Cannabinoids and Neuroprotection in Mouse Models of Demyelination

Thesis submitted for the degree of Doctor of Philosophy

Samuel James Jackson

Institute of Neurology, University College London

ProQuest LLC
789 East Eisenhower Parkway
P.O. Box 1346
Ann Arbor, MI 48106-1346

Abstract

The symptoms of multiple sclerosis (MS), an immune-mediated, degenerative disease of the central nervous system (CNS), are thought to be due to demyelination and axonal damage leading to impairment of neurotransmission. In a mouse model of MS, chronic relapsing experimental allergic encephalomyelitis (CREAE), cannabinoid compounds have been shown to protect axons and improve disease severity. In this study, CREAE and rotation-mediated CNS aggregate cell cultures were used to examine the role of cannabinoid receptor 1 (CB_1R) in endocannabinoid-mediated modulation of demyelination and neurodegeneration.

The aggregate cell culture system was developed and characterised in mouse to exploit CB_1R knockout (CB_1R-KO) animals. CREAE was induced in CB_1R-KO mice and wildtype counterparts, and CNS aggregate cell cultures derived from the same mouse strains were demyelinated with interferon gamma. CREAE animals were assessed for functional deficit by clinical scoring and in an open field activity chamber. CREAE spinal cords and aggregate samples were assessed for myelin content and axonal damage by measurement of myelin basic protein and neurofilament. Axonal vulnerability was assessed using a monoclonal antibody (SMI-32) against a dephosphorylated neurofilament epitope and caspase 3 expression and activation were measured to gauge cell death.

Neurofilament loss following demyelination was increased in CB_1R-KO animals and cultures when compared with wildtypes while myelin levels did not differ between the two strains. This indicates that the presence of CB_1R may be partially responsible for restricting damage to axons in inflammation, but has a less marked effect on myelination or remyelination. Neurofilament loss correlated with functional deficit,

suggesting that axonal or neuronal loss was responsible for neurodegeneration in CREAE. SMI-32 immunoreactivity was also increased, indicating axonal vulnerability or damage through alteration of neurofilament phosphorylation state. Increased activation of caspase 3 in knockout animals and cultures was evident, but not accompanied by increased procaspase 3 expression, signifying higher caspase activation rates. Caspases may therefore be involved in the death of neurons or axonal compromise in these two models.

Manipulation of the cannabinoid pathway by exogenous agonist-mediated CB_1R activation or indirect upregulation of endogenous ligands could slow disease progression in demyelinating diseases such as multiple sclerosis, indicating a potential therapeutic benefit.

Contents

List of Figures

List of tables

List of Abbreviations

Δ9-THC	Δ9-tetrahydrocannabinol
^{125}I	Iodine-125
2AG	2-arachidonoyl glycerol
ABH	Biozzi antibody high
ABL	Biozzi antibody low
ABTS	Azino-bis (ethylbenzthiazoline) sulphonic acid
BAME	Benzoylarginine methyl ester
BBB	Blood-brain barrier
Bcl	B-cell lymphoma
BrdU	Bromodeoxyuridine
BSA	Bovine serum albumin
CAII	Carbonic anhydrase 2
CB_1R	Cannabinoid receptor 1
CB_1R KO	Cannabinoid receptor 1 knockout
CB_2R	Cannabinoid receptor 2
cDNA	Complimentary deoxyribonucleic acid
CNP	Cyclic nucleotide phosphodiesterase
CNS	Central nervous system
CREAE	Chronic relapsing experimental allergic encephalomyelitis
CSF	Cerebrospinal fluid
DAB	Diaminobenzadine tetrahydrochloride
DEPC	Diethylpyrocarbonate
DIV	Days *in vitro*
DMEM	Dulbecco's modified Eagle's medium
DNA	Deoxyribonucleic acid
dNTP	Deoxyribonucleoside triphosphate
DPX	Distrene 80:plasticiser:xylene
E	Embryonic day

EAE	Experimental allergic encephalomyelitis
EGTA	Ethylene gycol-bis (2-aminoethylester)-N,N,N',N'-tetracetic acid
ELISA	Enzyme-linked immunosorbant assay
ER	Endoplasmic reticulum
FGF	Fibroblast growth factor
GalC	Galactocerebrocide
GAPDH	Glyceraldehyde-3-phosphate dehydrogenase
HRP	Horseradish peroxidase
IAP	Inhibitor of apoptosis
IFN	Interferon
Ig	Immunoglobulin
IGF	Insulin-like growth factor
IL	Interleukin
IPL	Interperiodic line
KSP	Lysine-serine-proline
LTP	Long term potentiation
Mab	Monoclonal antibody
MAG	Myelin-associated glycoprotein
MBP	Mylein basic protein
MDL	Major dense line
MHC	Major histocompatibility complex
MMLV	Maloney murine leukaemia virus
MOG	Myelin oligodendrocyte glycoprotein
MRI	Magnetic resonance imaging
mRNA	Messenger ribonucleic acid
MS	Multiple sclerosis
Na^+	Sodium ion
Na^+/Ca^{2+}	Sodium ion/calcium ion
Na^+/K^+-ATPase	Sodium/potassium adenosine triphosphatase
NCAM	Neuronal cell adhesion molecule
NCBI	National centre for biotechnology information
NF	Neurofilament
NF-H	Neurofilament heavy
NF-L	Neurofilament light

NF-M	Neurofilament medium
NFH^{SMI32}	SMI-32 reactive neurofilament
NFH^{SMI35}	SMI-35 reactive neurofilament
NMDA	N-methyl D-aspartate
NO	Nitric oxide
noR	Node of Ranvier
OPC	Oligodendrocyte precursor cell
OPD	Orthophenylenediamine
P	Postnatal day
PBS	Phosphate-buffered saline
PCR	Polymerase chain reaction
PDGF	Platelet-derived growth factor
PLP	Proteolipid protein
PNS	Peripheral nervous system
PP-MS	Primary progressive multiple sclerosis
PSA	Polysialic acid
RIA	Radioimmunoassay
RNA	Ribonucleic acid
RNase	Ribonuclease
RR-MS	Relapsing remitting multiple sclerosis
SDS	Sodium docecyl sulphate
ssDNA	Single stranded deoxyribonucleic acid
TAME	Tosylarginine methyl ester
Taq	*Thermus aquaticus*
TBE	Tris boric acid-EGTA
TGF	Transforming growth factor
TMB	Tetramethylbenzidine
TMEV	Theiler's murine encephalomyelitis virus
TNF	Tumor necrosis factor
TPCK	Tosylphenylalanyl chloromethane
Tris	Tris (hydroxymethyl) aminomethane
TTBS	Tween 20 – Tris buffered saline
WT	Wildtype

List of Abbreviated Companies

Aimer	Aimer products, Enfield, UK
Amersham	Amersham Pharmacia Biotech UK Ltd., Little Chalfont, UK
B & K	B & K Universal, Grimston, UK
Chemicon	Chemicon International Ltd., Harrow, UK
Cymbus Biotech	Cymbus Biotechnology Ltd., Chandlers Ford, UK
Fisher	Fisher Scientific UK, Loughborough, UK
Gibco	Gibco BRL Life Technologies ltd., Paisley, UK
Invitrogen	Invitrogen Ltd., Paisley, UK
Nybolt	Nybolt, Zurich, Switzerland
Perkin Elmer	Perkin Elmer Applied Biosystems, Norwalk, USA
Philip Harris	Philip Harris Scientific, Ashby de la Zouch, UK
Promega	Promega Biosciences Inc., Southampton, UK
R and D	R and D Systems Ltd., Abingdon, UK
Research Diagnostics	Research Diagnostics Inc., Flanders, USA
Santa Cruz	Santa Cruz Biotech, Santa Cruz, USA
Seralab	Seralab Ltd., Loughborough, UK
Serotec	Serotec Ltd., Oxford, UK.
Sigma	Sigma-Aldrich Co. Ltd., Poole, UK
Southern Biotech	Southern Biotechnology Associates Ltd., Birmingham, USA
Sternberger	Sternberger Monoclonals Inc., Lutherville, USA
TAG	TAG Inc., Burlingame, USA
VWR	VWR International, Lutterworth, UK

Acknowledgements

I would like to thank my supervisors Dr. Lara Diemel and Dr. David Baker, and Professor Louise Cuzner for their unswerving support throughout my PhD. Thanks also to Gareth Pryce for his invaluable advice and the Brain Research Trust for their generous funding of this project.

This thesis is dedicated to my family.

1. Introduction

1.1. The Cellular Pathology of Multiple Sclerosis

Multiple sclerosis (MS) is a relapsing and often progressive neurodegenerative disorder predominantly affecting young adults, with an immune-mediated aetiology but potentially incorporating viral, bacterial and/or genetic triggers. With a prevalence of around 1 in 800 in the United Kingdom, the disease renders about 89% of patients unable to walk without assistance 25 years after onset. Two main forms of MS exist. 60% of MS patients are diagnosed with relapsing remitting MS (RR-MS), with predominance in females of 2:1. This subtype is characterised by symptoms which develop over a period of several days, stabilise, and then typically improve over a period of a few weeks or months; the disease may progress in-between relapses, and eventually reach a stage of continuing decline without remission, termed secondary progressive MS. About 20% of people exhibit benign MS where following initial presentation, there is relatively little clinical disease activity. In contrast, the remaining 20% of MS patients have a form known as primary progressive MS (PP-MS), characterised by a gradually progressive clinical course from diagnosis, and has a similar incidence in men and women as RR-MS (Bashir & Whitaker, 1999). Demyelinated areas in the central nervous system (CNS) termed lesions cause MS-associated deficit, with the symptoms and nature of deficit depending on lesion location in the CNS. The disease is diagnosed with the aid of magnetic resonance imaging (MRI) to identify and quantify lesions (Figure 1-1), a key feature of which being the demonstration of disseminated lesion development in space and time, cerebrospinal fluid (CSF) analysis to identify intrathecal immunoglobulin (Ig)-G production (termed oligoclonal banding – Figure 1-2), as well as by clinical motor tests.

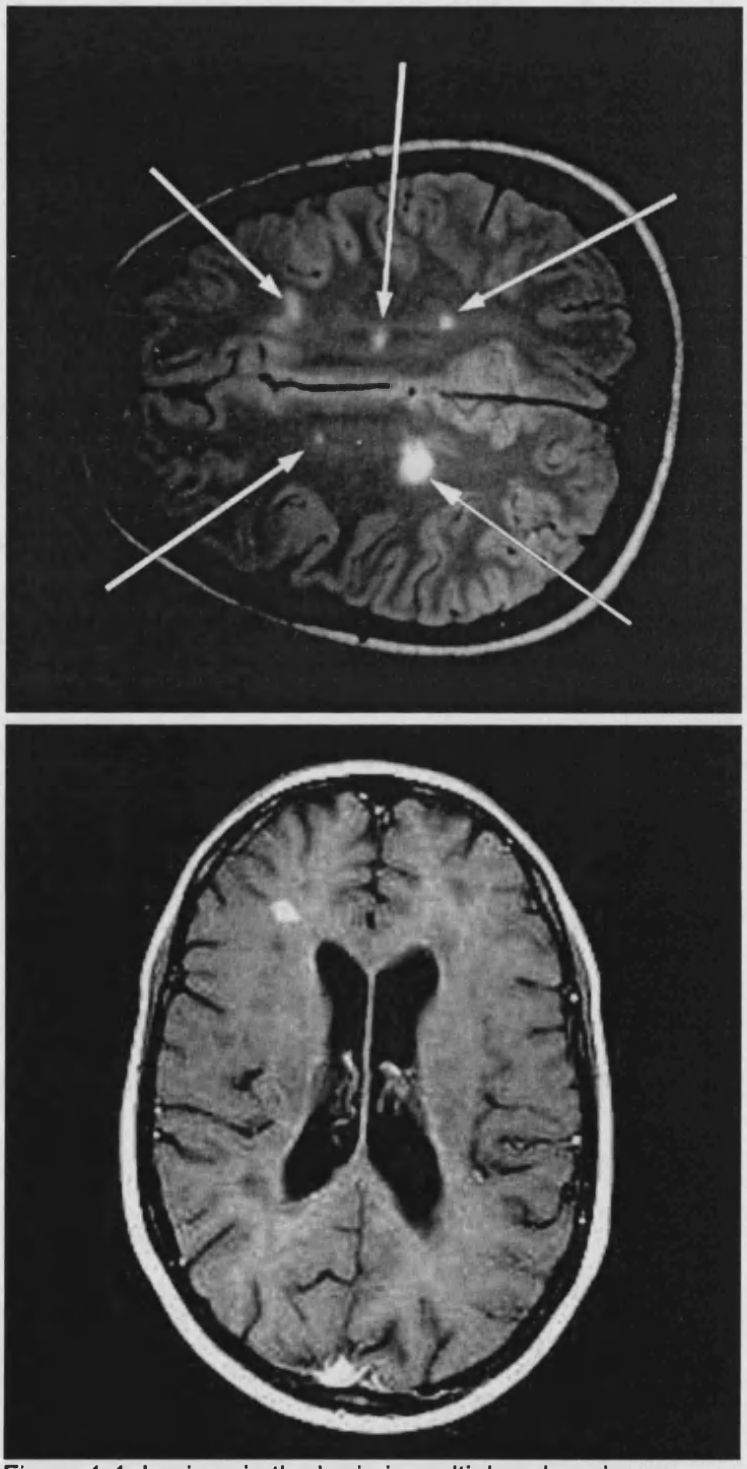

Figure 1-1: Lesions in the brain in multiple sclerosis, as visualised by magnetic resonance imaging, appear as light areas on a darker background. Location of a lesion in a brain structure dictates whether it is a "silent" lesion, or if it will elicit clinical symptoms. For instance, a lesion in the motor cortex can cause tremor or loss of movement function.
From: Multiple Sclerosis (Edited by Paty D.W., Ebers G.C.; 1997; Philidelphia, Pa. F.A. Davis)

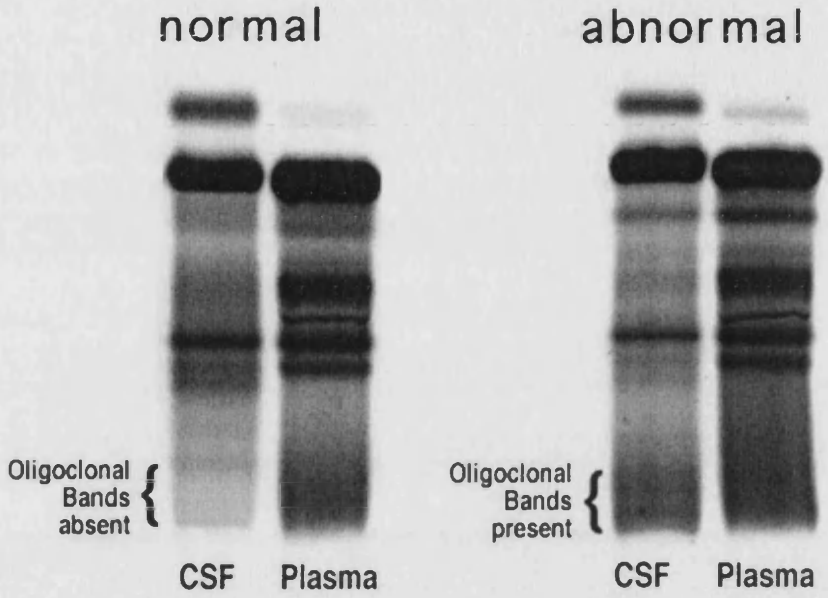

Figure 1-2: Oligoclonal bands present in the cerebro-spinal fluid are a diagnostic feature of multiple sclerosis. The presence of immunoglobulins usually only present in the blood indicates a breach of the blood-brain barrier. The figure shows banding produced on a Western blot gel stained with Comassie blue to visualise protein. Banding indicating blood-brain barrier breach occurs at the lower end of the gel. From: Multiple Sclerosis (Edited by Paty D.W., Ebers G.C.; 1997; Philidelphia, Pa. F.A. Davis)

1.1.1. Invasion of the CNS in MS

A key early event in multiple sclerosis is the invasion of the CNS by activated leucocytes, T-cells and macrophages (Figure 1-3). This occurs in a multi-stage process. Firstly, the invading cell tethers to the vessel endothelium via selectin molecules. Facilitated by a reduction in blood flow via cytokine-mediated vasoconstriction, this slows down the cell in the bloodstream and causes it to roll along the endothelial cell wall. In the second stage, termed triggering, cytokines produced by the invading cell cause integrins and other strong adhesion molecules to be upregulated or activated on the epithelium and invading cell surface. Strong adhesion then occurs, accompanied by a flattening of the cell. Finally the cell is able to diapese probably directly through the endothelial cell wall, stimulated by chemotactic cytokines (Brown, 2001; Gran & Rostami, 2001; Greenwood *et al.*, 2003).

1.1.2. Pathophysiology of the MS lesion

It had generally been accepted that similar pathophysiological mechanisms lead to the symptoms of all types of MS. However, recent studies have demonstrated a degree of heterogeneity in pathological processes, with different processes bringing about similar symptoms. Such a divergence of distinct mechanism patterns may split patients into distinct subgroups based on the dominant subtype present in lesions in an individual (Lucchinetti *et al.*, 1996). In spite of this, there remains a large degree of similarity between pathological processes in MS patients.

Dual inflammatory responses are observed in the CNS. Innate immunity acting through active microglia produces a focal and limited response to, for instance, an invasive body; the adaptive immune response produces antigen-specific T-lymphocytes to a more global and temporally extended attack (Lucchinetti *et al.*, 2001). The most

potent immunogens for the latter are present in myelin, with an autoimmune response consisting of recruited T- and B-cells priming resident and infiltrating macrophages to degrade myelin and secrete a range of damaging factors (Figure 1-4) (Gay & Esiri, 1991; Van Noort & Amor, 1998; Wekerle,1997).

Inflammation of this type occurs in MS in focal demyelinating lesions or plaques, characterised as active (or inactive) by the presence (or absence) of autoimmune attack, macrophages containing myelin fragments and by activation markers. Perivascular cuffs formed at sites of invasion contain macrophages, lymphocytes, B cells and plasma cells; only macrophages and lymphocytes progress further into the parenchyma. The majority of the lymphocytes are T-cells, with both $CD4^+$ (helper) and $CD8^+$ (cytotoxic) cells being involved. The $CD4^+$ cells are often further subdivided into proinflammatory (Th1) and anti-inflammatory (Th2); the proportions and activity of these cells may control overall lesion activity, although the distinction of activities is less clear cut in humans compared to their rodent counterparts (Markovic-Plese & McFarland, 2001).

The central pathophysiological event in MS is axonal conduction block, which worsens with disease course becoming irreversible. Axonal loss in the brain and spinal cord correlates with inflammation and demyelination (Trapp *et al.*, 1998). The potential mechanisms for this are numerous, and include cell-mediated cytotoxicity, damage via secreted effector molecules including tumour necrosis factor alpha (TNF-α), matrix metalloproteinases and reactive oxygen species, auto-antibodies and damage via glutamate release from microglia and activated leucocytes. Oligodendrocytes are highly sensitive to glutamate toxicity, with elevated glutamate levels in the CSF correlating with disease severity (Werner *et al.*, 2001). A role for nitric oxide (NO) has been

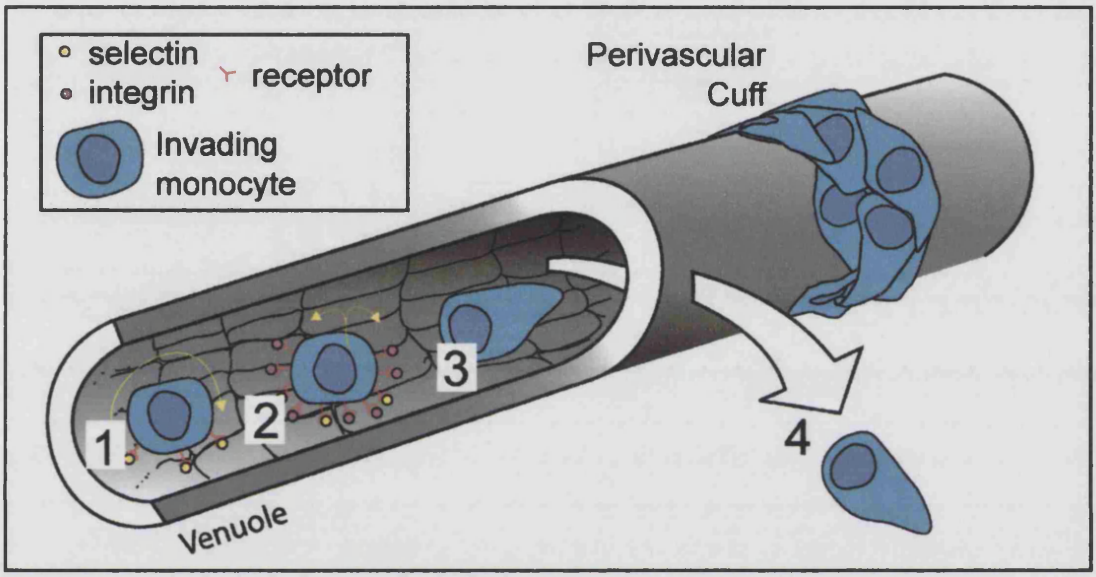

Figure 1-3: A model of invasion of the CNS by lymphocytes in inflammatory disease
1 - Tethering/Rolling: Selectins slow down the lymphocyte in the blood flow.
2 - Activation: Endothelium chemokines activate the lymphocyte to release pro-inflammatory cytokines and express integrins.
3 - Strong adhesion: Integrins adhere to the endothelium; the lymphocytes flatten.
4 - Transmigration: Aided by proteases and directed by chemokines, the lymphocyte forces through the endothelial cell wall.

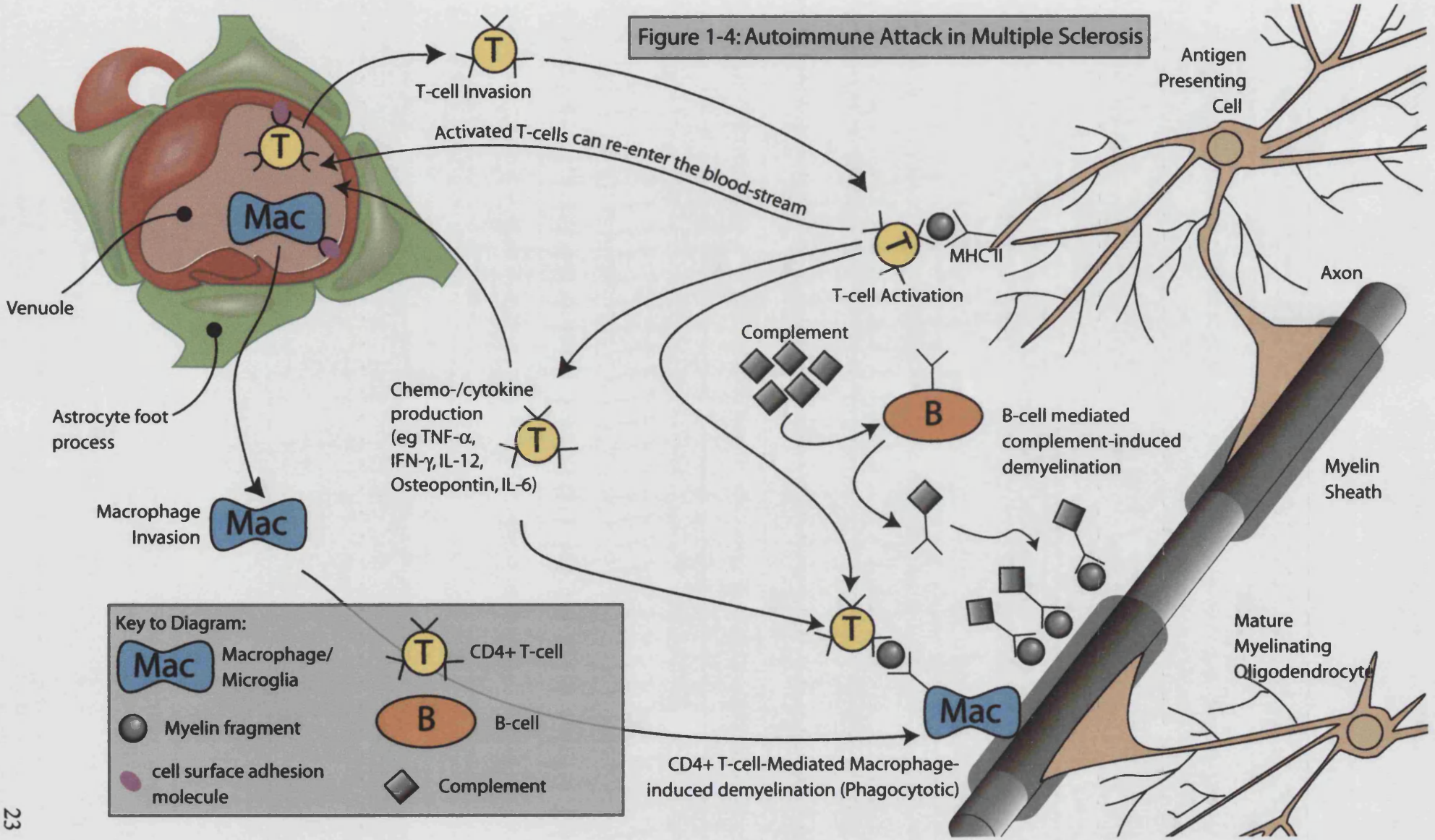
Figure 1-4: Autoimmune Attack in Multiple Sclerosis
T-cell Invasion
Activated T-cells can re-enter the blood-stream
Antigen Presenting Cell
MHC II
T-cell Activation
Axon
Venuole
Astrocyte foot process
Complement
B
B-cell mediated complement-induced demyelination
Myelin Sheath
Chemo-/cytokine production (eg TNF-α, IFN-γ, IL-12, Osteopontin, IL-6)
Macrophage Invasion
Mac
Mature Myelinating Oligodendrocyte
CD4+ T-cell-Mediated Macrophage-induced demyelination (Phagocytotic)
Key to Diagram:
Macrophage/ Microglia
CD4+ T-cell
Myelin fragment
B-cell
cell surface adhesion molecule
Complement

proposed (Smith *et al.*, 2001), where sustained impulses in conducting axons produce intermittent conduction failure in MS patients. Increased NO at the site of inflammation may cause permanent deficit in conduction. Tissue plasminogen activator in excitotoxic lesions can damage neurons through disruption of axon-laminin interactions (Gveric *et al.*, 2001).

Whether the product or cause of axonal damage, the destruction of the myelin sheath is a hallmark of pathology in MS. Pro-enzymes in serum and plasma can, once activated, cause myelin sheath disruption even in the presence of serum/plasma proteinase inhibitors (Pescovitz *et al.*, 1978). Lysis may occur through the formation of membrane attack complexes or by complement receptor-mediated opsonic phagocytosis (Silverman *et al.*, 1984), and myelin can be phagocytosed by macrophages and polymorphonuclear leucocytes. Astrocytes have also been implicated through the presence of ingested myelin in chronic demyelinated MS plaques. Activated microglia and macrophages in the presence of an antibody can effect myelin uptake via receptor-mediated mechanisms *in vitro* (Prineas,1985), and T-cells can, via production of TNF-α and -β, be effective cytotoxic mediators . Finally the concept of "frustrated" phagocytosis may induce demyelination, where macrophages or microglia are unable to internalise myelin membrane, leading to discharge of lysosomal enzymes (Young & Zygas, 1987).

1.2. Experimental Allergic Encephalomyelitis: An in vivo model of MS

Experimental allergic encephalomyelitis (EAE) is a demyelinating disease of the CNS inducible in a number of inbred animal strains. It can take an acute or chronic, potentially relapsing disease course, with inflammatory and sometimes demyelinating lesions. The disease can be triggered following sensitisation with white matter or

purified myelin proteins such as myelin basic protein (MBP) or myelin oligodendrocyte glycoprotein (MOG) (Martin & McFarland,1997). This T-cell mediated autoimmune disease is used as a model of MS. It is worth noting that susceptibility to EAE varies greatly from strain to strain (Levine & Sowinski, 1973) and is reflective of the contribution of polymorphic genetic components. For example, ABH mice described below are highly susceptible to the disease, whereas the closely related ABL strain is not (Baker *et al.*, 1990).

EAE can be induced using a variety of sensitising antigens (Amor *et al.*, 1993; Amor *et al.*, 1994; Amor *et al.*, 1996; Morris-Downes *et al.*, 2002), but chronic relapsing EAE (CREAE) in the ABH mouse strain is most reproducibly induced by injecting the animal sub-cutaneously with syngeneic spinal cord homogenate in complete Freund's adjuvant. The disease course is scored on a clinical scale of 1-5 (Figure 2-3). Following significant weight loss, the acute attack that occurs around day 15-17 is evident by the development of hind limb paralysis. This usually remits within 3-6 days, and is associated with weight gain. After a period of remission, a series of relapses occur, developing at around day 35-40 and at 2-3 week intervals thereafter. Each relapse is associated with a loss of weight and an increase in clinical score of at least 1 grade, but usually increasing to grade 4 – complete hind limb paralysis. Increased residual clinical scores are evident during remission, and these accrue over a series of relapses, indicating a level of cumulative and permanent CNS damage (Baker *et al.*, 1990; Baker *et al.* 2000).

Injection of spinal cord and adjuvant acts as a trigger to set the stage for EAE development. Autoreactive T-cells, a normal and constant part of the mature T-cell repertoire, are then activated by the injected myelin antigen. These cells differentiate

into primed T cells and circulate through tissues. This is facilitated by cell adhesion molecules on both T-cells (CD11a and CD49d) and cerebrovascular endothelial cells (CD54 and CD105) which are upregulated during CNS inflammation (Kalman *et al.*, 1995; Lee & Benveniste, 1999). Activated T-cells are then able to migrate through the blood brain barrier (BBB) and also into the CNS parenchyma, where they activate resident perivascular and paranchymal and glial cells and attract further influx of monocytes and other T-cells via chemoattractant chemokines and cytokines (Leonard *et al.*, 1995; Ruddle *et al.*, 1990).

1.2.1. Cellular infiltrates in EAE

Depending on the model, the spinal cord is a pathological focus for CNS cellular infiltrates, with lesions in the brain often being confined to the cerebellum (Baker *et al.*, 1990). Infiltrate density is comparable during acute and relapse phases of the disease, and is mainly of a similar composition, with the exception of a more prevalent acute phase polymorphonuclear cell population (Allen *et al.*, 1993). Perivascular cuffs containing 30-50% T-lymphocytes, mostly $CD4^+$, were observed, with further paranchymal infiltration of macrophages also occurring. There is extensive immunoglobulin deposition in the CNS lesions of relapsing animals, with lower paranchymal levels. In remission, the degree of infiltration falls with very few $CD4^+$ T cells and active macrophages observed (Baker *et al.*, 1990).

1.2.2. Neuronal damage in EAE

Axonal damage, neuronal death and demyelination in EAE and MS are likely to occur through a number of routes. Again, the direct toxic effects of TNF-α and -β and oxidative stress from T-cells and microglia which are likely to be responsible for demyelination, as mentioned previously, are in direct proximity to the axon and may

cause damage. Secondly, it has been found that sodium channel blockers such as phenytoin can protect neurons in culture (Lo *et al.*, 2002). During EAE, mitochondrial function is impaired, reducing sodium/potassium adenosine triphosphatase (Na^+/K^+-ATPase) activity and causing axonal depolarisation (Sathornsumetee *et al.*, 2000). Also, loss of myelin reduced trophic support available to the axon (Bjartmar & Trapp, 2003). It is hypothesised that the resulting sodium ion (Na^+) influx causes a reverse in the function of the sodium/calcium ion (Na^+/Ca^{2+}) exchange pump, leading to an increase in intracellular calcium levels (Carafoli, 1988). This may cause the activation of calcium-dependent proteolytic enzymes, such as calpain, and proteolysis of neurofilaments and other neuronal cytoskeletal components. Similarly, activation of calmodulin would cause upregulation of protein phosphatase 2B, dephosphorylating and destabilising neurofilaments (Groth *et al.*, 2003). Increased calcium at the presynaptic membrane would trigger excess neurotransmitter release, and excitotoxic effects on the post-synaptic cell. High levels of intracellular calcium can also trigger apoptosis via release of mitochondrial cytochrome c (Mattson, 2003). Nitric oxide, another potential agent of damage, has been found to act as a modulatory factor in the induction of the immune response. As such, different pathological environments induce NO to fulfil opposing roles as a degenerative or protective molecule (Willenborg *et al.*, 1999). Contributing to degeneration, NO can be directly cytotoxic, or can act via peroxynitrite free-radical formation, causing oxidative damage to the BBB, myelin and axons (Hooper *et al.*, 2000). Nitric oxide also increases levels of intracellular cyclic guanidine monophosphate, activating T-cells and macrophages, leading to increased proinflammatory cytokine-induced toxicity, as well as the direct damage caused by these cell types (Sherman *et al.*, 1992). In contradiction, it has been shown that NO

produced by NO synthase 2 (NOS-2 or iNOS), the inducible form of the enzyme, can inhibit T-cell proliferation, leukocyte adhesion/migration and down-regulate major histocompatibility complex (MHC) class II expression on macrophages, thereby inhibiting antigen presentation (Kahl *et al.*, 2003; Singh *et al.*, 2000). Owing to its small size, NO also has access to intramolecular sites, allowing diverse effects on key mechanistic molecules of the immune response, including ion channels, tyrosine kinase, phosphatases and transcription factors (Singh *et al.*, 2000). This presents a dichotomous role for NO-mediated protection in early disease and for later NO-mediated pathology.

1.2.3. Apoptosis in EAE

Most of the pathways described above will have an apoptotic final outcome. Oxidative stress combined with high intracellular Ca^{2+} concentrations leads to cytochrome c release from mitochondria, which is a vital part of the apoptosome, the caspase-9 based macromolecule responsible for a high degree of apoptotic end-point activity. Similarly, deoxyribonucleic acid (DNA) damage caused by free radicals or Ca^{2+}-activated enzyme pathways leads to cytochrome c release via p53 upregulation. Loss of trophic support from damaged surrounding cells causes deregulation of cell-cycle signals and activation of the CD95 death receptor by TNF-α both leading directly to triggering of the caspase activation cascade, and ultimately to apoptosis (described in section 1.5.7) (Lossi & Merighi, 2003).

1.3. Rotation-mediated aggregate cell culture: An in vitro model of demyelinative disease

Aggregation of dissociated embryonic cells was first performed in the late 1960s by Moscana (Moscona,1965). Since that time, the system has been exploited extensively for a wide variety of applications. Honegger and associates took up the

system in the mid 1970s as a developmental model of myelination and remyelination (Honegger & Richelson, 1976).

1.3.1. Developmental characteristics

Methodology for the use of rat tissue involves mechanical dissociation of the rat telencephalon by sieving, and incubation at an optimal density under constant rotation. The cells in suspension spontaneously form 3-dimensional aggregated structures under constant rotation (Honegger & Richelson, 1976). Following a short period of time *in vitro*, differentiated neurons, astrocytes and oligodendrocytes are observed, arranged into a specific and highly reproducible structure (Trapp *et al.*, 1979). In the rat, cells from foetal and early neonatal tissue yield viable aggregates. Developmental patterns of enzymatic activity varied with the age of starting tissue, with relatively undeveloped tissue yielding the highest levels of neuron specific enzymes (Honegger & Richelson, 1976). Mitosis occurs, as confirmed by bromodeoxyuridine (BrdU) incorporation, and aggregates can be maintained for up to 48 days in culture (Copelman *et al.*, 2000). Morphologically, synaptic contacts and myelinated axons appear with further maturation, but, while experimentally acceptable, myelin levels are lower than in organotypic cultures or *in vivo* (Trapp *et al.*, 1979). Synthesis, storage and release of neurotransmitters were confirmed by radiolabelling studies, indicating that the synapses present are electrically active (Honegger & Richelson, 1979).

1.3.2. Remyelination in the aggregate cell culture system

The CNS aggregate culture model has been extensively characterised for myelin synthesis. It was found that commitment of myelination *in vitro* occurred after the same period required *in vivo*, and was temporally coupled with the expression of 2'-3'-cyclic nucleotide phosphohydrolase and cerebroside sulphotransferase, two myelin-specific

enzymes (Sheppard *et al.*, 1978). Furthermore, isoforms of MBP are differentially expressed in development, with exon 2-containing isoforms being expressed early on, and possibly playing a role in the onset of myelination (Kruger *et al.*, 1999).

Further to the studies of myelination, the aggregate cell culture system has been used to study remyelination after a demyelinative insult *in vitro*. Myelinated axonal processes can be found in the intermediate shell of the aggregate (Trapp *et al.*, 1979). They are therefore accessible to exogenous factors added to the medium. Honegger et al. (1989) used the MOG-specific antibody 8-18-C5 to effectively demyelinate aggregate cultures (Honegger *et al.*, 1989). Since then, other anti-MOG antibodies have shown a similar effect, along with the cytokines IFN-γ and TNF-α, and IL-1β (Loughlin *et al.*, 1997). One line of study using this system has been to investigate the roles of macrophages in demyelination and remyelination (Copelman *et al.*, 2000; Copelman *et al.*, 2001; Loughlin *et al.*, 1997). The culture system is used to model a simplified demyelinating MS lesion, where it is thought that macrophages can have damaging or repairing effects dependent on the immediate microenvironment (Diemel *et al.*, 1998). Supplementation of demyelinated cultures with peritoneal macrophages severely curtails their ability to remyelinate, while addition to an undamaged environment promotes myelinogenesis (Diemel *et al.* 2003). Another study investigated the role of macrophages in response to oxidative stress, where oxidative insult induced using menadione was significantly higher in macrophage-supplemented cultures (Bartnik *et al.*, 2000).

1.3.3. Benefits of the aggregate system

The ability to add endogenous factors or other cell types (e.g. macrophages) to culture flasks and compare them with identical cultures from the same source is a major

benefit of this system. A reproducible culture population can be seeded and treated in a highly flexible manner. The ability to maintain a relatively large volume of tissue *in vitro* for long periods of time allows temporal studies to be undertaken, sampling one culture flask at successive time points. The production of CNS specific structures and pharmacological systems by the aggregates makes possible the accurate assessment of a substance prior to whole animal studies, presenting a more humane method of animal testing. Finally, the aggregate culture allows development of cells in a three-dimensional context, more closely mimicking brain development than monolayer cultures.

1.4. Myelination and oligodendrocyte development

1.4.1. Myelination of the axon

With a few exceptions, myelination occurs only in vertebrates and can therefore be considered necessary for the evolution of higher nervous function. The process of myelination occurs in a highly reproducible manner, caudo-rostrally in the brain, and rostro-caudally in the spinal cord. Myelination in the mouse starts at around birth, and is complete by around 20 days postnatally in the spinal cord and 60 days postnatally in the brain (Bird *et al.*, 1980; Siegrist *et al.*, 1981) and slightly later in the rat. The stage of differentiation can be identified by a group of molecular markers, as outlined in Figure 1-5.

Initiation of myelination

Although *in vitro* uncompacted myelin-like structures can form in the absence of an axon (Sarlieve *et al.*, 1983), *in vivo*, oligodendrocytes form myelin sheaths solely around axons. Proliferation of oligodendrocyte precursor cells (OPCs) appears to be

dependent on axonal electrical activity (Barres & Raff, 1993), and oligodendrocyte numbers correlate closely with axonal numbers (Burne *et al.*, 1996) suggesting direct and controlled glial-axonal signalling, although the precise nature of this signal has not yet been elucidated. Axonal diameter also plays a critical role, acting as a control of myelin thickness (Elder *et al.*, 2001). However, axons are myelinated in internodal sections, requiring a more spatially specific signal. Pharmacologically, the Na^{2+} channel blocker tetrodotoxin has been shown to block the initiation of myelination (Crespo *et al.*, 1995), while α-scorpion toxin has the opposite effect (by slowing Na^{2+} channel activation, and thus repolarisation) (Demerens *et al.*, 1996). These findings again illustrate the importance of axonal activity for myelination.

Myelination begins with the extension of processes which, aided by astrocytic guidance (Meyer-Franke *et al.*, 1999), align with and adhere to the axon in an adhesion molecule-dependent process. The oligodendrocyte cell processes then form loose cups around an axonal segment. As the sheath envelops the axonal process, so one lip (the future inner tongue) becomes forced under the other lip. The lamellae develop by rotation of the inner tongue around the axon, and this is quickly followed by compaction (Figure 1-6). One oligodendrocyte may myelinate up to 40 segments (termed internodal areas) on different axons in this way, creating a mesh of axons, myelinating oligodendrocytes and supportive astrocytes (Raine,1984).

Internodal areas are flanked by nodes of Ranvier (noR), and are 150-200μm in length, with around 12nm between each layer (Butt & Ransom, 1989). Myelin thickness seems to be influenced by axon diameter, with thicker axons receiving thicker layers of myelin (Waxman & Sims, 1984). Following the spiralling of an axon by the sheet of myelin, the layers compact around the fibre, with the layers being assigned labels

dependent on their intra- or extracellular orientation. The major dense line (MDL) is comprised of the intracellular cytoplasmic interface of the myelin, whereas the intraperiodic line (IPL) refers to the opposition of the external faces of the oligodendrocyte membrane (Figure 1-7) (Sjostrand, 1949). Separating the MDL and IPL is the lipid bilayer, containing the variety of myelin proteins (Figure 1-8).

The noR is an axonal membrane specialisation related to the saltatory conduction of action potentials down the axon. Prior to myelination, the axon membrane contains a low density of sodium channels, randomly distributed along its length. During myelination, the sodium channels become localised to the noR, with potassium channels concentrated in the juxtanode. This arrangement facilitates saltatory conduction by causing changes in membrane polarisation, and to regulating ion flow (Hildebrand *et al.*, 1993; Waxman & Black,1995).

Molecular Aspects of Myelinogenesis

In the mouse, gene activation for transcription of myelin proteins occurs in the late pre-natal period, when the switch from immature oligodendrocytes (expressing galactocerebrocide (GalC) and 2'-3'-cyclic nucleotide 3'-phosphodiesterase (CNP)) to mature oligodendrocytes (expressing MBP, proteolipid protein (PLP) and myelin associated glycoprotein (MAG)) occurs (Monge *et al.*, 1986). These molecules are transported by a variety of routes. MBP, which is required for myelin compaction by adhering to the cytoplasmic leaflet of the lipid bilayer, is likely to be non-specifically adhesive to organelle membranes. Therefore, MBP messenger ribonucleic acid (mRNA) is specifically transported to areas of myelination, where translation occurs (Colman *et al.*, 1982). In contrast, PLP is likely to be transported in vesicles, with proteins involved in such transport having been identified in oligodendrocytes (Allard *et al.*, 1998;

Figure 1-5: The Developing Oligodendrocyte

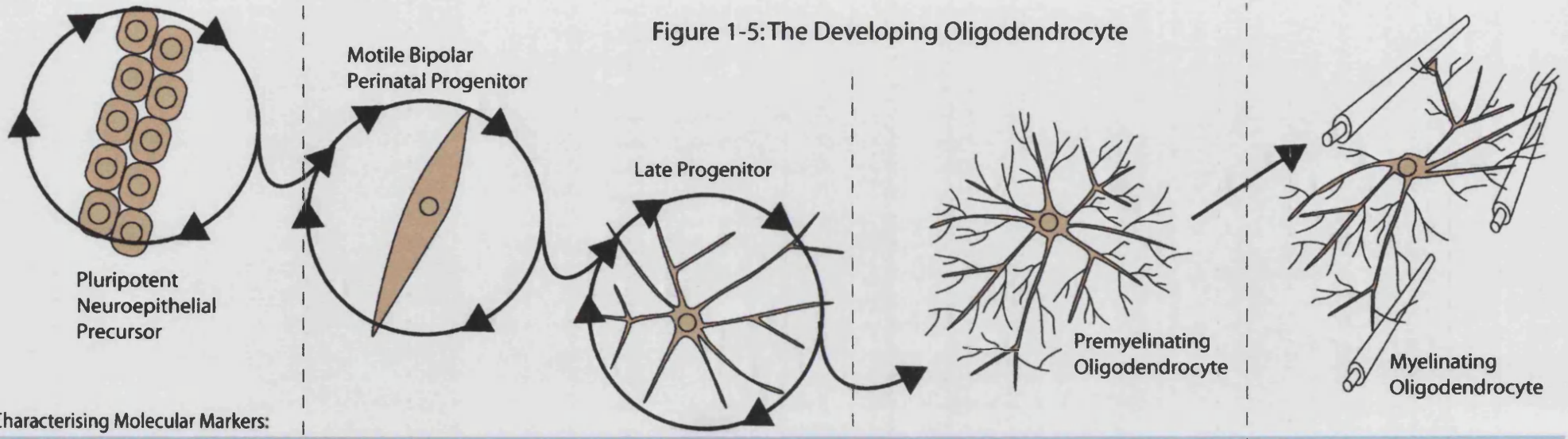

Characterising Molecular Markers:					
PDGF alpha Receptor +		PDGF alpha-R +	PDGF alpha-R +	NG2 -	Galc +
O4 -		O4 -	O4 +	GalC +	MBP +
NG2 -		NG2 +	NG2 +	O4 +	PLP +
A2B5+		A2B5 -	GalC -	PLP/DM20 +	CNP +
					MOG +
Factors Involved and Role					
PDGF:	Mitogenic	Promotes survival and motility			
bFGF:		Mitogenic, upregulates PDGF-R			
IGF-1		Mitogenic			
NT-3:	Mitogenic*	Mitogenic**			
GGF:				Mitogenic and survival factor	
TGF-beta:		Promotes Differentiation, inhibits PDGF actions			

Key to Symbols and abbreviations

*Dependent on High PDGF or insulin levels
**Dependent on BNDF
PDGF: Platelet Derrived Growth Factor
NG2: NG2 Proteoglycan
GalC: Galactocerebroside
PLP: Proteolipid Protein
MBP: Myelin Basic Protein
CNP: C-type Natriuretic Peptide
MOG: Myelin Oligodendrocyte Glycoprotein
bFGF: basic Fibroblast Growth Factor
IGF-1: Insulin-like Growth Factor 1
NT-3: Neurotrophin 3
GGF: Glial Growth Factor
TGF-b: Transforming Growth Factor beta

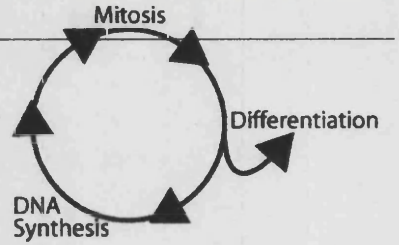

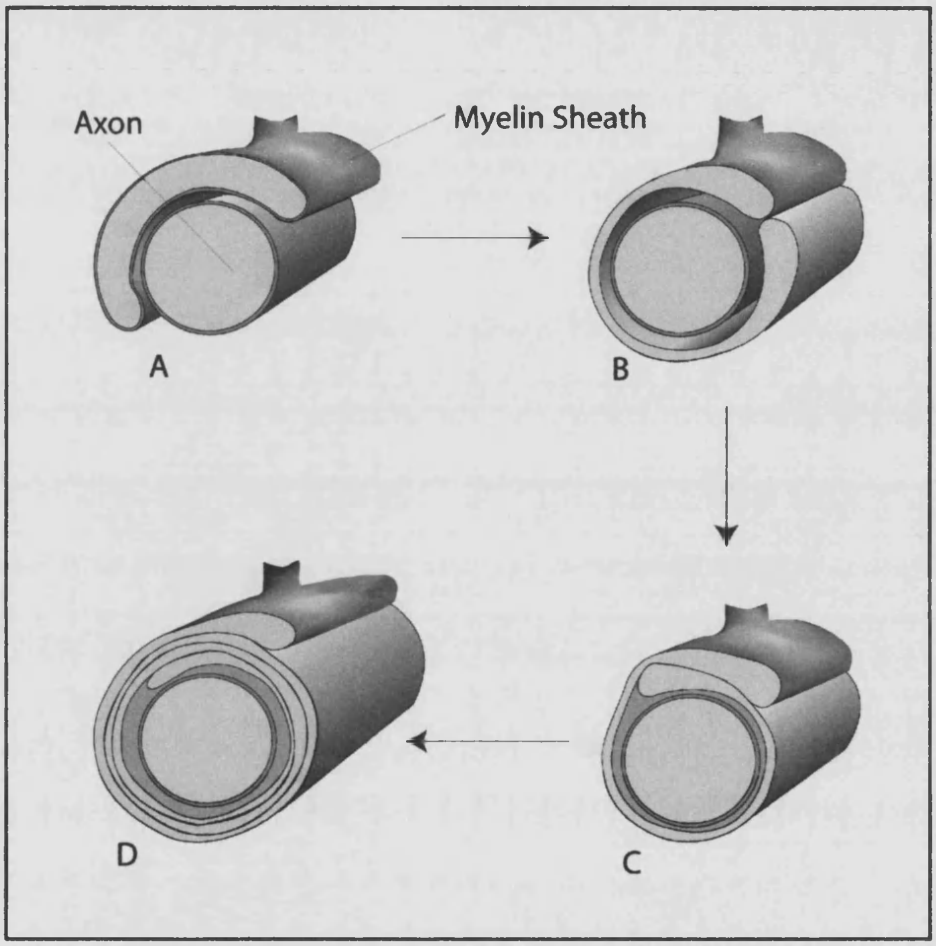

Figure 1-6: the morphological events surrounding the myelination of an axon. (A) Oligodendrocyte processes begin to form a sheet-like myelin structure upon axonal contact; (B) This sheet wraps around the axon until the two ends meet; (C) One end extends further underneath the other, forming inner and outer tongues; (D) Myelin continues to encircle the axon, and the multi-layered structure compacts by virtue of the electron-dense proteins in the membrane. After: Myelin, 2nd ed. (edited by Morell,P.; 1984; New York Plenum Press).

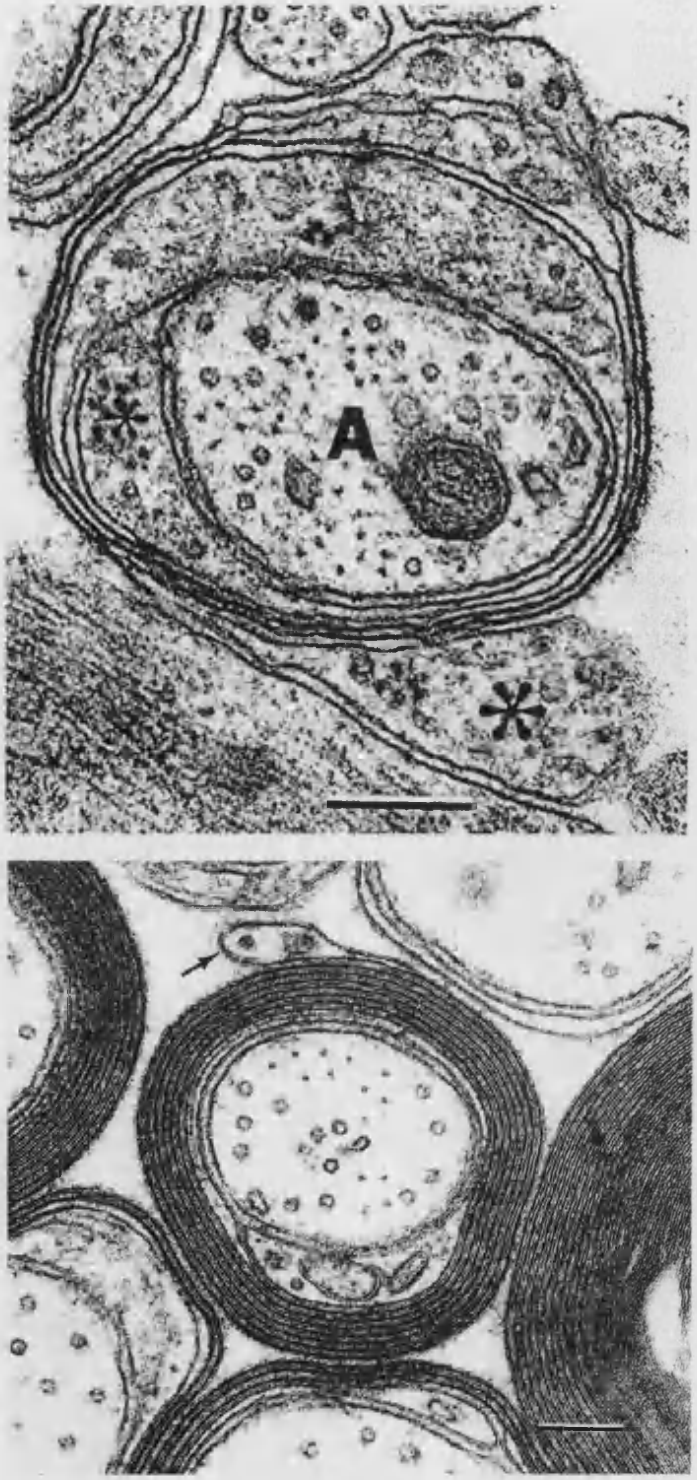

Figure 1-7: Electron micrographs showing CNS myelin. The top panel shows partially compacted myelin with the inner (small *) and outer (large *) tongues (A - axon); the lower panel shows compacted myelin, with the arrow indicating the outer tongue. From: Myelin, 2nd ed. (edited by Morell, P.; 1984; New York Plenum Press)

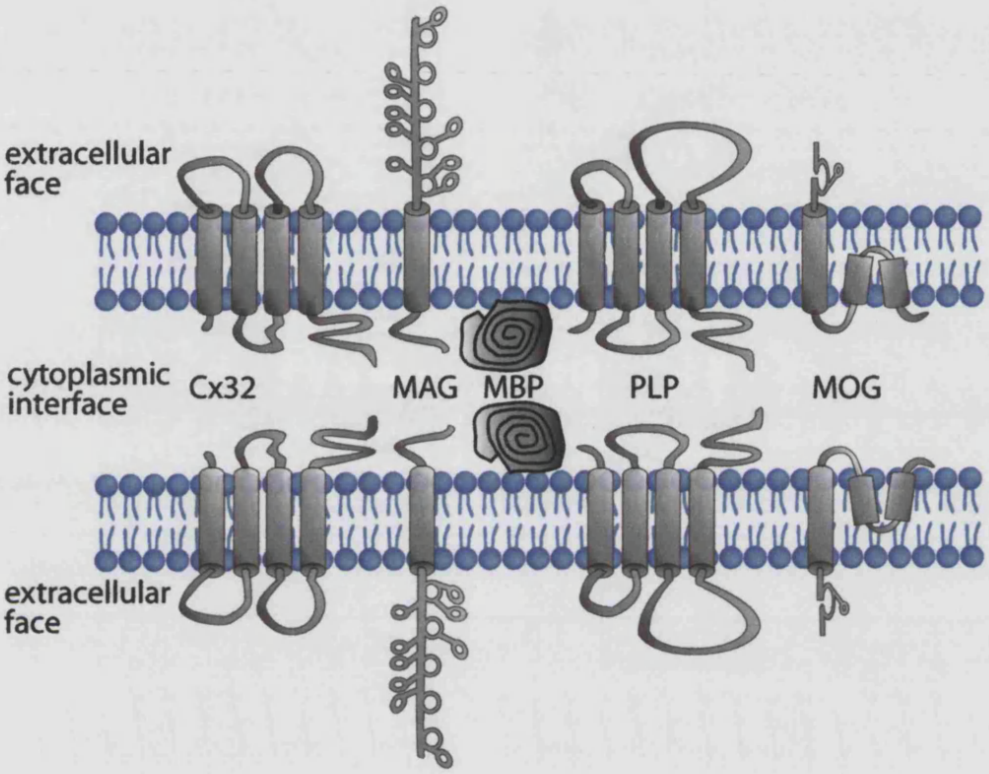

Figure 1-8: Proteins of the myelin sheath. The main constituent glycoproteins of the myelin sheath are arranged so as to maximise interactions at the cytoplamsic interface and allow compaction to occur. Abbreviations: Cx32 - Connexin 32; MAG - Myelin Associated Glycoprotein; MBP - Myelin Basic Protein; PLP - Proteolipid Protein; MOG - Myelin/ oligodendrocyte glycoprotein. After: Myelin, 2nd ed. (edited by Morell,P.; 1984; New York Plenum Press)

Madison *et al.*, 1996; Madison *et al.*, 1999). As well as specific molecular transportation mechanisms, the activation of enzymes associated with lipid processing is closely temporally related to myelinogenesis. Myelination hits a peak rate at around 18 days post-parturition in both the rat and mouse, as do the levels of a number of myelin-constituent processing factors (Lachepelle *et al.*, 1994; Sarlieve *et al.*, 1974; Schulte & Stoffel, 1993; Schutgens *et al.*, 1985).

The formation of lipid and protein complexes in myelinogenesis is essential for the correct construction of myelin. Oligodendrocytes are rich in glycolipids, which have been shown to co-cluster with proteins, and form microdomains during transport from the Golgi apparatus. The presence of myelin vesicular protein in oligodendrocytes and in myelin strengthens the theory of lipid-protein microdomain complexes as a method of extending the specialised plasma membrane to form the sheath (Magyar *et al.*, 1997). From electron micrographs (see Figure 1-7), the myelin membrane appears to have layers of protein (dark lines) and lipid hydrocarbon chains (unstained lines) (Morell, Quarles, & Norton,1994).

Each leaflet of the myelin lipid bilayer has a different molecular composition. Glycolipids are positioned on the extra-cellular face of the membrane, with the head groups protruding into the IPL; in contrast, the negatively charged amino-headed groups form the intracellular face. This differentiation is essential for correct myelin compaction. The most abundant proteins in the bilayer are MBP and PLP. It is thought that PLP stabilises the IPL, and, by interaction with acidic lipids in the opposite membrane, facilitates compaction of the major dense line (Stoffel *et al.*, 1997).

1.4.2. Origin and fate of oligodendrocytes

Oligodendrocytes originate from neuroepithelial precursor cells in the developing CNS, mainly from the subventricular zone (SVZ) which is present throughout development and persists into later life in some mammals (Doetsch *et al.*, 1997). Precursor cells of the SVZ are often multipotent, but can also have a restricted lineage (Levison & Goldman, 1993), with the fate and survival of a given cell being influenced by the immediate microenvironment (Jensen & Raff, 1997). Migration, proliferation and differentiation of precursor cells is controlled by growth factors (such as platelet-derived growth factor (PDGF), basic fibroblast growth factor (bFGF or FGF-2), insulin-like growth factor-1 (IGF-1), neurotrophin-3 (NT-3), glial growth factor (GGF), neuregulin), hormones (especially thyroid hormone) and neurotransmitters (Johe *et al.*, 1996). Like neurons, glial cells undergo apoptosis postnatally due to a lack of trophic support, with the death of each cell type being regulated by competition for limiting amounts of specific factors (Barres *et al.*, 1992; Levison & Goldman, 1993). Due to the multipotent effects of many growth factors, it is often difficult to elucidate their exact functions *in vivo* where two or more growth factors may act together to fine-tune a response (McMorris & McKinnon, 1996). The roles played by growth factors are outlined in Figure 1-5.

Hormones, neurotransmitters and Notch

Thyroid hormone has long been a candidate for the control of neural development; hyper- or hypothyroidism during development severely increases the risk of a child being born with mental retardation (Eayers & Taylor, 1951). Thyroid hormone exerts effects in three major areas through the active form of the hormone. Firstly, it can act as a signal for generation of oligodendrocytes, and enhances the

proliferation of committed precursors (Ahlgren *et al.*, 1997). Secondly, thyroid hormone directly promotes differentiation of precursor cells, and thus regulates the numbers generated (Ben Hur *et al.*, 1998). Finally, it can directly stimulate myelin protein gene expression, including PLP and MBP (Tosic *et al.*, 1992).

Oligodendrocytes have been shown to carry receptors to known neurotransmitters, and voltage and ligand-gated ion channels have been identified in oligodendrocyte cell membrane. AMPA (dl-α-amino-3-hydroxy-5-methylisoxazole-4-propanoic acid), kainate, GABA-A (γ-aminobutyrate-A), dopamine and opioid receptors have been identified on oligodendrocytes (Sontheimer *et al.*, 1989).

The Notch pathway is instrumental in priming oligodendrocyte development. Activation of the Notch1 receptor by the ligand Jagged1 prevents differentiation of stem cells, and Jagged1 is down regulated in retinal ganglion cells in a manner that temporally parallels myelination (Givogri *et al.*, 2002). Axons are myelinated in the days following target innervation, leading to the hypothesis that axonal Jagged1 down regulation occurs in response to target innervation, and triggers the onset of myelination (Wang *et al.*, 1998). Therefore, the Notch pathway may play a role in keeping some stem and precursor cell populations elevated in adult tissues, forming a pool of progenitors which can be recruited for tissue repair and remyelination (Artavanistsakonas *et al.*, 1995).

Early oligodendrocyte progenitors will migrate possibly large distances, to form a skeletal outline of the future white matter throughout the developing brain (Lachepelle *et al.*, 1984; Levison & Goldman, 1993). This has to occur prior to maturation, as late progenitors have reduced migratory potential (Reynolds & Wilkin, 1991) and therefore,

the environmental conditions have to be correct to prevent premature maturation (Wang *et al.*, 1998).

Maturation is controlled by a variety of extracellular matrix molecules. For example, tenascin-C is found to be expressed at elevated levels in the junction of the retina and optic nerve, an area through which progenitors do not migrate (ffrenchConstant *et al.*, 1988). Modified (with the addition of polysialic acid or PSA) neural cell adhesion molecule (NCAM) has been identified in explant cultures, and PSA structures have been found to negatively modulate cell adhesion during development. In these cultures, removal of PSA-NCAM results in a complete blockade of oligodendrocyte progenitor migration (Durbec & Cremer, 2001).

1.4.3. Markers of mature myelin

Just as the stages of oligodendrocyte development can be characterised by a range of markers (as illustrated in Figure 1-5), the maturing oligodendrocytes can be followed during myelination. Glycolipids are early cell surface markers which remain present throughout oligodendrocyte maturity (Raff *et al.*, 1979), and include GalC and sulphogalactosylceramides (sulphatides).

The specific myelin proteins discussed previously are translated at various stages of oligodendrocyte maturation. CNP, MBP, PLP/DM20, MOG and MAG are all vital constituents of the compacted myelin sheath, and can be used to quantify the development of myelin (Figure 1-8).

Carbonic anhydrase II is the only one of the seven isoforms of carbonic anhydrase to be expressed in the CNS, and is present exclusively in glial cells. It can be used to differentiate between oligodendrocytes and other glial cell types as oligodendrocytes have a higher abundance of the enzyme (Ghandour *et al.*, 1980).

1.4.4. Functions of myelin

Saltatory conduction of nerve impulses

The noR, where the axon is exposed to the extracellular space, maintain the velocity and integrity of salutatory conduction over distances. Na^+ channels are anchored in place at the node by a network of filamentous molecules just below the surface (Lambert *et al.*, 1997). These include ankyrin and spectrin, which also bind Na^+/K^+-ATPase molecules, as well as various cell adhesion molecules (Black *et al.*, 1990). The flanking paranodal regions, where the terminal loops of myelin can be found, are rich in potassium channels. The tight association of the terminal loops with the axolemma in the paranodal regions have been associated with paranodin (or caspr), a transmembrane glycoprotein unique to neural tissue (Einheber *et al.*, 1997). In the unmyelinated axon, a depolarisation in the axonal membrane causes current production that quickly attenuates, resulting in a loss of signal. After myelination, sodium channels are localised to the naked areas of axolemma – the noR – separated from localised potassium channels in the juxtanode. Insulation of the axon in the sheathed segments improves current flow along the axon. Once at the next noR, the localised sodium channels produce a further membrane depolarisation, leading to repropagation of the signal. It is these three events – formation and maintenance of internodal myelin segments, ion channel clustering and axonal insulation – that comprise the primary role of the myelinating cell.

Role of oligodendrocytes in axonal development and maintenance

Oligodendrocytes play an important role in the development and maintenance of functional axons. Axonal calibre has long been associated with conduction velocity, with myelin thickness being closely controlled to provide an optimal conduction

velocity for a given axonal diameter (Rushton, 1951). The mechanisms for this parallel axoglial development are mostly elusive. It has been shown that oligodendrocytes can regulate full axonal growth and development in the absence of myelin, as demonstrated using three transgenic mouse strains – shiverer, jimpy and quaking (Sanchez *et al.*, 1996). Shiverer and jimpy mice have mutations in the MBP (Roach *et al.*, 1983) and PLP (Philips, 1954) genes respectively, while quaking mice have an unknown mutation (Campagnoni, 1988), and all of them produce a dysmyelinating phenotype. In all three mutant strains, normal axonal development occurs in non-myelinated axons, an effect that is thought to be controlled by an oligodendrocyte derived factor. It has also been demonstrated that radial growth of axons is promoted by oligodendrocytes independent of myelination, by induction of neurofilament bundling. Reduced axonal calibre correlates with reduced neurofilament bundling and phosphorylation in non-myelinated areas.

Specific myelin proteins support axonal integrity. Although PLP knockout mice produce near-normal myelination, axonal integrity is compromised in these animals. Axonal swelling and widespread axonal degeneration occur, with the presence of spheroids – membranous, mitochondria-rich inclusions (Griffiths *et al.*, 1998). The location of spheroids at the distal paranode suggests an impairment of axonal transport. Transgenic mice with an extra autosomal copy of the PLP gene exhibited a phenotype characterised by severe hypomyelination, astrocytosis, seizures and premature death, indicating that genetic control of PLP expression is a critical determinant for oligodendrocyte differentiation and function (Readhead *et al.*, 1994). Individually the two isoforms of PLP (PLP and DM-20) had no effect on the jimpy phenotype, but when introduced together, a substantial increase in the number of myelinated axons was

observed, coupled with an increase in axonal integrity. This indicates vital and distinct roles for PLP and DM20 in axoglial interaction (Nadon *et al.*, 1994).

Inhibition of axonal growth and regeneration by oligodendrocytes

The inhibition of regeneration in damaged or lesioned axons is a major problem following brain or spinal cord trauma or disease (Jackowski, 1995). Studies point to the ability of myelin-derived proteins to block the regrowth of axons. Late developing axons have been shown to be directed by oligodendrocyte associated neurite growth inhibitors (specifically NI-35 and NI-250) in the rat spinal cord (Schwab & Schnell, 1991), providing a guide for the development of new tracts. This positive developmental role becomes detrimental in the event of CNS damage. The potential for regeneration is limited in the CNS, in contrast to the peripheral nervous system (PNS) where NI-35 and NI-250 are expressed at far lower levels (Caroni & Schwab, 1988b). NI-35 and NI-250 are membrane-bound proteins which can be neutralised by the monoclonal antibody IN1 (Caroni & Schwab, 1988a). When applied *in vivo* following unilateral transection of the corticospinal tract in the rat brainstem (Thallmair *et al.*, 1998), IN1 produced sprouting of lesioned and intact fibres both above and below the lesion site, with rats demonstrating full recovery in sensory and motor tests. This study demonstrates that by altering the permissiveness of the glial environment, axonal regeneration can be stimulated, a finding supported by the spontaneous regeneration of lesioned CNS axons grafted into the PNS (Richardson *et al.*, 1980), but not *visa-versa* (David & Aguayo, 1981). The myelin protein MAG mediates a second form of inhibition. This protein is inhibitory as opposed to non-permissive, causing growth cone collapse *in vitro* (Li *et al.*, 1996). It has a soluble extracellular domain, which has been

identified *in vivo* (Moller, 1996), and inhibits axonal regeneration *in vitro* (Tang *et al.*, 1997).

1.5. Innervation and neuronal development

1.5.1. Origins and differentiation

The hundreds of nerve cell phenotypes found in the adult vertebrate are descendants of a single population of embryonic ectodermal cells and the divergence is due to one of two proposed mechanisms: lineage (also known as intrinsic) and inductive (extrinsic) specification (Sulston & Horvitz, 1977). The lineage route involves asymmetric cell division where some cytoplasmic contents are divided unequally between daughter cells at mitosis. In the inductive route, cell division is equal and position-dependent cell-cell interactions define the phenotype. Most neuronal precursor division occurs by the inductive route, where daughter cells are conferred their fate from their position in the ectoderm. It is recognised, however, that invariant patterns of cell division can be due to highly reproducible cell-cell interactions, and that both lineage and inductive specification mechanisms can give rise to uniform lines of cells.

The number of neurons created during development is dependent on a group of cell cycle genes, (Schuurmans & Guillemot, 2002; Tzeng, 2003; Whitford *et al.*, 2002), which regulate the production and segregation of neuroblasts, embryonic neuronal precursors. Interactions between neurons and glial cells control the number of oligodendrocytes produced, and ensure that there are enough myelinating and support cells for the number of neurons generated.

1.5.2. Migration

Early on in development, the neural tube develops by a folding up of the neural ectoderm. Precursors in the neural tube have to migrate potentially large distances in

order to take their place in the embryonic CNS. Mitoses occur on the inner (ventricular) surface of the tube, migrating outwards between other cells to the outer (pial) surface. The ventricular face retains cells of mitotic potential, and becomes defined as the ventricular germinal zone. In laminar brain regions such as the cerebral and cerebellar cortices, post-mitotic cells continue to migrate outwards to the more superficial levels in an "inside-out" manner (Angevine, Jr., 1970). In nuclear regions such as the hypothalamus, the "outside-in" proliferation occurs (Rakic, 1977). Other hotspots of neuronal proliferation exist, including the SVZ, which forms above the ventricular germinal zone. It is thought that post-mitotic neurons from both the ventricular and the sub-ventricular zones are guided by radially orientated glial cells, which extend from the ventricular to the pial surface (Rakic, 1972). The radial unit hypothesis, where discrete ventricular proliferative zones exist and their progeny migrate along a group of radial glial cells, has been shown to be a basis for the columnar organisation of the adult cortex (Rakic, 1988). Regional differences in cell division rate contribute to the increasingly complex folding of the neural tube, eventually creating primitive brain and spinal cord structures.

Some neurogenesis occurs in the mature mammalian CNS, as studied in the olfactory and hippocampal regions of the rodent brain (Altman,1969; Lois & Alvarez-Buylla, 1993).

1.5.3. Initial innervation

Axonal growth from differentiated neurons occurs at the growth cone, an area containing the cellular machinery for manufacture of the extending axon – mitochondria, vesicles, microtubules and microfilaments. Axon guidance is handled by this leading-edge structure of the axon. Small outgrowths, or filopodia, dynamically

branch out and retract according to the underlying substrate and in response to guidance cues (Letourneau, 1981). Filopodia attachment, mediated via actin and myosin, is graded according to substrate – the processes will have a stronger affinity for one substrate than another. A single filopodia can change the direction of axonal growth by adhesion to a preferable substrate – relatively weak preferential differences can be crucial in this decision – then the filopodia are swept backwards and to the side of the growth cone, pulling the axon in that direction (Bray, 1979). Glycolipid-containing vesicles in the growth cone undergo Ca^{2+}-dependent fusion to the membrane in order to increase surface area for filopodia or axonal outgrowth. The tension produced through actin in an attached filopodia appears to initiate tubulin polymerisation and microtubule formation, thus axonal extension, indicating a functional link between actin and tubulin.

The polarity of the neuron is not attributed until late on in development at the point of axon outgrowth. All processes will start to grow at the same rate, with one accelerating and becoming the axon. It then develops unique biochemical and structural properties, as do the dendrites (Goslin & Banker, 1989). These include microtubule orientation – in the axon the 'positive' end (where subunits are added) are at the growing tip, where as the dendrites have microtubules of each orientation (Black & Baas, 1989). This allows transport of ribosomes and Golgi body products into the dendrites, which are not present in the axon.

On arrival in the target tissue, stop signals allow the axon to slow or stop in order to find a target for synaptogenesis. Growth factors may be involved, with a drop in FGF concentration slowing axon advance (McFarlane *et al.*, 1995), and the presence of neurotransmitters such as serotonin and dopamine eliciting a similar response

(Haydon *et al.*, 1984; McCobb *et al.*, 1988). The growth cone changes shape from a consolidated mass with fine filopodia to an arborised, innervating structure.

1.5.4. Neurofilament construction/degradation

Neurofilaments (NFs) are the primary cytoskeletal component of the mature axon, extending along its length and providing structure and mechanical stability. Physiologically, protein subunits form protofilament polymers in a helical, rope-like structure, which in turn polymerise to form 10nm thick filaments. The three polypeptide subunits of NF, named NF-L, NF-M and NF-H after their low, medium and high molecular weights respectively, differentially construct these polymerised protofilaments. Carboxyl-tail cross-links between filaments contribute to regular spacing of filaments and ensure a high tensile strength in this unusually long structure. NFs are known to be anchored in the plasma membrane and the nuclear envelope, and also associate with cytoskeletal microtubules and actin filaments (Hoffman *et al.*, 1987; Leterrier *et al.*, 1996). NFs are frequently modified by changes in their phosphorylation state, and are assembled and disassembled on this basis. Mammalian NF-H and NF-M have distinctive lys-ser-pro (KSP) motif repeats, with between 8 and 53 repeats in mouse and human NF-H, clustered in the crosslink-forming tail domains of the protein. Each of these can be phosphorylated twice, making this one of the most highly phosphorylated proteins in the CNS. NFs can also be less extensively phosphorylated in the amino-terminal head domain (Shetty *et al.*, 1993). NF deconstruction or degradation may result in aggregation of the protein, an event which has long been regarded as a marker of disease processes, and is increasingly thought to be directly responsible for CNS disease. In either case, the destruction of a vital member of the axonal cytoskeletal

repertoire is a potential trigger for cell death, possibly by activation of the apoptotic pathway.

Neurofilament protein synthesis and transport

In a developmental situation, the neuronal cytoskeleton needs to accommodate behavioural and morphological transitions, from the early migratory target-seeking stage to the stable functioning neuron. Neuronal precursors express a range of intermediate filaments in addition to NFs, including nestin, vimentin, alpha-internexin, and peripherin, the presence and phosphorylation states of which have been characterised by a group of monoclonal antibodies. Small regional and temporal variations occur, but there is a general pattern of intermediate filament expression. The swap from non-neurofilamentous intermediate filament to NF expression indicates a transition between the proliferative and differentiating stages of neuronal development with the prior group acting as a dynamic scaffold for NF assembly *in vivo* (Grant & Pant, 2000).

NF proteins are transported at 0.1-3mm per day, but unlike with other organelles, movement is interrupted by prolonged pauses with an estimated 90% of NF in transport being stationary at any one time (Roy *et al.*, 2000; Wang *et al.*, 2000). These studies also found that transport of NF can be in either an anterograde or retrograde direction. Transport mechanisms are likely to involve association with members of the kinesin and dynein families, but the exact transport proteins are unknown (Shah *et al.*, 2000). NF is thought to be transported in either small oligomers or as more complete filaments. Clearly, though, entire filaments need to be dissociated from the matrix prior to transport (Yabe *et al.*, 1999).

Phosphorylation of NF plays a regulatory role in construction, and also may be involved in controlling association with motor proteins. Side-arm domains can be highly phosphorylated, and a correlation between the degree of phosphorylation and the speed of transport exists. In addition a high degree of phosphorylation on the side-arms leads to bundling of NF and thus decreased motility (Archer *et al.*, 1994).

Neurofilament construction and phosphorylation

Following transport, NF subunits become highly phosphorylated, and therefore heavily cross-linked via the side-arm domains. Light and medium chain subunits are expressed first in development, with the heavy chain being expressed shortly after that in a mixture of partially phosphorylated and non-phosphorylated forms (Ackerley *et al.*, 2003). Phosphorylation occurs after transport in a gradient fashion along the axon in a proximal-to-distal direction, and continues into early postnatal life, correlating with synaptogenesis and myelination as a mature cytoskeleton is assembled (Szaro *et al.*, 1989; Willard & Simon, 1983). Indeed, myelination seems to provide a signal for further NF phosphorylation, with MAG being one putative signalling molecule (Yin *et al.*, 1998).

Assembly of the heteropolymeric filament relies on the correct phosphorylation of NF-L and –M head domains, where phosphorylation of certain single serine residues can completely inhibit assembly of subunits, or may induce disassembly of constructed filaments (Sakaguchi *et al.*, 1993).

It is thought that a highly sensitive stoichiometric balance regulates the calibre of a given axon (Sakaguchi *et al.*, 1993). Phosphorylation of the NF subunits contributes to the inter-filament spacing, but interactions with other components such as

microtubules and actin filaments are essential for the construction of a dynamic cytoskeletal lattice (McQuarrie *et al.*, 1986).

Phosphorylation effector molecules in this system fall into three categories – proline and non-proline directed NF-associated kinases, and phosphatases. The serine-55 residue of NF-L is the key, with phosphorylation of this site blocking assembly. This site is dephosphorylated on entering the axon by the non-proline directed kinase CK1, to allow NF construction (Nakamura *et al.*, 2000). Proline-directed kinases, especially of the cyclin-kinase and MAP-kinase families, are responsible for control of KSP-repeat phosphorylation, which occurs during and after construction. The repeat residues are usually stably phosphorylated during myelination and radial axonal growth as the mature cytoskeleton is established. This stability may, in part, be due to rendering NFs resistant to proteolytic digestion (Veeranna *et al.*, 1998). Phosphatases are involved in the more labile stages of axon outgrowth, with dephosphorylated NF more likely to disassemble and dissociate from other cytoskeletal components. This not only has implications in development, but also in plasticity, and potentially in learning and long-term potentiation mechanisms (Hashimoto *et al.*, 2000).

1.5.5. Synaptogenesis

Properties of the pre-synaptic cell, post-synaptic cell and surrounding membrane need to change in order for synaptogenesis to take place. Structural specialisation at the pre-synapse and input from oligodendrocytes is also required. Synaptogenesis is regarded as a multi-step process at sites of axonal contact with dendrites, neuronal soma or other axons. Initial contact is followed by the establishment of stable sites of cell-cell contact, and subsequently by pre- and post-synaptic specialisation (Figure 1-9). Presynaptic differentiation involves the assembly of complex and elaborate

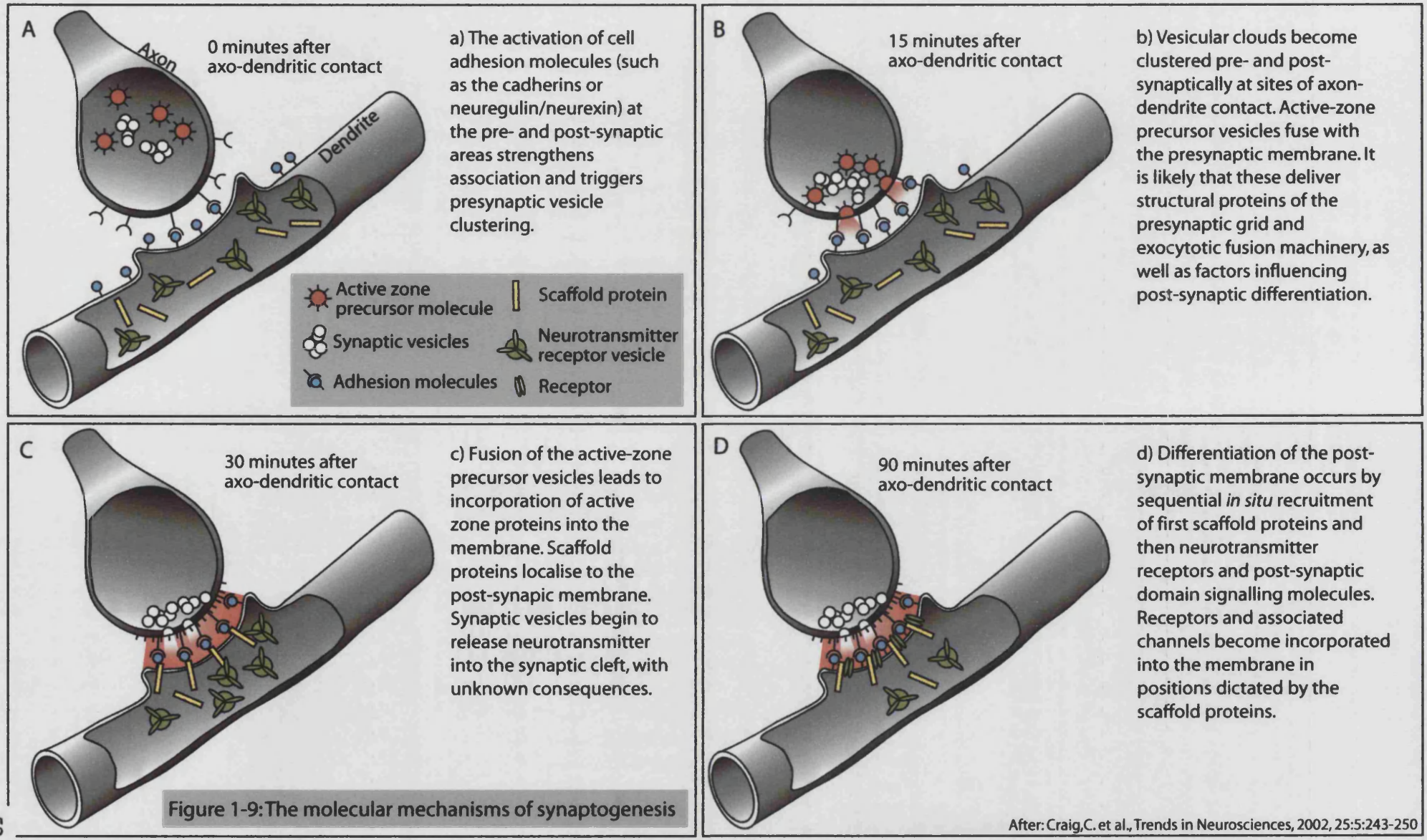

Figure 1-9: The molecular mechanisms of synaptogenesis

After: Craig,C. et al., Trends in Neurosciences, 2002, 25:5:243-250

macromolecular protein complexes which are rapidly assembled sequentially from cytosolic pools (Yamada & Miyamoto, 1995). As the neuron is a large and complex cell, unique molecular trafficking and sorting problems arise. Two subsets of synaptic vesicle proteins are transported from the Golgi apparatus in one of two "precursor" synaptic vesicle types. Maturation of the presynaptic apparatus occurs following recycling of synaptic vesicles with the plasma membrane. The vesicles are then filled with neurotransmitter and unregulated fusion and neurotransmitter release begins to occur, the role of which in synapse formation is unclear (Hannah *et al.*, 1999). Some vesicle contents remain in the membrane, while some are released into the synaptic cleft, presumably to initiate or influence postsynaptic membrane specialisation. It is thought that channels, receptors and transporters are dynamically cycled between the synaptic membrane and the plasma membrane in vesicles (Roos & Kelly, 2000).

The post-synaptic membrane holds large, diverse molecular complexes constructed in-situ from individual elements, or using distinct classes of vesicular intermediates carrying limited repertoires of molecules. Receptors can be individually recruited to the membrane via signalling or activity dependent pathways (Sheng, 2001). It has been postulated that scaffold proteins cluster and stabilise receptors. Loss of one of these molecules does not perturb the lattice they form, suggesting that there is a degree of functional redundancy in the system (McGee *et al.*, 2001). Glial cells, particularly oligodendrocytes, play a vital role in neuronal maturation, as outlined in section 1.4.4.

1.5.6. Elimination of excess connections

Shortly after connections are made, the nerve cell population undergoes a period of cell death, eliminating half of the neurons in some sites, less in others (Hamburger &

Oppenheim, 1982). This seemingly wasteful event has developed during evolution to generate accurate neuron numbers and to perfect axon guidance (Clarke, 1981), and is highly flexible allowing for rapid evolutionary changes in brain anatomy and function. Cell death occurs at this stage to eliminate neurons whose axons have failed to reach their target (Hamburger & Levi-Montalcini, 1949), to scale down neuronal numbers to match the number of targets (Cowan,1973) and to eliminate connection errors (Rakic *et al.*, 1986). The lack of electrical activity and competition for trophic factors are likely to determine the pattern of cell death.

1.5.7. The caspase pathway in neuronal cell death

The caspases are a growing family containing around 10 cysteine-dependent aspartate-specific proteases involved in the execution of the apoptotic cell death pathway (Philchenkov, 2003). This pathway plays an important role in the physiological development and homeostasis of brain cell numbers, but is also implicated in many CNS disease states (Bilsland & Harper, 2002). The caspases have been highly conserved throughout evolution, with mammalian caspase 1 (ICE) having been identified via the *Caenorhabditis elegans* homologue, ced-3 (Schwartz & Osborne, 1994). The family contains a conserved active site composed of the pentapeptide QACXG, where X is variably R, Q or G in different isoforms. Caspases are synthesised as inactive proenzymes (zymogens) with an N-terminal peptide (prodomain), and usually one small subunit and one large subunit. In caspase 1 and 3, and possibly in other isoforms, the active enzyme is a hetero tetramer composed of two small and two large subunits. The caspase prodomains vary in length, with caspases 3, 6 and 7 having short prodomains compared to the other family members (Chang & Yang, 2000). The function of the prodomain in caspase 8 (and possibly caspase 10) is to directly link to

the death receptors CD95 and TNF receptor 1 in the plasma membrane, and trigger the caspase activation cascade (Chinnaiyan *et al.*, 1996). In the other caspases, the function of the prodomain is unclear. Caspases are cleaved at specific aspartate residues, leading to theories of sequential activation by other caspases in a hierarchical manner (Boatright & Salvesen, 2003). An initiator caspase (caspase 8) could activate an amplifier caspase (caspase 1), which in turn could activate machinery caspases (caspases 3 and 7) to cleave substrates. This model requires a factor or event to activate the caspases at the apex of the hierarchy, such as CD95 and TNF receptor 1 (Hengartner, 2000).

Caspase activation and induction of apoptosis

Activation of the caspases is effectively the trigger for the start of the apoptotic process (Figure 1-10). Caspases appear to be cleaved via three main mechanisms – by an upstream caspase, by induced proximity activation or by association with a regulatory subunit. In the first, activation by a previously activated caspase would involve proteolytic cleavage of the zymogen between the prodomains (Fraser & Evan, 1996). These are separated by aspartate residues, suggesting that caspases could be activated by "auto-cleavage" events. It is thought that this activation method is used extensively to activate caspases 1, 6 and 7, which act as signal amplifiers contained within a positive feedback loop (Budihardjo *et al.*, 1999). This method, however, cannot explain how the first caspase is activated. The second activation theory, which concerns apex caspase activation, is termed induced proximity activation (Muzio *et al.*, 1998). Upon ligand binding, cell death receptors including CD95 and TNF receptor aggregate to form membrane-bound complexes. Via adapter molecules, these then recruit and bind a number of caspase 8 molecules, bringing them closer together (Chang *et al.*, 2003b). The concentration of zymogen molecules into a small space means that their combined

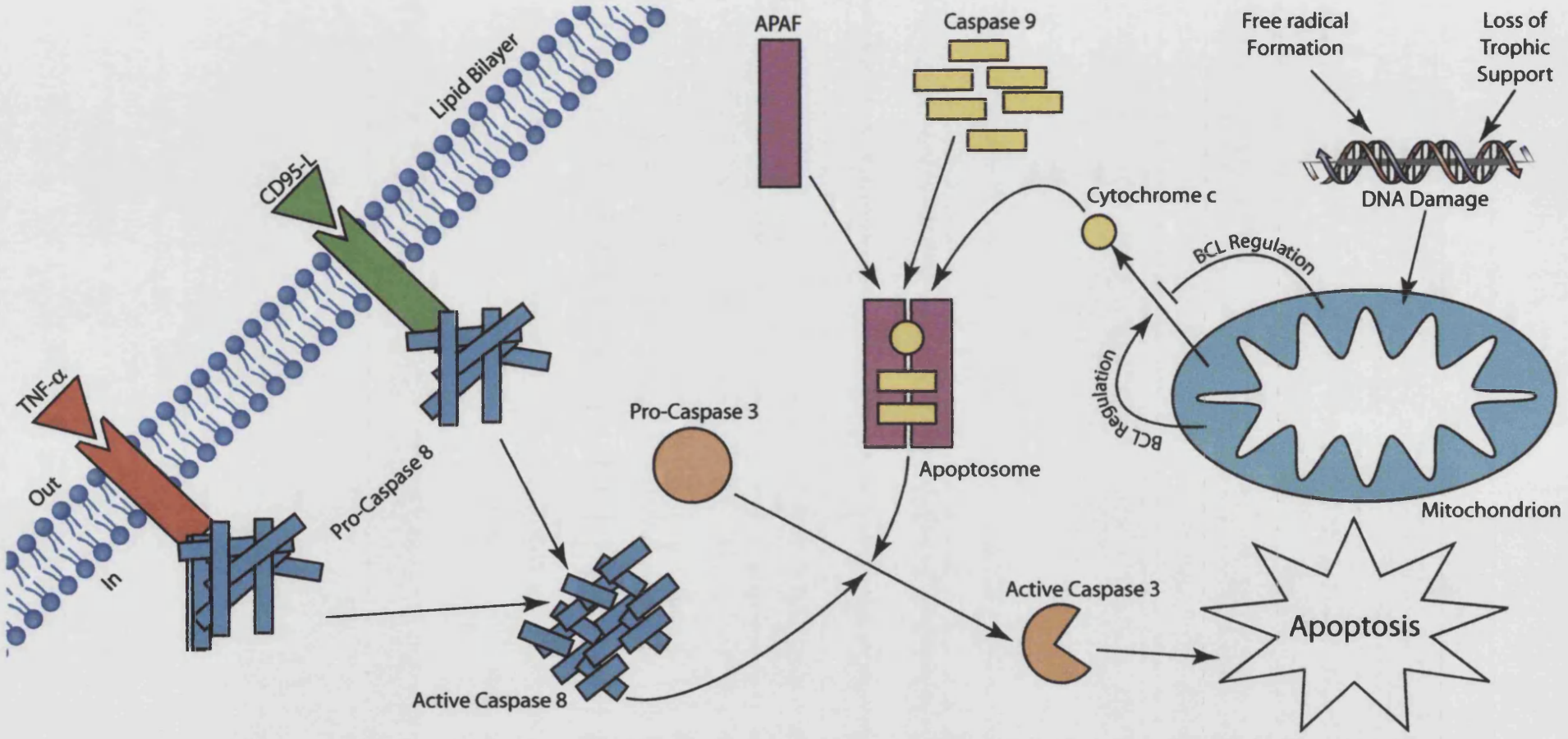

Figure 1-10: The caspase activation cascade: Caspase activation can be initiated via two main pathways: 1 - TNF-α and CD95 ligand can activate cell surface receptors, triggering activation of upstream caspases; 2 - DNA damage can trigger release of cytochrome c from mitochondria, leading to caspase 9 mediated apoptosome formation, and processing of downstream caspases. Caspase 3 is thought to be a major effector molecule in the pathway, cleaving vital cellular proteins.

low intrinsic protease activity is sufficient to begin cleavage of the inactive caspase 8 molecules, triggering the activation cascade. It is likely that other levels of control exist *in vivo* to regulate this activation pathway (Chang *et al.*, 2003a). The third activation process is associated with caspase 9. Cleavage of pro-caspase 9 only produces a small increase in proteolytic activity and full activation only occurs via association with a regulatory subunit, Apaf-1, with the complex of these two molecules and possibly others constituting the true active form of caspase 9. The resulting complex enzyme, known as the apoptosome, exerts the effects of active caspase 9 (Li *et al.*, 1997). Formation of the apoptosome relies on mitochondrial damage, as outlined below.

The regulation of apoptosis by Bcl-2 family

One important group of molecules involved in the caspase pathway are the B Cell Lymphoma (Bcl)-2 family of proteins (Burlacu, 2003). They have been divided into three structurally or functionally distinct groups, with group 1 being anti-apoptotic, and groups 2 and 3 displaying pro-apoptotic actions. These proteins can form active homodimers and inactive heterodimers with one another, where competitive binding regulates their activity. A higher concentration of group 1 proteins will bind pro-apoptotic group 2 and 3 proteins, neutralise them and exert an anti-apoptotic effect within the cell (Reed, 1997). The pro-apoptotic role of Bcl-2 group 2 and 3 proteins is focussed in the mitochondria. Housed inside the mitochondrion outer membrane is a cocktail of pro-apoptotic molecules, including cytochrome c. The release of cytochrome c enables it to join the apoptosome formed by caspase 9 furthering activation and increasing apoptosomal proteolytic activity (Li *et al.*, 1997). There are several putative methods for Bcl-2 induced cytochrome c release from mitochondria. One pro-apoptotic member Bcl-X_L has sequence homology with the pore-forming unit of diptheria toxin.

Bcl-2 could induce conformational changes in the outer membrane by forming pores (Muchmore *et al.*, 1996). Secondly, it is known that several Bcl-2 proteins can bind to and regulate the activity of the voltage-dependent anion channel, a subunit of the mitochondrial permeability transition pore, which when opened, results in rapid loss of membrane potential and in mitochondrial swelling. Although this channel is too small to allow large molecules like cytochrome c to pass, significant Bcl-2 induced conformational change could reconfigure the channel proteins to form a larger pore (Shimizu *et al.*, 1999). Finally, Bcl-2 family members could induce rupture of the outer mitochondrial membrane, bypassing the need for a large-pore channel by allowing diffusion of molecules through tears in the bilayer. This would occur through control of mitochondrial homeostasis by Bcl-2 members, either directly or through intermediate proteins.

The protein substrates of caspases

To date, caspases have been found to cleave hundreds of potential substrates, a handful of which have vital structural or housekeeping roles within the cell, and are considered key substrates of caspases in apoptosis. Upon proteolysis, destruction of these substrates leads to a widespread shutdown of cellular functions, with chromatin condensation, changes in membrane permeability leading to cell shrinkage, and eventual phagocytosis (Earnshaw *et al.*, 1999).

1.6. Remyelination

1.6.1. Physiological remyelination

The CNS has an innate capacity to remyelinate following a demyelinative episode, but in these so-called "shadow plaques", myelin takes the form of thin sheaths

with a reduced intranodal length compared to development (Blakemore, 1974). One school of thought is that a recapitulation of events seen in development occurs, as developmental genes, such as MBP exon 2, become expressed in correlation with remyelination in MS (Capello *et al.*, 1997). The process is not identical to developmental myelination however, as thyroid hormone does not play a critical role (Franklin & Gilson, 1996) and other growth factors are also differentially expressed (Copelman *et al.*, 2000). Another view is that the migratory and proliferative functions of OPCs are preserved in the remyelinating lesion, but that the microenvironment of the lesion is weighted against differentiation and remyelination. Studies indicate that recruitment of precursors occurs effectively (Carroll & Jennings, 1994; Franklin *et al.*, 1997), but that the recruited cells do not differentiate, possibly due to inhibitory cytokines, chemokines and PSA-NCAM or Notch pathway protein expression (Franklin, 2002). Remyelinative potential decreases with age, an effect attributed to delayed growth factor expression and reduced capacity for OPC recruitment (Hinks & Franklin, 2000) and differentiation (Sim *et al.*, 2002).

Where it has been found to be effective, the consensus view of remyelination is based on this model of progenitor proliferation within, or migration to, the lesion site and differentiation into myelinating cells. Evidence has been presented for differentiated oligodendrocyte-derived remyelination, with MOG-positive cells found to produce new myelin sheaths in demyelinated MS plaques (Wolswijk, 2000). However, in experimental demyelination (Keirstead & Blakemore, 1997) and transplant studies (Crang *et al.*, 1998), this has not been observed leading to the conclusion that remyelination may also be carried out by adult progenitor cells (Scolding *et al.*, 1995).

The signals thought to be required for remyelination are thus far limited to growth factors, the expression sequences of which have been elucidated from rodent models, which may differ from the human scenario (Copelman *et al.*, 2001; Hinks & Franklin, 1999). Also, the potential reduction in remyelinative capacity with the age of animal has often not been duly taken into account (Hinks & Franklin, 2000). Perhaps more importantly, the pathology of an inflammatory disease is multifaceted and heterogeneous, involving a large number of growth factors, chemokines and cytokines (Baranzini *et al.*, 2000). Links between remyelination and inflammation have been postulated, with TNF-α (Arnett *et al.*, 2001) and IL-1β (Mason *et al.*, 2001), enhanced migration of OPCs (Tourbah *et al.*, 1997), and expression of brain-derived neurotrophic factor (Kerschensteiner *et al.*, 1999) and ciliary neurotrophic factor (Linker *et al.*, 2002) all thought to be beneficial in remyelination. In addition, the depletion of macrophages has been found to impair the remyelinative process (Kotter *et al.*, 2001).

1.6.2. Problems with remyelination in multiple sclerosis

Speculations as to the reason for a breakdown in the remyelinative repertoire of the CNS have been further confused by the identification of MS as a heterogeneous disease with distinct patterns of demyelination, as discussed in section 1.1 (Lucchinetti *et al.*, 2000). However, failures in several key areas combine to bring about remyelinative deficit.

In relapsing-remitting disease, an initial demyelinative attack may deplete OPC numbers in the lesion vicinity available for repair, followed by subsequent demyelinative episodes (Keirstead *et al.*, 1998). In addition, endogenous OPC migration is slow and covers only short distances, limiting repair capacity in large lesions (Blakemore *et al.*, 2000). This, however, is not thought to be the major rate-limiting step

in remyelination, as OPCs are usually found in sufficient numbers in lesions. Axons are not receptive to remyelination following an episode in MS, due to the re-emergence of expression of PSA-NCAM (Chang *et al.*, 2002). This molecule is expressed in development as an anti-myelinative factor, preventing interaction of the late OPC and the axon.

The astrogliosis accompanying the emergence of plaques in MS may be a stimulatory factor to OPCs, encouraging their proliferation and differentiation through the range of astrocyte-derived growth factors (Ridet *et al.*, 1997). A failure of astrocytes to generate the correct signals in the MS plaque may lead to impairment of OPC recruitment. Astrocyte-derived neuregulin, a growth factor responsible for OPC differentiation, is found to be reduced in MS plaques (Viehover *et al.*, 2001). Also, abnormal expression of jagged1 by astrocytes in active lesions may be a negative regulatory factor for OPC differentiation, acting via the Notch receptor, an effect not observed in remyelinated lesions (John *et al.*, 2002).

1.6.3. Experimental models of remyelination

Toxic demyelination

In this type of widely used model, a toxin such as lysolecithin or ethidium bromide is injected into the white matter of an experimental animal, causing myelin loss (Woodruff & Franklin, 1999b). The area and extent of demyelination is highly reproducible in these models. There is, however, some traumatic insult to the lesion area cause by the injection itself, and therefore localised blood brain barrier breach and inflammatory cell recruitment, independent of demyelination (Woodruff & Franklin, 1999a). Cuprizone, a diet-administered copper chelator elicits complete and consistent demyelination in the corpus callosum and the superior cerebellar peduncle (Matsushima

& Morell, 2001). In preparation for transplant studies, demyelination by ethidium bromide injection can be combined with irradiation techniques to kill proliferating cells and prevent endogenous remyelination (Blakemore & Patterson, 1978). Irradiation damages astrocytes, however, so the astrocytic reaction to demyelination is altered. None of these models take into account the inflammatory aspects of demyelinative disease, as are seen in MS (Stangel & Hartung, 2002b).

Inflammatory demyelination

As previously discussed, EAE is a widely used and highly representative model of CNS inflammatory disease (Gold *et al.*, 2000). Induced by the injection of myelin or CNS antigens, the disease can show signs similar to MS, with a relapsing-remitting disease course and accumulating movement deficit. As it mimics many of the pathological features of inflammatory CNS diseases, EAE is considered an accurate model of demyelinative disease. Inflammatory disease can also be induced by injection of GalC antibodies plus complement (Woodruff & Franklin, 1999a), or by the implantation of a GalC-secreting hybridoma (Rosenbluth *et al.*, 1999). These models specifically damage oligodendrocytes, but again injection leaves a small traumatic lesion along the injection canal. Administration of an antibody against MOG has been found to augment demyelination in an acute EAE model of MS (Stefferl *et al.*, 2000). Large confluent demyelinated plaques are produced (Linington *et al.*, 1988), allowing the study of demyelination and potential repair mechanisms in the immunocompromised experimental environment of the EAE model (Iglesias *et al.*, 2001).

Viral demyelination

Several virus-mediated models of demyelination exist. The Theiler's murine encephalomyelitis virus (TMEV) persists within oligodendrocytes following injection, and gives rise to CNS inflammation and demyelination (Rodriguez *et al.*, 1983). Neurotrophic mouse hepatitis virus (MHV) and Semliki Forest virus (SFV) are also used in experimental investigations of remyelination (Mokhtarian *et al.*, 1999; Soilu-Hanninen *et al.*, 1994). The latter is thought to induce demyelination via molecular mimicry with MBP, where sufficient sequence homology or similarity between the viral and self peptides are able to induce autoimmune responses that lead to disease (Oldstone, 1987).

1.6.4. Promotion of endogenous remyelination

Growth Factors

Enhancing the inadequate endogenous remyelination system is an attractive therapeutic target in MS. Growth factors play a large role in remyelination, and their administration initially seems like a straightforward strategy. NGF has been found to be protective against demyelination in EAE (Villoslada *et al.*, 2000), and neuregulin can reduce damage to oligodendrocytes in EAE (Cannella *et al.*, 1998). FGF-2 gene therapy ameliorates the course of EAE (Ruffini *et al.*, 2001), and injection of PDGF speeds up recovery following toxin-mediated demyelination (Allamargot *et al.*, 2001). However, growth factors have pleiotropic effects. IGF-1 enhanced remyelination in the acute phase of EAE but this was transient, and was not observed when IGF-1 was injected in the chronic phase (Cannella *et al.*, 2000). In addition, IGF-1 did not promote remyelination following toxic insult (O'Leary *et al.*, 2002). A number of growth factors are expressed sequentially in remyelination, and often one growth factor will modulate

the activity or response of another (Copelman *et al.*, 2000). Therefore, administration of a single factor is probably not going to be sufficient for the long-term stability of remyelination; a complimentary group of factors may be required. It is worth bearing in mind that, even if growth factor repertoires sufficient for remyelination in rodents are elucidated, responses in human patients are likely to differ (Scolding *et al.*, 1995).

Intravenous immunoglobulins

Antibodies against spinal cord homogenate and specifically against MBP, have been made which have been found to promote remyelination in TMEV (Asakura & Rodriguez, 1998). All of these antibodies have an IgM isotype and the capacity to bind oligodendrocytes, but do not share epitope specificity. These antibodies also accelerate the rate of remyelination in chemically induced demyelination (Pavelko *et al.*, 1998) and in EAE (Miller *et al.*, 1997). The exact mechanism of action of these immunoglobulins is not yet known, but it is likely that they elicit an indirect, immunomodulatory effect, producing a permissive environment for remyelination, as opposed to acting via direct oligodendrocyte stimulation (Stangel & Hartung, 2002a).

Cell transplantation

Transplanting oligodendrocytes, precursors, Schwann cells, olfactory ensheathing cells and stem cells into the CNS to promote remyelination has varied in success (Blakemore, 1977; Franklin, 2003; Keirstead *et al.*, 1999; Lakatos *et al.*, 2003; Targett *et al.*, 1996). The attempts which showed the most promising results often used tissue from ethically sensitive sources. In addition, it is likely that the hostile lesion environment which prevents remyelination by endogenous precursors will not permit proliferation or differentiation of transplanted cells. Finally, lesions are disseminated

throughout the CNS, and therefore it is likely that multi-site transplantation would be necessary.

1.7. Cannabinoid signalling and neuroprotection

1.7.1. Cannabinoids in the physiological brain

Receptors

The isolation and purification of Δ^9-tetrahydrocannabinol (Δ^9-THC), the major psychoactive component of cannabis, was carried out and the structure elucidated in the 1960s (Mechoulam & Gaoni, 1965). Synthetic analogues mimicking the effects of Δ^9-THC were produced (Dewey, 1986), exposing the high stereoscopic specificity of the ligands (Mechoulam *et al.*, 1980), and were used subsequently to identify the brain cannabinoid receptor, CB_1R (Devane *et al.*, 1988). The receptor was then cloned (Matsuda *et al.*, 1990), and the anatomical distribution (Herkenham *et al.*, 1990) and neuropharmacology (Howlett, 1995) elucidated.

The cannabinoid receptor 2 (CB_2R) was cloned from a human cell line some time after CB_1 (Munro *et al.*, 1993), and shares only partial homology. It is predominantly expressed in the periphery (Matsuda, 1997), especially on cells of the immune system, but has been reported in some CNS cell types (Facci *et al.*, 1995; Skaper *et al.*, 1996; Walter *et al.*, 2003).

There is evidence from several pharmacological studies for a putative novel non-CB_1 non-CB_2 CNS cannabinoid receptor, but one has not yet been identified or sequenced (Breivogel *et al.*, 2001; Calignano *et al.*, 1998; Calignano *et al.*, 2001; Di, V *et al.*, 2000).

Caligano et al (1998, 2001) found that the endogenous fatty acid amide palmitoylethanol induces antinociceptive effects that can be attenuated by antagonists

acting at CB_2R but not CB_1R. The molecule has been shown not to have affinity for either CB_1R or CB_2R (Lambert *et al.*, 1999; Sheskin *et al.*, 1997), leading to the proposition of a novel "CB_2-like" receptor.

Di Marzo et al. (2000) and Breivogel et al. (2001) have demonstrated G-protein mediated second messenger pathway activity following administration of anandamide and WIN55-212-2 in tissue from the CB_1R-KO mouse. These effects were not produced by other CB_1R or CB_2R agonists. Furthermore, it has been reported that the receptor stimulated by WIN55-212-2 may not signal via adenylate cyclase, unlike that occurring with CB_1R and CB_2R (Monory *et al.*, 2002).

Agonists and activating agents

Following identification of Δ^9-THC, synthetic agents were produced with generally high binding affinity for the cannabinoid receptors, and have been recently officially classified into four groups – classical and non-classical cannabinoids, aminoalkylindoles and eicosanoids. Classical cannabinoids have a tri-cyclic structure and a benzopyran moiety, examples of which include the natural extracts of cannabis (Howlett, 2002). Non-classical cannabinoids include bi- and tri-cyclic analogues of classical cannabinoids, lacking the pyran ring structure (Howlett, 2002). Examples include CP55-940, which was instrumental in the discovery of CB_1R (Devane *et al.*, 1988). Aminoalkylindoles are a group of molecules not structurally derived from THC (Pacheco *et al.*, 1991), and include WIN55-212-2, a highly studied molecule shown to produce many of the effects of THC (Compton *et al.*, 1992). Finally, eicosanoids include the endogenous cannabinoid agonists anandamide and 2-arachidonoyl glycerol (2-AG). Anandamide (arachidonoyl ethanoamide) is produced at synapses, and in macrophages and other leukocytes (Felder *et al.*, 1996). 2-AG has a binding affinity

similar to anandamide and was first isolated from the canine gut (Mechoulam *et al.*, 1995). Fatty acid amide hydrolase is thought to be the principle enzyme responsible for the breakdown of anandamide and 2-AG, and as such plays a key role in the endocannabinoid signalling pathway (Di, V *et al.*, 1999). Other putative endocannabinoid compounds have been reported.

Endocannabinoid signalling

Depolarisation-induced suppression of inhibition (DSI) describes the phenomenon of transient suppression of inhibitory GABAergic cellular events by brief depolarisation of the cell. It was first described by Marty in cerebellar Purkinje cells (Glitsch *et al.*, 1996), and by Alger in hippocampal pyramidal neurons (Alger *et al.*, 1996). DSI demonstrates that a post-synaptic signalling event can alter pre-synaptic neurotransmitter release, requiring a retrograde synaptic messenger. In the hippocampus, DSI only applies to GABAergic inhibitory neurons. In the cerebellum on the other hand, glutamatergic neurons can also be affected, resulting in depolarisation-induced suppression of excitation (DSE) (Wilson & Nicoll, 2001).

Studies carried out to investigate the role of CB_1R at the synapse found that CB_1R agonists blocked DSI and DSE, and that antagonists reverse this effect. DSI is missing in the hippocampus of CB_1R KO mice (Yoshida *et al.*, 2002). Both hippocampal and cerebellar neurons produce enzymes required for endocannabinoid synthesis and degradation, and the retrograde suppression of synapses and formation of endocannabinoids are calcium dependent. CB_1R is located in the pre-synaptic membrane of hippocampal pyramidal synapses, and on both inhibitory and excitatory inputs to cerebellar neurons (Ohno-Shosaku *et al.*, 2002). It has also been found that CB_1R activation can downregulate cyclic adenosine monophosphate production by

interaction with adenylate cyclase, indicating control via this second messenger pathway.

The mechanism of signalling can be divided into post- and pre-synaptic events (Figure 1-11). In the post-synaptic cell, neurotransmitter-receptor interactions cause depolarisation, thus opening calcium channels, allowing influx, at the same time as a separate glutamate pathway induces cannabinoid synthesis via metabotropic glutamate receptor 1. The cleavage of N-arachidonoylphosphatidylethanolamine (NAPE) by phospholipase D (PLD) liberates the active cannabinoid, anandamide, which crosses the synapse in a retrograde fashion and activates CB_1R on the pre-synaptic membrane. This G-protein coupled receptor then inhibits Ca^{2+} influx into the pre-synaptic cell via direct interaction between the $G\beta\gamma$ subunit and the calcium channel, with no second messenger involvement. The drop in calcium influx leads to a reduced probability of vesicle fusion, and therefore a reduction in neurotransmitter release (Maejima *et al.*, 2001).

1.7.2. Cannabinoids in EAE and MS

Anecdotal evidence for the use of cannabinoids as a treatment for the symptoms of multiple sclerosis is long-standing, but has more recently been backed up by pre-clinical and clinical data. A large proportion of that evidence has come from rodent EAE models of inflammatory disease, suggesting that cannabinoid compounds may have efficacy for symptom relief. Studies using purified Δ^9-THC (Lyman *et al.*, 1989) and subsequently the more stable Δ^8-THC (Wirguin *et al.*, 1994) demonstrated an improvement in the signs of treated rats and guinea pigs. Recent, more detailed studies have shown that cannabinoids may control spasticity and tremor, and potentially act as neuroprotective agents (discussed in Section 1.7.3). The non-psychotropic cannabinoid dexanabinol (HU211, an NMDA-receptor antagonist) inhibited the acute course of EAE

in the Lewis rat, significantly reducing clinical score (Achiron *et al.*, 2000). This seemed to be due to a reduction in CNS infiltrates as assessed by histology; however, having little efficacy at the cannabinoid receptors, these effects are clearly not via the CB1R. Cannabinoid receptor activation using the synthetic agonist WIN 55,212-2, the active constituent of cannabis, Δ^9-tetrahydrocannabinol, the anandamide analogue methanandamide and the CB2-selective agonist JWH-133all produced a significant reduction of tremor and spasticity in the ABH mouse chronic relapsing EAE model (Baker *et al.* 2000). CB1 and CB2 antagonists exacerbated the signs, suggesting involvement of the endocannabinoid system in symptom control. Further investigation into enhancement of the endocannabinoid pathways in EAE showed that anandamide reuptake and hydrolysis inhibitors ameliorate spasticity, an effect reversed by cannabinoid receptor 1 and 2 antagonists (indicating cross reactivity of antagonists between CB1 and 2). Blocking G protein-coupled phosphodiesterase activity downstream of the CB1 and 2 receptors exacerbated spasticity and tremor. The same study also identified that endocannabinoid levels are increased in spastic CREAE mice but not in non-spastic immunised animals, suggesting that endocannabinoids increase in an attempt to compensate for the spastic deficit. This finding was followed up and confirmed by the same group (Baker *et al.*, 2001). Cannabinoid receptor levels have been found to be elevated in striatal and cortical neurons in the Lewis rat EAE model, postulated to be a compensatory mechanism for motor dysfunction (Berrendero *et al.*, 2001).

Numerous clinical trials of cannabinoid compounds have been carried out in recent years, investigating the potential for symptom control in humans. Δ^9-THC was first assessed in single patient or small scale trials in the 1980s and 1990s (Clifford,

1983; Martyn *et al.*, 1995; Meinck *et al.*, 1989; Petro & Ellenberger, Jr., 1981; Ungerleider *et al.*, 1987), with varied patient responses. Larger scale trials have tested a range of compounds administered via several routes. Oral administration of Δ^9-THC and *cannabis sativa* plant extract on patients (n=16) who presented with severe spasticity found no beneficial effects (Killestein *et al.*, 2002). Both substances were deemed safe for further trial, but neither reduced spasticity, and both worsened the patient's global impression. A second study using orally administered cannabis extract found an improvement in spasm frequency (n=57; $p<0.05$), and a tendency towards an increase in mobility (Vaney *et al.*, 2004). Spasticity as assessed by the Ashworth scale, tremor, sleep disturbance and bladder control were not improved. One of the largest studies to date has been the CAMS study, investigating the use of orally administered cannabis extract and Δ^9-THC on 667 established MS patients with muscle spasticity (Zajicek *et al.*, 2003). This study found no improvement in spasticity (again assessed by the Ashworth scale), but some improvement in secondary outcome measures were observed, including improved mobility and a more positive perception of symptoms.

The sublingual spray may provide an alternative route of administration, potentially allowing higher cannabinoid bioavailability, avoiding the high 1st pass metabolism and long-term body-fat storage of ingested cannabinoids. Wade et al (Wade *et al.*, 2003) found that Δ^9-THC, cannabidiol or a combination of the two could bring about improvements in relief of pain and muscle spasms, and an improvement in bladder control and spasticity in a small cohort (n=20). An unpublished phase III clinical trial with larger groups of patients also using the sublingual route of administration found improvements in neuropathic pain ($p<0.05$; n=66), sleep

disturbance ($p<0.05$; n=70), and a reduction in spasticity ($p<0.01$; n=160). Carried out by GW pharmaceuticals, these results have yet to be subjected to peer-review.

While there are clearly potential benefits from cannabinoid compounds in MS, it would appear that trials so far have not uncovered definite therapeutic avenues. Studies have tended to be poorly performed with little attention paid to the pharmacokinetics of cannabinoid compounds, revealing the insensitivity of outcome measures employed. Changes to the administration route, characterisation of inferred novel receptors and of the endocannabinoid system as a whole, and development of new agonists may help to elucidate strong clinical targets.

1.7.3. Evidence for cannabinoid-mediated neuroprotection

The evidence for cannabinoid-mediated neuroprotection comes from a wide range of experimental models both *in vitro* and *in vivo*. Evidence has been found for protection mediated via cannabinoid receptors against excitotoxic and ischaemic insult and via non-receptor mediated pathways for excitotoxic, ischaemic, oxidative and traumatic damage.

Excitotoxic damage via glutamate release and calcium influx has been studied the most extensively. Two *in vitro* studies, from Shen and Thayer (Shen & Thayer, 1998) and Abood et al (Abood *et al.*, 2001) agree that damage can be attenuated by application of WIN55212-2, a cannabinoid receptor agonist and Δ^9-THC, the active form of cannabis, respectively. Furthermore, the effect is attributed to activation of the CB_1R, as SR141716A, a CB_1R antagonist, can block protection. Protection is most likely afforded through CB_1R-linked inhibition of synaptic glutamate release, since concomitant addition of agonist and extracellular glutamate results in neuronal damage. A third excitotoxic study by Hansen et al (Hansen *et al.*, 2002) found that antagonism of

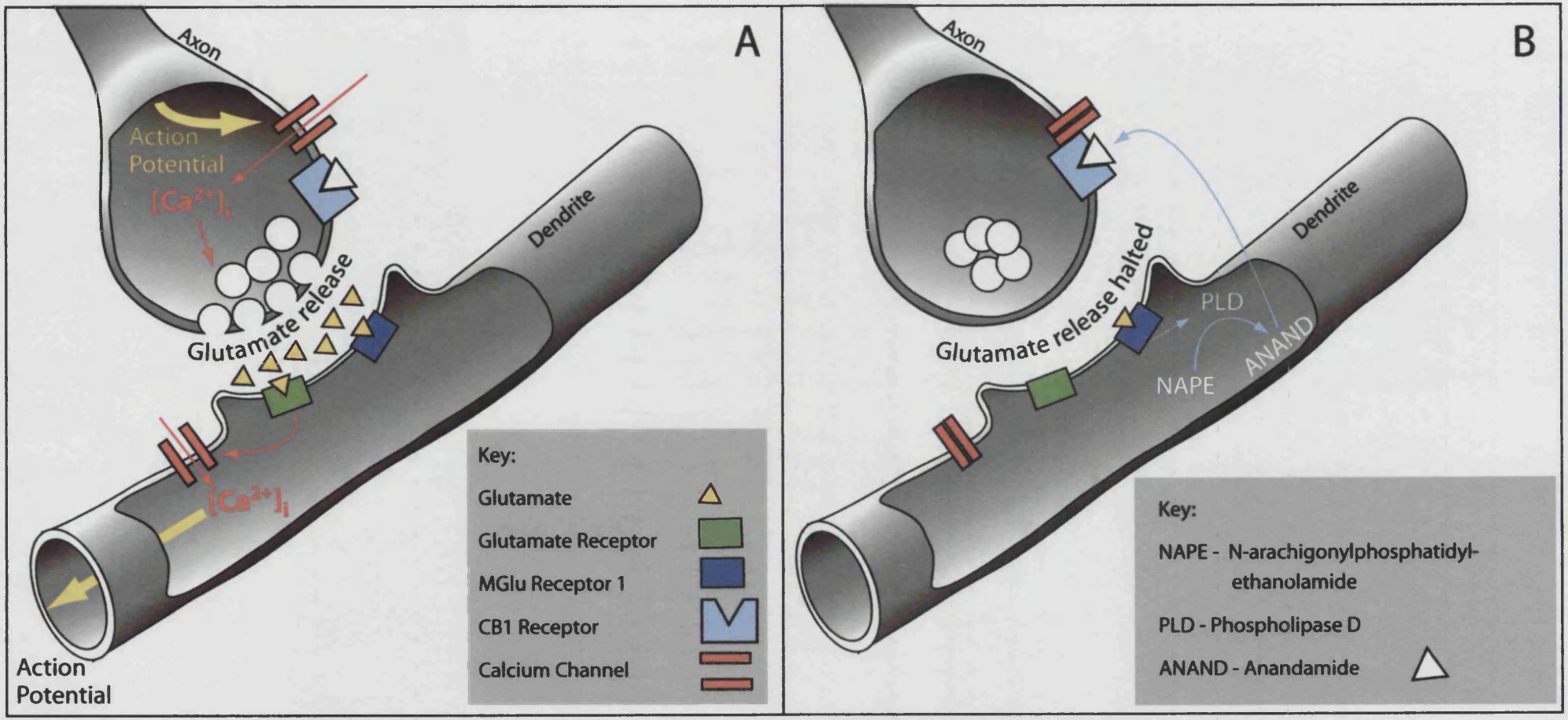

Figure 1-11: Endogenous cannabinoid signalling at a glutamateric synapse. (A) Action-potential medaited glutamate release from the presynaptic membrane activates postsynaptic glutamate receptors to depolarise the cell. (B) Among the receptors activated is MGluR 1, which upregulates phospholipase D activity. In turn, PLD processes NAPE, liberating anandamide which crosses the synapse in a retrograde manner. Activation of presynaptic CB1 receptors closes calcium channels and halts synaptic vesicle fusing and glutamate release. This retrograde synaptic negative feedback mechanism may be implicated in excitotoxic damage.

the CB_1R elicited reduced neuronal cell death, and that CB_1R agonists had no effects. The disparity between this and previous studies was put down to substantial differences between models, with the Hansen model being N-methyl-D-aspartate (NMDA) specific. Finally, a study by Hampson et al (Hampson *et al.*, 1998) looked at excitotoxic and oxidative damage, and concluded that cannabidiol and Δ^9-THC can be neuroprotective, but that the effect is not mediated via cannabinoid receptors. A second study into the effect of cannabinoids in oxidative stress (Marsicano *et al.*, 2002) examined protection by a range of classical and non-classical cannabinoid and non-cannabinoid compounds. These were split into three groups, based on their structure and binding profiles. Results from these studies suggest that presence of a phenolic ring structure is sufficient to protect against non-receptor mediated oxidative stress (Marsicano *et al.*, 2002).

Protection from ischaemic insult has been studied *in vivo*, in the four-vessel transient occlusion and the middle cerebral artery permanent occlusion models (Nagayama *et al.*, 1999), and *in vitro* in hypoxic cerebellar cortical neuron cultures (Sinor *et al.*, 2000). The *in vivo* studies both confirm that WIN55212-2 can protect brain tissue against ischemic injury via receptor-mediated mechanisms. The authors concluded that the effect could be due to cannabinoid receptor-mediated G-protein coupled reduction of flux through Ca^{2+} channels, or via second messenger pathways, such as cyclic adenosine monophosphate and phospholipase A2-cyclooxygenase.

A model of closed head trauma showed that 2-AG reduced oedema (intracranial swelling) significantly in the damaged hemisphere, and that recovery from the injury was transiently expediated. Infarct volume and hippocampal cell death were also attenuated. Again, this effect appeared to be receptor mediated (Panikashvili *et al.*, 2001). Increased levels of endocannabinoids have also been reported in head trauma

models following injury, indicating a potential autoprotective mechanism (Hansen *et al.*, 2001).

Finally two parallel studies using an novel MRI methodology found that two compounds – Δ^9-THC and anandamide protect brain tissue via different routes (van der Stelt *et al.*, 2001b; van der Stelt *et al.*, 2001a). Both studies used the Na^+/K^+-ATPase inhibitor oubain to induce acute insult to the striatum, followed by longitudinal (7 days duration from insult) MRI analysis to record recovery. Δ^9-THC was found to protect striatal neurons from insult for 7 days, mediated by CB_1R. Conversely, anandamide protected neurons in the early stage (up to 24 hours after insult) via non-receptor mediated routes. This was reversed in the late stage (7 days after insult) when SR141716A abolished neuroprotective properties. The authors speculate that the early protective effect could be due to the affinity of anandamide for other molecular targets, including the serotonin, NMDA and vanilloid receptors (van der Stelt *et al.*, 2001b; van der Stelt *et al.*, 2001a).

1.7.4. Cannabinoid receptor-1 knockout mouse characteristics and traits

Two mutant mouse strains with disrupted CB_1R gene (the CB_1R KO mouse) have been engineered and used in studies since 1999, one on the CD1 mouse background (Ledent *et al.*, 1999) and one on the C57BL/6 mouse background (Zimmer *et al.*, 1999). These strains allow for the investigation of the role of CB_1 on axonal and neuronal loss in CREAE.

Behavioural Traits

CB_1R-KO mice on the CD1 strain background have been shown to have a mild increase in locomotor activity when newly exposed to an open field, and exhibit

increased exploratory behaviour, compared with wildtypes (WT) (Ledent *et al.*, 1999). Both of these effects are transient, as the mice become quickly habituated and may be due to changes in short term memory. Conversely, some studies have shown that CB_1R-KO on the C57BL/6 background are hypoactive in the open field (Zimmer *et al.*, 1999). However, we have found that there is no difference in locomotor activity between wildtype and knockout mice on the ABH background.

Developmental differences and mortality

Although CB_1R knockout mice have no gross anatomical or functional deficits at birth (Zimmer *et al.*, 1999), both hetero- and homozygous knockout animals are under-represented at birth when compared to wildtype. This indicates the death of pre- or early post-natal pups, possibly due to a deficit in embryo implantation mechanisms. General life expectancy has been reported to be lower in the knockout animals, with % survival changing from approx. 95% in wildtypes to 70% in knockouts after 24 weeks (Zimmer *et al.*, 1999). It has been found that antagonist administration reduces the probability of blastocyst development in the preimplantation mouse embryo and administration of anandamide promotes blastocyst implantation in vitro at 14nM, but inhibits it at higher concentrations (Paria *et al.*, 2001). Cannabinoid antagonist administration also inhibits suckling in new-born pups, potentially leading to death (Fride *et al.*, 2001). These effects are likely to be strain dependent, since animals bred on the C57BL/6J background are susceptible, while those backcrossed on to the ABH background show no evidence of changes in postnatal survival compared to knockout mice on the CD1 background (D.Baker, personal communication).

1.8. Aims

Exogenous cannabinoids have been reported as being neuroprotective through CB_1R in a range of neuropathological conditions, including immune-mediated EAE models. In view of this, the aims of this project were to assess the degree of axonal and myelin pathology in an animal lacking the receptor during EAE *in vivo* and IFN-γ mediated demyelination in the aggregate cell culture model.

To assess the CB_1R knockout mouse, the aggregate cell culture system was modified to use tissue from the mouse telencephalon. Enzyme-linked immunosorbent assays (ELISAs) for NF and MBP were set up to assess axonal loss, demyelination and neuron damage/compromise in both systems, and the activation of caspase 3 was investigated as a harbinger of cell death. Clinical assessment of EAE by score and weight loss correlated with functional impairment in an activity chamber.

Modification of endogenous cannabinoid pathways is a preferable route to therapy for demyelinating inflammatory conditions, as, while effective, administered cannabinoids are unpredictable in their dosing attributes, and elicit numerous undesirable side-effects. This study aims to shed light on the endogenous pathway as a therapeutic target by investigating pathology in the absence of that system.

2. Materials and Methods

All chemicals were from Sigma-Aldrich Co. Ltd., Poole, UK, unless otherwise stated.

2.1. Mouse Aggregate Cell Culture System

2.1.1. Media

Mechanical dissociation and subsequent washes/centrifugation were carried out in D1 solution (Honegger,1985), containing 138mM NaCl, 5.4mM KCl, 0.17mM Na_2HPO_4, 0.22mM KH_2PO_4, 5.55mM D-glucose, 58.43mM sucrose, 5mg/l phenol red (Gibco BRL Life Technologies Ltd, Paisley, UK). Aggregates were cultured in serum-free high glucose Dulbecco's modified Eagle's medium (DMEM) without sodium pyruvate (Gibco), supplemented with 0.8μM bovine insulin and other trace hormones, vitamins and elements. The above media was supplemented with 100U/ml penicillin and 100μg/ml streptomycin antibiotics (Gibco).

2.1.2. Preparation of foetal mouse telencephalon

Foetuses were removed from outbred BK1 (B&K Universal, Grimston, UK), inbred C57BL/6 (B&K Universal) and inbred ABH mice (in-house stock) at 16-19 days after gestation, and placed separately in sterile, ice-cold D1 solution. New born pups of 0, 1 and 2 days post-parturition were decapitated and the heads placed in ice-cold D1 solution. The telencephalon of these foetal/new born mice were dissected out and placed in 50ml centrifuge tubes (Philip Harris Scientific, Ashby-de-la-Zouch, UK) containing ice-cold sterile D1 solution.

2.1.3. Mechanical dissociation and seeding of telencephalon cells

After washing twice by replacing the D1 solution in each tube and allowing the material to settle under gravity, brain tissue was dissociated by sieving through a nylon mesh with 200μm pores (Nybolt, Zurich, Switzerland) submerged in D1 solution, using

a sterile 5ml pipette outside the sieve to gently break up tissue (see Figure 2.1). The suspension was then poured through a nylon mesh sieve with 115μm pores (Nybolt) under gravity. Tissue of each foetal age was sieved separately. The filtrates were made up to 50ml with D1 solution, and centrifuged in a Sorvall RT6000B centrifuge (Dupont Ltd, Stevenage, UK) at 300g for fifteen minutes at 4°C with no brake. After discarding the supernatant, the pelleted cells were thoroughly re-suspended in D1 solution. A sample was diluted in 0.1% trypan blue/phosphate-buffered saline (PBS; 1.84mM KH_2PO_4, 10mM $K_2HPO_4.3H_2O$, 154mM $NaCl_2$, pH 7.2-7.4) to enable counting of viable cells by trypan blue exclusion, following which the suspension was re-centrifuged. The remaining pellet was re-suspended in the appropriate volume of DMEM to produce a cell suspension of 10^7 viable cells per ml, and 4ml of this suspension was seeded into 25ml capped DeLong flasks (Aimer Products, Enfield, UK) to give a total of $4x10^7$ cells per flask. The cells were incubated at 37°C in a humid 10% CO_2/90% O_2 atmosphere (Heraeus incubator; Philip Harris Scientific, Ashby-de-la-Zouch, UK) under constant rotation (Kuhner Shaker; Philip Harris). The rotation speed was increased from 68rpm to 80rpm over the first week of incubation to ensure optimal cell aggregation. The day of seeding is termed Day *in vitro* (DIV) zero.

2.1.4. Culture Maintenance

On DIV2, the aggregates were transferred to 50ml DeLong flasks (Aimer) containing 4ml of pre-warmed DMEM, bringing the total volume in each flask to 8ml. On DIV5, 8, 11, 14 and then every other day, 5ml of complete DMEM was replaced in each flask with pre-warmed DMEM.

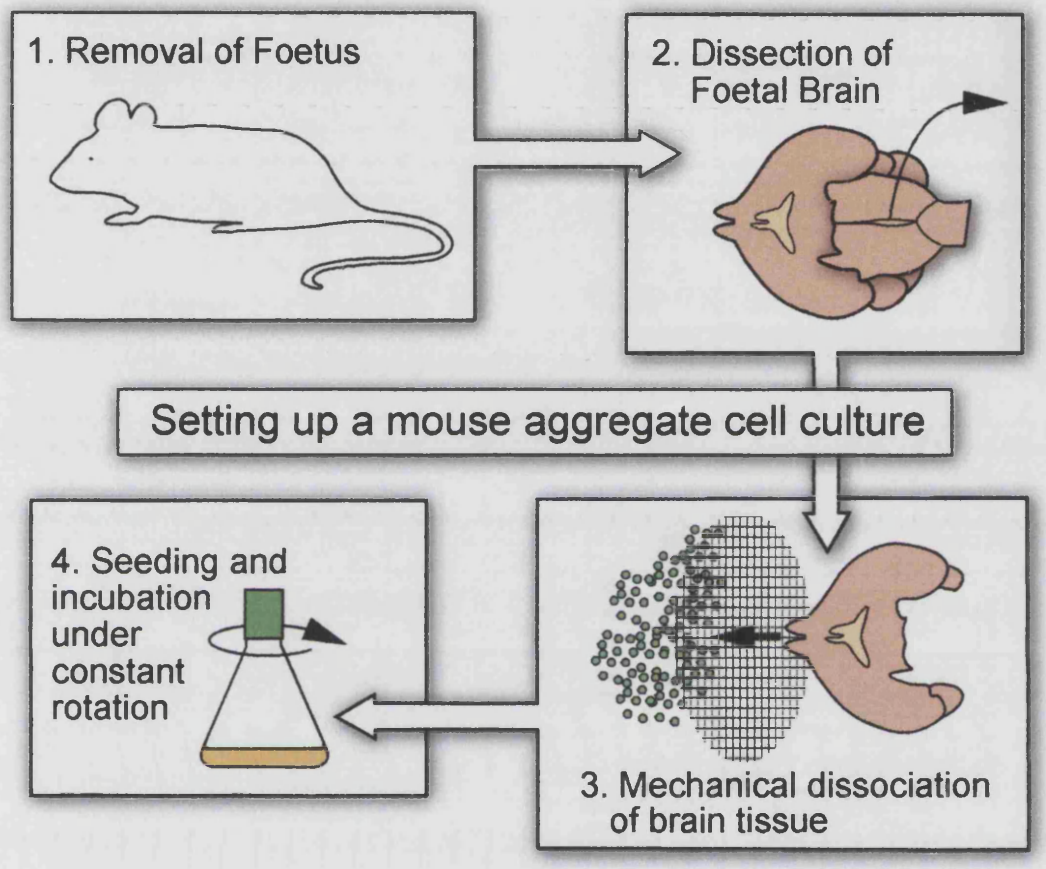

Figure 2-1: Setting up the aggregate cell culture. Foetuses are removed from the mother at embryonic day 16-18 under sterile conditions. The telencephalon is dissected out by removal of the cerebellum, and mechanically dissociated by sieving. Cells are seeded and incubated under constant rotation, forming aggregates over the following 2 days.

2.1.5. Demyelinating treatment of aggregate cultures

Aggregate cultures were treated with the cytokines IFN-γ and TNF-α, and the anti-MOG antibodies 8-18C5 and Z12.

Cytokine treatment: Stock solutions of cytokine were prepared by dilution in sterile PBS, aliquoted to avoid repeated freeze-thaw cycles and stored at -20°C. Murine recombinant IFN-γ (23ng/ml or 200U/ml; Chemicon International Ltd., Harrow, UK) or TNF-α (20ng/ml or 500U/ml; Chemicon) were added to pre-warmed culture medium. Cultures were then maintained as normal, substituting medium for cytokine-supplemented medium, on DIV 21 and 23. Flasks were then flushed of cytokine by washing with fresh prewarmed medium three times on DIV 25. Control flasks were also subjected to triple washing.

Antibody Treatment: Stock solutions of antibody were prepared by dilution in sterile PBS, aliquoted to avoid repeated freeze-thaw cycles and stored at -20°C. An IgG_1 mouse monoclonal antibody derived from clone 8-18C5 (Linington *et al.*, 1984) or the IgG_{2a} mouse monoclonal antibody, Z12 (Piddlesden *et al.*, 1993) were added to pre-warmed culture medium in the presence of complement (guinea pig serum; Serotec Ltd, Oxford, UK). Cultures were then fed as normal, substituting medium for antibody and complement-supplemented medium, on DIV 21 and 23. Flasks were flushed of antibody and complement by washing as described above. When using antibodies to demyelinate, the addition of complement is necessary to successfully demyelinate aggregate cultures, providing the need for a second set of control flasks, containing complement only.

2.1.6. Aggregates from rat tissue

For verification of the new mouse tissue method, comparison with rat aggregates was necessary. The protocol for establishing an aggregate culture from rat tissue was as for the mouse culture, with the exception that embryonic day 16 Sprague-Dawley rat foetuses were used as a tissue source.

2.1.7. BrdU incorporation

Harvested aggregates were transferred directly into a 6-well cell culture plate (VWR International, Lutterworth, UK) into 2ml of pre-warmed medium containing 10μM BrdU. This was incubated under constant rotation at 37°C for 4 hours. Following BrdU incorporation, aggregates were fixed for 10 minutes in 4% paraformaldehyde and washed in PBS. Aggregates were subsequently stored in PBS containing 0.01% sodium azide as a preservative.

2.1.8. Sampling of cultures

Samples of aggregates were harvested at desired time points through the culture period for biochemical, molecular biological or morphological analysis. Harvesting regimens varied according to experimental design, and care was taken not to over sample, to maintain aggregate microenvironment homeostasis.

Sampling aggregates for biochemical analyses:

The flask was gently agitated to ensure even distribution of aggregates, and a volume of medium with aggregates was transferred to a conical 10ml polypropylene tube (Fisher Scientific UK, Loughborough, UK) on ice. The aggregates were allowed to settle, the medium aspirated away, and the pellet was washed twice in 10ml of

barbitone buffer (63mM Sodium Barbital, 11mM Barbital, 1.2mM EDTA). Most of the barbitone buffer was removed, and the aggregates were transferred to a 1.5ml microfuge tube (VWR), where the remaining buffer was removed, and the sample frozen at minus 70°C.

Sampling aggregates for mRNA analysis:

Sampling was performed as above, with extra care being taken to minimise RNA degradation, involving the use of ribonuclease (RNase)-free tubes and PBS.

Sampling aggregates for analysis by confocal microscopy:

Sampling was performed as for biochemical analyses, with the addition of a fixation step. After removal of remaining barbitone buffer, the aggregates were fixed for 10 minutes in 500µl of 4%-paraformaldehyde. Following 2 washes with 10ml Barbitone buffer, the samples were stored in 200µl of PBS containing 0.01% sodium azide as a preservative.

Sampling aggregates for immunocytochemical analysis:

Aggregates were harvested and washed as for biochemical analysis. They were then treated with 200µl of 2% dispase in PBS at 37°C for 20 minutes while being agitated in order to disaggregate the cells. The remaining cell suspension was affixed to a microscope slide using a cytocentrifuge (Thermo Shandon UK, Runcorn, Cheshire, UK) at 600rpm for 5 minutes. After 10 minutes drying time the slides were placed in boxes with care taken not to disturb the cells, and frozen at –20°C.

2.2. *Measurement of total protein concentration*

The total protein concentration of aggregate homogenates was assessed using the Folin phenol method (Lowry *et al.*, 1951), which is based on a two-step colour reaction. In an alkali solution copper associates with protein and subsequently reduces the Folin reagent to form a blue coloured product. To maximise the colour resulting from the reduction, 0.4M sodium hydroxide is present to neutralise any acid released on addition of the Folin's solution and sodium carbonate is added to buffer the reagents to an optimal pH of 10. The optical density, read at 750nm, is proportional to the copper-bound protein.

Aggregates were homogenised in 500µl of homogenisation buffer (Barbitone buffer, as previously described, supplemented with 20µg/ml leupeptin, 20µg/ml pepstatin A, 200µg/ml benzoylarginine methyl ester (BAME), 200µg/ml tosylarginine methyl ester (TAME), 200µg/ml trypsin inhibitor, 200µg/ml tosylphenylalanyl chloromethane (TPCK), 200µg/ml aprotinin and 4mM ethyl glycol tetraacetic acid (EGTA)). This was done using a high-intensity ultrasonic processor (Jencons Scientific Ltd, Leighton Buzzard, UK). An aliquot of each sample was then diluted to 1 in 26 using 0.05M NaOH, and standard concentrations of BSA (bovine serum albumin) were prepared (0, 5, 10, 15, 20 and 30µg/ml) in a volume of 150µl. Samples and standards were assayed in duplicate. 50µl of each diluted sample was placed in a 10ml conical tube (Fisher) with 100µl distilled water. 50µl of 0.4M NaOH was added to each tube (standards and samples), followed by 1ml of freshly prepared solution X (2% Na_2CO_3, 0.02% K_2 Tartrate in 0.1M NaOH added to 1% $CuSO_4.5H_20$ in a ratio of 99:1). All tubes were vortexed, and left for 15 minutes. 100µl of Folin and Ciocalteu's reagent (diluted 1:1 with water; VWR) was added to each tube. After vortex mixing the tubes,

they were incubated in the dark for a further 30 minutes. The absorbance of each sample at 750nm was read on an Ultraspec 2000 spectrophotometer (Amersham Pharmacia Biotech UK Ltd., Little Chalfont, UK), and the generation of a linear standard curve allowed conversion of optical density to μg of protein per sample.

2.3. *Measurement of myelin basic protein and neurofilament content by ELISA*

MBP content correlates with the extent of myelination in the CNS as assessed by electron microscopy (Shine *et al.*, 1992). MBP content had previously been assessed using a radioimmunoassay (RIA) technique, using potentially dangerous radioactive chemicals. This was replaced by a novel sandwich-type ELISA for MBP.

2.3.1. Measuring MBP by ELISA

Sample and standard preparation:

Aggregates sampled for biochemical analysis were homogenised as for the measurement of total protein, and then diluted to 1 in 2.5 in diluent solution (0.2% BSA, 0.5% Tween-20 in barbitone buffer). An MBP concentration of 1000ng/ml was prepared from isolated human MBP and this was serially diluted 6 times in diluent to produce a standard curve. The final standard concentration was zero, using diluent alone to control for background activity. For reproducibility between assays, batches of standards were prepared and frozen for use in multiple assays.

ELISA protocol

Coat antibody (rat anti-MBP 36-50, Serotec) was diluted to 1:2000 in coating buffer (100mM Na_2HPO_4 adjusted to pH 9.0 with 100mM NaH_2PO_4), and 100μl was added to each well of a 96-well Nunc Maxisorp plate (VWR). The plate was then

incubated overnight at 4°C. After bringing the plate to room temperature, non-specific binding was blocked by incubation with 200µl of 1% BSA in barbitone buffer to each well for 1 hour at room temperature. Following blocking, the plate was washed once using barbitone buffer with 0.5% Tween-20 (PBS-T) and then incubated with samples and standards for 2 hours at room temperature under gentle agitation. After washing 4 times as above, the detect antibody (polyclonal rabbit anti-MBP; Chemicon) was diluted to 1:1000, 100µl was added to each well, and the plate incubated at room temperature under gentle agitation for 1 hour. Following a further 4 washes, horseradish peroxidase (HRP)-conjugated anti rabbit antibody (Amersham) was diluted to 1:1000 in diluent as previously, and 100µl was added to each well. The plate was incubated for 1 hour at room temperature under gentle agitation. Tetramethylbenzadine (TMB) substrate (R and D systems UK Ltd., Abingdon, UK) was removed from refrigeration and prepared in a light-excluded 50ml centrifuge tube to allow it to rise to room temperature. Following 4 final washes, 100µl of substrate was added to each well, and the colorimetric reaction observed for 5-10 minutes before being stopped with 1M phosphoric acid. The plate was read on a dedicated photometer (Anthos Labtec Instruments, Salzburg, Austria) at 450nm wavelength, using 620nm wavelength as a reference measurement.

Analysis of MBP ELISA results

Using Microsoft Excel, an equation representing the standard curve was determined, and used to predict the concentration of MBP in each sample from the optical density reading. This figure was then divided by the total protein for that sample, as determined by the Folin phenol method (see Section 2.2), to give the concentration of MBP per mg of total protein. In this way differences in sample concentration caused by non-identical sample sizes were normalised, allowing direct comparison of samples.

2.3.2. Measuring neurofilament by ELISA

Samples were prepared as for the MBP ELISA and diluted to 1 in 5 with diluent. Standards were prepared from recombinant NF H (Affiniti Research Products, Exeter, UK) by serially diluting 6 times in diluent solution from a stock of 250ng/ml. The final standard was zero, using diluent alone. The protocol and analysis for the ELISA (Petzold *et al.*, 2003) was the same as for MBP. The antibodies used were as follows: coat antibody – SMI35 (Sternberger Monoclonals Inc, Lutherville, USA) at ; detect antibody – rabbit anti-NF 200; HRP-linked antibody – HRP-conjugated anti-rabbit (Amersham). All antibodies were diluted to 1:1000. SMI-32 and SMI-35 reactive NF is termed NFH^{SMI35} or NFH^{SMI32} accordingly.

2.4. Measurement of MBP by radioimmunoassay

The radioimmunoassay (RIA) is a limited reagent assay which provides a quantative measure of ligand using a specific antibody exhibiting high affinity for that ligand. By binding a fixed concentration of antibody to a fixed concentration of radiolabelled ligand in the presence of an unknown quantity of unlabelled ligand, labelled and unlabelled ligand compete for antibody binding(Kruger *et al.*, 1999).

2.4.1. Radiolabelling MBP

^{125}Iodine (^{125}I) was used to radiolabel purified human MBP (supplied by N.Groome, Oxford Brookes University, Oxford, UK) using Iodogen iodination reagents (Peirce and Warriner UK Ltd., Chester, UK). Iodine needs to be in its oxidised reactive form to be successfully substituted into aromatic ring structures such as tyrosine, a step which is facilitated by use of these reagents. Iodogen Iodinating Reagent (tetrachlorodiphenylglycouril) was coated on to glass pyrex tubes (Bibby Sterilin Ltd, Stone, UK) by addition to the tube and evaporation overnight in a fume hood.

10µl purified human MBP (1mg/ml in 0.05M sodium phosphate buffer, pH7) was added to an iodogen coated tube containing 10µl of sodium phosphate buffer, pH 7, followed by 5µl of sodium ^{125}I (approx. 18.5 MBq) in dilute sodium hydroxide, pH 7-11, to provide a final concentration of around 74MBq/20µl. The tube was incubated for 30 minutes at room temperature. The iodination reaction was stopped by adding 0.5ml of 1M sodium phosphate buffer containing tyrosine (1mg/ml) and 1mg of blue dextran to the reaction vessel. The contents were then pipetted on to a PD10 column containing Sephadex G-25 M (Amersham) in order to desalt and separate labelled from non-labelled fractions. The dextran blue-stained fraction containing iodinated MBP was collected in a plastic screw-top phial and stored at 4°C in a lead container until required.

The success of iodination was estimated by activity counting using the LKB-Wallac 1275 mini gamma counter (EG & G Wallac, Milton Keynes, UK).

2.4.2. Measurement of sample MBP

Buffer for the RIA (0.05M sodium phosphate, pH7, 1.2% w/v sodium chloride, 0.5mg/ml calf thymus histones type II-S, 0.05% hexadecyltrimethyl ammonium bromide (CTMB)) was prepared and used to suitably dilute aggregate homogenate samples. A 50µl aliquot of diluted sample was added to gamma-counter compatible tubes in duplicate. Stock ^{125}I-labelled MBP was diluted in RIA buffer to give approximately 20,000cpm per 50µl, and this amount was added to each tube. A non-specific binding (NSB) tube containing 50µl ^{125}I-MBP and 50µl RIA buffer (to determine the percentage counts in the absence of antibody) and a total (T) tube containing 50µl ^{125}I-MBP alone (to measure total radioactive counts) were also prepared in duplicate. Each tube was vortex mixed and incubated overnight at 4°C to enable

components to reach a binding equilibrium. Separation of bound and free ligand was accomplished by using the Sac-Cel method (IDSLtd, Tyne and Wear, UK): a cellulose-linked secondary antibody raised against the IgG type of the primary anti-MBP antibody was added. This binds to ^{125}I-MBP and can then be removed by centrifugation (2 minutes, 18°C, 1000g). The supernatant was then discarded and the ^{125}I radioactivity (cpm) retained in the bound fraction within the pelleted cellulose was counted.

2.5. Immunocytochemical analysis of aggregates

Immunocytochemical staining of prepared slides (see Section 2.1.8) was carried out to assess the types and morphology of cells within the aggregate. The prepared slides were fixed in ice-cold methanol for 5 minutes at –20°C. After washing with PBS, non-specific binding was blocked by incubation for 30 minutes with normal goat serum (Vector Laboratories Inc., Burlingame, USA) diluted to 1 in 40 with PBS. Following 3 five-minute washes with PBS, 75µl of the relevant primary antibody was applied (see Table 2-1) and incubated for 1 hour at room temperature. Following a further 3 five-minute washes, the relevant biotinylated secondary antibody was applied to the slide at a 1 in 200 dilution, and incubated for 1 hour at room temperature. After 3 five-minute washes, the sensitivity of the staining was augmented by using the Vectastain Elite ABC kit (Vector Laboratories Inc., Burlingome, USA) avadin-biotin system. The reagents were applied as per the manufacturers instructions, and slides were incubated for 1 hour at room temperature. Following 3 final PBS washes, the slides were placed in PBS with 2% 3,3'-diaminobenzidine tetrahydrochloride (DAB) and 5µM H_2O_2 for 5 minutes in order to develop colouration. Slides were then washed under running tap water, and counterstained in freshly filtered haemotoxylin for 30 seconds, followed by a 5-minute wash under running tap water. Dehydration of the stained slides was carried

out by immersion in 90% ethanol (VWR), then two immersions in 100% ethanol (VWR), followed by two immersions in 100% xylene (VWR), each for 45 seconds. Slides were mounted using Distrene 80:plasticiser:xylene (DPX) medium and allowed to dry overnight before viewing.

2.6. Histochemistry of spinal cord transverse sections

8μm paraffin-wax spinal cord sections fixed in 4% paraformaldehyde were cut (Bright Instruments, Huntingdon, UK) from ABH mice (in-house stock), and mounted on to poly-lysine coated microscope slides (VWR). Sections were provided by AstraZeneca Sweden.

2.6.1. Luxol fast blue staining for myelin

Sections were incubated in Luxol fast blue solution (Salthouse, 1964) (Luxol fast blue 1% w/v in ethanol with 2% acetic acid) overnight at 37°C, rinsed in 95% ethanol and then distilled water. Staining was differentiated by immersion in 0.05% lithium carbonate, followed by 70% alcohol and water washes, and slides were counterstained in eosin and cresyl violet (0.25% cresyl violet, 0.1% acetic acid) before dehydration and mounting with a coverslip.

2.6.2. Bielschowsky's silver stain

Following hydration, slides were placed in preheated 20% silver nitrate solution at 37°C for 15 minutes. After three washes in distilled water, slides were placed in ammoniacal silver solution for 10 minutes at 37°C, and then in developer solution (5% formaldehyde, 20% absolute alcohol in distilled water) until the stain had developed appropriately (1-5 minutes) (Yamamoto & Hirano, 1986). Slides were toned in 0.1%

gold chloride for 2 minutes, and fixed in 5% sodium thiosulphate for 2 minutes. Sections were mounted in DPX (VWR).

2.7. Aggregate analysis by confocal microscopy

Immunofluorescent staining of whole aggregates and subsequent analysis by confocal microscopy was performed to allow identification of cell types and their spatial organisation within the aggregates. Aggregates were fixed and stored as described in Section 2.1.8. The free-floating whole aggregates were then stained by incubation overnight at 4°C with 50µl of a relevant primary antibody (see Table 2-1). After washing three times with PBS, the relevant fluorochrome-conjugated secondary antibody was applied, and aggregates incubated overnight at 4°C. Where double staining was required, aggregates were incubated overnight with a second primary antibody with a different IgG subtype, followed by three washes with PBS, and a final overnight incubation with directly conjugated secondary antibodies against those IgG subtypes. After immunolabelling, 3-10 aggregates were placed on a glass microscope slide (VWR) followed by a drop of glycerol containing 22mM 1,4-diazobicyclo[2,2,2]octane (to reduce fluorochrome fading). A glass cover slip was then placed on top of the aggregates, squashing them slightly, and sealed with clear nail varnish. Aggregates were analysed on a Zeiss 410 inverted scanning confocal microscope (Zeiss UK Ltd, Welwyn Garden City, UK) with three separate excitation lasers, and images were prepared using Adobe Photoshop 7.0.

Cell type	Primary	Source
Pluripotent oligodendrocyte precursor; perinatal and late OG progenitor; adult OG precursor.	**Rabbit anti-PDGF-α receptor; 1:1000**	R and D Systems
Perinatal and late OG progenitor; Adult OG precursor.	**Rabbit anti-NG-2; 1:1000**	Gift (G.Wolswijk)
Late OG progenitor; Adult OG precursor.	**Mouse monoclonal O4 (tissue culture supernatant); 1:2**	Gift (G.Wolswijk)
Oligodendrocyte cell body and myelin	**IgG3 Mouse anti-Galactocerebrocide C; 1:4**	Chemicon
Myelin	**Rabbit anti-myelin basic protein; 1:200**	Chemicon
Neuron	**IgG1 mouse anti-neurofilament; 1:500**	Sigma
Dividing cells	**IgM mouse anti-BrdU; 1:100**	Cymbus Biotchnology
Vulnerable or compromised subset neurons	**Mouse IgG1 anti-dephosphorylated neurofilament (SMI-32); 1:1000**	Sternberger
Oligodendrocyte Cell Body	**Rabbit anti-carbonic anhydrase II; 1:1000**	Gift (G.Wolswijk)

Table 2-1: Primary antibodies for immunocytochemistry and fluorescent confocal microscopy

Antibody		Source
rabbit-Cy3 conjugate; 1:400	Donkey	Research Diagnostics Inc
mouse IgG1-CY5 conjugate	Goat	Southern Biotechnology
mouse IgG1-TRITC conjugate; 1:500	Goat	Serotec
mouse IgG2a-FITC conjugate 1:500	Goat	Cymbus Biotechnology
mouse IgG3-FITC conjugate 1:100	Goat	Serotec
mouse IgM-TRITC conjugate 1:100	Goat	TAG Inc
rabbit IgG-TRITC conjugate; 1:500	Goat	Sigma
rat IgG-TRITC conjugate; 1:500	Goat	Seralab
goat- FITC conjugate; 1:100	Rabbit	Sigma
rat IgG-FITC conjugate; 1:100	Rabbit	Sigma
mouse IgG1-FITC conjugate; 1:100	Sheep	Serotec

Table 2-2: Secondary antibodies for confocal microscopy analysis

2.8. *Extraction of Total RNA from aggregates*

Total RNA was extracted from aggregate samples using a modified version of the Chomczynski and Sacchi procedure (Chomczynski & Sacchi, 1987). Guanadine thiocyanate and guanadine hydrochloride were used to disrupt cell membranes, including nucleoprotein complexes, allowing RNA to be released into solution and purified free of protein. These compounds, along with β-mercaptoethanol and sodium acetate also serve to inactivate RNases released from cell membrane-bound organelles on disruption. Purification by phenol:chloroform extraction separates RNA from contaminating DNA and proteins, which can then be alcohol precipitated.

2.8.1. Cell disruption and RNA extraction/precipitation

Isolation was performed on ice to slow the rate of RNase activity and RNase free equipment was used and gloves worn throughout. Aggregates in RNase-free 1.5ml Eppendorf tubes were thawed on ice. In an extraction hood, 750µl of filter-sterilised guanidine thiocyanate (4.215M guanidine thiocyanate, 25mM sodium citrate pH7, 0.5% N-lauroyl sarcosine, 0.1M β-mercaptoethanol, 12.5ml dipyrocarbonate (DEPC)-treated water) was added to each tube, and aggregates triturated by passing through a 23-gauge needle several times. After transferring to a 2ml lock-cap Eppendorf tube, RNA was extracted by sequentially adding 75µl of sodium acetate (2M sodium acetate, 2M glacial acetic acid, pH 4), 750µl of saturated phenol containing 1mg/ml hydroxyquinoline (Gibco), and 150µl of chloroform:isoamyl alcohol (24:1), with each tube being inverted to mix the contents between additions. The samples were then thoroughly vortex-mixed, incubated on ice for 15 minutes, and centrifuged at 8000g for 15 minutes at 4°C. The remaining lysate consisted of an aqueous upper phase containing RNA, and an organic lower phase containing DNA and proteins. The aqueous phase was transferred to a fresh

1.5ml Eppendorf tube and RNA was precipitated by mixing with 750µl of isopropanol, followed by an overnight incubation at –20°C.

Following incubation, samples were centrifuged as above to pellet the RNA, and the supernatant carefully removed and discarded. The pellet was resolubilised in 750µl of filter-sterilised guanidine hydrochloride (6M guanidine hydrochloride, 0.1M sodium acetate pH 5, 5mM dithiothreitol, 5.1ml DEPC-treated water), gently vortexed, and incubated on ice for 15 minutes. A 375µl aliquot of absolute ethanol was used to reprecipitate the RNA, again during an overnight incubation at –20°C.

Following centrifugation, the supernatant was removed and discarded, and the pellet was resuspended in 375µl of 70% ethanol. Samples were further dehydrated by vortexing and resuspending in 80% and then 100% ethanol. Samples were air-dried in a sterile environment to remove remaining ethanol, and the pellets resuspended in 40µl of RNase-free water before heating to 60°C for 10 minutes. After freeze-thawing the sample, the RNA was quantified by spectrophotometric analysis.

2.8.2. Spectrophotometric determination of RNA concentration and purity

To determine the concentration of RNA in each sample, the samples were suitably diluted, and measured at 260nm (UV wavelength) on an Ultrospec 2000 spectrophotometer (Amersham). An optical density of 1 corresponds to 40µg of RNA in 1ml, so the concentration in µg/ml was calculated (i.e. RNA conc. = OD at 260nm x 40 x dilution factor). Also, by measuring the 280nm wavelength OD, a ratio was obtained to estimate the purity of RNA extracted, with ratio values close to 2 indicating little contamination by DNA, protein or an extraction agent.

2.9. *Reverse-transcription of extracted RNA*

RNA extracted from aggregates was reverse transcribed into single-stranded DNA for analysis by the polymerase chain reaction method. Using retroviral reverse transcriptase, incubation of messenger RNA with oligo d(T) primers and free deoxyribonucleoside triphosphates (dNTPs) under the correct conditions allows the retroviral enzyme to reverse transcribe single-stranded DNA from the extracted RNA. Again, extreme care was exercised in the handling of RNA, as contamination with RNases would produce degradation.

A 3µg aliquot of total RNA was placed in a RNase free 1.5ml Eppendorf tube with 40 units of recombinant RNase inhibitor (Promega Biosciences Inc., Southampton, UK) and made up to 13.5µl with DEPC-treated water. Oligo d(T) primers (0.5ng) were added to each tube, and samples were incubated at 70°C for 10 minutes to allow annealing of the primer to the poly-A tail of the RNA. These were transferred directly to ice to prevent the formation of secondary structures in the RNA, and 3µl of 0.1M dithiothreitol, 40 units of RNase inhibitor, 1.5µl of 10mM dNTPs, 600 units of Malarey murine leukaemia virus (MMLV) reverse transcriptase (Promega), and 6µl of 5 x reverse transcription buffer (50mM Tris (hydroxymethyl) aminomethane (Tris)-HCl pH 8.3, 7mM $MgCl_2$, 40mM KCl, 0.1mg/ml BSA, 0.01% NP-40; Promega) were added. The samples were then incubated with this mixture for 1 hour 20 minutes at 37°C to allow primer extension and complimentary DNA (cDNA) production. This was followed by MMLV reverse transcriptase denaturation with a 10 minute incubation at 70°C. After transferring directly to ice, the samples were made up to 150µl with DEPC-treated water, and the mRNA:cDNA hybrids were denatured at 100°C for 5 minutes. Samples were then cooled on ice and stored at -20°C.

2.10. Amplification of CB_1R cDNA by Polymerase Chain Reaction

The polymerase chain reaction (PCR) is a technique for amplifying areas of DNA using complimentary fragments of DNA flanking the region of interest (primers). Primer design requires knowledge of the DNA sequence of a gene. Following DNA denaturation, primers anneal to the single-stranded DNA (ssDNA) at specific temperatures related to their basic structure. The temperature is then changed to allow activation of a heat-tolerant DNA polymerase that extends the primer in a 5' to 3' direction using surplus free dNTPs. A third temperature change denatures the DNA strands and the cycle can repeat, allowing the number of cycles to determine the degree of DNA amplification. The amplification is exponential up to a point then plateaus out, with DNA polymerase being the limiting factor. Taq DNA polymerase (from *Thermus aquaticus* bacteria) is heat stable, and therefore ideal for this application. It requires the presence of free magnesium ions to function, with the magnesium acting as a cofactor.

2.10.1.Primer design

Primers for the mouse CB_1 receptor were designed using the Lasergene software from DNAstar Inc. (Madison, USA) and the National Centre for Biotechnology Information (NCBI) nucleotide database (http://www.ncbi.nlm.nih.gov). The primers used for CB_1R (accession number: NM007726) in the mouse were as follows:

Forward: 5'-CAT CAT CAC AGA TTT CTA TGT AC-3'

Reverse: 5'-GAG GTG CCA GGA GGG AAC C-3'

PCR conditions for these primers were optimised by altering the magnesium chloride concentration for the reactions, and then by changing primer extension time and cycle number so that a single clear band was visible in each lane. The cycle number used was still in the linear phase of exponential duplication.

2.10.2.PCR protocol

A 5µl aliquot of each RT product was loaded into a sterile PCR reaction tube (Perkin-Elmer Applied Biosystems, Norwalk, USA; 8 tubes per strip) with 200mM dNTPs, 1.25mM $MgCl_2$, 1 x PCR Buffer (200mM Tris-HCl pH 8.4, 500mM KCl; Invitrogen Ltd, Paisley, UK), 1mM forward and reverse primers (Qiagen Ltd., Crawley, UK), 2.5 units of Taq DNA polymerase (Invitrogen), in a final volume of 50µl. The tube strips were loaded into a Geneamp PCR System 9700 (Perkin-Elmer), caps applied to each tube strip, and incubated under thermal cycling conditions for 40 cycles at an optimum annealing temperature of 55°C. Following incubation, products were stored at 4°C.

2.10.3.Analysis of PCR products by 1% agarose gel electrophoresis

Separation of the 366bp DNA fragment was performed on a 1% agarose gel, and visualised under ultra-violet light using ethidium bromide. The sizes of PCR products were determined by comparison with a DNA ladder. Agarose in Tris-boric acid-EGTA (TBE) buffer (Gibco) with 0.5µg/ml ethidium bromide was prepared and loaded into a gel box with well-forming comb, and allowed to set for 45 minutes. Once set, the combs and barriers were removed, and the gel was mounted in an electrophoresis box and covered by TBE buffer (Gibco) containing 0.5µg/ml ethidium bromide. Samples and a 100 base pair DNA ladder (Promega) were prepared by diluting 5µl of PCR product/ladder with 5µl of dH_2O and 2µl of 6x orange G dye. Samples were loaded into separate wells, flanked by wells containing DNA ladder, and the gel was run at 110V/ 0.05 amps for 1 hour 30 minutes. After running, the gel was destained in dH_2O under agitation for 15 minutes, photographed using dedicated CoolSnapPro-cf monochrome

camera and analysed using the GelPro image analysis package (Media Cybernetics, Berkshire, UK).

2.11. Measurement of active and total caspase 3 by Western blotting

Western blotting is a technique for quantifying specific protein levels in a given sample. The technique entails running the protein in a sample through a gel under high electric current to separate protein by molecular weight – smaller proteins will travel further than large proteins in a given time. These are then transferred on to a membrane and probed with antibodies raised against the protein of interest. Bands on an autoradiograph can then be quantified using computer techniques.

A 40μg aliquot (20-30μl) of protein was diluted in running buffer (2% sodium docecyl sulphate [SDS], 10% Glycerol, 2.5% β-mercaptoethanol, 125mM Tris-HCL pH 6.8, 0.02% bromophenol blue), denatured at 100°C and loaded on to 5% stack, 12% resolve gels (Biorad, Hemel Hempstead, UK), which were placed in a Biorad Mini-Protean 3 gel-running box. Any empty wells were topped up with sample buffer prior to the addition of running buffer (0.25M Tris base, 1.92M Glycine, 1% SDS) to the chamber. The gel was then run under 180 volts for ~45 minutes until the bromophenol blue dye-front had reached the bottom of the gel. Following removal of the gel, it was equilibrated in transfer buffer (0.25M Tris base, 1.92M Glycine, 20% Methanol) along with Immobilon P polyvinylidene fluoride blotting membrane (Millipore, Massachusetts, USA). Mini Protean 3 fibre pads and 3mm blotting paper were also soaked in transfer buffer. The transfer sandwich was constructed according to the manufacturer's instructions, and loaded into a transfer block. This was then immersed in transfer buffer in the Mini Protean 3 chamber and proteins transferred to the membrane using 22v current overnight at 4°C. Following removal of the membrane and one 10

minute wash in Tris-buffered saline and Tween-20 (T-TBS; 0.01M Tris-HCL, 0.15M sodium chloride, 0.05% tween-20; Sigma Aldrich), non-specific binding sites were blocked using 5% Marvel fat-free milk (Premier International Foods (UK) Ltd, Lincs, UK) dissolved in T-TBS. After another single 10 minute wash in T-TBS, primary rabbit antibody specific for caspase 3 (Santa Cruz Biotechnology, California, USA) was diluted to 1:1000 in 5% Marvel in T-TBS and incubated with the membrane for 2 hours at room temperature. The membrane was washed 3 times for 10 minutes in T-TBS, followed by incubation with goat antibody specific for rabbit IgG (secondary antibody) diluted to 1:1000 (Santa Cruz) for 1 hour at room temperature. Three further 10 minute T-TBS washes were followed by incubation with ECL reagents (Amersham) for 1 minute according to the manufacturers instructions. The blot was then visualised using ECL x-ray film (Amersham), with exposures for 1, 5 and 20 minutes. Film was developed and fixed in Kodak reagents, and analysed using the GelPro software package.

2.12. Induction of EAE

ABH mice (in-house stock) were injected subcutaneously in the flank on day 0 and 7 with 0.3ml of an emulsion of lyophilized spinal cord homogenate (SCH) reconstituted in PBS, and mycobacterium-supplemented Freund's incomplete adjuvant (BD Biosciences Ltd, Oxford, UK). Each animal received 1 mg of SCH and 60 μg Mycobacterium (*Mycobacterium tuberculosis* H37Ra, *butyricum* (4 : 1) per injection) (Baker et al., 1990).

2.13. Assessment of functional deficit in EAE

2.13.1. Clinical scoring of mice

Mice with EAE were scored from day 11 onwards on a clinical scale of one to five, as illustrated in Figure 2-2, and photographed in Figure 4-2. Diagnostic criteria are as follows: 1 – loss of muscular tone in the tail; 2 – impaired righting reflex when the animal is turned on to its back; 3 – partial hind limb paralysis, with one limb affected; 4 – complete hind limb paralysis, with both limbs affected; 5 – moribund and unable to move. In order to more effectively facilitate use of the ranking with statistical analyses, neurological signs of a lower severity than typically observed for a defined grade were scored 0.5 lower. Therefore, animals in remission have tail movement and tone, but the tail is also limp, so is scored as a 0.5. Animals which are slowly able to right themselves following inversion are scored 1.5, and animals showing a small degree of partial limb paralysis are scored 2.5. Bilaterally paralysed animals showing only minor hind limb movement are scored as 3.5. Accompanying these clinical signs, weight loss occurs 1-2 days prior to onset of disease, and is an accurate predictor of changes in disease, with animals regaining weight prior to recovery in remission.

2.13.2. Movement in an open-field activity chamber

Mice were placed in a 27 x 27 cm open-field activity chamber (Med Associates, Georgia, VT, USA) at varying stages of disease severity and movement around the chamber was recorded over a five-minute period. Total distance moved was recorded via computer, and data analysed using the SigmaStat V.2 (Jandel Scientific, San Rapheal, USA).

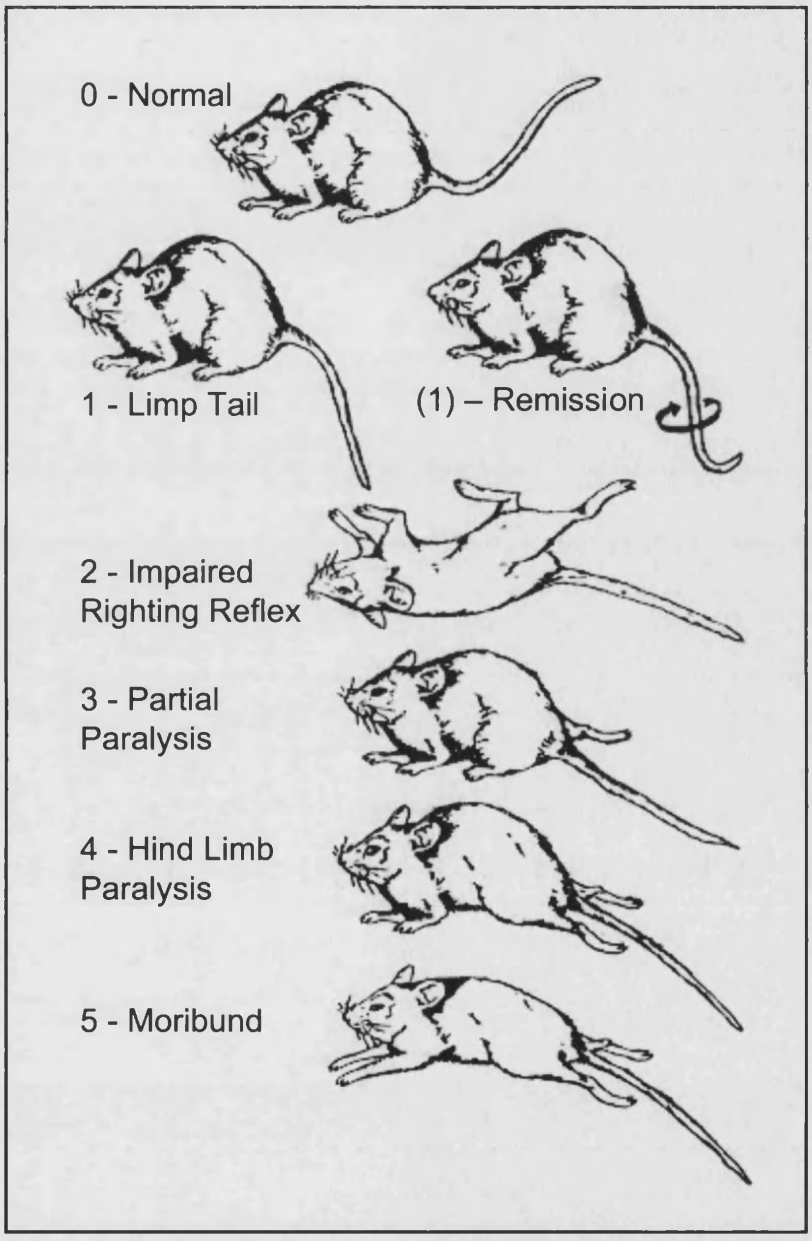

Figure 2-2: The clinical scoring criteria in relapsing-remitting EAE. Signs become more severe as the disease course progresses, and are accompanied by weight loss prior to acute attack or relapse onset, and weight gain prior to remission.

2.14. Statistical evaluation

Data was analysed with the GraphPad Prism computer package (GraphPad Software, San Diego, USA). Datasets were compared with either one or two-way analysis of variants (ANOVA) with 95% confidence limits, and errors calculated as the standard error of the mean (SEM). P-values were taken as proof of significance with the following nomenclature: * - $p<0.01$; ** - $p<0.005$; *** - $p<0.001$. N-numbers were 11 and above for the spinal cord analyses, and 15 and above for the aggregate analyses. Individual n-numbers are given in each results chapter.

3. Characterisation of a mouse aggregate cell culture system

3.1. Introduction

The aggregate cell culture system was developed using rat tissue, and has been extensively characterised and used to investigate myelination and remyelination, as well as growth and differentiation of cells over time (Almazan *et al.*, 1985; Honegger *et al.*, 1979; Honegger & Lenoir, 1980), developmental expression of opiates (Lenoir *et al.*, 1983; Lenoir *et al.*, 1984), neurotransmitters and growth factors (Honegger & Guentert Lauber, 1983; Honegger & Lenoir, 1982), adhesion molecule expression (Jorgensen *et al.*, 1984), viral infection (Pulliam *et al.*, 1984) and toxicological studies (Honegger & Werffeli, 1988), amongst others. The volume of tissue that can be cultured, relative ease of technique, lack of exogenous supportive factors, three dimensional arrangement and flexibility of experimental variables makes the system ideal for examining cell types in conjunction with others. This environment models the *in vivo* situation more closely than a monolayer culture, allowing the interactions between cells to be examined. This is one reason why myelination, a process which intrinsically links nerves and oligodendrocytes, has been extensively studied using the aggregate system. Advances in gene knockout technologies in mice have presented an invaluable tool with which to elucidate the effects of a single factor on a system. A combination of the aggregate cell culture with gene knockout technology would provide a methodology with which to examine in detail processes such as myelination and neurogenesis, and the cellular interactions they represent.

The mouse strains employed in these studies were chosen for specific strain-dependent properties. BK1 mice are outbred, and mate reliably giving consistently large litter sizes. This means that a high number of flasks can be set up for each experiment. C57BL/6 mice are an inbred strain commonly used as the background strain for

knockout mice. As this work was done with a view to using knockout animals, it was important that tissue from the background strain formed viable aggregates. However, C57BL/6 mice are relatively resistant to EAE induction (Levine & Sowinski, 1973), except where MOG is the immunogen (Slavin *et al.*, 1998). Therefore, ABH mice were tested for aggregate cell culture suitability, as CREAE can be effectively induced in these animals, as described previously. This was done with a view to backcrossing a gene deletion on to the ABH background strain.

3.2. Results

3.2.1. Aggregate molecular and cellular characteristics

The n-numbers used for all statistical evaluations in Section 3.2 were at least n=15 flasks. When examined under the light microscope, aggregates from mouse tissue were smaller than published data on rat aggregates, being 150-200μm in diameter, compared to 360-400μm in the rat (Figure 3-1). Variation in aggregate size was evident in the earlier stages of development, but was considerably reduced by 14 DIV. Aggregates had a spherical gross structure which remained intact for the duration of the 42 day culture period.

The morphology of the aggregates was similar to that of aggregates from rat tissue. As can be seen from Figures 3-2 and 3-3, an astrocytic shell surrounds an intermediate layer of neuronal processes, myelin and oligodendrocyte cell bodies. Neuronal cell bodies can be found in the core of the aggregate. Expression of markers for early and late oligodendrocyte progenitors occurred in concordance with the *in vivo* situation, as well as with rat aggregate development (Figure 3-4). NG2-positive cells, an early progenitor marker, appear to be present in greater numbers at DIV 5 than O4-positive late progenitors. The early progenitors persist until DIV 14, apparently

reducing in numbers between DIV 14 and 21, whereas late progenitor numbers remain high until at least DIV 21. These progenitors have a morphology similar to that seen in rat aggregates. NG2-positive cells are round with few processes; O4-positive cells have a similar rounded shape, but often have more complex morphology with higher numbers of processes. Expression of O4 and NG2 and a third marker, PDGF-α, variably overlap at different stages of progenitor maturation. Simultaneous immunostaining for these three markers enables identification of progenitors in different stages of the lineage (see Figure 1-8). As can be seen from Figure 3-5, early and late progenitors dominate until DIV8, after which more pre-myelinating oligodendrocytes are seen. In conjunction with Figure 3-4, this indicates the progressive nature of oligodendrocyte development *in vitro* in the presence of other cell types.

3.2.2. Development of an ELISA for myelin basic protein

Whilst performing the first biochemical studies on mouse tissue aggregates using an RIA to measure MBP, it became clear that a less time consuming and safer technique was required to efficiently analyse aggregate myelin content, as the RIA took a minimum of 48 hours to complete. An ELISA was developed for MBP employing a two-antibody sandwich around the antigen. Three candidate capture antibodies (which is bound to the plastic surface of an ELISA plate in order to capture the antigen) were identified and tested for sensitivity (Figure 3-6). These antibodies were all monoclonal and sourced from readily available clones. They were coated on to a ELISA plate at a concentration of 1:1000 (see methods for a detailed description) and exposed to doubling dilutions of MBP. It was found that clone 12 was the most sensitive to MBP, detecting levels of around 7ng/ml above background. Clones 22 and 14 were sensitive to around 50ng/ml. Following selection of the coat antibody, the concentration of coat,

detector and reporter antibodies were optimised by varying the concentration of each individually (Figure 3-7). Taking into account background and sensitivity, it was found that the optimum concentration for all three antibodies was 1:1000.

A comparison of three chromogenic substrates, 2,2'-azino-bis (3-ethylbenz-thiazoline) 6-sulfonic acid (ABTS), TMB and orthophenylenediamine (OPD) was undertaken to establish the most suitable for use in the assay (Figure 3-8a). OPD was found to produce a highly chromogenic and very rapid reaction producing saturated results and was therefore discarded. TMB was found to be more sensitive than ABTS, producing a well-paced reaction. Two proteins were tested for efficacy at blocking non-specific binding on the ELISA plate – bovine serum albumin and histones. Both have been used in past methodologies, and as can be seen from Figure 3-8b, there is a negligible difference between the two. BSA was chosen over histones due to being readily available and more cost effective.

To verify that colour production was due to the presence of antigen and not cross-reaction between components, experiments were conducted omitting pertinent components of the ELISA, with the aim of getting no colour production. For example, to test that the coat and detect antibodies did not cross-react, one ELISA was performed with no antigen present. Cross-reaction between coat, detect and report antibodies, the plastic plate, the BSA blocking agent and the TMB chromogenic substrate were all negative (Figure 3-9a). A comparison was carried out between the ELISA and RIA techniques to verify that the results were comparable between the two (Figure 3-9b). Samples in which MBP had previously been quantified using the RIA were retested

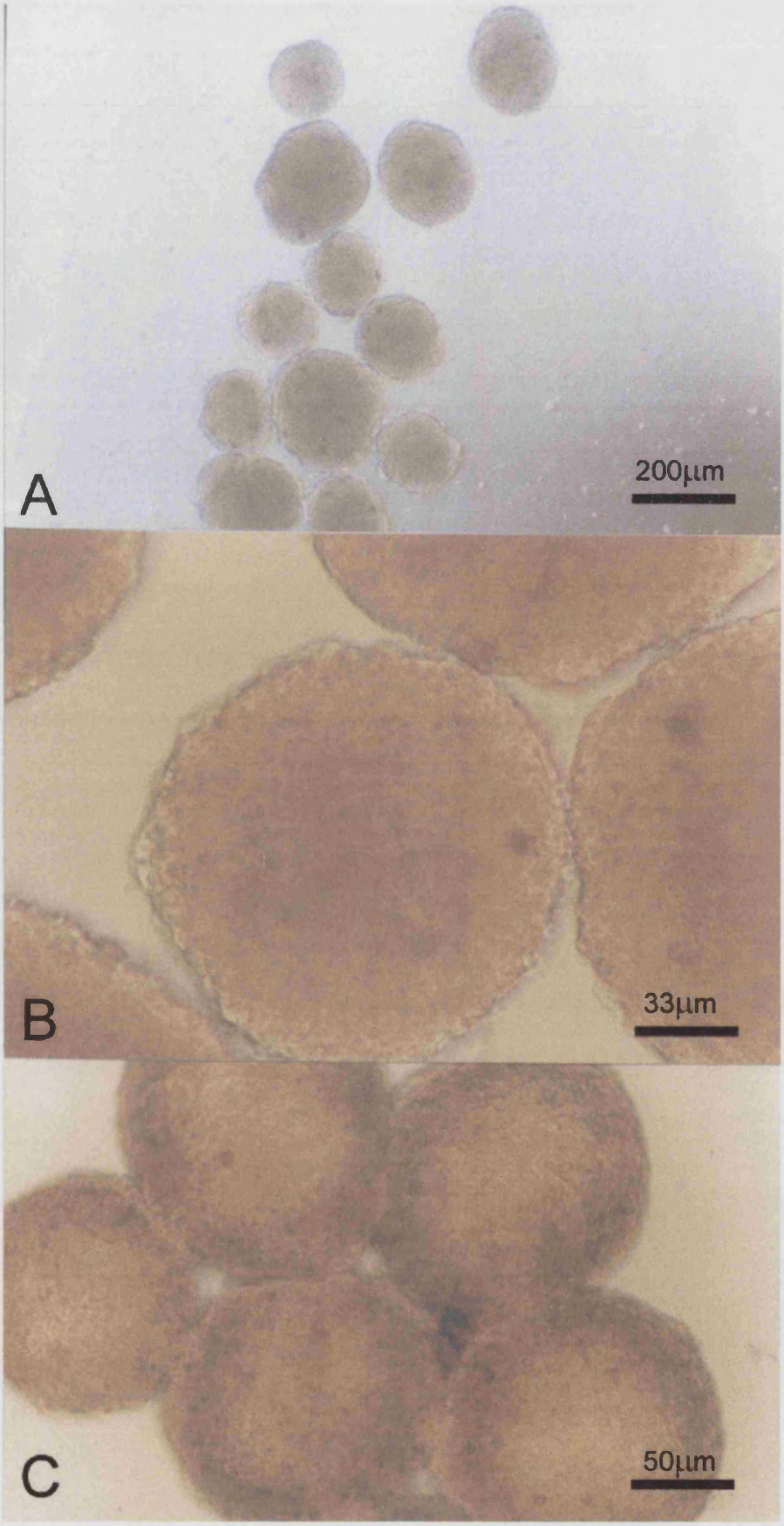

Figure 3-1: Mouse aggregates after 21 days *in vitro* form the characteristic sphere morphology, at around 200µm in diameter. Aggregates from rat tissue averaged around 340µm in diameter. Shown at (A) 5x (B) 30x and (C) 20x magnifications.

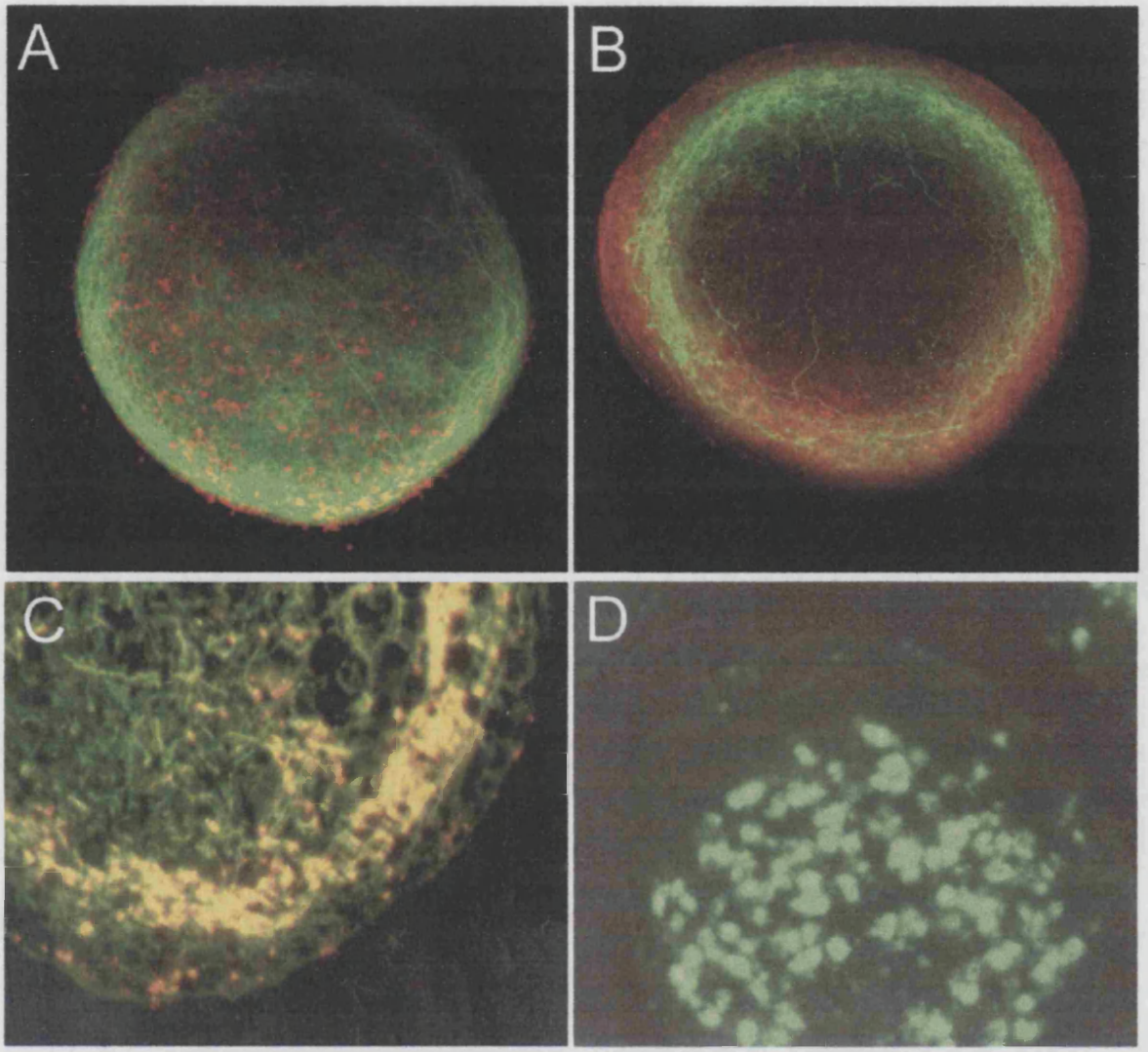

Figure 3-2 - Immunofluorescent labelling and confocal microscopical analysis of aggregates highlighting morphology and cellular arrangement.
(A) The intermediate layer of axonal processes interspersed with oligodendrocyte cell bodies. Neurofilament (axons - green) and carbonic anhydrase (oligodendrocyte cell bodies - red); magnification x30;
(B) - The same intermediate axonal layer, with the outer astrocytic shell. Neurofilament (axons - green) and glial fibrillary acid protein (astrocytes - red); magnification x30;
(C) - Axonal processes and myelin in an aggregate are indicated by yellow double staining. Neurofilament (axons - green) and myelin basic protein (myelin - red); magnification x40
(D) - Neuronal nuclei. Hu (neuronal cell bodies - green); magnification x30.

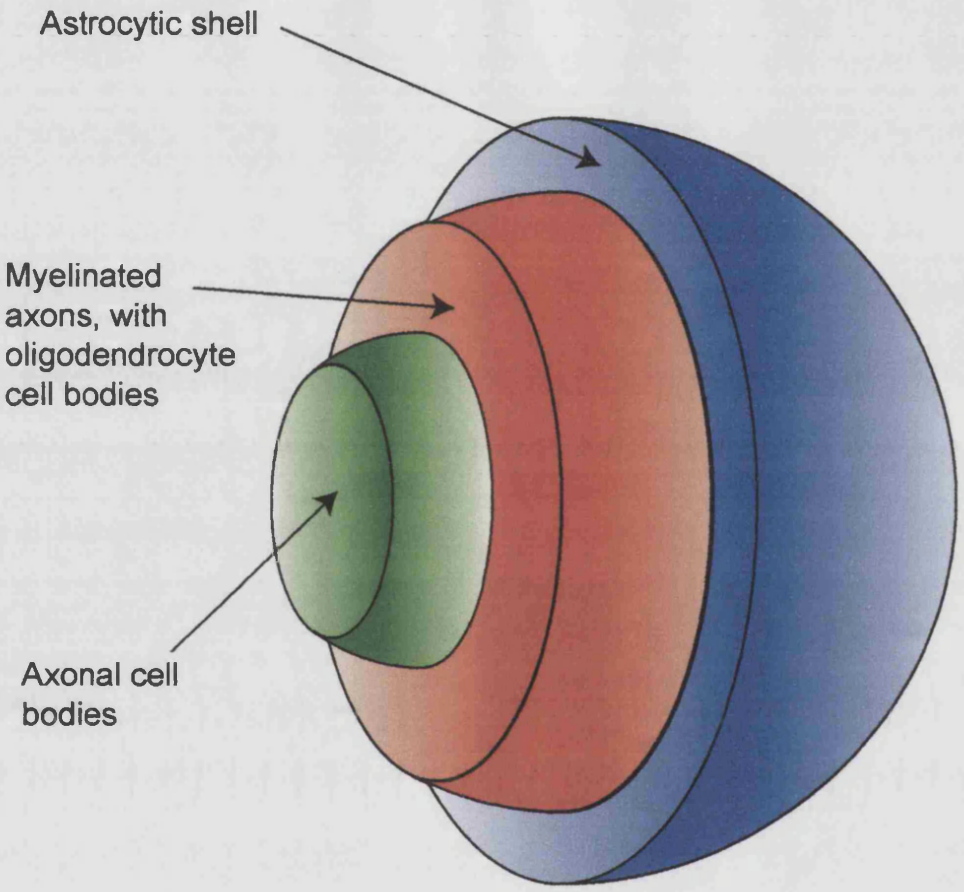

Figure 3-3: General 3-D cellular organisation of an aggregate. A shell comprising mostly astrocytes surrounds an intermediate layer containing myelinated axons and oligodendrocytes cell bodies. The aggregate core comprises mostly neuronal cell bodies.

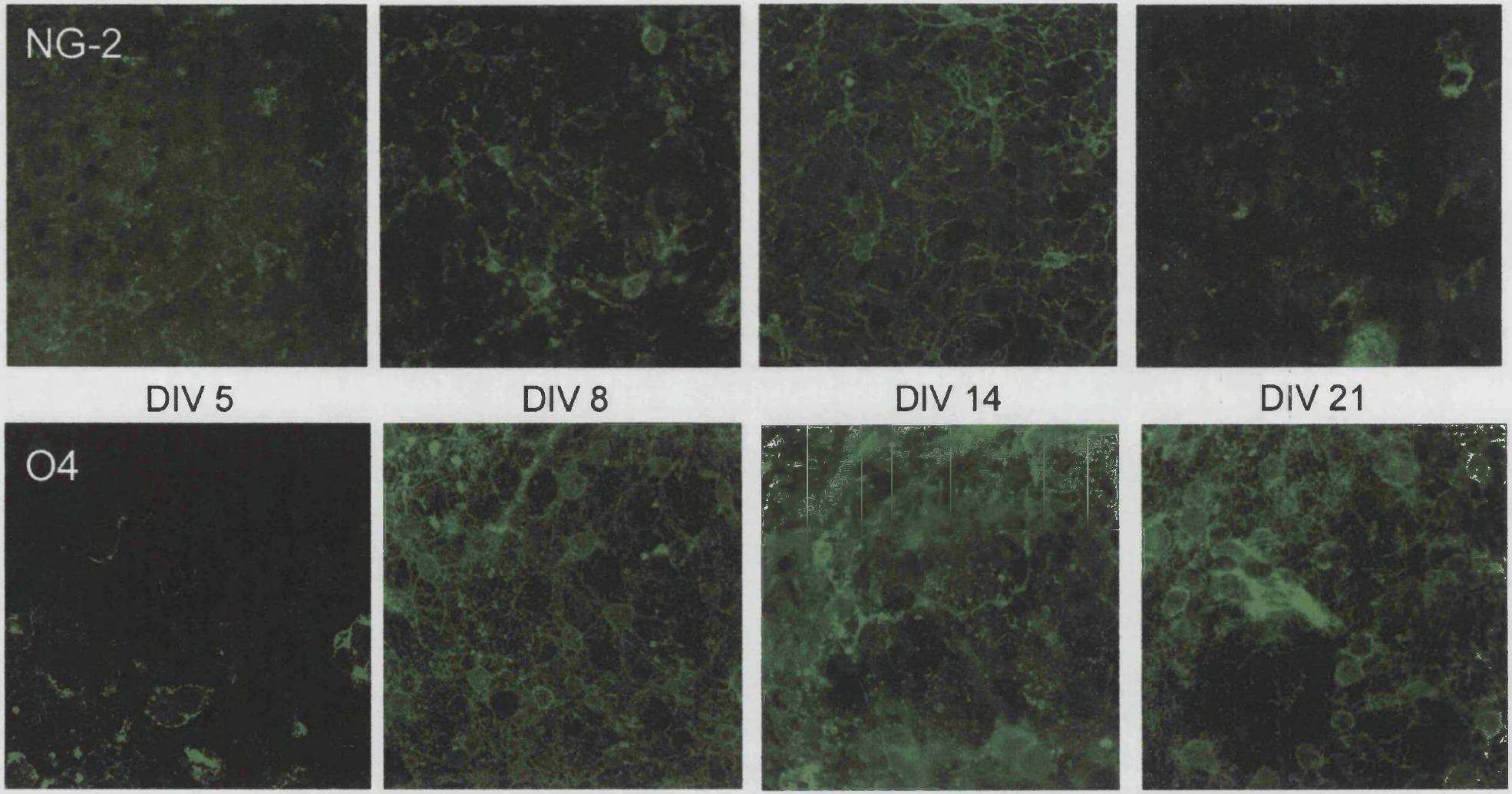

Figure 3-4: Confocal staining of NG2 (top) and O4 (bottom), markers for early and late oligodendrocyte progenitors respectively, over development of the aggregates from wildtype animals. NG2-positive cells appear first, with O4-positive cells being less abundant in the first instance. Both subsets persist to DIV 21.

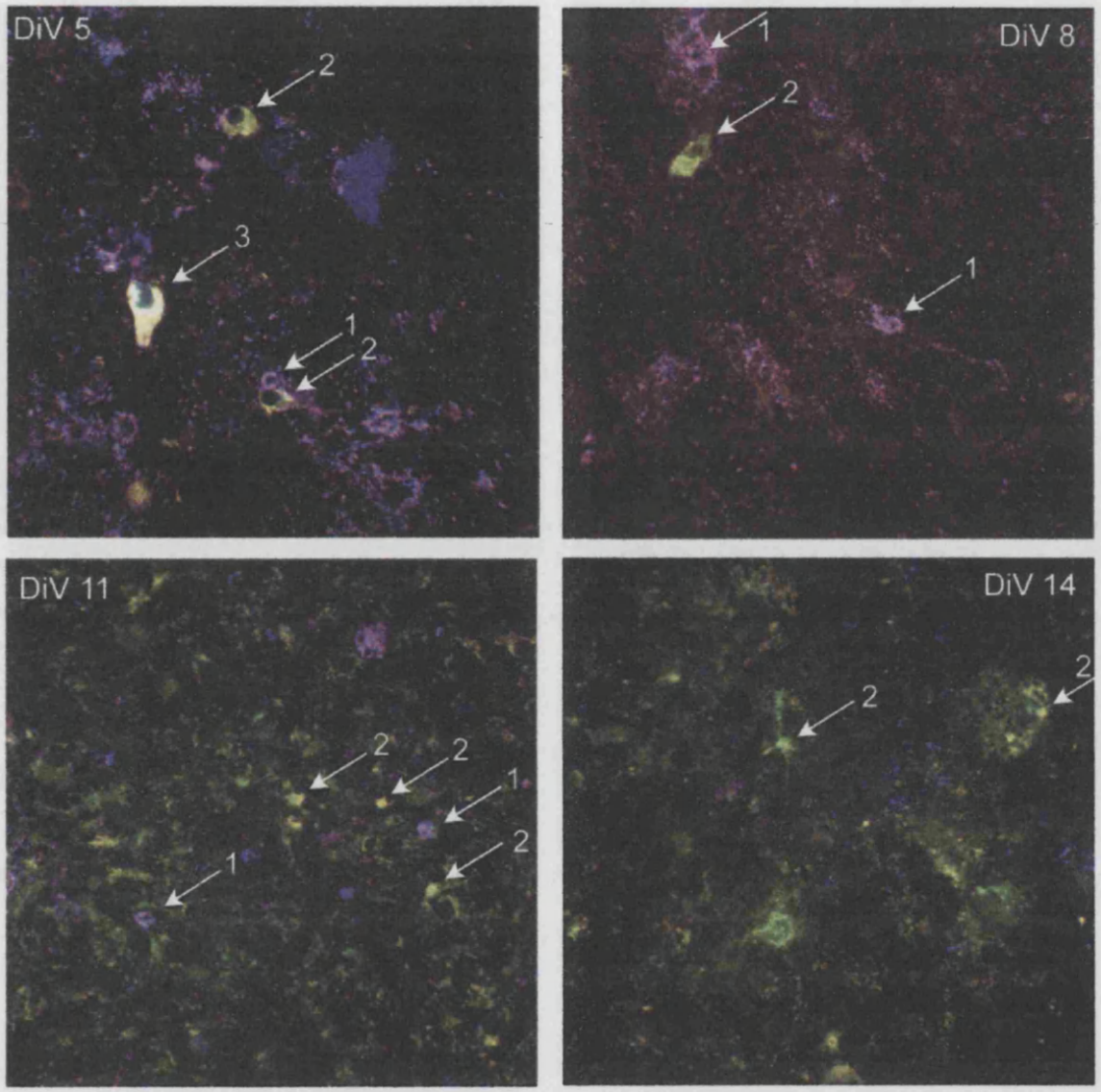

Figure 3.5: Confocal microscopy of early oligodendrocyte cell markers confirms the presence of oligodendrocyte progenitor and precursor cells in the aggregate cell culture. All progenitor subtypes appear to persist in lower numbers throughout the cell culture period, but are most abundant in the first 14 days *in vitro*.

Dual or triple staining indicates subtypes of progenitor cell, as described below and indicated by numbered arrows. Red - NG2; Green - O4; Blue - PDGFα-R.
1 - Purple: early (perinatal) oligodendrocyte progenitor
2 - White: late oligodendrocyte progenitor
3 - Yellow: Premyelinating oligodendrocyte

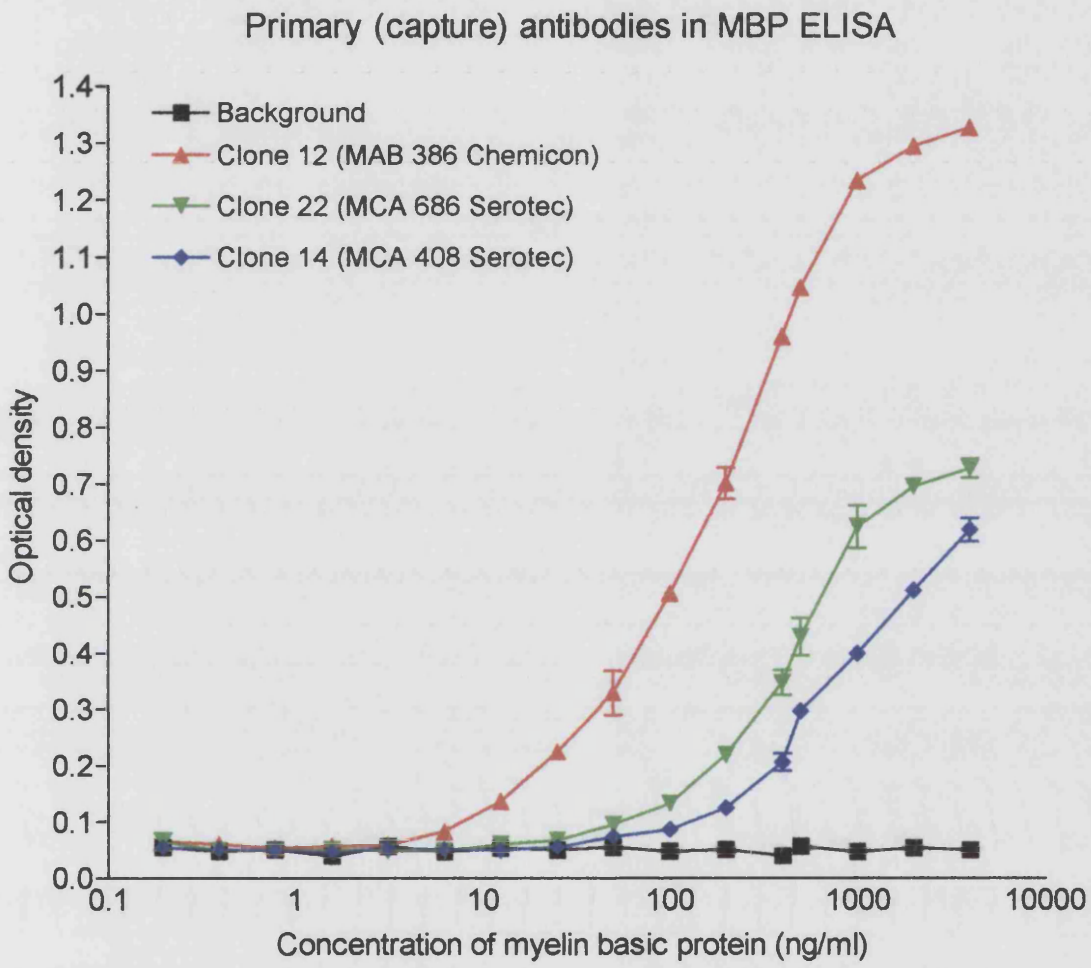

Figure 3.6: Comparing three monoclonal candidate antibodies for antigen capture in an MBP ELISA. Plates were coated with capture antibody at a diulution of 1:1000 and exposed to differing concentrations of MBP. Detect and report antibodies were also applied at 1:1000 prior to chromogenic substrate reaction to determine the most sensitive coat antibody with the lowest background reactivity at these concentrations. Clone 12 was used in subsequent ELISAs, as it yielded a high level of sensitivity without proportionally-increased background.

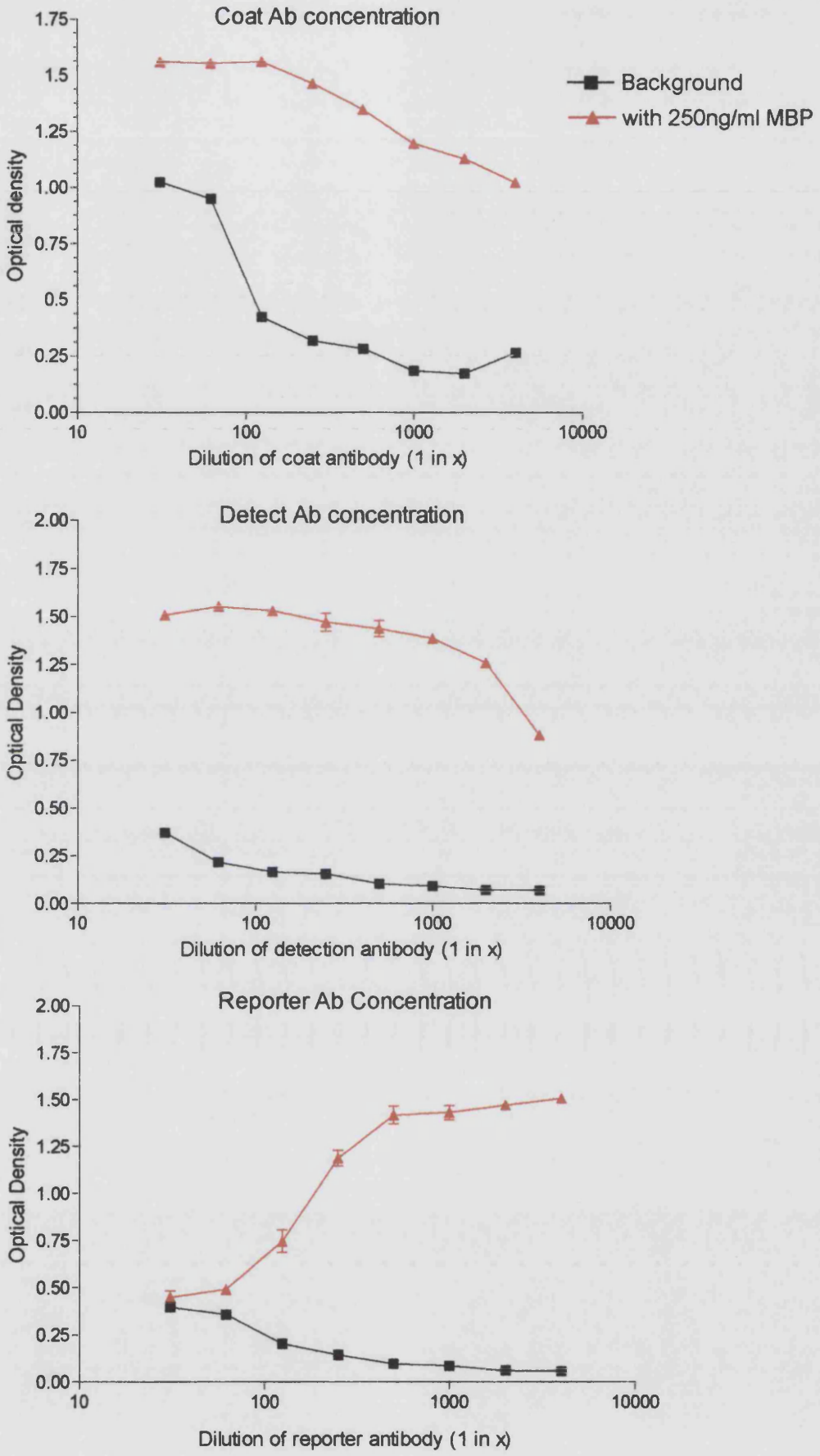

Figure 3.7: Optimisation of antibody dilutions for the MBP ELISA. ELISA antibodies were applied at varying dilutions (1:4000 to 1:31) and tested for optimum sensitivity with minimal background. All other antibodies were applied at 1:1000, and the antigen, purified human MBP, was used at 250ng/ml. In all cases, antibodies were found to be optimally sensitve at a dilution of 1:1000

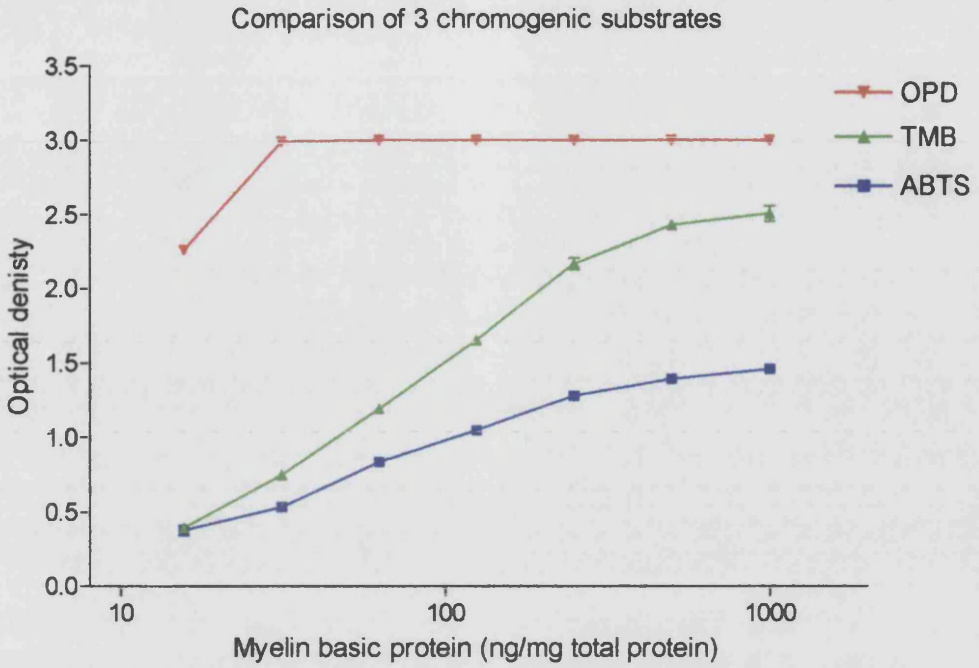

Figure 3.8a - 3 colour-producing peroxidase reactive substrates were tested for suitability and sensitivity in the ELISA. A standard test ELISA was used, with antibodies at 1:1000, and varied concentrations of antigen (purified human MBP). These chemicals vary in the intensity of colour produced over a five minute period. TMB was found to be the most suitable, producing a wide-ranging near-straight curve which did not saturate quickly.

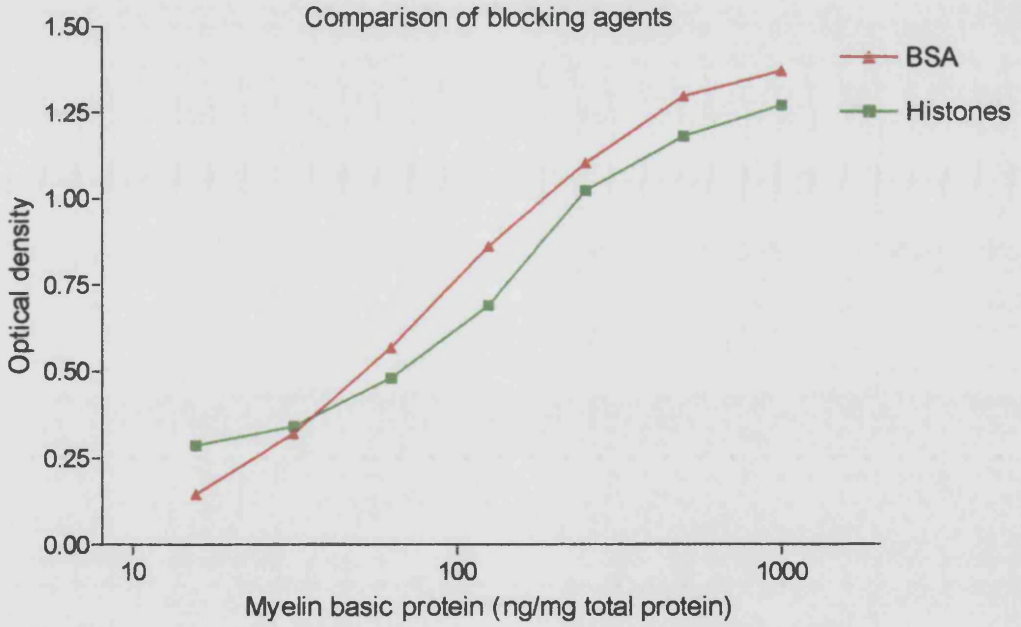

Figure 3.8b - Bovine serum albumin and histones were compared for blocking of non-specific binding over a range of MBP dilutions. The standard test ELISA was used, with antibodies at 1:1000. Standard curves were similar, and BSA was chosen as the blocking protein due to availability and low cost.

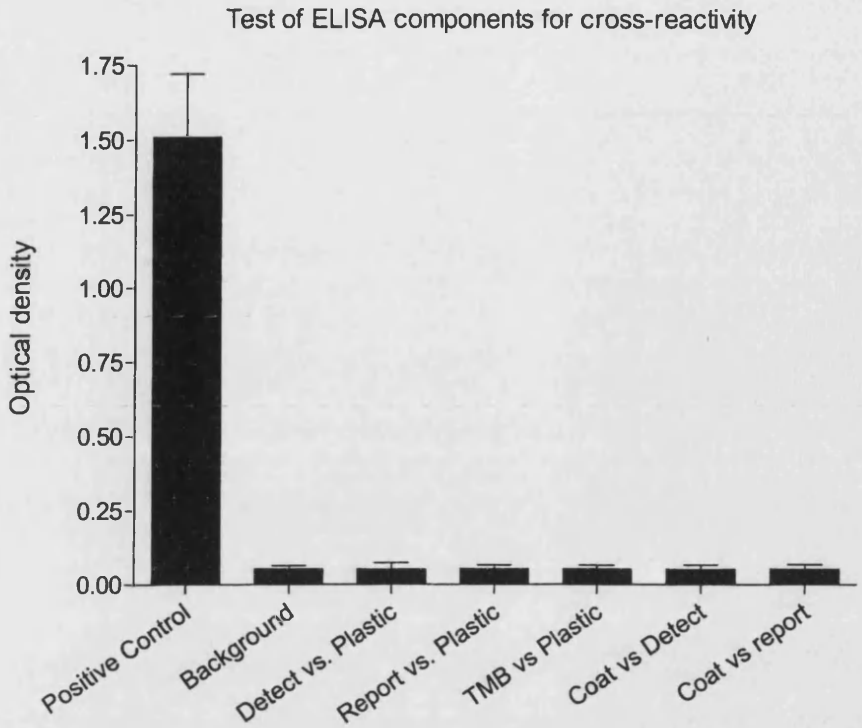

Figure 3.9a - Reagent cross reactivity may produce false-positive results in ELISA. Cross reactivity between ELISA antibodies was tested by omitting a component each time. For example, to test for cross-reactivity between the coat and detect antibodies, no antigen was applied. The assay was then run as normal and optical density produced was compared with background. None of the components were found to be cross reactive.

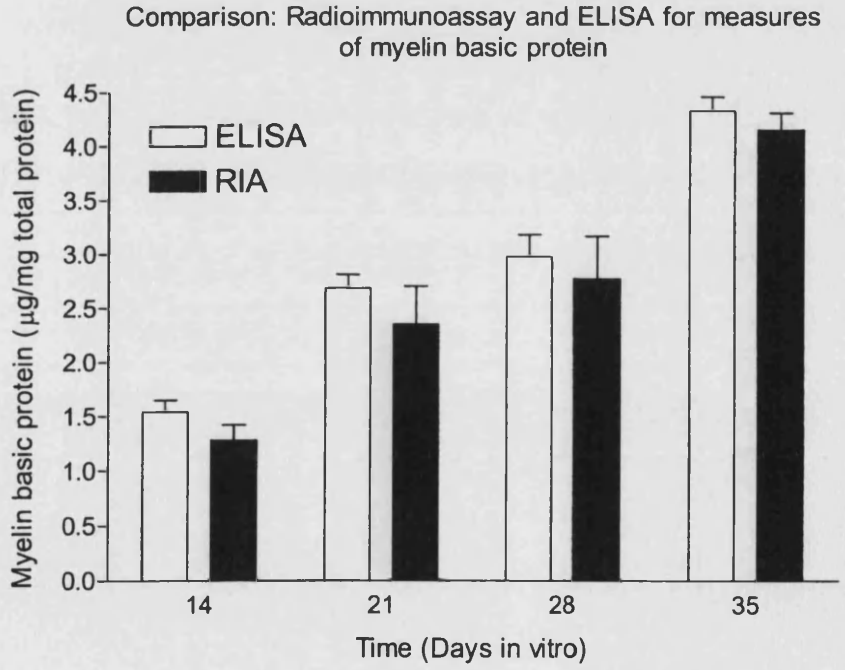

Figure 3.9b - Aliquots from a group of samples were measured with both the ELISA and Radioimmunoassay[1] techniques to test for inter-assay reproducibility. MBP values obtained were not significantly different between the two techniques indicating that the ELISA provides a reliable quantification of MBP. The ELISA results also have smaller errors.

[1]Copelman et al 2000 Glia 30 (4) p342-351

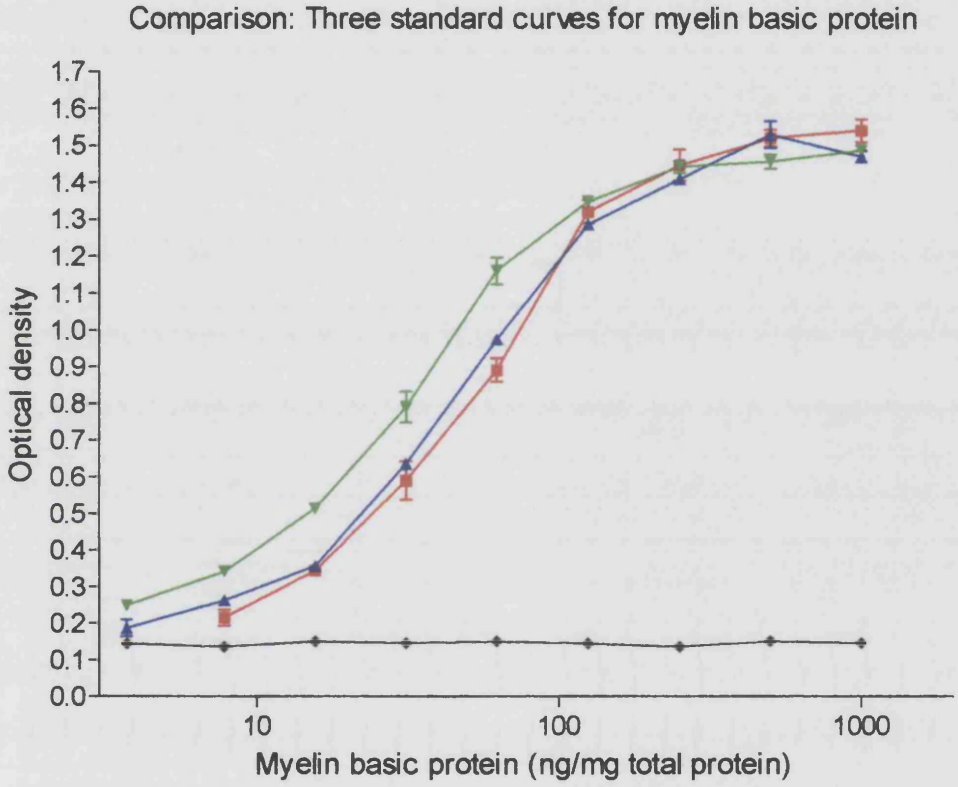

Figure 3.10 - Three assays were performed at different times to test the reproducibility of the MBP ELISA. Standard curves (MBP concentrations of 3.5 to 1000 ng/ml) were not found to be significantly different between tests. Even so, internal control samples were used in future assays which used more than one plate, to ensure interplate comparability.

using the ELISA, and no significant differences were found. Finally, three separate standard curves were run to test inter-assay reproducibility. All three experiments were performed using the same methodology but on different days, and as can be seen in Figure 3-10, they produced highly comparable standard curves, verifying reproducibility between assays.

3.2.3. Quantification of myelination and neurofilament accumulation

The ELISA for MBP was used, along with another in-house ELISA for NF (Petzold *et al.*, 2003) to characterise the development of mouse aggregates in terms of myelin accumulation and neuronal process growth. The C57BL/6 mouse strain is an inbred strain commonly used as the background in genetically modified mouse lineages. The use of inbred animals limits the biological variation that can occur in outbred populations. Initially, aggregates from BK1 and C57BL/6 animals were evaluated for MBP and NF content over the time-course of the culture. It was found that, while there were no significant differences in NF accumulation (Figure 3-11), the BK1 mice had significantly lower MBP levels at each time point. Following this, the C57BL/6 and ABH inbred strains were compared. ABH mice were found to accumulate significantly higher levels of myelin and NF *in vitro* (Figure 3-12), and were used in all subsequent experiments. With the intention of examining knockout mouse models for myelination and neuronal development, experiments were carried out to optimise the foetal dissection age. Pups were taken at embryonic day 16 and 18 (E16 and E18), at postnatal day 0 (shortly following parturition; P0), P1 and P2. As can be seen in Figure 3-13, MBP levels rose steadily in aggregates from E16 and E18 pups, with each expressing similar levels. Aggregates from pups dissected at P0 had high initial levels of myelin, which fell over the culture period. Foetal brain tissue dissected at postnatal

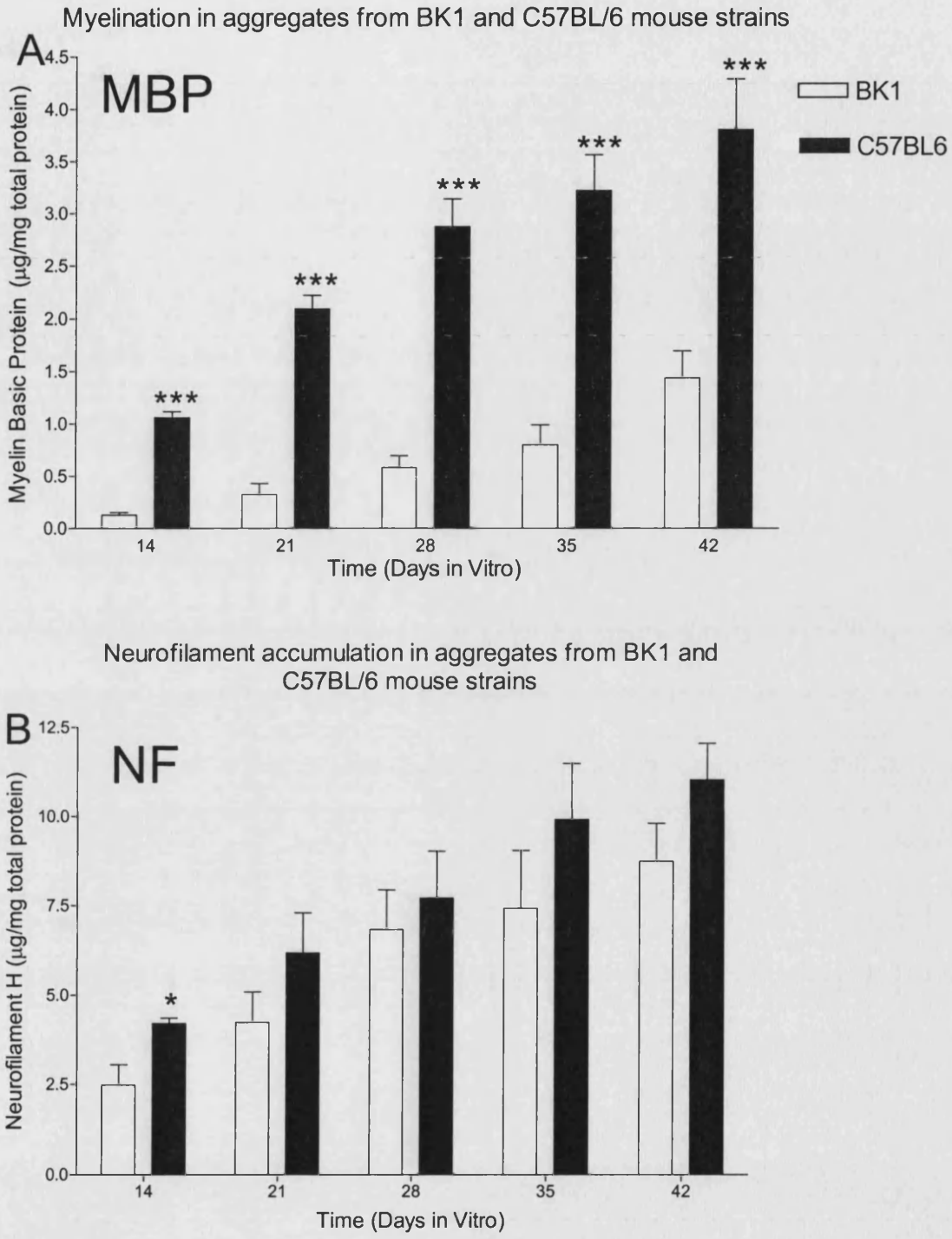

Figure 3-11: Myelination (A) and Neurofilament accumulation (B) was measured in aggregates from BK1 and C57BL/6 mice by ELISA for myelin basic protein and neurofilament H respectively. A higher degree of myelination was observed in the C57BL/6 strain, although neurofilament levels differed less. Outbred BK1 mice were chosen due to their high litter production, and inbred C57BL/6 mice are the background strain from which many gene knockout animals are engineered. Error bars represent SEM, and significances were evaluate by one-way ANOVA.

* - $P<0.05$ *** - $p<0.001$

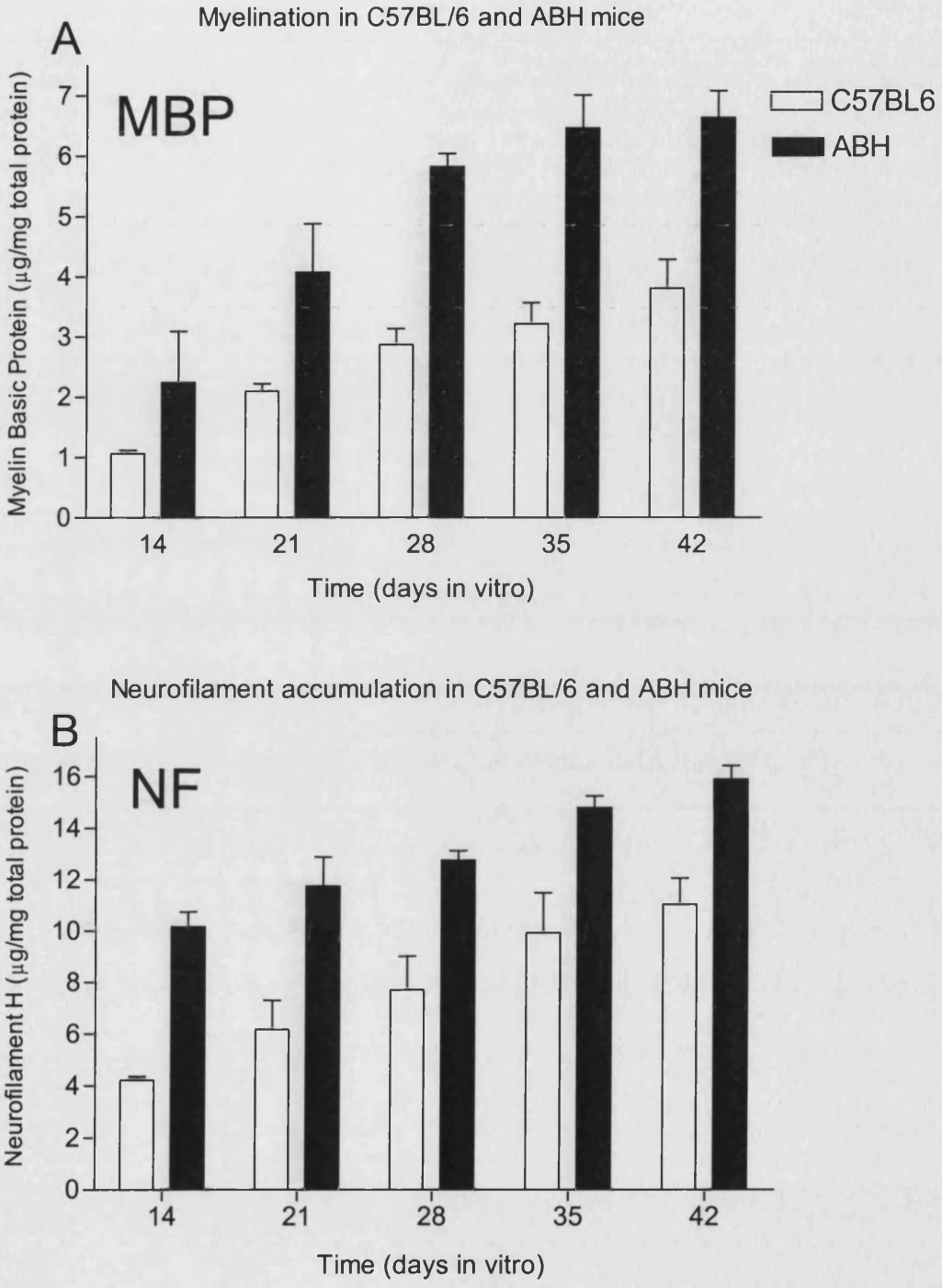

Figure 3-12: Myelination (A) and Neurofilament accumulation (B) in aggregates from the C57BL/6 and ABH mouse strains as measured by ELISA for myelin basic protein and neurofilament H respectively. ABH mice accumulate more myelin and neurofilament over the culture period than C57BL/6 mice so ABH mice were used in subsequent experiments. Each strain is inbred, with an inherent lack of genetic variation between animals. C57BL/6 is commonly used as a background strain in genetically modified animal lineages, whereas a well-characterised form of crEAE can be induced in the ABH mice.

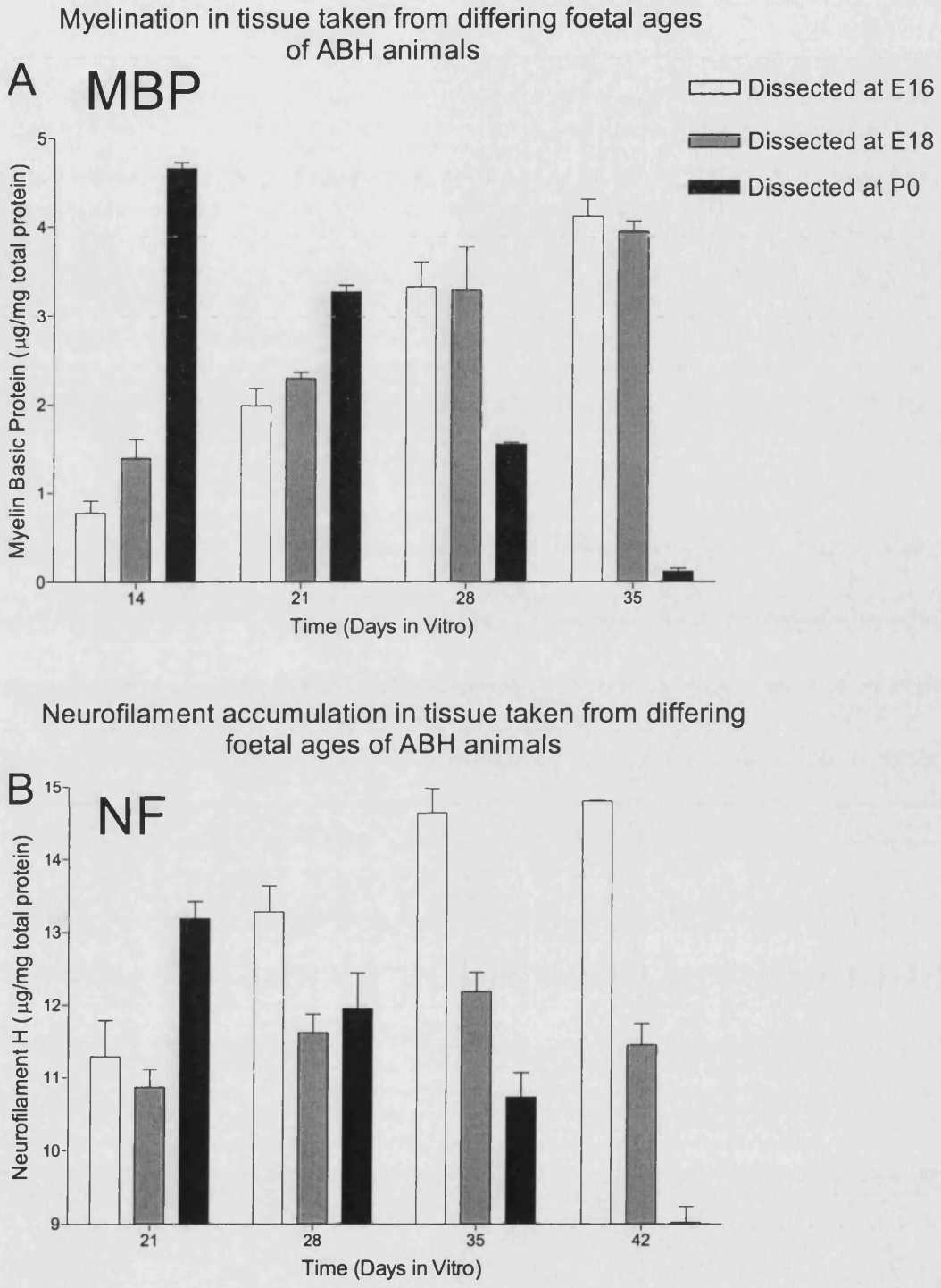

Figure 3-13: Myelination (A) and Neurofilament accumulation (B) in aggregates from ABH mouse tissue dissected at varying foetal ages as measured by ELISA for myelin basic protein and neurofilament H respectively. Tissue from pups taken at E16-E18 (1-3 days prior to birth) myelinate and accumulate neurofilament effectively; tissue from newborn pups (P0) lose both markers over the culture period. E16-18 pups were used for all subsequent culture experiments.

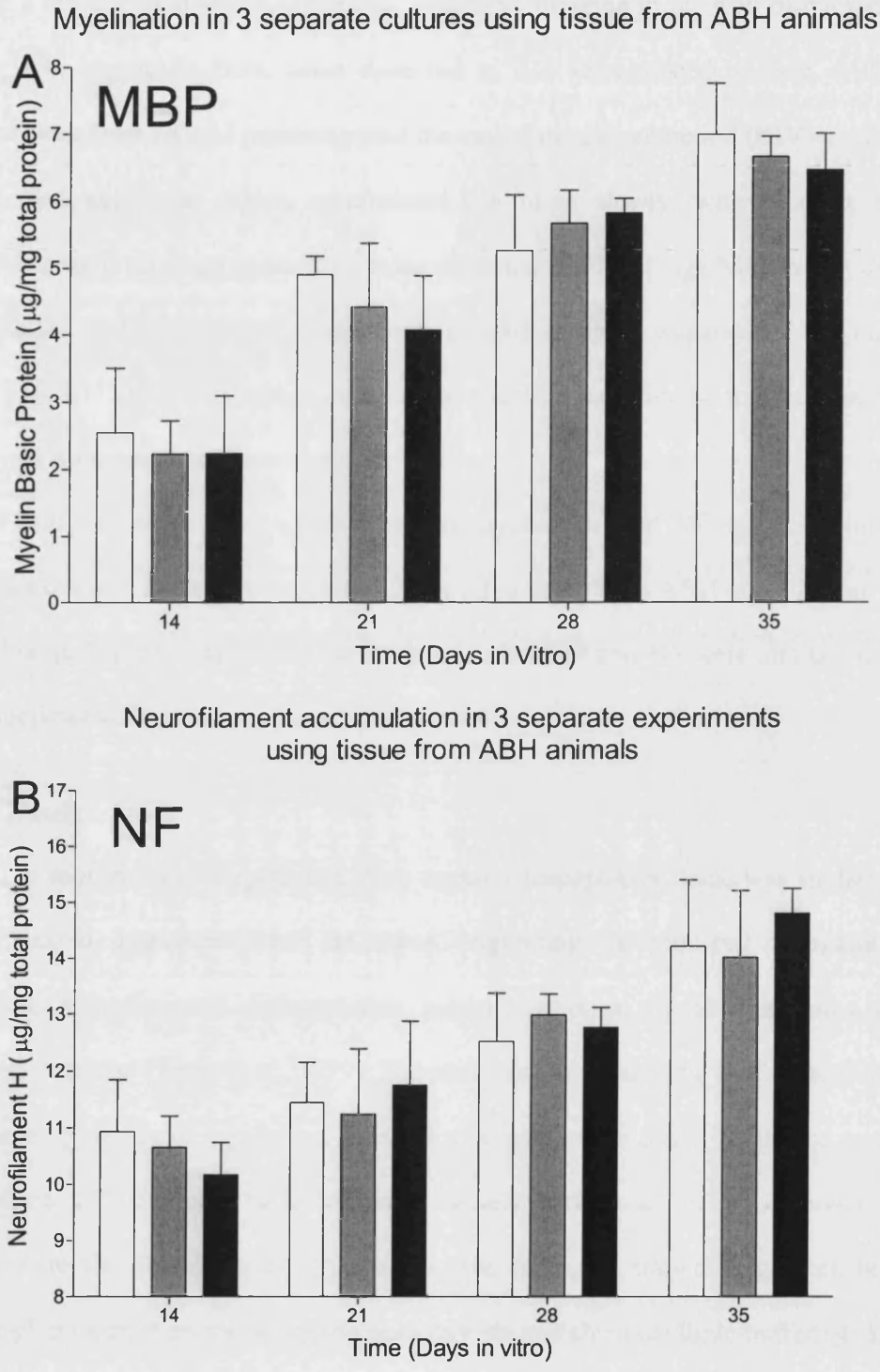

Figure 3-14: Myelination (A) and Neurofilament accumulation (B) was measured in aggregates from three separate ABH mouse cultures by ELISA for myelin basic protein and neurofilament H respectively. No significant differences were found, indicating that the culture preparation technique was reproducible, and that cultures developed on a similar time frame.

day 1 or 2 did not form viable aggregates, with cells adhering to the wall of the flask. NF levels in aggregates from tissue dissected at E16 accumulated quickly, with a sustained peak from DIV 35 persisting until the end of the culture period (DIV 42). E18 mice formed aggregates which accumulated NF more slowly, with a lower but acceptable peak level. Aggregates from tissue dissected at P0 had high NF levels at DIV 14, which fell rapidly thereafter, in tandem with MBP levels. It was decided that mice of ages E16, E17 and E18 would be used for future culture experiments to maximise the tissue yield from one set of time-matings.

Finally, reproducibility of the levels of myelination and NF accumulation *in vitro* was examined in three successive cultures using tissue from ABH mice. As can be seen if Figure 3-14, it was found that levels of both MBP and NF were similar in all three experiments.

3.3. Discussion

The morphology of aggregates from mouse telencephalon tissue was similar in arrangement to aggregates from rat tissue, suggesting that cell-cell recognition, interaction, migration and differentiation patterns observed in rat aggregates are conserved in mouse (Trapp *et al.*, 1979). The predominantly astrocytic shell surrounds a layer made up mostly of myelinated neuronal processes which could be likened to the interposition of astrocytes between blood vessels and axons *in vivo*. However, astrocytes are also found dispersed throughout the aggregate, providing support, both 'passively' in nutrient provision, debris phagocytosis and chemical/ionic buffering, and 'active' in neuronal survival and possibly synapse formation. The astrocytic layer may also play a more mechanically protective role to the fragile processes within, as aggregate collision with other aggregates is inevitable. Neuronal cell bodies are

concentrated in the centre of the aggregate in a position least vulnerable to chemical or mechanical damage. Astrocytes have been found radiating inwards from the shell, providing support for the neuronal cells bodies at the centre (personal communication, L.Diemel). Retrograde axonal transport may be responsible for some nutrient provision to the soma. The temporal pattern of myelination in mouse aggregates is similar to that of rat aggregates, which in turn has been likened to myelination *in vivo* (Kruger *et al.*, 1999; Matthieu *et al.*, 1978), confirming the mouse aggregate system as being a relevant model for studying developmental myelination. A reduction in myelin levels observed after around 30 DIV in the first rat aggregate experiments (Matthieu *et al.*, 1978) was not mirrored in this system, or in preceding experiments with rat tissue (Copelman *et al.*, 2001; Kruger *et al.*, 1999; Loughlin *et al.*, 1997), making it possible to carry out valid experiments with culture periods of six weeks. This improved longevity of culture may be influenced by a reduction in the time period between termination of the mother and getting cells into culture, meaning that more viable cells were seeded. By confocal microscopy, oligodendrocyte progenitors follow a similar developmental pattern to those in rat aggregates (Diemel *et al.* 2003). Markers for NG2 and PDGF-α receptor appearing early on in the culture period, followed by O4, galactocerebrocide and MBP–positive cells as maturation and differentiation take place. Oligodendrocyte progenitor cell markers persist throughout the culture period. This provides a potential pool of replacement oligodendrocytes following demyelinative insult (Nait-Oumesmar *et al.*, 1999). As these progenitors are situated in the intermediate aggregate layer alongside neuronal processes, and in direct proximity to both astrocytes and neuronal cell bodies, they have access to chemical cues from these cells which may control development or differentiation.

MBP and NF levels appeared to be lower in the initial cultures from BK1 out-bred animals, increasing in the C57BL/6 inbred mice and highest in ABH inbred animals. This could be attributed to inter-species variation. It also could be due to improvement in dissection techniques over the first months of culture work. The amount of time it took to seed one culture, from termination of the mother to seeding, was reduced dramatically by the time ABH mice were being used. However, culture MBP and NF levels were found to be highly reproducible in ABH cultures, suggesting that an optimum dissection technique and time had been reached by this point. Despite aggregates from mouse tissue being smaller than their rat counterparts, MBP levels are comparable between the two, suggesting that there are similar numbers of smaller myelinated fibres in the mouse culture, as opposed to less myelinated processes. The size of a comparable neuron and its dendritic arbour is greater in rat than in mouse (Purves & Lichtman, 1985), supporting this hypothesis. The age of foetal dissection is a crucial variable controlling effective aggregate formation and development. For example, myelination in cultures using postnatal tissue fell over the culture period as aggregates shrank and disintegrated. This is likely to be due to changes which occur at birth, as foetal pups taken the day before birth form viable aggregates. Birth may be a trigger for large-scale differentiation of oligodendrocytes and myelination; differentiated cells may not be as well equipped as progenitors for survival after mechanical dissociation. Differentiation may also elicit changes in cell-cell recognition or interaction, so that cells form weaker bonds and therefore non-viable aggregates. NF levels in cultures from E16 mice are markedly higher than those in cultures from E18 mice, despite the fact that they have very similar levels of MBP. Again, it is possible that a higher proportion of undifferentiated neural precursors in the E16 animals at

dissection may confer survival, and thus higher NF accumulation, with dissociation causing death of differentiated neurons. The same MBP levels indicate that there are more unmyelinated axon-like processes in cultures from E16 animals, or that MBP is present in a form not associated with myelin at higher levels in E16 cultures.

4. Evidence for cannabinoid mediated neuroprotection *in vivo*

4.1. Introduction

EAE is an inflammatory demyelinating disease of the CNS inducible in a variety of species. CREAE in the ABH mouse has been found to be a representative model of multiple sclerosis (Baker *et al.*, 1990). Animals have a relapsing-remitting time-course of paralysis, with worsening residual functional deficit over the course of the disease. The events of blood brain barrier dysfunction, cellular infiltration demyelination and axonal loss are similar to that occurring in multiple sclerosis and are most evident in the spinal cord. This means that a few strategic lesions can cause a relatively high functional deficit, enabling accurate disease scoring using a scale of well-defined clinical signs in addition to stereotypical weight change fluctuations. The CB_1R-KO mouse, originally on the EAE-resistant CD1 mouse background (Ledent *et al.*, 1999) was bred on to the ABH background by back-crossing to enable induction of CREAE and study the role of the cannabinoid system in this model (Brooks *et al.*, 2002). For these studies, spinal cords were removed from adult CB_1R-KO and ABH wildtype mice either during the acute attack, first, second, third or fourth remission for assessment of the accumulation of axonal dysfunction. The CB_1R-KO mouse accumulates neurological deficits that rapidly reach unacceptable severity limits following the first relapse of disease where there is chronic paralysis, so data for the second, third and fourth remissions is confined to wildtype animals. Spinal cord tissue was homogenised and tested for MBP, NFH^{SMI35} and NFH^{SMI32}. SMI-35 and -32 are monoclonal antibodies against phosphorylated and dephosphorylated NF respectively (Sternberger & Sternberger, 1983). Phosphorylated NFs are stable in the developed neuron, with dephosphorylated NF representing a damaged subset of NFs, compromising the cytoskeletal structure (Howland & Alli, 1986; Meller *et al.*, 1993; Trapp *et al.*, 1998).

As there is no standard against which to compare dephosphorylated NF, and as it represents a subset of NFH^{SMI35}, it is presented as a ratio over NFH^{SMI35}. Finally, caspase 3 is investigated as a potential death effector mechanism of function loss in EAE (Ahmed *et al.*, 2002). Total and cleaved (activated) caspase 3 were quantified by Western blotting and computer analysis.

4.2. Results

4.2.1. Clinical and pathological features of EAE in wildtype and CB_1R knockout animals

The n-numbers used for statistical analyses in Section 4.2.1 were all 11 or above, except for remission 2 and 3 spinal cords, where the n=5 and 6, respectively. To confirm lack of the CB_1 receptor in knockout animals, PCR for reverse-transcribed CB_1R mRNA was carried out. As can be seen in Figure 4-1, there is no receptor expressed in the knockout mice, or in cultures derived from them. Lack of the receptor was also functionally tested using WIN55-212-2, a cannabinoid agonist (20mg/kg intraperitoneal injection in dimethyl sulphoxide:Cremophor:PBS (1:1:18)) and failed to induce significant catalepsy, visually assessed hypomotility or hypothermia. The relapsing-remitting disease course is associated with increasing functional deficit over a series of relapses in CREAE (Figure 4-2). These are associated with hind-limb paralysis, as illustrated photographically in Figure 4-3. It was found that, when initiating EAE in CB_1R-KO mice, the disease onset and acute attack proceeded in a similar manner to the wildtype, with a peak clinical score of around 4. Following this however, the almost-complete recovery associated with the disease in wildtype animals did not usually occur. Instead, a residual deficit represented by a score of around 2.5 was observed in the first remission period (Figure 4-4). Following the second attack,

knockout animals exhibited chronic limb paralysis that reached unacceptable severity limits and demanded euthanasia. In an open-field activity monitor, motor function impairment can be quantified by measuring the distance an animal travels in a given amount of time. In wildtype animals, movement is reduced with each successive disease state (Figure 4-5). A more severe deficit was observed in knockout animals, with deficit following the first attack being equivalent to that following four paralytic attacks in the wildtype mouse. Immunostaining for MBP in the spinal cord shows progressive loss over the course of the disease (Figure 4-6). Accompanying immunostaining for NF shows a marked lack of neuronal somata and processes, indicating that NF loss and demyelination are parallel processes.

4.2.2. Demyelination and loss of neurofilament in EAE

Myelin levels as quantified by ELISA for MBP showed a trend towards demyelination over the course of the disease (Figure 4-7). In wildtypes, there was no significant ($p<0.01$) difference between control, acute attack and 1st remission animals, but a trend was evident signifying demyelination. By the third remission, a highly significant ($p<0.001$) drop in MBP levels was observed, with no change in the MBP levels following that. Knockout animals did not have significantly different MBP levels at any disease stage, but again there was a trend towards demyelination at each point. NF levels, as quantified by ELISA, also showed reduction over the disease period. In wildtype mice, the trend was towards loss of NF over the disease course, culminating in a highly significant loss in fourth remission animals. Samples from remission 2 and 3 agreed with this trend, but errors were larger in these samples. Knockout levels were

A - Aggregate cell culture

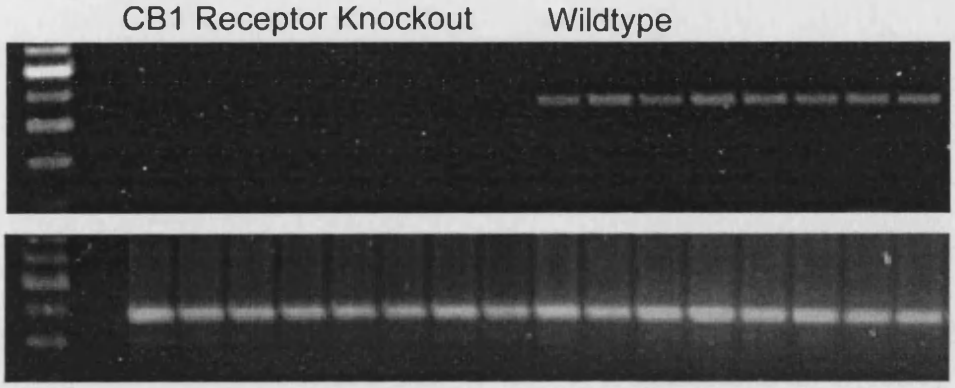

GAPDH

B - ABH mice

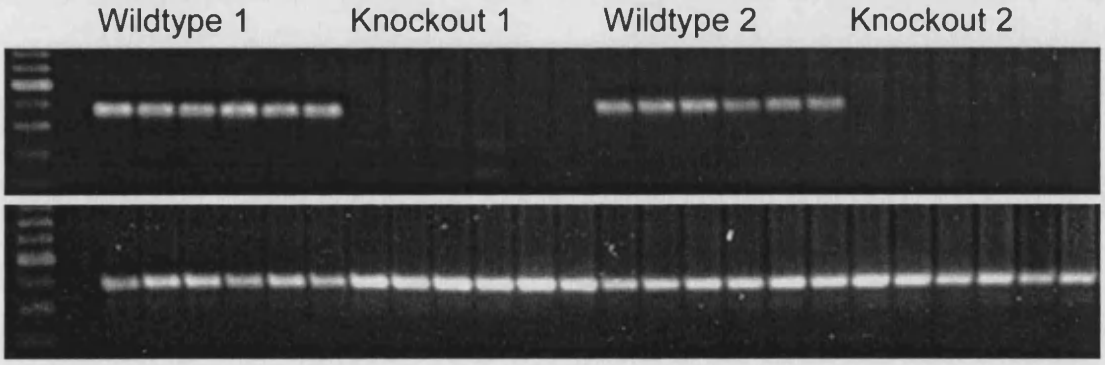

GAPDH

Figure 4-1: PCR for cannabinoid receptor 1 gene (Cnr1) mRNA confirms that this receptor is not expressed in knockout animals, but is present in their wildtype counterparts. (A) Tissue from the aggregate cell culture (B) Spinal cord tissue from ABH mice. The lower panel in both (A) and (B) shows the mRNA expression of GAPDH, a housekeeping protein, to validate equal RNA loading onto the gel.

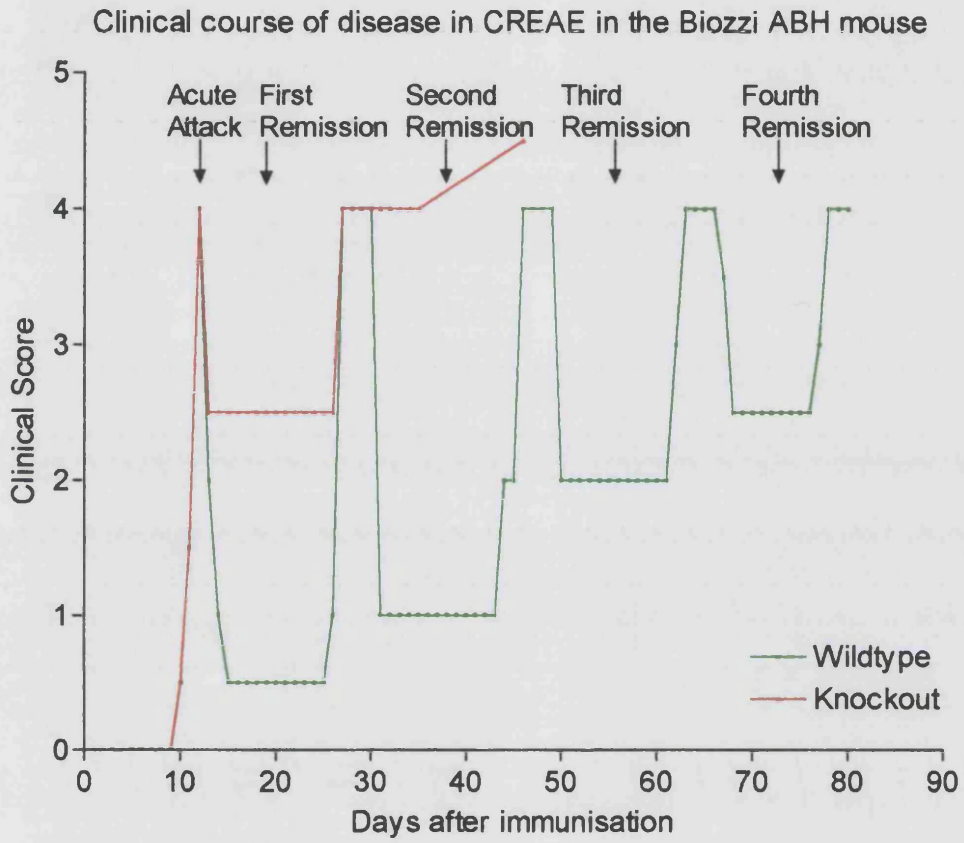

Figure 4.2 - Graph illustrating the clinical course of disease in biozzi ABH mice with chronic relapsing EAE. The green line represents the course in a wildtype mouse, the red in a CB1-R knockout mouse. Wildtype mice have a relapsing-remitting disease course with a step-wise increase in functional deficit with each remission. Spinal cords were taken from mice without disease (control), and in the acute, first remission second, third and fourth remission stages of disease (fourth remission is clinically equivalent to a chronic disease state). Knockout mice often survive until the first relapse, from which they do not remit and either die or are terminated. Therefore, it is not possible to sample from knockout mice following the first relapse.

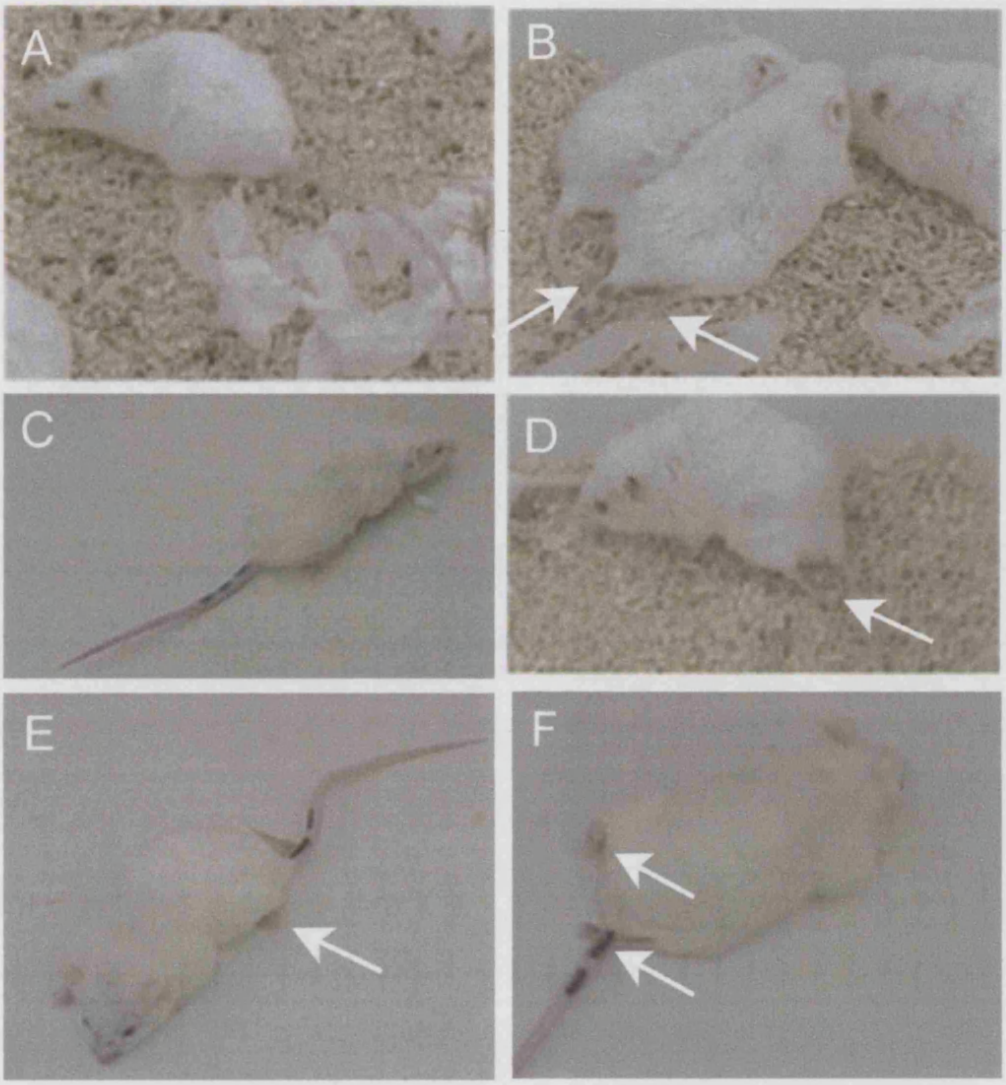

Figure 4.3: Photographs of the stages of disease in CREAE in ABH mice. Following injection of 1mg of spinal cord homogenate in Freund's adjuvant on day 0 and 7, animals developed a relapsing-remitting disease course. Each attack and relapse is characterised by tail and hind limb paralysis, indicated by white arrows. This is not seen in remissions, but by remission 4, chronic paresis and hind limb paralysis has often become permanent.

A - Normal, pre-disease control B - Paralysis in acute attack
C - Recovery in remission 1 D - Paralysis in relapse 1
E and F - Permanent paresis in remission 4

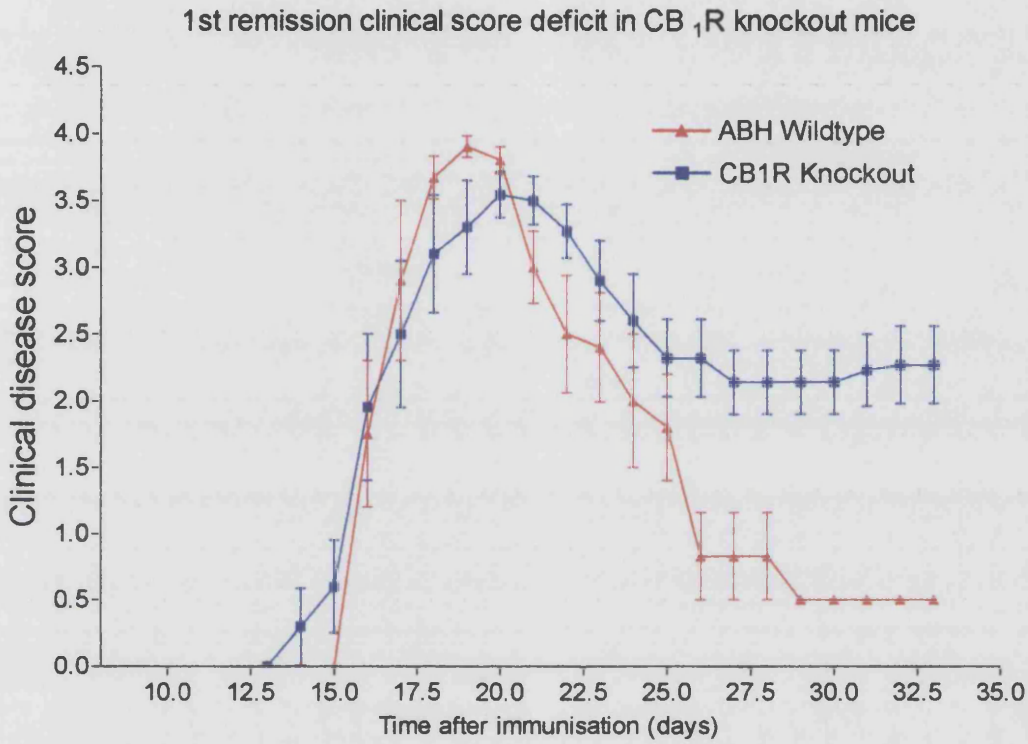

Figure 4.4: Increased clinical score deficit is observed following the acute CREAE attack in knockout mice compared with wildtypes. Following injection of 1mg of spinal cord homogenate in Freund's adjuvant on day 0 and 7, animals developed a relapsing-remitting disease course.The course of clincal disease as assessed by scoring differs between wildtype and knockout animals over the first relapse. Knockout animals accumulate more clinical deficit after the first acute attack.

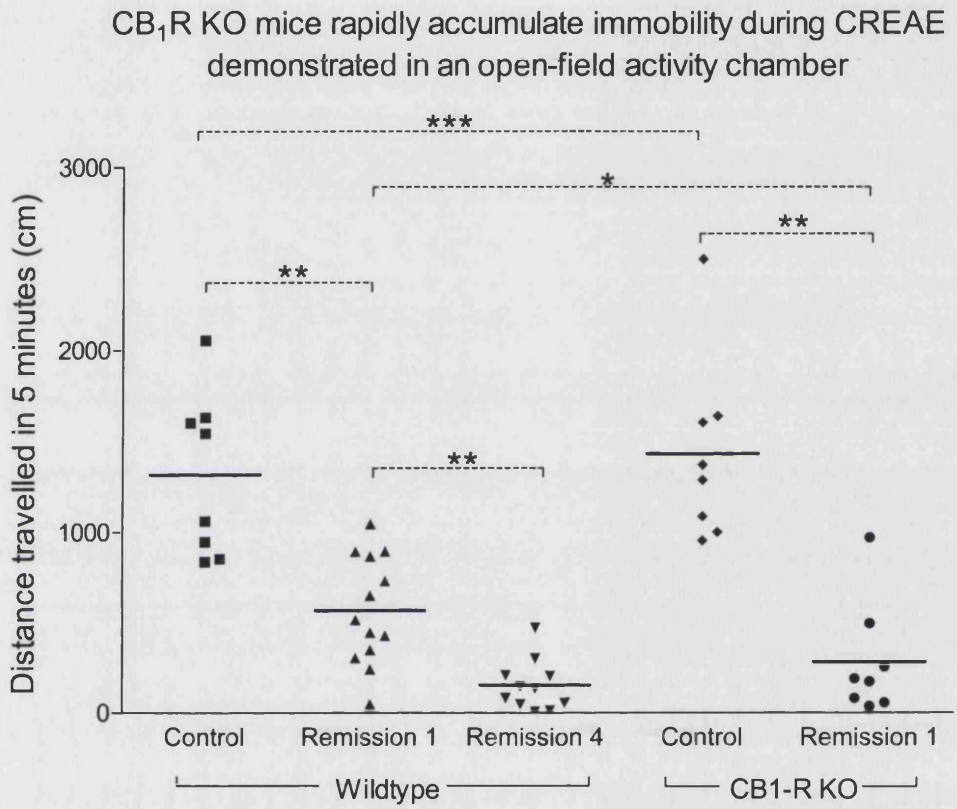

Figure 4.5: Motility deficit in crEAE increases with worsening disease condition. This is illustrated using an open-field activity chamber, where the distance travelled by a mouse in 5 minutes is recorded. The distance travelled by wildtype mice is reduced in each sucessive disease state, with each symbol representing movement in one individual animal. The deficit observed in CB1R-KO animals, however, worsens more quickly. Fourth remission wildtype mice are comparable with first remission knockout mice in this test, illustrating the increased functional deficit in CB1R-null animals.

* - $p<0.05$; ** - $p<0.0005$; *** - $p<0.00001$

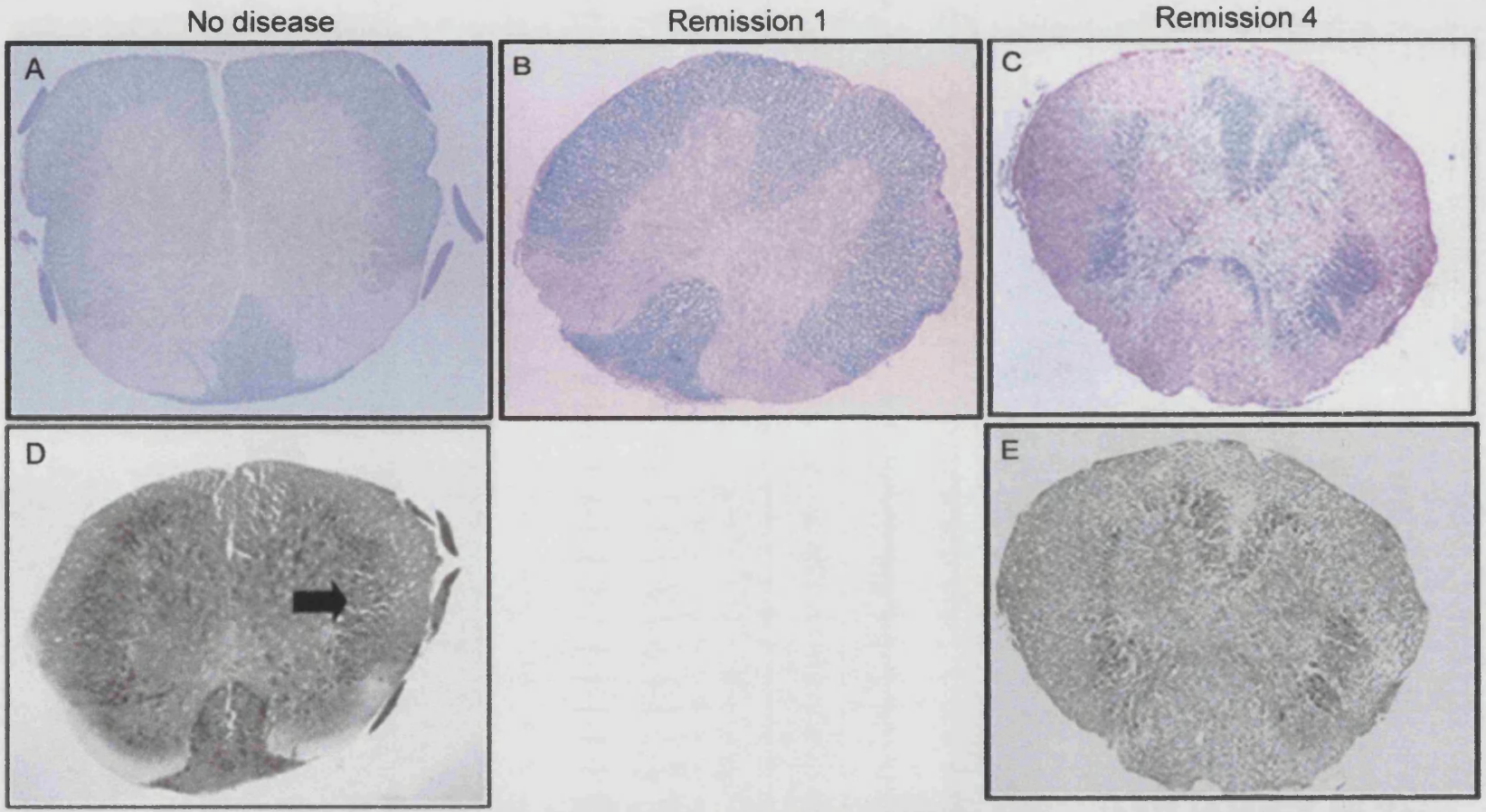

Figure 4.6: Staining of decalcified wax sections for myelin (colour) and neurofilament (greyscale) illustrating progressive loss of each from the spinal cord over the course of EAE. Luxol fast staining for myelin shows early degradation around peripheral regions at remission 1 (B), and marked loss by remission 4 (C). A similar pattern is observed with axonal processes (D and E), as stained with the Bielschowsky silver stain method.

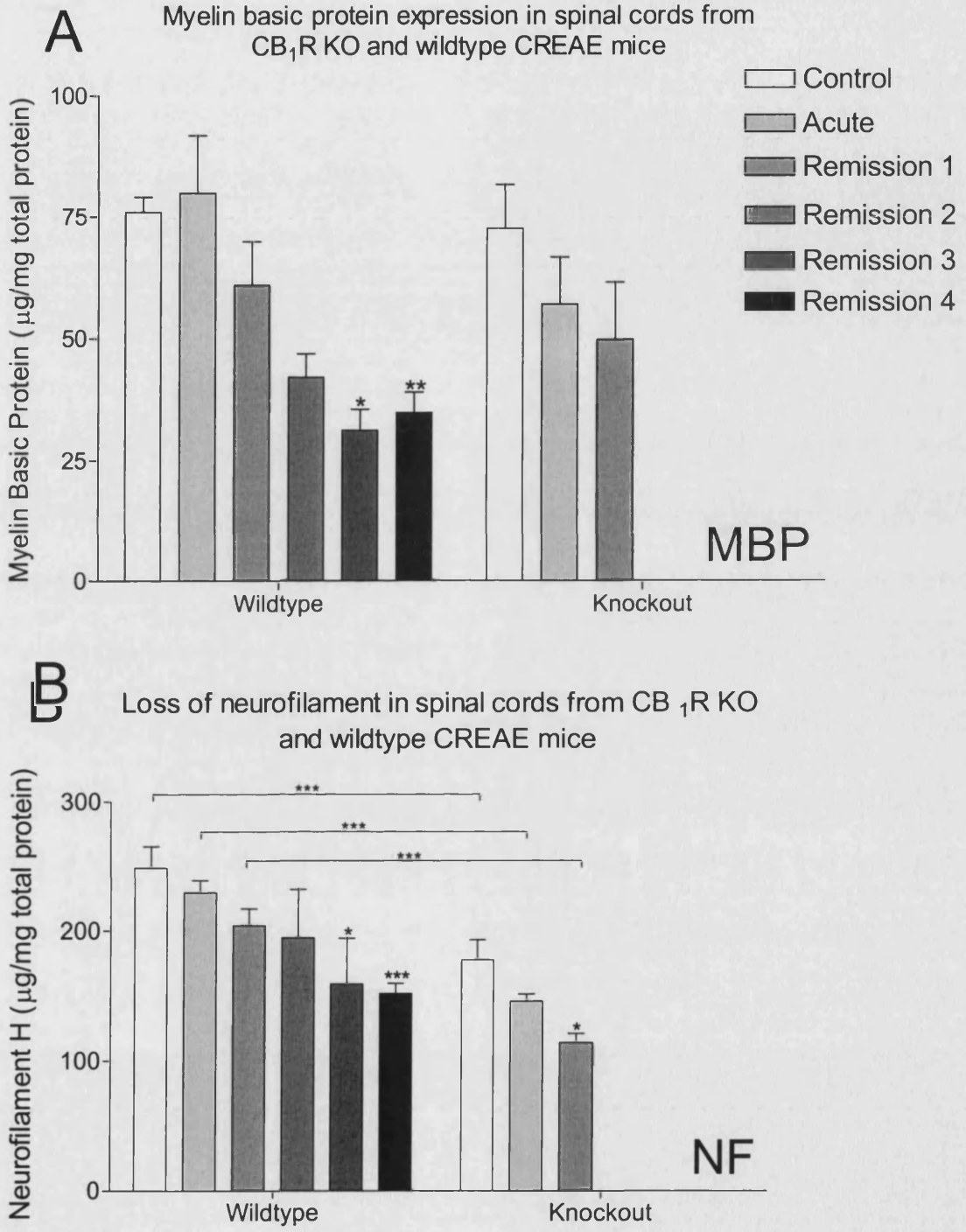

Figure 4.7: Significant demyelination (A) and Neurofilament loss (B) in spinal cords from mice with cr-EAE over the timecourse of the disease as measured by ELISA. Demyelination is not significantly different between wildtypes and knockouts, but loss of NfH^{SMI35} is increased in CB1R KO mice, indicating that the CB1R is neuroprotective in the demyelinative state. * - $p<0.05$; ** - $p<0.01$; *** - $p<0.001$

significantly lower at all disease stages than in their wildtype counterparts, and fell by around 33% by remission 1, compared to 20% drop in wildtypes over the same period.

4.2.3. Increase in the NFH^{SMI32}:NFH^{SMI35} ratio in EAE

SMI-32 reactive NF is considered to be damaged or compromised due to dephosphorylation, and can be measured by ELISA. In wildtype animals, it was found that levels of NFH^{SMI32} normalised over total protein increased from control in the acute phase, and then fell to near baseline levels during remission 1, remaining so into remission 2 (Figure 4-8). Levels increased in subsequent remissions so that by the fourth remission, levels were 8 times that of control. In control CB_1R KO mice, prior to disease induction, NFH^{SMI32} levels were elevated over wildtype controls. Levels increased proportionally to wildtypes in the acute phase and fell in remission. When NFH^{SMI32} was presented as a ratio to NFH^{SMI35}, these trends held true, but the differences between wildtype and knockout animals were accentuated.

4.2.4. Differentially Increased Caspase 3 levels in wildtype and CB_1R-KO animals with EAE

Analysis of caspase 3 by Western blotting allowed quantification of the total and active isoforms of the protein, by virtue of the polyclonal antibody used (Figure 4-9). Total caspase 3 expression, normalised over actin expression, was at negligible levels in control wildtype animals (Figure 4-10). During the acute attack, these levels rose sharply to as much as 45 times the control level, and fell slightly to around 30 times control in remission 1. Levels rose again in remission 4 to around those observed in the acute attack. Total caspase 3 levels in knockout control animals were similar to those in wildtype controls. The levels rose in the acute phase, but remained significantly lower than their wildtype counterparts. In the first remission, levels of total caspase did not

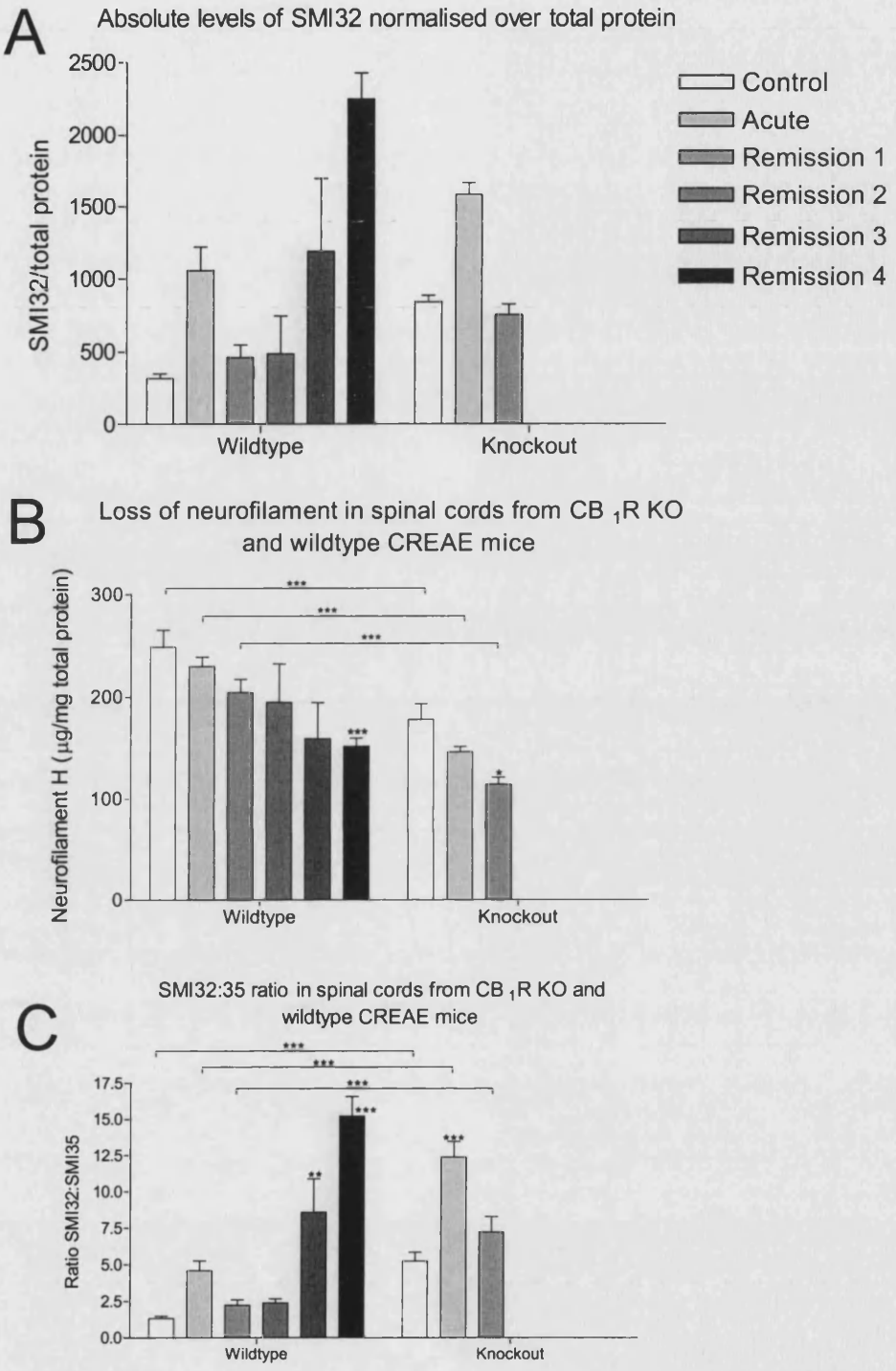

Figure 4.8:(A) - NfH^{SMI-32} in spinal cord from CREAE animals as measured by ELISA. Expressed as a proportion of total protein. (B) - Levels of NfH^{SMI-35} expressed as a proportion of total protein. (C) - Ratio of NfH^{SMI32} to NfH^{SMI35} levels. In wildtype animals, a rise in the acute phase, is followed by a drop in NfH^{SMI-32} in the first remission and subsequent accumulation. CB_1R KO mice have a higher degree of NfH^{SMI32} prior to disease induction, and have higher levels in the two tested disease stages. * - $p<0.05$; ** - $p<0.01$; *** - $p<0.001$

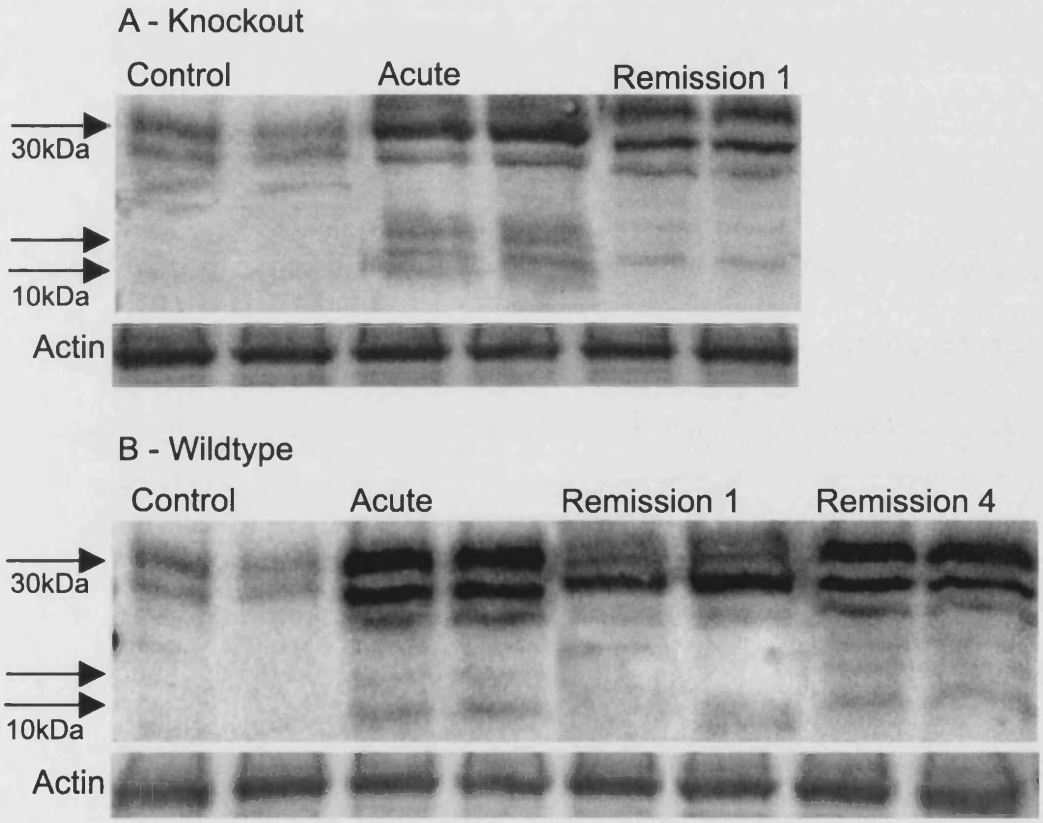

Figure 4.9 - Representative Western blots showing caspase 3 expression in spinal cord homogenates from (A) knockout and (B) wildtype animals in CREAE. Animals were terminated at the relavent disease stage and the spinal cord homogenised for Western blot analysis. Samples were also probed for actin to demonstrate equal sample loading on the gel. Blots were quantified using computer analysis, the result of which are shown in Figure 4.10.

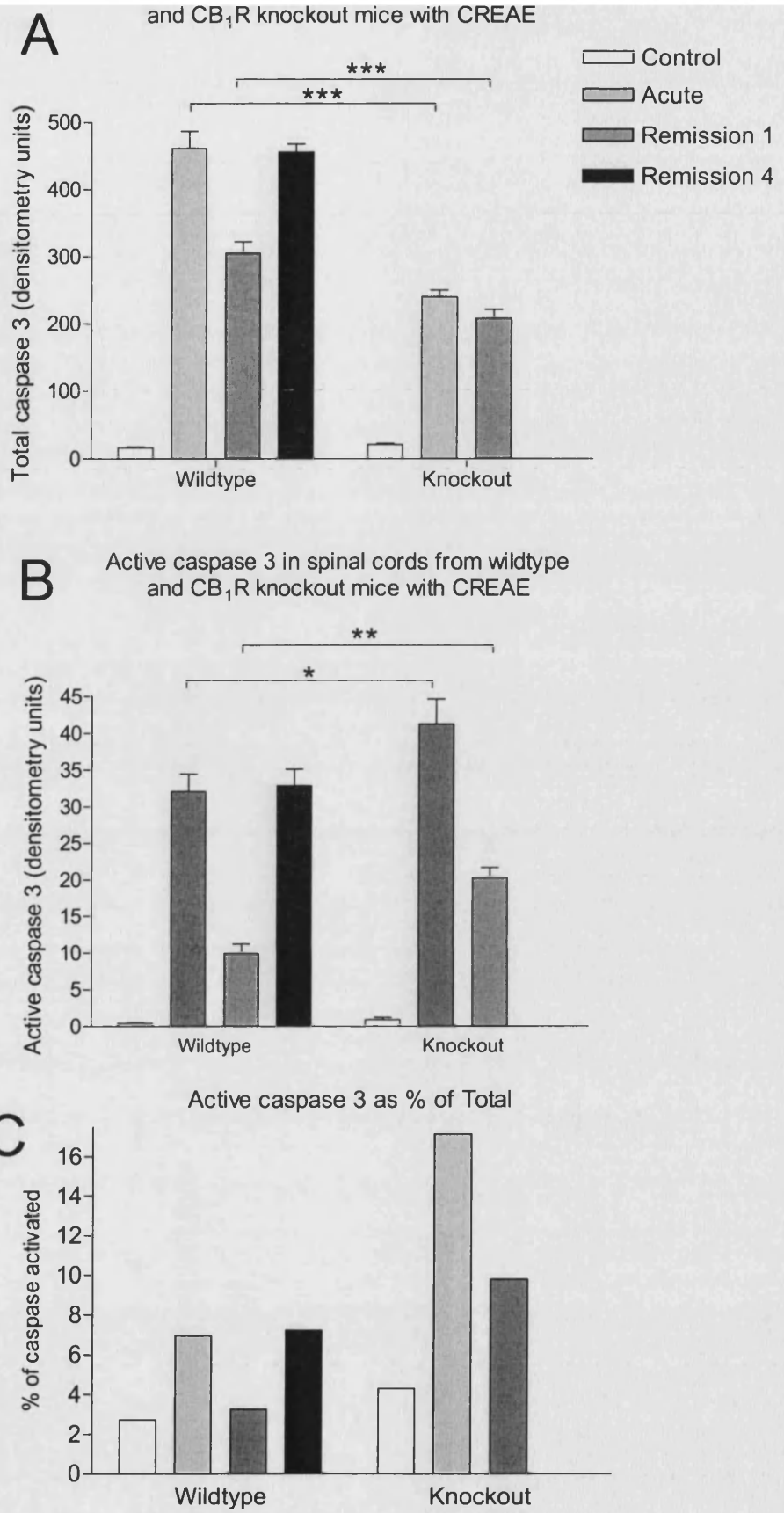

Figure 4.10 : (A) Total caspase 3 expression rises sharply in the acute phase of disease in WT mice, and is elevated for the disease duration, but is reduced In KO animals. (B) In contrast, the increase in activation of caspase 3 in disease is elevated in knockout animals. (C) Active caspase 3 expressed as a percentage of total caspase 3.
* - $p<0.05$ ** - $p<0.01$ *** - $p<0.001$

significantly change from those seen in the acute attack. Levels of active caspase 3 were measured by quantifying smaller cleaved caspase 3 moieties using western blotting and computer aided densitometry techniques. In wildtype animals, a similar pattern to total caspase 3 expression was seen. Very low levels in control animals increased dramatically in the acute phase of disease, falling in the first remission and rising again by the fourth remission. In contrast to total caspase 3, the active subunits occurred at significantly ($p<0.05/0.01$) higher levels in knockouts than in wildtype animals.

Expressions of the active caspase 3 measurements as a percentage of total caspase 3 clarifies the significant difference between the levels of active caspase 3 in wildtype and knockout animals, being higher in knockout animals at each disease point.

4.3. Discussion

Neuronal damage in autoimmune disease is likely to be caused through a variety of mechanisms and pathways, via glutamate toxicity (Pitt *et al.*, 2000; Smith *et al.*, 2000b), oxidative damage (Liu *et al.*, 2003) and cytokines, including TNF-α (Kollias & Kontoyiannis, 2002) and IL1 (Huitinga *et al.*, 2000). Evidence has been presented which shows that CB_1R knockout mice have a more severe disease course in EAE. Following an initial acute paralysis phase, recovery does not occur as effectively as it does in their wildtype counterparts and CB_1R knockout mice show increased movement deficit. Histology and quantification of nerve proteins show loss of neurofilament and myelin basic protein from immunostained spinal cord sections and accelerated emergence of transacted axons and axonal end-bulbs associated with pathology. These findings may indicate that the CB_1 receptor confers neuroprotective properties in the mouse CNS.

Quantitative measures of NF content in the spinal cord shows that NF levels are reduced in the CB_1R knockout mouse prior to disease induction. Although this could represent slow, underlying neurodegeneration in these mice this may also reflect brain and CNS modelling events during development. This suggests that the cannabinoid system may play an important role in developmental neural plasticity. Cannabinoid receptors appear early in foetal mouse development, and at atypical locations compared to postnatal distribution (Fernandez-Ruiz *et al.*, 1999). They are found on neurite growth cones, influencing migration and motility (Zhou & Song, 2001), and have been shown to modulate synapse formation *in vitro* (Kim & Thayer, 2001), as well as modulation of neurotransmitter production (Fernandez-Ruiz *et al.*, 1999). Alternatively, endogenous cannabinoids could prevent inherent neurodegeneration that occurs during brain modelling during development. Although recent studies have reported that cannabinoids can induce apoptosis *in vitro*, (Galve-Roperh *et al.*, 2000; Sarker *et al.*, 2000) these studies were conducted with high doses of synthetic cannabinoid compounds, producing a pharmacokinetic environment that may be different from the developing brain. Galve-Roperh et al (2000) reported apoptosis induction by cannabinoid compounds in tumourous tissue, but with 'no significant neurotoxic effects'. One study reported protection via CB_1 against vanilloid-receptor mediated apoptosis (Maccarrone *et al.*, 2000). The diversity of the results produced in such studies may be a consequence of the numerous intracellular signalling pathways by which cannabinoid compounds act, and the developmental stage of the cell on which they are acting. This complexity, coupled with the limitations of cell culture techniques, may partly explain the published differences between *in vitro* studies and the findings stated here.

It is evident that the inflammatory insult in wildtype mice causes accumulating axonal pathology. This has recently been demonstrated in another mouse strain (SWXJ ($H\text{-}2^{q,s}$), where the histological axon content inversely correlated with the number of relapses (Wujek *et al.*, 2002). Counting of axons indicated that 10-20% of nerve loss was clinically silent, residual paresis was evident with >30% axonal loss. Chronic paralysis in MS was associated with a loss of 68% of axons (Bjartmar *et al.*, 2000). The results of this study using the quantitative ELISA technique show close parallels with histological counting of axons in sections. Whilst lesions can occur along the entire neuraxis (Baker *et al.*, 1990), there may be regional variations as shown by differences in cervical and lumbar cord axonal loss in CREAE (Wujek *et al.*, 2002). Analysis of the whole cord will average this regional effect. The use of this ELISA is significantly faster than labour-intensive counting, and provides an estimate of axonal content in the whole cord.

Knockout mice lose more NF than wildtypes with each successive disease stage, indicating that inflammatory insult elicits a greater neuropathological effect on mice lacking the receptor. This demonstrates the neuroprotective effects of endogenous CB_1 receptor activation. CB_1R agonism has been shown to protect against a range of insults *in vivo* and *in vitro*, including ischemia (Nagayama *et al.*, 1999), hypoxia (Sinor *et al.*, 2000), excitotoxicity (Shen & Thayer, 1998) and oxidative damage (Marsicano *et al.*, 2002). Indeed, the latter two have been implicated in EAE pathology (Espejo *et al.*, 2002; Pitt *et al.*, 2000), and can occur as a result of microglial activation. Excesses of glutamate and TNF-α are directly toxic to neurons and oligodendrocytes and can also lead to production of reactive oxygen and nitrogen species. Whether the excitotoxic effects of glutamate or the oxidative stress caused by reactive species is the primary

pathological agent is as yet unknown. It is interesting to note that the increased damage to neurons in knockout mice does not appear to be due to primary demyelination, as MBP loss is not significantly different between knockouts and wildtypes. This indicates that the degree of neuronal loss is not necessarily dependent on the degree of demyelination in EAE.

The vulnerability of a neuron to damage can be assessed by the ratio of dephosphorylated NF to phosphorylated NF, as measured by the SMI-32 and SMI-35 antibodies, respectively (Petzold *et al.*, 2003). The SMI32:35 ratio is increased in acute phase EAE in wildtype animals, and then falls in remission. This indicates a transient dephosphorylation during the active disease stage, making the neuron unstable and vulnerable to degradation. The effect is reversed in the first remission, in a pattern mirroring that of inflammatory-cell infiltration into the CNS. Accumulation of dephosphorylated NF occurs over subsequent remissions, with levels being high by remission four, indicating a high number of vulnerable or damaged neurons. The possibility of dephosphorylation being linked to infiltrating cellular entities is illustrated by the ability of macrophages and microglia to produce kinases and related molecules. Alternatively, infiltrating leucocytes may stimulate resident CNS cells to produce these molecules. In CB_1R knockout animals, the SMI32:35 ratio follows the same pattern as the wildtypes, but levels are higher after disease development. This indicates that, while dephosphorylated NF is not a physiological feature of the knockout mouse, lack of the receptor may confer greater vulnerability of axonal processes in the pathological state. This, however, is dependant on the notion of dephosphorylated neurofilament as a marker of axonal injury. As can be seen from the model of NF phosphorylation in Figure 4-11 (after (Grant & Pant, 2000)) changes in calcium influx, growth factor

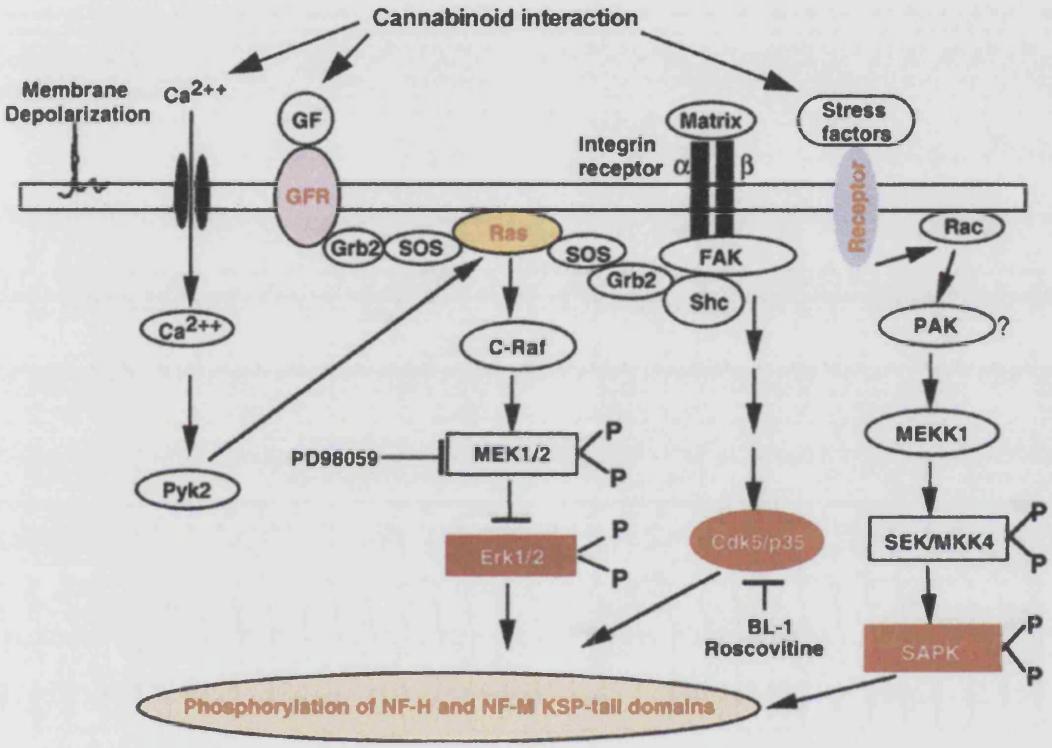

Figure 4.11: MAP Kinase (ERK1/2) cascade hypothesis of neurofilament protein phosphorylation. Activation of CB_1R can potentially lead to effects on growth factor receptors, calcium channels and stress factors, all of which may modulate neurofilament phosphorylation through the protein kinase pathways indicated. After Grand and Pant, 2000 (Journal of Neurocytology 29, 843–872)

receptor activation and stress factors could all contribute to NF phosphorylation by various intracellular pathways. CB_1R activation has been shown to modulate these processes (Takahashi & Linden, 2000; Williams *et al.*, 2003), and is therefore a candidate molecule for regulating NF stability. This also provides a mechanism whereby cannabinoid receptor activation protects neurons against dephosphorylation, and therefore vulnerability. Alternatively, phosphorylation of NF is associated with stabilising the molecule in CNS development, and there is evidence to suggest that in neuronal repair, a similar situation is encountered (Hall & Yao, 2000). Rebuilding or appending to NFs would require the transport of further NF polymers from the soma, increasing the level of non-phosphorylated NF epitopes. So, in addition to being a marker of damage, antibodies to non-phosphorylated NF epitopes may indicate repair.

Caspase 3 is a ubiquitous cell-death effector molecule, responsible at least in part for apoptotic cell death. In wildtype mice, levels of both total and active caspase 3 rose during disease, indicating that apoptotic cell death is a factor in EAE. Increased total caspase 3, the benign precursor isoform, indicates that expression is upregulated. Increased active caspase 3 indicates an increase in the rate of processing of precursor to active caspase 3. It is possible, however, that the caspase increases observed are a result of glial, as well as of neuronal, cell death. This could be due to death receptor-activated processing of upstream caspases, indicating an upregulation of other caspase molecules. Alternatively, more active caspase 3 could be due to a higher incidence of mitochondrial membrane breach related to Bcl-family member activity, contributing to higher levels of apoptosomal activity via cytochrome c incorporation. Thirdly, inhibition or down-regulation of the inhibitor of apoptosis molecules (IAPs), possibly due to the release of

smac/DIABOLO from compromised mitochondria, may contribute to this effect (Gottlieb, 2000).

Wildtype mice have higher levels of total caspase 3 than knockout mice, but have lower levels of active caspase 3. This finding could simply reflect the fact that more of the pool of total caspase 3 is being cleaved in the knockout animals, leaving less total and producing more active caspase 3. It is possible that endogenous activation of the CB_1R inhibits apoptosis. *In vitro* studies on cortical neurons show that CB_1R agonists can elicit the opposite effect, and induce apoptosis (Campbell, 2001). However, as mentioned previously in this chapter, high doses of synthetic cannabinoid agonists were used in these experiments that may not accurately reflect the *in vivo* physiology, and are used in a context that may be very different from the post-mitotic neural environment of the adult CNS.

5. Evidence for cannabinoid mediated neuroprotection *in vitro*

5.1. Introduction

The aggregate cell culture system, a 3D multicellular system representative of the CNS physiology, has been used in numerous studies investigating demyelination and remyelination *in vitro* (Copelman *et al.*, 2000; Honegger & Matthieu,1990). Aggregates develop axon-like processes with which myelin associates, synaptic contacts and the full repetoir of CNS cell types, organised in a 3D fashion mimicking the brain. The system allows for complex treatment regimens and repeated sampling. A flask with $4x10^4$ cells can be maintained in rotational culture for 21 days and split immediately prior to treatment, giving rise to two identical cultures that can be differentially treated. This increases the 'n' numbers for statistical analyses providing more reliable results with more robust internal controls.

The three-dimensional morphology of the aggregates allows studies on the myelin sheath and neuronal processes to be carried out. Several demyelinative agents have been used in conjunction with the aggregate cell culture, including complement-dependent and -independent antibodies and the cytokines IFN-γ and TNF-α (Kruger *et al.*, 1999). Addition of an agent to the culture medium elicits demyelinative effects, without the need for additional manipulation. The agent can be easily removed by replacing the culture medium several times after the required demyelinative period. Use of a single cytokine has advantages over the use of demyelination-inducing antibodies which typically require complement activation, as it requires less control cultures.

For these studies, IFN-γ was used as the demyelinative agent, as it was found to be more effective in bringing about demyelination than TNF-α, and at lower concentrations. IFN-γ levels are elevated in the CNS during EAE (Begolka *et al.*, 1998),

and the cytokine has been used effectively in previous studies of demyelination using this cell culture system.

5.2. Results

5.2.1. Development of aggregates from knockout tissue

N-numbers used for statistical analysis in Section 5.2 were at least n=18 flasks. Aggregates set up using telencephalon tissue from CB_1R knockout mice do not appear to differ morphologically over the normal time course of *in vitro* development than their wildtype counterparts. There is no discernable difference between the O4 and NG-2 markers for early oligodendrocyte progenitors (Figures 5-1 and 5-2). Staining for the CB_1 receptor shows restricted co-localisation with NF, while as expected in knockout cultures, only background staining was evident (Figure 5-3). When measured by ELISA, there were no significant differences in NF levels between wildtype cultures and cultures from heterozygous and homozygous knockout animals (Figure 5-4). MBP levels were also consistent, until DIV 42, by which point homozygous knockout cultures appear to have accumulated more myelin. These results show that, *in vitro*, the CB_1 receptor has few significant effects on normal myelination and NF production.

5.2.2. Demyelination in aggregates from knockout cultures

In order to mimic demyelination *in vitro*, a subgroup of flasks was supplemented with IFN-γ for four days from DIV 21 to DIV 25. During this time, the cytokine caused significant ($p<0.001$) loss of myelin basic protein in the aggregates. This loss was found to induce differentiation of some oligodendrocyte progenitors into pre-myelinating oligodendrocytes, as shown by dual staining for GalC and incorporated BrdU (Figure 5-5). The number of double labelled cells in both wildtype and knockout cultures

appeared to increase following IFN-γ treatment, and persist to DIV 42. Figure 5-6 shows the development of myelinated fibres over the first 21 days *in vitro*, and the effects of demyelination at 25 days. Yellow double staining for myelinated fibres is much reduced in culture from wildtype and knockout animals treated with IFN-γ. After a period of recovery, double staining had reappeared, albeit not to the same degree seen in control cultures. When measured by ELISA, developmental MBP levels in untreated cultures were comparable between wildtype and knockout cultures at each time point (Figure. 5-7). Cultures from both wildtypes and knockouts that were treated with IFN-γ lost a highly significant ($p<0.001$) amount of MBP directly following treatment before levels recovered to normal by DIV 42.

5.2.3. Loss of neurofilament in aggregates from knockout tissue

NF levels in untreated control cultures were not significantly different between wildtype and knockout controls. Interferon-γ treatment had no effect on the NF levels in wildtype cultures. However, significantly reduced levels of NF were observed in cytokine-treated cultures from knockout animals. NF levels in all culture flasks returned to that of control by DIV 42.

5.2.4. Increased NFH^{SMI-32}:NFH^{SMI-35} in aggregates from knockout tissue

NF^{SMI-32} was more evident in immunostaining (Figure 5-8) following demyelination, and persisted until DIV 42. When measured by ELISA and expressed as a ratio with SMI-35, NF^{SMI-32} did not change over the course of the culture period in control cultures. However, levels were higher initially in knockout cultures, and remained higher at each time point. In wildtype IFN-γ treated cultures, NF^{SMI-32} levels

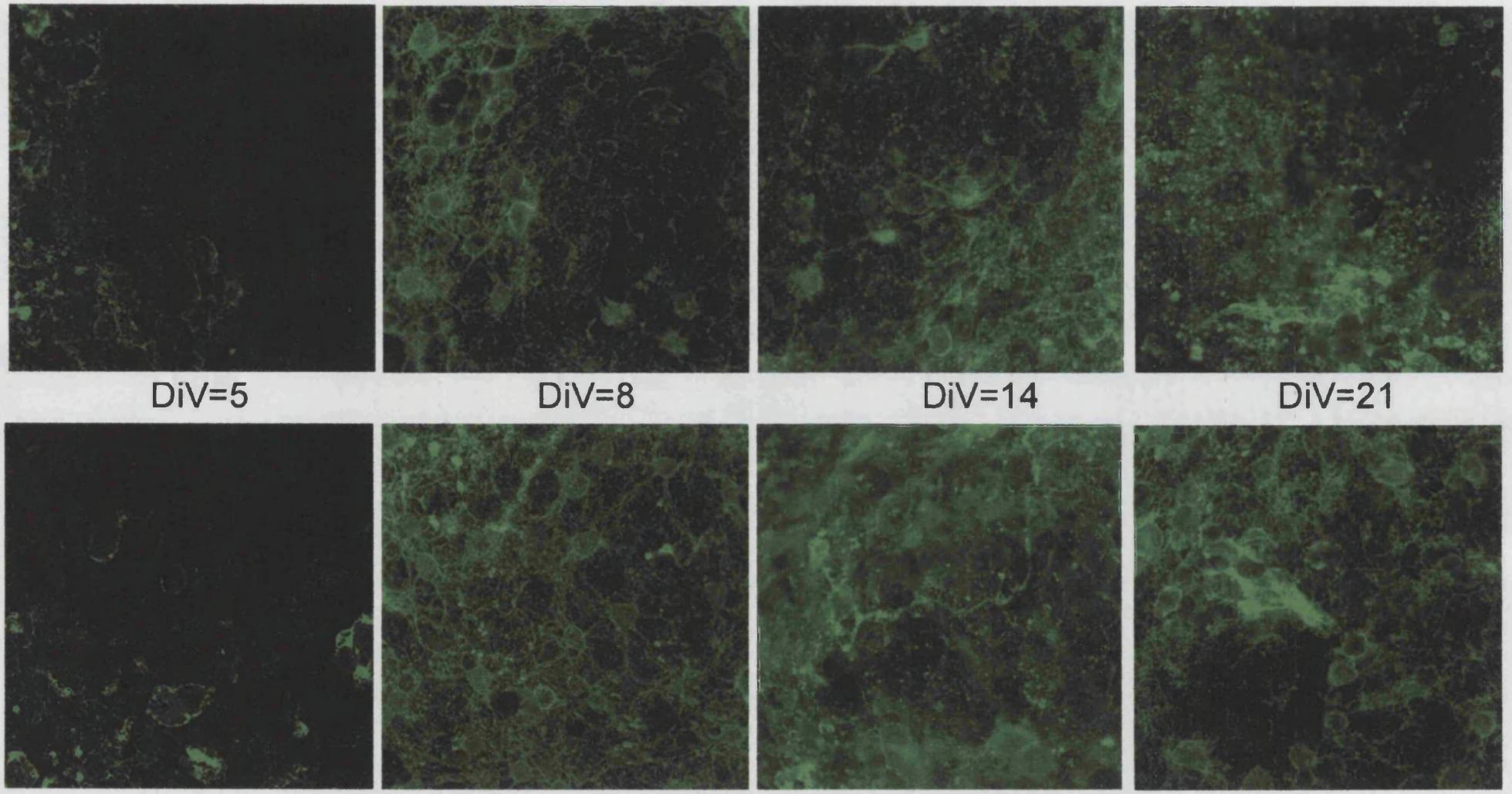

Figure 5-1: Confocal staining of O4 antigen, a marker for oligodendrocyte progenitors and precursors, over development of the aggregates. The top panel shows aggregates taken from CB_1-R KO animals, the bottom panel wildtype. O4-positive cells are less abundant in the first instance, peaking at around DiV 14, and persisting to DiV 21.

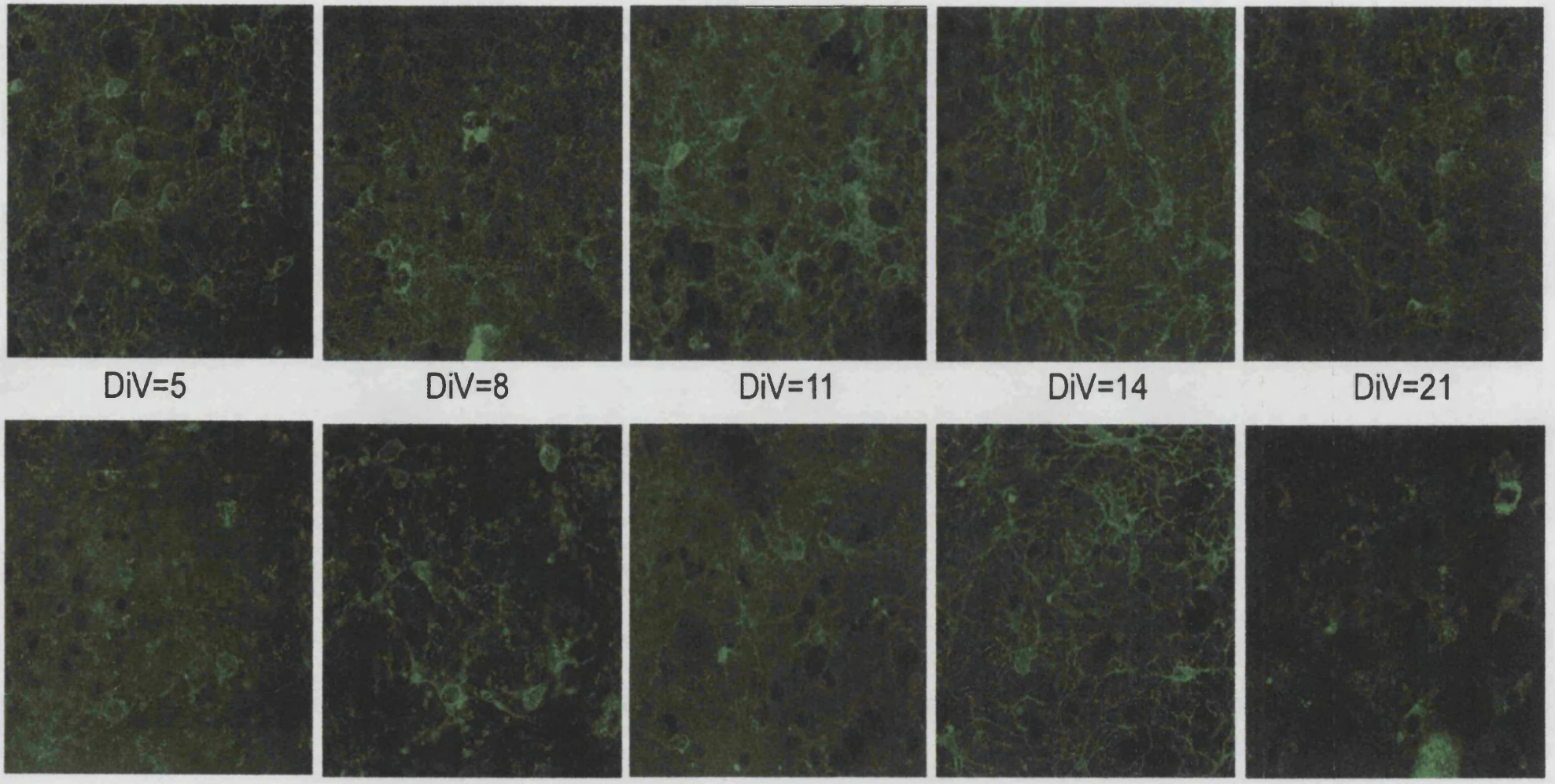

Figure 5-2: Confocal staining of NG2 proteoglycan, a marker for early oligodendrocyte progenitors, over development of the aggregates. The top panel shows aggregates taken from CB_1-R KO animals, the bottom panel wildtype. NG2-positive cells appear to peak in density at around day 14 in vitro, with a low number of cells persisting to DiV 21 and further (data not shown).

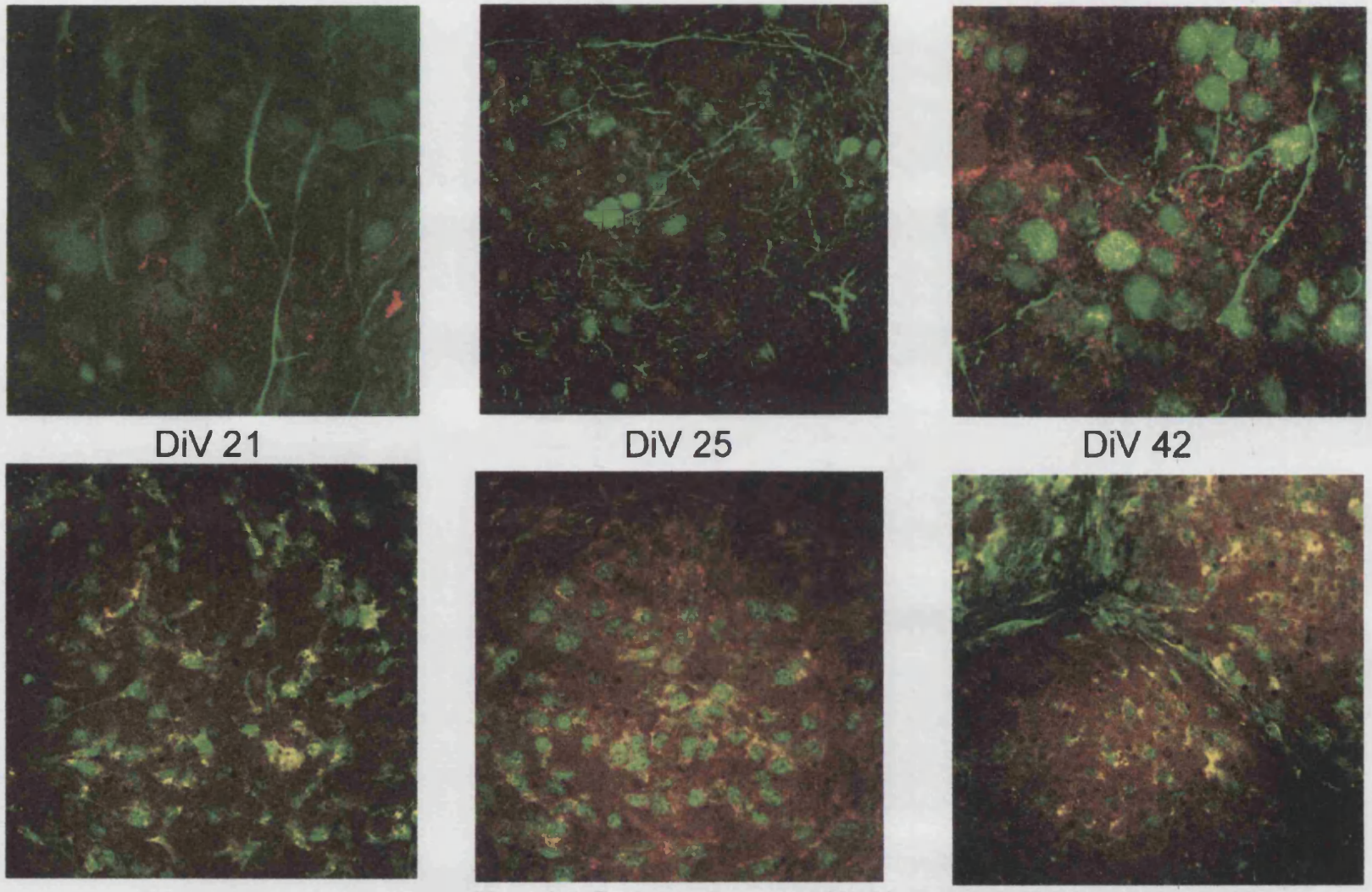

Figure 5-3: Confocal microscopy of NfH (green) and CB_1R (red) in CB_1-R KO (upper panel) and wildtype (lower panel) cultures. Some non-specific staining is observed in knockout aggregates, but the receptor can be seen co-localised with neurofilament in wildtype aggregates.

A

Myelination in aggregates using tissue from wildtype and CB1-R knockout animals

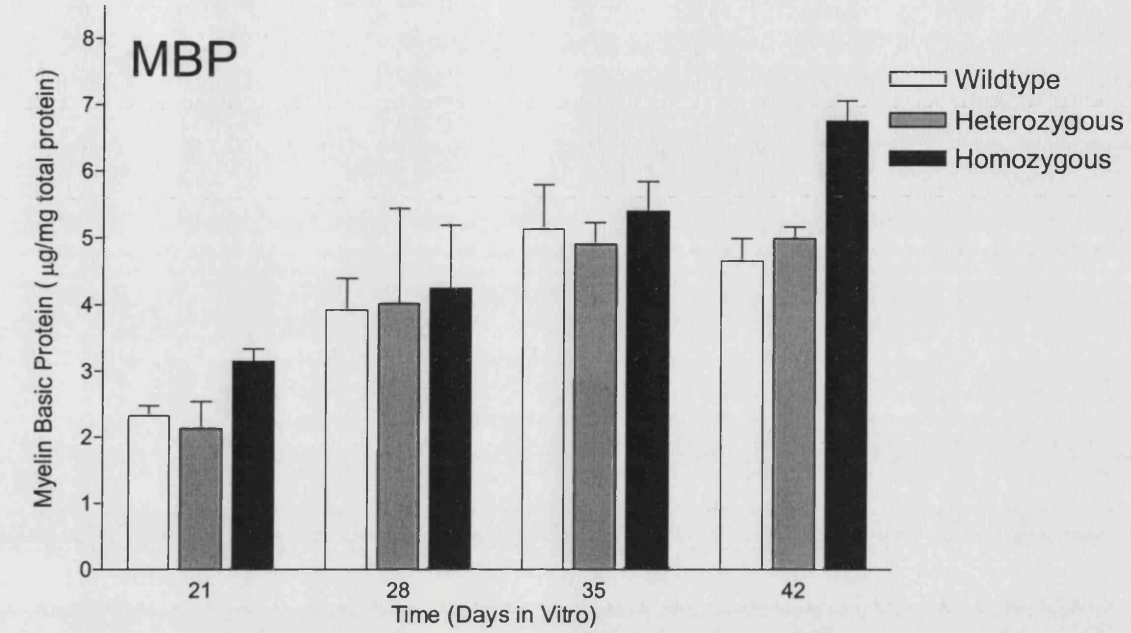

B

Neurofilament accumulation in aggregates using tissue from wildtype vs knockout animals

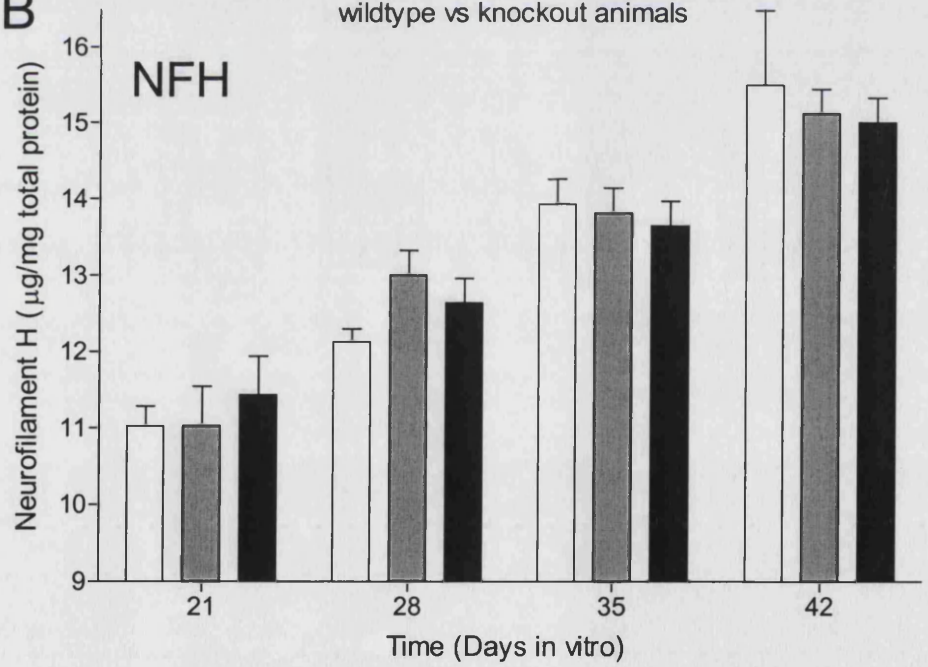

Figure 5-4: Myelination (A) and neurofilament accumulation (B) in aggregates from wildtype ABH, homozygous CB_1R knockout ABH mice and heterozygous CB_1R knockout ABH mice proceeds in a manner akin to the *in vivo* situation, and at a comparable rate/extent to previously characterised rat aggregate cultures. there is no significant difference between wildtype ABH, hetero- or homozygous knockout animals.

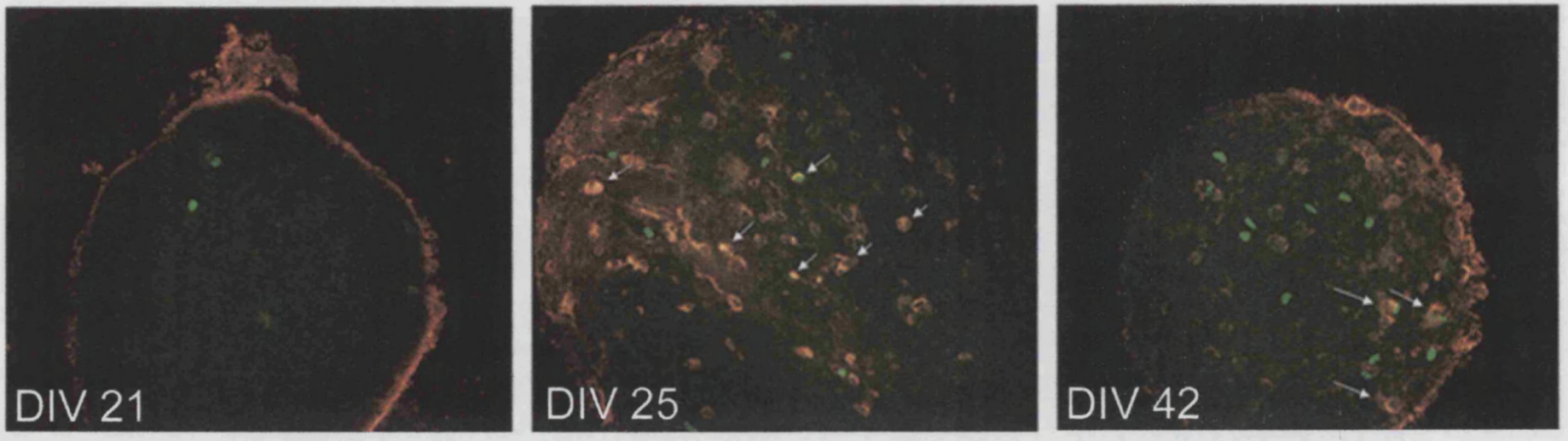

Figure 5-5: Galactocerebrocide (red) and incorporated BrdU (Green), indicating increased proliferation of oligodendrocytes following demyelination, which persists until the end of the culture period. The BrdU pulse was applied for 4 hours prior to fixation and immunolabelling.

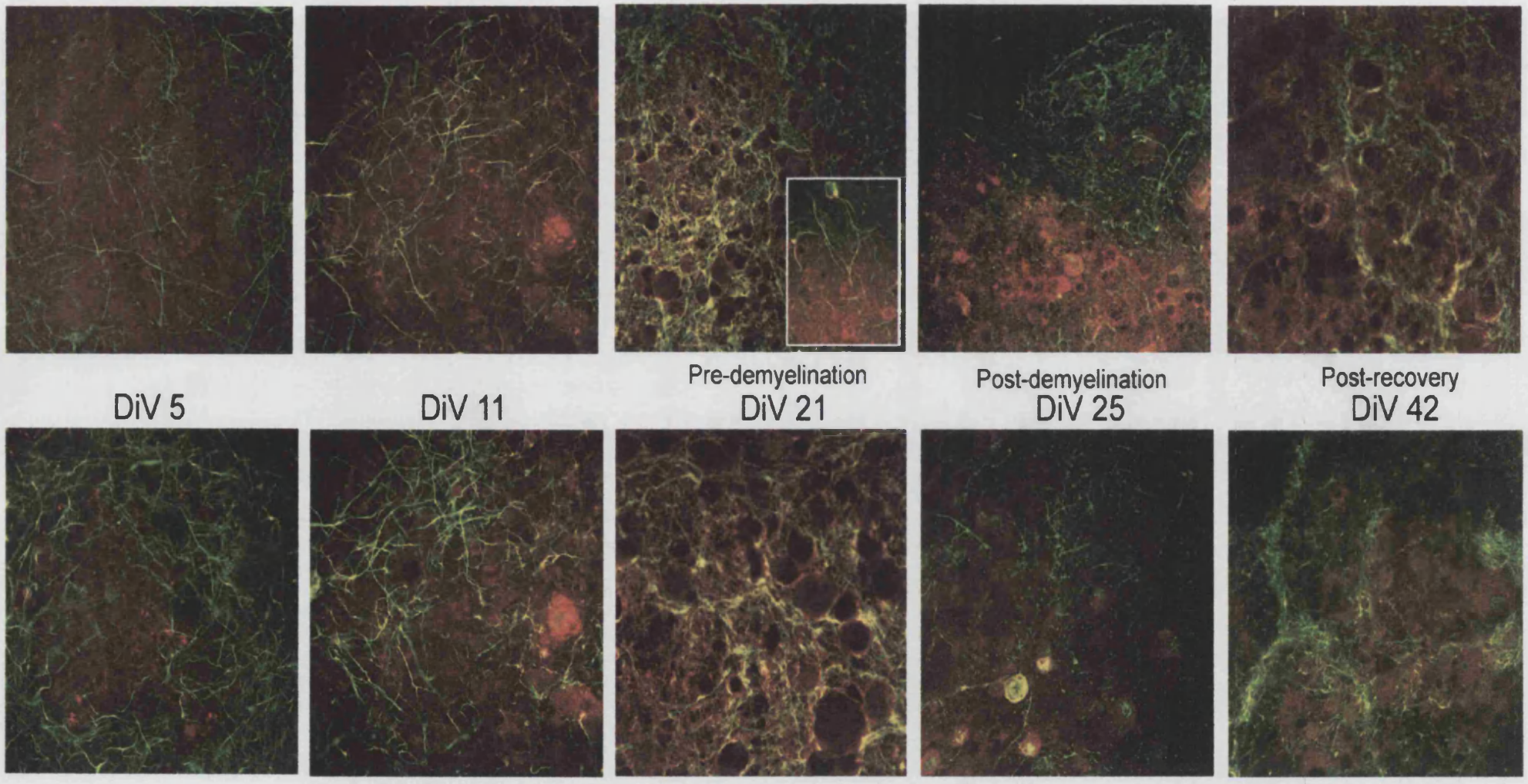

Figure 5-6: Confocal staining for myelin basic protein (red) and neurofilament (green) during development of the aggregates. The top panel shows aggregates from CB_1-R KO animals, the bottom wildtypes. Demyelination was induced using interferon gamma on DiV 21-25.

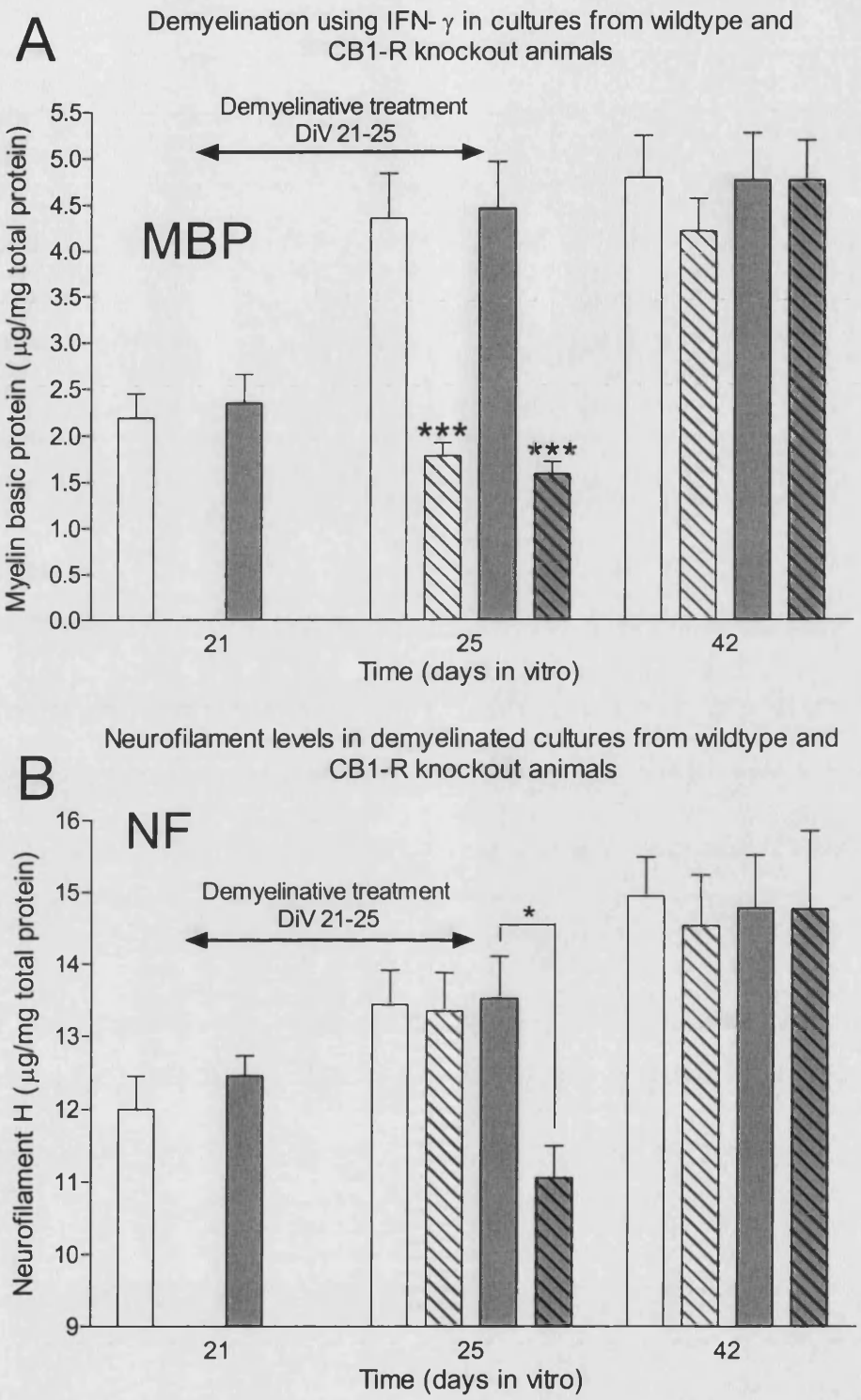

Figure 5-7: Cytokine-induced demyelination (A) and neurofilament loss (B) in the aggregate cell culture. Demyelination induced by an acute IFN-γ insult significantly reduces neurofilament levels in cultures from CB_1R KO animals only. This indicates that the CB_1R plays a neuroprotective role in demyelination. Levels of both MBP and NfH^{SMI35} recover to that of controls by DIV 42.

* - p<0.05; *** - p<0.001

Wildtype control
Wildtype demyelinated
Knockout control
Knockout demyelinated

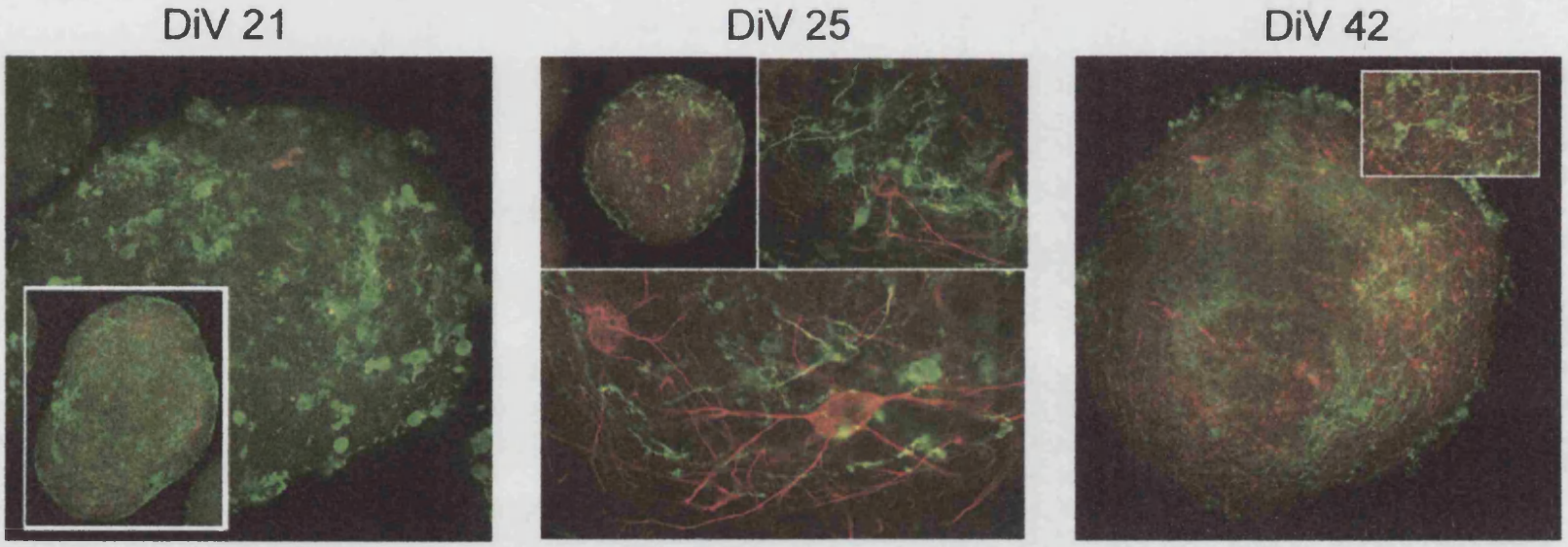

Figure 5-8: Confocal staining for MBP (green) and SMI-32 (red - a marker of compromised dephosphorylated neurofilament), indicating an increase in SMI-32 reactivity following demyelination, which persists after recovery.

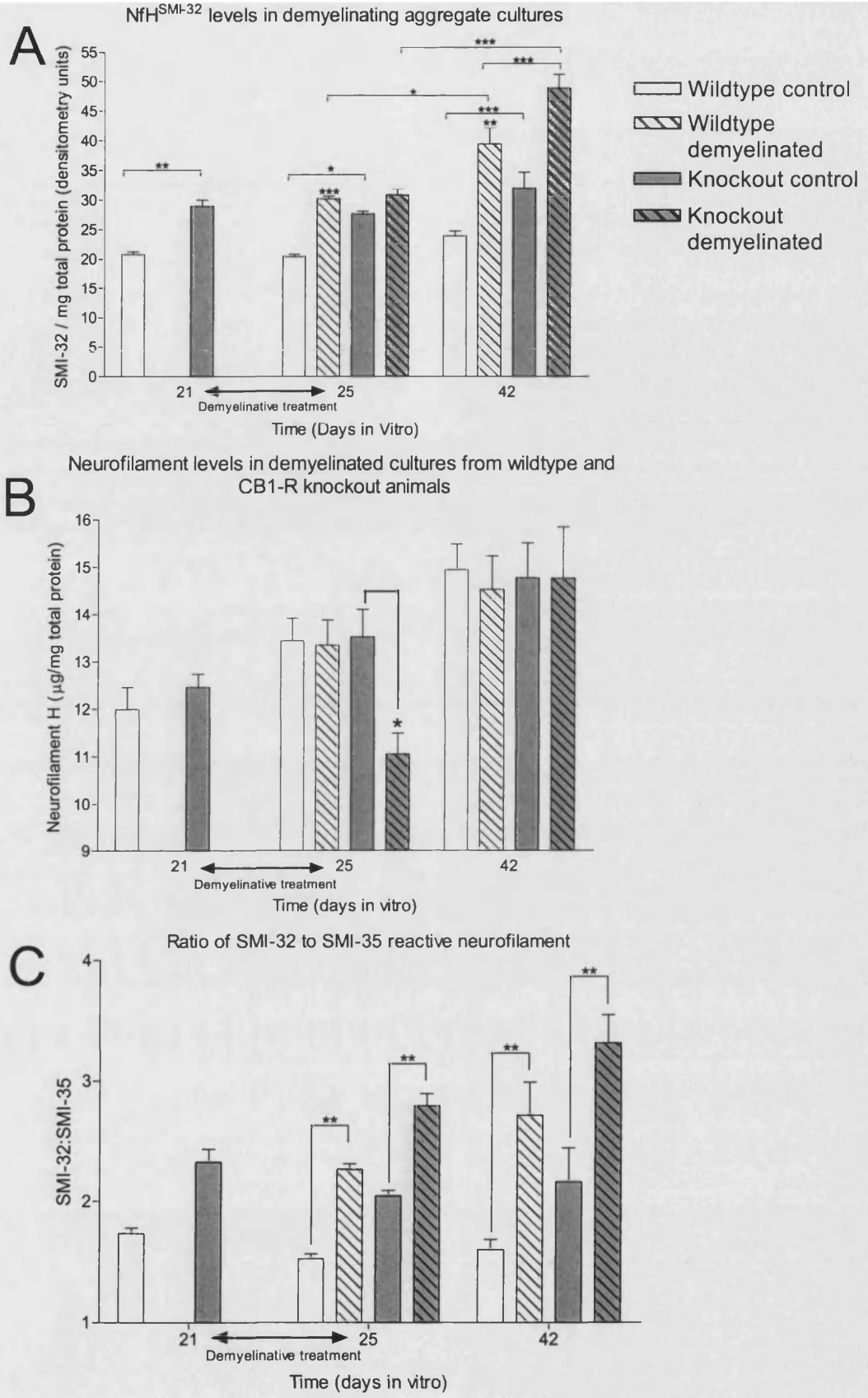

Figure 5-9: Absolute levels of NfH^{SMI-32} expressed as a proportion of total protein(A) . NfH^{SMI-35} expressed as a proportion of total protein (B). Ratio of NfH^{SMI-32} to NfH^{SMI-35} (C) in foetal aggregate cell cultures. NfH^{SMI32} is expressed as a ratio with NfH^{SMI35} due to the lack of a reliable standard for dephosphorylated neurofilament. Ratio values from KO or WT controls do not change significantly over the course of the culture. The ratio in aggregates from both WT and KO animals increases following demyelination, with the larger increase being evident in cultures from knockout animals.
* - $p<0.05$; ** - $p<0.01$; *** - $p<0.001$

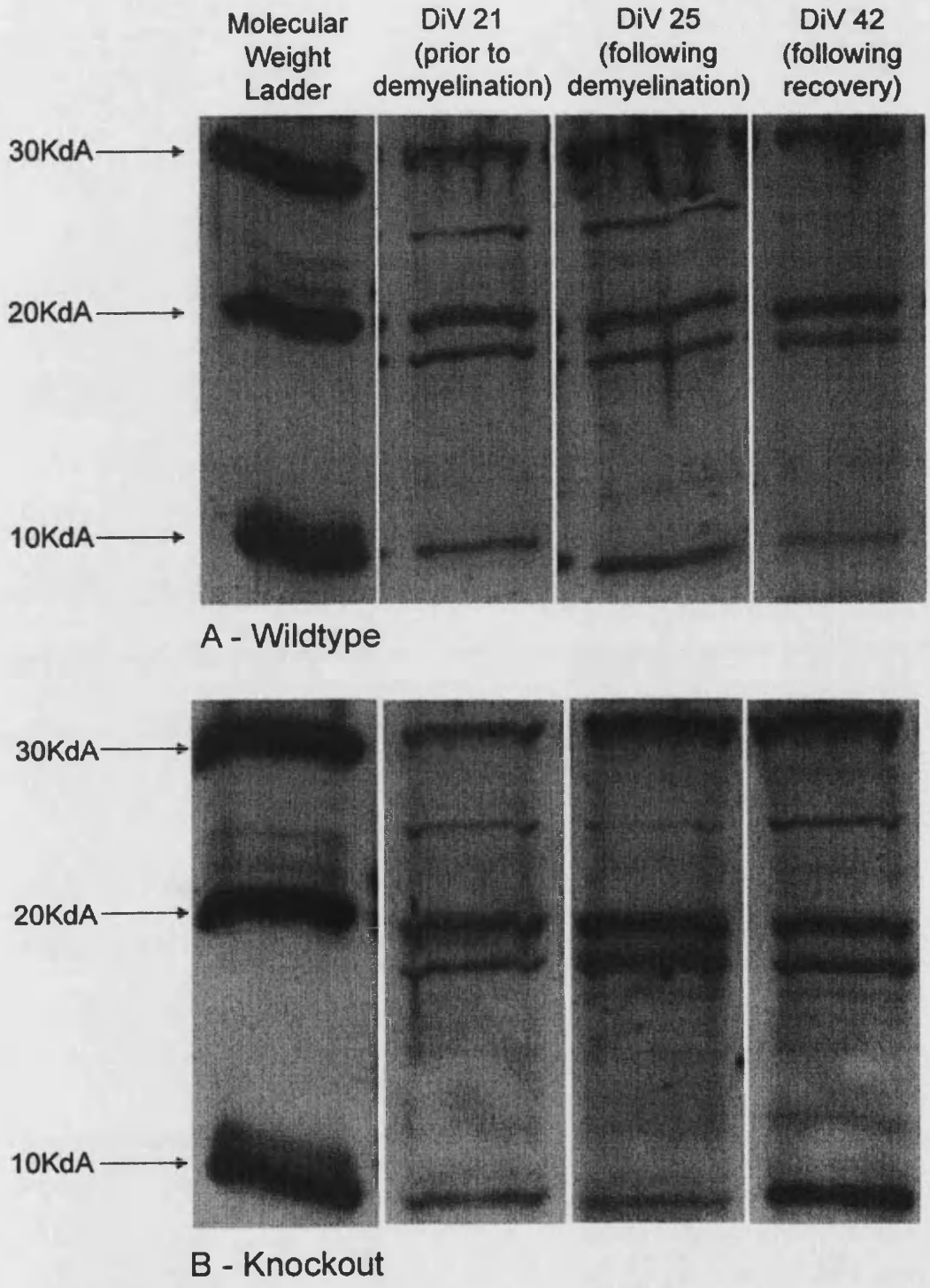

Figure 5-10: Two representative Western blots showing caspase 3 expression in (A) wildtype and (B) knockout aggregate cultures over time. Bands at around 20kDa and below represent active caspase 3.

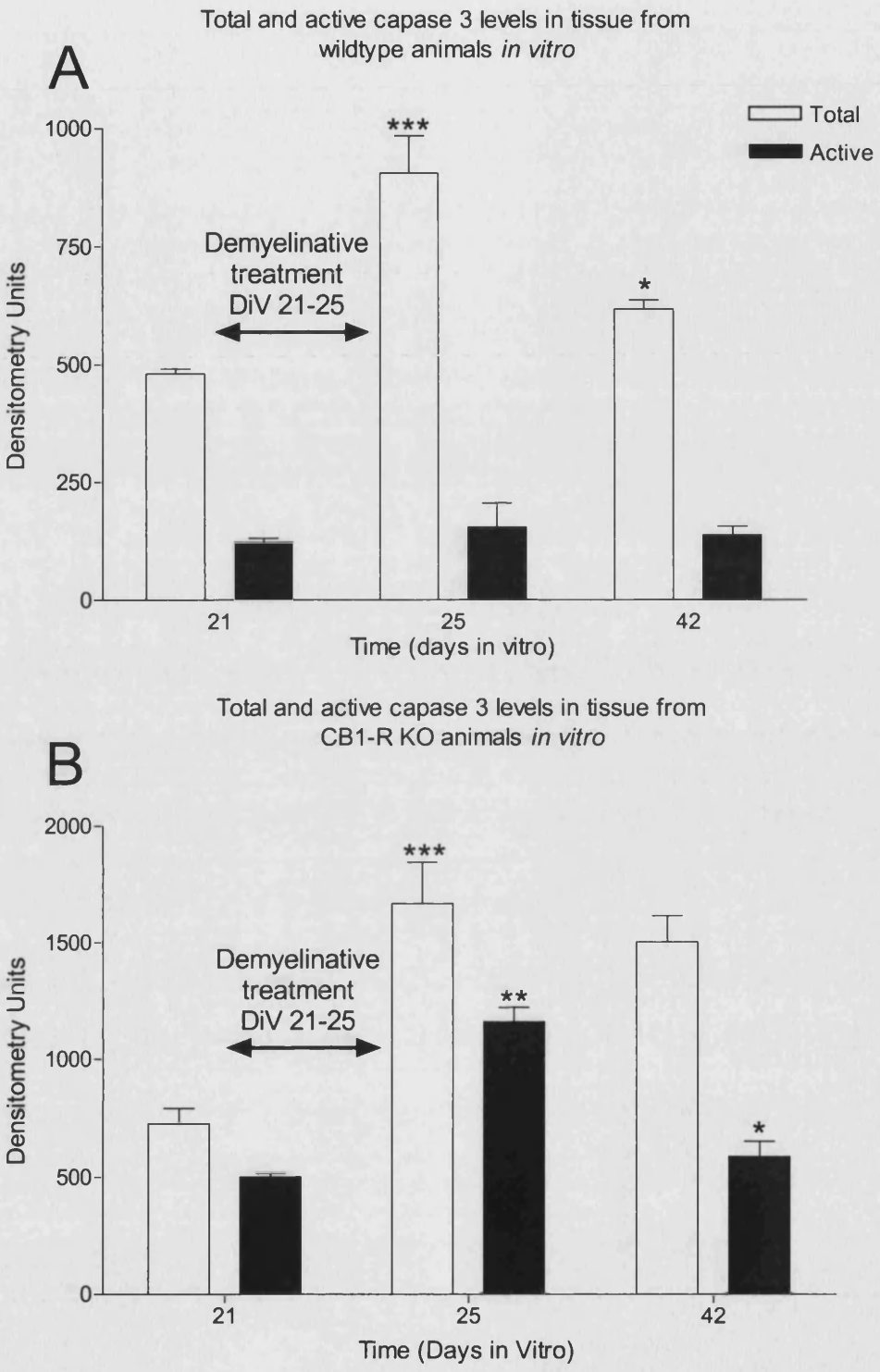

Figure 5-11: Graph of caspase 3 in aggregate cell cultures from (A) Wildtype and (B) CB1R-KO over time. In wildtype animals (A), total caspase 3 is upregulated following demyelination, but activation of the procaspase to the proteolytic form remains at a constant low level. In CB_1R KO cultures (B), both total and active caspase 3 are increased following IFN-γ treatment. This indicates that presence of the CB_1R downregulates caspase activation but not expression.

* - $p<0.05$ ** - $p<0.01$ *** - $p<0.001$

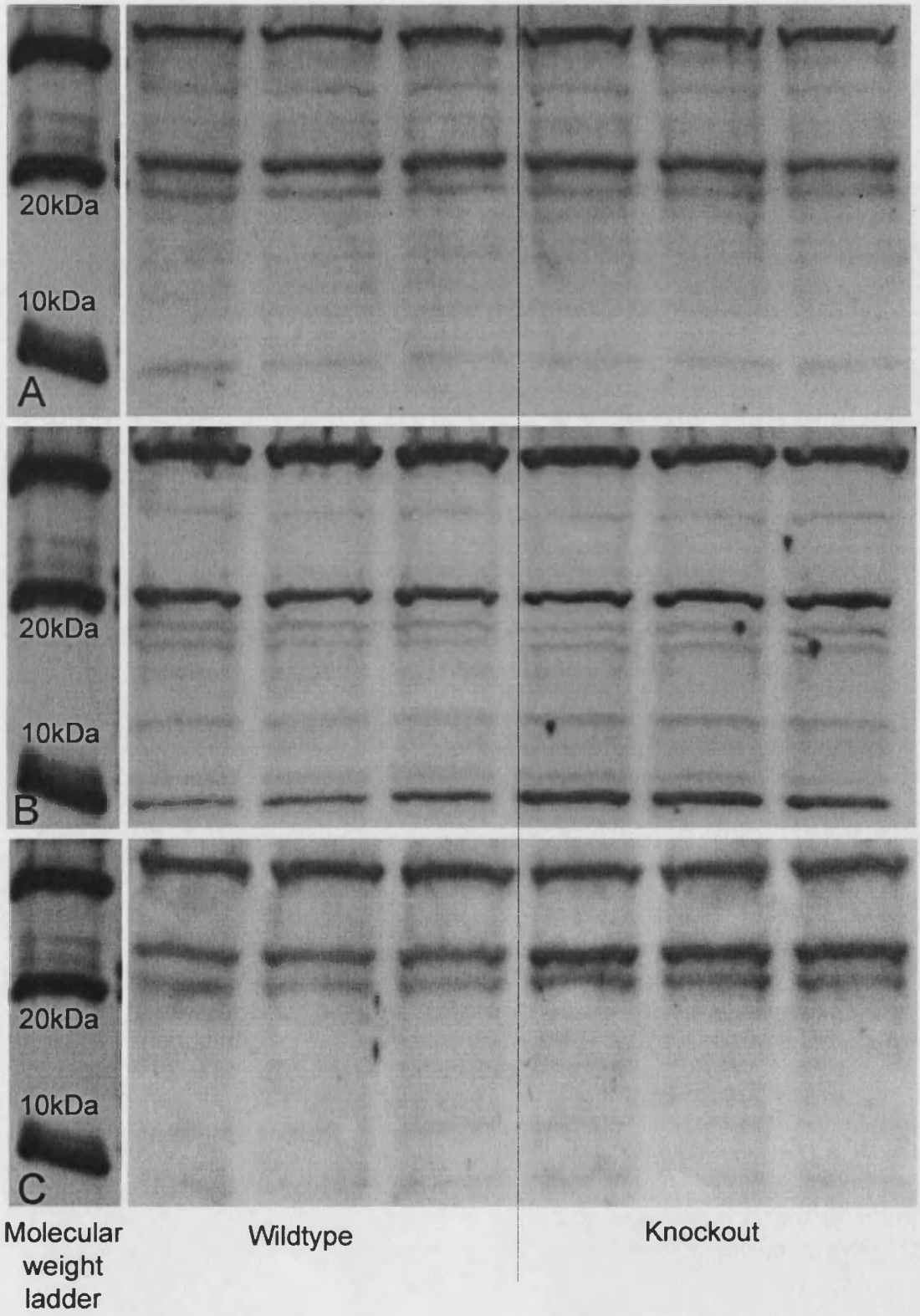

Figure 5-12: Western Blots for Caspase 3 comparing knockout and wildtype aggregate cultures (n=3) at (A) DiV 21; (B) DiV 25; (C) DiV 42. Active caspase 3 is represented by the bands at 20kDa and below.

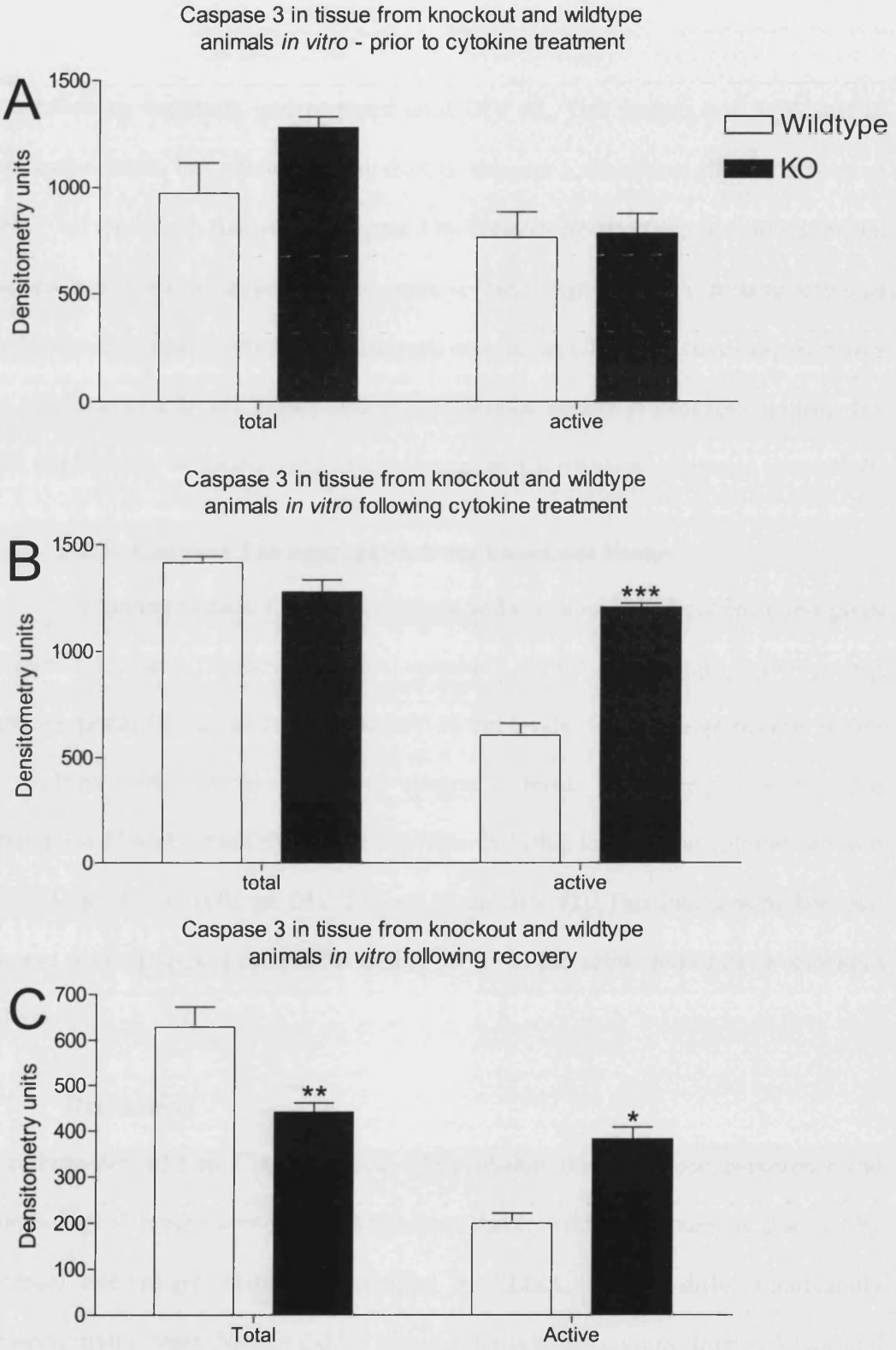

Figure 5-13: Comparison of active and total caspase 3 levels between knockout and wildtype cultures (A) prior to demyelination, (B) following demyelination and (C) following recovery. Total caspase 3 is not significantly different until the recovery phase, where wildtype cultures retain a higher level. Active caspase 3 is higher in knockout cultures following demyelination, and remains so into the recovery phase.

*** - $p<0.001$ ** - $p<0.01$ * - $p<0.05$

rose following treatment, and persisted until DIV 42. This pattern was replicated in knockout cultures, but cultures lacking the CB_1 receptor accumulated significantly more NF^{SMI-32} (Figure 5-9). Analysis of caspase 3 by Western blotting (Figure 5-10 and 5-11), showed that in the wildtype cultures, cytokine insult significantly increased levels of total caspase 3, which were still significantly elevated at DIV 42. Active caspase 3 was not significantly affected. Figure 10B shows a similar pattern in knockout animals, but with significantly increased levels of active caspase 3 at both post-treatment time points.

5.2.5. Caspase 3 in aggregates from knockout tissue

Comparing caspase 3 levels in wildtype and knockout cultures at each time point (Figures 5-12 and 5-13) shows that total caspase 3 did not differ significantly between culture types at DIV 21 or 25. Only at DIV 42 did levels rise to be significantly higher in wildtype mice. Conversely, active caspase 3 levels were comparable between wildtype and knockout at DIV 21, but significantly higher in knockout cultures between DIV 25 and 42 ($p<0.001$ on DIV 25; $p<0.05$ on DIV 42). This indicates higher total caspase 3 in wildtype cultures, but higher levels of the active molecule in knockout cultures.

5.3. Discussion

In cultures derived from CB_1R knockout telencephalon, the emergence, persistence and morphology of progenitors did not differ from that in wildtype culture, as assessed by confocal microscopy. MBP, as quantified by ELISA, did not differ significantly between culture types. Neither did NF levels differ between cultures from wildtype and knockout animals, indicating that the CB_1 receptor does not play an inherent role in NF construction, degradation or expression. Although this could be contradictory to previous findings (see chapter 4), where NF levels were reduced in spinal cords from

control knockout animals compared with control wildtypes. Spinal cords were taken from mice where disease had been induced at 6-8 weeks of age; these animals were terminated at anything up to remission 4, at around 16 weeks of age. This time frame is significantly larger than the 42-day culture period. Experimental myelination and remyelination has been shown to be significantly affected by the age of the animal used.

The discrepancies may also be due to a compensatory molecule in the culture system. It has been demonstrated that cannabinoids can inhibit thyroid function *in vivo*, reducing serum levels of thyroid hormone (Porcella *et al.*, 2002). The lack of endogenous cannabinoid stimulation in CB_1R KO mice could lead to an elevated level of thyroid hormone, which in turn would promote NF assembly (Stein *et al.*, 1991). However, there are supra-physiological levels of hormone in the culture medium, ruling this out as a putative explanation. The culture medium also contains supra-physiological levels of insulin (800nM). Insulin has been known to interact with both growth factor receptors and integrin receptors (Van Obberghen *et al.*, 2001), two triggers for NF phosphorylation via the microtubule-associate protein kinase cascade hypothesis (Figure 4-11). Furthermore, CB_1R agonism causes a rise in insulin production *in vivo* (Li *et al.*, 2001), implying that the lack of endogenous CB_1R activation, as in CB_1R knockout mice, would lead to a reduction in insulin. Therefore, high levels of insulin in knockout cultures but low levels in knockout animals may explain the discrepancy between models. The effects of insulin are multipotent, so this explanation is just one hypothetical mechanism by which altered NF levels could be explained. Likewise, cannabinoids can regulate many other neuroendocrine systems that could affect development and influence nerve growth *in vivo* (Murphy *et al.*, 1998; Romero *et al.*, 2002).

Treatment of the cultures with IFN-γ caused significant loss of MBP, followed by full recovery over time. IFN-γ-induced demyelination can occur through a variety of routes. Activation of microglia and macrophages may lead to NO (Merrill *et al.*, 1993) and TNF-α (Selmaj *et al.*, 1991) production, and direct phagocytosis of myelin, possibly linked to Fc receptor upregulation (de Andres *et al.*, 1994). Upregulation of this receptor may cause super-oxide production and release of pro-inflammatory cytokines and mediators, exacerbating the effect (Roberts *et al.*, 1990). Induction of the normally-absent MHC class I expression in oligodendrocytes (Suzumura *et al.*, 1986) may cause a 'traffic jam' effect in the endoplasmic reticulum (E.R.), leading to release of Ca^{2+} from this organelle (Baerwald *et al.*, 2000). This calcium release from the E.R., one of the biggest intracellular calcium stores may in turn lead to production of reactive oxygen species (Pahl & Baeuerle, 1997). Due to its lipid constitution, myelin is particularly sensitive to oxidative damage (Smith *et al.*, 1999). Upregulation of protease molecules has been demonstrated following IFN-γ treatment (Rivett *et al.*, 2001), and this could also contribute to the damaging environment.

Demyelination induces division of late oligodendrocyte precursors and remyelinating oligodendrocytes, as assessed by BrdU incorporation and confocal microscopy. This is a well-documented event following demyelinative episode, and has been shown to occur in MS (Reynolds *et al.*, 2002) and in a variety of models (Arenella & Herndon, 1984; Ludwin, 1984; Sato *et al.*, 1997). It is hypothesised that the stimulation of oligodendrocyte and precursor division is an attempt to repopulate and remyelinate areas of myelin damage. Oligodendrocyte cell division is much reduced by DIV 42, and levels of MBP as assessed by ELISA have risen to those of control cultures

by this time point, indicating myelin recovery. It is likely, though not proven in this study, that the dividing cells are responsible for remyelination.

Treatment with IFN-γ induced MBP loss in all treated cultures. However, this was accompanied by loss of NF in cultures from CB_1 receptor knockout animals only. This finding presents *in vitro* data for neuroprotection by cannabinoids, supporting data from mouse CREAE presented in Chapter 4. The vulnerability of neuronal processes *in vitro* shows that damage is not entirely dependent on the adaptive autoimmune response seen in EAE animals. In EAE, a wide variety of damaging responses contribute to neuronal injury . In the aggregate model, IFN-γ alone is used to elicit demyelination. While this is designed to mimic the *in vivo* pathology, it is essentially missing many of the adaptive immune effectors seen in EAE. It has been found that IFN-γ can induce apoptosis via cell surface receptor activation, causing upregulation of upstream caspases and cell death receptors (Ossina *et al.*, 1997; Takahashi *et al.*, 1999). It has also been demonstrated that pathology akin to apoptosis can occur in transected or damaged axons (Coleman & Perry, 2002; Peterson *et al.*, 2001) . Cannabinoids have been shown to reduce excitotoxic and oxidative damage to neurons through CB_1 activation (Hampson & Grimaldi, 2001; Howlett, 2002). As the data here suggest, the lack of the CB_1 receptor may confer increased vulnerability to damage by these IFN-γ mediated pathways.

Levels of NFH^{SMI-32} rose following cytokine treatment, lending support to the notion that IFN-γ treatment conferred vulnerability to neurons. This effect was markedly greater in CB_1 receptor knockout cultures, in agreement with the hypothesis that endogenous CB_1R activation protects neurons from damage via a modification of the NF phosphorylation pathways mentioned previously in Chapter 4. Treatment with

IFN-γ induced a rise in the level of caspase 3 precursor (procaspase 3) but not of the active form in wildtype culture and a rise in both pro- and active caspase 3 in cultures from knockout mice. This indicates that caspase 3 plays a role in the pathology of IFN-γ-induced demyelination and neuronal damage. The induction of caspase 3 precursor protein (procaspase 3) expression following demyelination may be due to the activation of cell death receptors and the caspase cascade. IFN-γ may induce microglial cells to produced TNF-α (Hu *et al.*, 1997) which could bind to cell death receptors causing processing of procaspase 8. This in turn, and possibly in tandem with calcium-induced caspase 9 complex formation (Adams & Cory, 2002), would lead to the activation of caspase 3 and to apoptosis by death effector pathways.

When comparing caspase 3 between wildtype and knockout cultures, levels of active caspase 3 were found to be higher in knockout cultures, while the total was higher in wildtype cultures. This reflects the level of caspase 3 processing following expression. As upregulation of procaspase 3 expression is similar in wildtype and knockout cultures, the activation of procaspase 3 in knockout cultures would appear to be enhanced. This could be due to higher levels of upstream caspases, e.g. caspase 8, which could be caused by greater death receptor agonism or expression. Alternatively, greater mitochondrial compromise, possibly caused by DNA damage and regulated by the Bcl protein family, could cause increased induction of the caspase-9 based apoptosome. This would also lead to release of the proapoptotic proteins from mitochondria, increasing caspase 3 cleavage.

Both myelin and neuronal processes recover by the last culture time-point, suggesting that at least some of the effects of damage are transient and not terminal to cells. The recovery following damage to axonal processes suggests that neuronal cell

death, for instance via apoptosis, is not occurring, but rather that localised axonal degradation accounts for the drop in NF levels observed. Increased caspase 3 levels in the cultures suggest otherwise. It is possible that demyelination is partially due to oligodendrocyte cell death via caspase 3-mediated apoptosis. Due to the morphology of the myelinated axon, oligodendrocytes are exposed to higher levels of IFN-γ for longer than axons, prior to demyelination and axonal exposure. They are also highly vulnerable to oxidative stress. This may tip the balance between transient damage and apoptosis induction. In this case, oligodendroglial recovery would be due at least in part to precursor maturation, pre-myelinating oligodendrocyte proliferation and consequently *de novo* myelination. Confocal evidence showing the increase in dividing oligodendrocytes following demyelination supports this. Confocal evidence for regeneration in nerves, however, is inconclusive, so it is unclear whether this represents full axonal recovery and remyelination of new neuronal outgrowth or remyelination of repaired axonal processes in the absence of neuronal regeneration.

The demyelinative insult applied in this study is a short-term exposure to IFN-γ akin to an acute lesion formation in multiple sclerosis. It has been demonstrated using magnetic resonance spectroscopy for N-acetyl aspartate, an axonal marker, that axonal recovery occurs following an acute MS episode (Davie *et al.*, 1994). Neuronal/axonal recovery may be due to sprouting of replacement processes or proliferation of neuronal progenitors, both of which have been shown to occur following acute attack in EAE (Bambakidis *et al.*, 2003; Picard-Riera *et al.*, 2002; Sandyk, 1999).

6. Conclusions and Future Studies

6.1. Conclusions

IFN-γ is one of a number of proinflammatory cytokines which are upregulated in autoimmune disease. The source of IFN-γ in vivo is thought to be invading Th1 and natural killer cells (Weber,1988). By supplementing cultures with exogenous recombinant cytokine, it was possible to observe the effects of a single factor *in vitro*. IFN-γ treatment resulted in a loss of MBP in the aggregate cell cultures, accompanied by a loss of NfH in CB1R-KO cultures only. Associated increases in dephosphorylated neurofilament and caspase 3 activation were observed. In EAE, IFN-γ is an important pathological mediator, and is upregulated in disease. This discussion will first focus on the deleterious effects of IFN-γ and potential routes by which they could occur, and then at mechanisms for cannabinoid-mediated neuroprotection inferred from this work.

6.1.1. Mechanisms for interferon gamma mediated cell damage

Macrophages – Macrophages are thought to be responsible for, or causative of, many of the deleterious effects observed in CNS inflammatory disease (Cuzner *et al.*, 1994). Activated macrophages, attracted by chemokines and facilitated by the upregulation of endothelial cell adhesion molecules, cross the blood brain barrier at sites of damage to form part of the inflammatory response (Brown, 2001). In the aggregate cell culture model, there is no blood brain barrier analogue, so the response can be examined as if looking at an isolated lesion. It has been shown that the cell culture system using rat tissue has a resident macrophage population, albeit limited in number (Copelman *et al.*, 2001). IFN-γ addition *in vitro* could induce macrophages to assume a phagocytotic phenotype, a process which may involve compliment receptor 3 (van der Laan *et al.*,

1996). Phagocytosis of myelin has been shown to upregulate macrophage production of TNF-α and NO, both of which damage oligodendrocytes and could contribute to demyelination (van der Laan *et al.*, 1996). TNF-α receptor activation can cause proximity activation of caspase 8 in oligodendrocytes and neurons, triggering the apoptotic cascade.

Nitric oxide and mitochondria - IFN-γ has been shown to induce NO production from astrocytes (Chao *et al.*, 1996) and macrophages (Misko *et al.*, 1995) in the CNS. As TNF-α is also produced by macrophages, there is potential for a feed-forward mechanism where NO levels are dramatically increased in disease (Nelson *et al.*, 2003). The damaging effects of NO are dualistic. Firstly, NO expression coupled with the super-oxide anion leads to formation of peroxynitrite, a potent oxidative effector (Lipton *et al.*, 1993). Increased levels of the reactive species can lead to demyelination via oxidation of lipids (Bongarzone *et al.*, 1995). Due to the high latent level of oxidative metabolism in the CNS, there is a relatively high level of super-oxide production in mitochondria. Oligodendrocytes are relatively poorly equipped to deal with oxidative insults, with low levels of antioxidant defences, high iron levels and a large membrane surface area (Smith *et al.*, 1999). The myelin membrane itself has a high lipid to protein ratio, making it a preferential target for reactive oxygen species (Verstraeten *et al.*, 1997).

Secondly, a role for NO in neuronal damage has been proposed by the disruption of mitochondrial function. As mentioned, cytokines including IFN-γ can stimulate astrocytic production of NO, leading to disruption of the mitochondrial respiratory chain (Moss & Bates, 2001). This is not terminal to astrocytes, as they can maintain

ATP production by glycolysis (Almeida *et al.*, 2001). Accumulated NO therefore has the opportunity to diffuse to adjacent cells, notably neurons. It has been demonstrated that NO can trigger synaptic glutamate release, leading to excitotoxic activation of NMDA receptors. The resulting increase in intracellular calcium levels would lead to neuronal nitric oxide synthase-related production of further NO species (Leist *et al.*, 1997). The increased calcium levels could also activate protease molecules, and trigger the apoptotic pathway. NO and peroxynitrite radicals could lead to mitochondrial damage and ATP depletion. Neurons do not generally have the ability to survive under glycolysis alone, so ATP depletion could lead to cell death by apoptosis. In addition to this, it has been shown that depletion of ATP by this route causes dysfunction of the sodium/potassium ATPase pump, leading to a reverse in the sodium/calcium exchanger due to increasing intracellular sodium concentrations (Kapoor *et al.*, 2003). The resulting calcium influx may add to the pro-apoptotic environment.Mitochondrial dysfunction is also associated with mitochondrial membrane disruption and the release of cytochrome c and free radicals, contributing to the pool of toxic cytoplasmic molecules. Cytochrome c has been shown to be necessary for apoptosome formation with procaspase 9, part of the apoptotic cascade (Schild *et al.*, 2001).

MHC Expression - IFN-γ is able to induce MHC expression on oligodendrocytes in the CNS giving these cells an antigen-presenting role, causing myelin perturbation (Turnley *et al.*, 1991). Oligodendrocytes are constantly replacing lipoprotein membrane constituents in their extensive membranes, putting a high workload on the Golgi apparatus and endoplasmic reticulum (ER) (Smith, 1968). When induced to express MHC II, it is likely that the oligodendrocyte is unable to transport histocompatibility complex proteins from the ER due to the absence of accessory molecules which

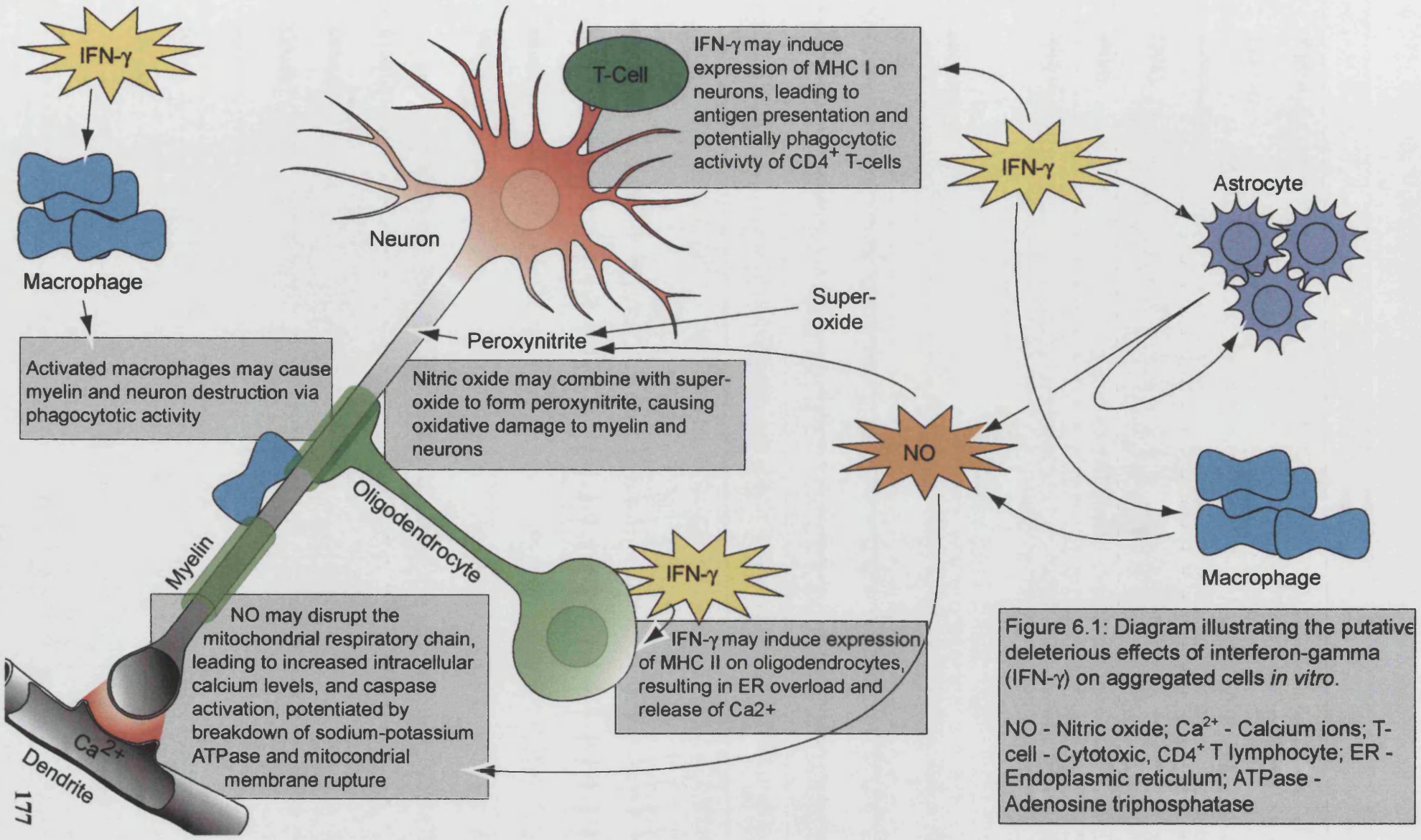

Figure 6.1: Diagram illustrating the putative deleterious effects of interferon-gamma (IFN-γ) on aggregated cells *in vitro*.

NO - Nitric oxide; Ca^{2+} - Calcium ions; T-cell - Cytotoxic, $CD4^+$ T lymphocyte; ER - Endoplasmic reticulum; ATPase - Adenosine triphosphatase

oligodendrocytes do not constitutively express (Baerwald *et al.*, 2000). There is however low-level expression on the cell surface membrane. It has been shown that accumulation of protein in the ER results in calcium ion release (Pahl & Baeuerle, 1996). This could trigger apoptosis as outlined above. Alternatively, disruption of the ability to process myelin proteins may result in demyelination and impaired remyelination.

IFN-γ can induce MHC class I expression in neurons (Neumann *et al.*, 1997), allowing for antigen presentation and subsequent recognition by cytotoxic CD4+ T-cells, opening up the cell to damage by cytotoxic mediators.

6.1.2. Mechanisms for endogenous cannabinoid-mediated neuroprotection

It has been shown in this thesis that lack of the CB1 receptor can lead to increased detrimental effects in neurons following an inflammatory insult both in vivo and in vitro. It can be conferred from this that increased activation of CB1R could be neuroprotective in these pathological states, and that this may be achieved by modulation of the endogenous cannabinoid signalling system. Putative pathways for neuroprotection via CB1, especially combating the effects of IFN-γ outlined previously, will be postulated.

Cytokines – Cytokine expression has been shown to be affected by treatment with cannabinoids in a range of models (Croxford & Miller, 2003; Facchinetti *et al.*, 2003; Gruol *et al.*, 1998; Molina-Holgado *et al.*, 1997). Cytokines are a vital control mechanism in disorders such as EAE, initiating and upregulating the immune response following disease induction and providing key effectors in almost all aspects of disease (Willenborg & Staykova, 2003). The effects of IFN-γ have been discussed previously.

With regards to IL-1 activity, one study using rat microglia in vitro indicated that THC administration elicits a reduction in the cytokine (Puffenbarger *et al.*, 2000). IL-1 has also been shown to be modulated by the cytokine IL-1 receptor antagonist (IL-1ra(Molina-Holgado *et al.*, 2003). In vitro application of various cannabinoid molecules can induce expression of IL-1ra. In vivo, mice injected with various cannabinoid agonists can induce expression of IL-1ra. In vivo, mice injected with lipopolysaccharide (LPS) to initiate an immune reaction were subsequently treated with a cannabinoid agonist or antagonist. The agonist induced and increase in IL-1ra, while the antagonist produced the opposite effect. Neuroprotection by the cannabinoid agonist HU210 in vivo following excitotoxic insult was abolished when applied to IL-1ra knockout mice, as was the inhibition of NO production, indicating that IL-1 plays a role in these effects.

LPS-mediated inflammation in vitro following administration of the cannabinoid agonists WIN55,212-2 and HU210 resulted in an reduction of TNF-α and IL-12 expression, and an increase in IL-10, producing an anti-inflammatory effect (Smith *et al.*, 2000a). The authors postulate that the effect may have been due to CB1R activation on immune cells. However, the agonists used, while being selective for CB1R, have lesser efficacy at CB2. The possibility of non-receptor mediated effects was illustrated in vitro when WIN55,212-2 applied to blood mononuclear cells elicited a reduction in TNF-α (Germain *et al.*, 2002). This was however not significantly reduced by antagonists at the CB1R or CB2R. In addition, a high concentration of agonist was required to elicit the effect.

It has been hypothesised that CB1R activation may elicit effects on cytokines via the hypothalamic-pituitary adrenal axis, leading to reduced TH1 activity via corticosterone modulation (Gallily *et al.*, 1997). Given that agonists do not appear to be

specifically efficacious at one receptor subtype, perhaps more likely is the direct effect of cytokine modulation via CB2 activation on immune cells. This could control the relative differentiation of Th1 and Th2 cell types, thus controlling cytokine production.

MHC expression, cAMP and kinase regulation – It has been reported that the CB1 agonist CP55,940 can block IFN-γ-induced MHC II expression in a mouse microglial cell line in vitro (Gongora *et al.*, 2004). It was found that the CB1R effected MCH expression changes through the MHC II transactivator (CIITA) following a modest dose of the CB1-preferential agonist. CIITA has also been found to bring about a wide range of gene expression changes, identified by DNA microarray to include genes responsible for antigen processing, signalling and cell proliferation, and may play a larger role in the physiology of antigen presenting cells.

One route of modulation of CIITA gene expression, and potentially transcription of other genes, is the negative coupling of CB1R to adenylate cyclase (Davis *et al.*, 2003). Activation of the receptor has been shown to inhibit the conversion of ATP to cAMP through a pertussis toxin-sensitive GTPα inhibitory protein. This reduces cAMP levels, one effect of which is to increase the cytosolic levels of microtubule-associated protein kinase (MAPK) molecules. These kinases have diverse effects on cell proliferation, differentiation and synaptic plasticity (Bozyczko-Coyne *et al.*, 2002; Waltereit & Weller, 2003). Such a large range of potential gene regulation triggered by CB1R could elicit changes supportive of neurodegeneration (Barone *et al.*, 2001). Signalling via various MAPK molecules (including FAK and ERK) has been shown to result in changes in expression of the proinflammatory cytokines IL6 and IL8, and plays a role in TNFα-mediated cytokine production via the transcription factor NF-κB. TGF-

β mediated neuroprotection in rodent hippocampal cell cultures has been shown to be elicited via NF-κB, and to be dependant on ERK (Zhu *et al.*, 2004). It is worth remembering that there are also studies illustrating regulation of NF-κB by CB2 receptors (Ouyang *et al.*, 1998), putative as yet uncharacterised cannabinoid receptors (Herring & Kaminski, 1999), and by receptor-independent mechanisms (Sancho *et al.*, 2003). Therefore, CB1 activation may not be wholly responsible for observed effects.

Excitotoxic inhibition, ion channels and apoptosis – Endocannabinoid signalling in the CNS plays a major role in the control of excitatory neurotransmitter release (Wilson & Nicoll, 2001). The arrival of an action potential at the terminus of the presynaptic cell triggers opening of calcium channels and the influx of the ion. This results in vesicle fusion with the presynaptic membrane and the release of neurotransmitter contents which cross the synaptic cleft to activate post-synaptic receptors and elicit a further action potential, involving again the influx of calcium ions. Prolonged synaptic presence or excessive release of glutamate could result in excitotoxicity, whereby intracellular calcium ion concentration is elevated, causing protease activation and leading to apoptosis (Arundine & Tymianski, 2003). However, glutamate binding to postsynaptic metabotropic glutamate receptor 1 stimulates phospholipase D to produce the endocannabinoid anandamide from NAPE, it's precursor (Hansen *et al.*, 1999). The endocannabinoid crosses the synapse in a retrograde direction and activates CB1R, closing associated calcium channels, causing membrane repolarisation and halting neurotransmitter release, thereby preventing excitotoxicity (Kreitzer & Regehr, 2002). This endogenous protective pathway is a strong candidate for the neuroprotective effect

presented here. Lack of the CB1 receptor in the knockout mouse would abolish this pathway, potentially leading to increased excitotoxic effects.

Nitric Oxide – As discussed previously, NO could act as a potent mediator of neuronal damage. Several studies have reported modulation of NO synthesis by CB1R activation. Inhibition of NO production by CB1R agonist Δ^9-THC from mouse peritoneal macrophages has been demonstrated following activation with LPS and IFN-γ (Coffey *et al.*, 1996), but the high concentrations of agonist required to elicit this effect may have promoted non-receptor mediated events. Cannabinoid treatment in the Thelier's virus model of inflammatory disease is also associated with NO production; anandamide treatment of virally infected astrocytes suppressed NO production in a dose dependant manner (Molina-Holgado *et al.*, 1997). Inhibition of potassium chloride induced activation of neuronal nitric oxide synthase was observed in an in vitro cerebellar granule neuron cell culture preparation following treatment with WIN55,212-2 (Hillard *et al.*, 1999). The CB1R antagonist SR141716A potentiated NO synthase activation, suggesting that tonic endocannabinoid activity at CB1R may be limiting NOS activity. In CNS resident microglia, NO production was inhibited by CP55940, with CB1 antagonists again reversing the effect, indicating functional linkage between CB1 and NO production (Waksman *et al.*, 1999). However, again the high levels of agonist used may indicate activation of receptor independent pathways. One study outlined differential roles for the nitric oxide pathway on cannabinoid CNS effects mediated by Δ^9-THC, suggesting that nitric oxide is involved in cannabinoid control of body temperature and locomotor activity, but not in nociceptive effects (Azad *et al.*, 2001).

The oxidative stress mediated by NO depends at least partially on the presence of elevated super-oxide radical levels, as discussed previously. In human blood mononuclear cells in vitro, WIN55,212-2 was found to reduce reactive oxygen species generation in LPS-primed cells (Germain *et al.*, 2002). However, any antioxidant effect may have been non-receptor mediated due to the high concentration of agonist required to elicit a response.

6.2. Future work

The work presented here is a step towards elucidating a therapeutic role for cannabinoids. Further experimental studies are needed to clarify the role of these compounds in protecting axonal processes.

Electron microscopical studies are required to confirm that, as in the rat-derived aggregate culture, myelin compaction occurs, and noR are present.

A fundamental question in neurodegenerative demyelinating disease is one of primary pathology – does demyelination lead to axonal damage, or is neurodegeneration a result of primary inflammatory attack? Although the two are not necessarily mutually exclusive, this could be investigated by transverse cutting, immunostaining for myelin and neuronal markers, and counting/characterising of neurons and myelin from EAE spinal cords. A larger number of time-points in the disease course could be used to elucidate the primary event. The use of an assay to quantify active caspase 3 at these time points would illustrate the role of this pathway in cell death.

The quantification of oligodendrocyte precursor proliferation and neuronal sprouting following demyelination would provide insight into the remyelinative capacity of cells in either system. Antibodies against markers for oligodendrocyte

precursors (e.g. NG2, O4, PDGFα receptor) and neuronal precursors (e.g. nestin), dual stained with a marker for proliferating cells (e.g. cyclin B1) would provide an insight into the proliferation of precursors. Neuronal sprouting could be identified by staining for a marker of growth cone extension or synapse formation (e.g. GAP-43 or synaptophysin), and the extent of this analysed by dual staining for a neuronal marker (e.g. NF) and cell counting. In this way, a ratio of total cells to dual-stained cells will give a measure of the extent of *de novo* neuronal outgrowth. Also, the concurrent analysis of growth factor expression such as through gene microarrays may shed light on the microenvironment needed to provide the optimum conditions for remyelination. Analysis of whole spinal cords may not be an effective method by which to do this, as any changes would be confined to lesion sites, and thus diluted in the whole cord. Ideally, the microarray approach would provide sensitive and wide-ranging quantification of growth factors and cytokines; however, this approach may be prohibited by cost. Therefore, longitudinal spinal cord sectioning and antibody-mediated staining would provide a sensitive and cost-effective method of analysis.

Investigations into the mechanisms of cell-death independent damage to myelin and axons following demyelination or conductance block are required. Immunocytochemical and confocal analysis of apoptotic nuclei (using the Hoescht or TUNEL stains) paired with cell-type markers will show which cell types are undergoing apoptosis. Use of an antibody against caspase 3 as well as staining for cell-type markers may give a better idea of sub-cellular localisation of proteolytic activity.

In vitro, both NF and MBP levels recover completely by the final culture day. It is unlikely that this recovery represents replacement of apoptotic cells by increased proliferation and migration of precursors. At least in part, it is likely to be that damaged

distal structures, such as myelin or axons, are replaced or repaired by a surviving soma. Apoptosis-independent mechanisms of cell damage are a potential research and therapeutic target, including analysis of proteinases such as the metalloproteinases, and examination of calcium-dependent proteolytic pathways.

Exogenous cannabinoids have been shown to effectively ameliorate EAE, at least with respect to control of some clinical signs. Therapeutics involving cannabinoid compounds have reached Phase III clinical trials for pain, spasticity and other disseminated symptoms of multiple sclerosis. Some have shown encouraging results, but none have provided an easily dosed, side effect free treatment profile. Smoking cannabis, as recreational users often do, is not an acceptable route of administration, as even tobacco-free cannabis smoke contains potent carcinogens (Roth *et al.*, 2001). Oral administration leads to problems of dosing, as the first pass metabolism of active cannabinoid compounds can be as high as 80%. In addition, cannabinoids are taken up into dietary fat, being released slowly, making accurate dosing difficult. Cannabinoids are also currently associated with psychotropic side effects which could be debilitating or prevent normal activities at effective doses.

Modulation of the endogenous pathway is perhaps the most promising target for therapeutic intervention which may reduce the side effects and possibly administration problems. Up regulation of endogenous cannabinoid production or down-regulation of degradation would increase cannabinoids in the CNS. Experimentally, this could be investigated by generating transgenic mice over-expressing endogenous CB_1 agonists, such as anandamide or 2-AG, by enhancing activity of enzymes involved in endocannabinoid agonist production (Sugiura *et al.*, 2002) or by disrupting genes

producing degradative proteins, such as fatty-acid amide hydrogenase (Cravatt *et al.*, 2001) or monoglycerol lipase (Dinh *et al.*, 2002).

Reference List

Abood, M. E., Rizvi, G., Sallapudi, N., & McAllister, S. D. (2001) Activation of the CB1 cannabinoid receptor protects cultured mouse spinal neurons against excitotoxicity. *Neurosci. Lett.*, 309,197-201.

Achiron, A., Miron, S., Lavie, V., Margalit, R., & Biegon, A. (2000) Dexanabinol (HU-211) effect on experimental autoimmune encephalomyelitis: implications for the treatment of acute relapses of multiple sclerosis. *J. Neuroimmunol.*, 102,26-31.

Ackerley, S., Thornhill, P., Grierson, A. J., Brownlees, J., Anderton, B. H., Leigh, P. N., Shaw, C. E., & Miller, C. C. (2003) Neurofilament heavy chain side arm phosphorylation regulates axonal transport of neurofilaments. *J. Cell Biol.*, 161,489-495.

Adams, J. M. & Cory, S. (2002) Apoptosomes: engines for caspase activation. *Curr. Opin. Cell Biol.*, 14,715-720.

Ahlgren, S. C., Wallace, H., Bishop, J., Neophytou, C., & Raff, M. C. (1997) Effects of thyroid hormone on embryonic oligodendrocyte precursor cell development in vivo and in vitro. . *Mol. Cell Neurosci.*, 9,420-432.

Ahmed, Z., Doward, A. I., Pryce, G., Taylor, D. L., Pocock, J. M., Leonard, J. P., Baker, D., & Cuzner, M. L. (2002) A role for caspase-1 and -3 in the pathology of experimental allergic encephalomyelitis : inflammation versus degeneration. *Am. J. Pathol.*, 161,1577-1586.

Alger, B. E., Pitler, T. A., Wagner, J. J., Martin, L. A., Morishita, W., Kirov, S. A., & Lenz, R. A. (1996) Retrograde signalling in depolarization-induced suppression of inhibition in rat hippocampal CA1 cells. *J. Physiol*, 496 (Pt 1),197-209.

Allamargot, C., Pouplard-Barthelaix, A., & Fressinaud, C. (2001) A single intracerebral microinjection of platelet-derived growth factor (PDGF) accelerates the rate of remyelination in vivo. *Brain Res.*, 918,28-39.

Allard, J., Barron, S., Diaz, J., Lubetzki, C., Zalc, B., Schwartz, J. C., & Sokoloff, P. (1998) A rat G protein-coupled receptor selectively expressed in myelin-forming cells. *Eur. J. Neurosci.*, 10,1045-1053.

Allen, S. J., Baker, D., O'Neill, J. K., Davison, A. N., & Turk, J. L. (1993) Isolation and characterization of cells infiltrating the spinal cord during the course of chronic relapsing experimental allergic encephalomyelitis in the Biozzi AB/H mouse. *Cell Immunol.*, 146,335-350.

Almazan, G., Honegger, P., & Matthieu, J. M. (1985) Triiodothyronine stimulation of oligodendroglial differentiation and myelination. A developmental study. *Dev. Neurosci.*, 7,45-54.

Almeida, A., Almeida, J., Bolanos, J. P., & Moncada, S. (2001) Different responses of astrocytes and neurons to nitric oxide: the role of glycolytically generated ATP in astrocyte protection. *Proc. Natl. Acad. Sci. U. S. A*, 98,15294-15299.

Altman, J.(1969)Postnatal Neurogenesis and the Problem of Neural Plasticity.

Amor, S., Baker, D., Groome, N., & Turk, J. L. (1993) Identification of a major encephalitogenic epitope of proteolipid protein (residues 56-70) for the induction of experimental allergic encephalomyelitis in Biozzi AB/H and nonobese diabetic mice. *J. Immunol.*, 150,5666-5672.

Amor, S., Groome, N., Linington, C., Morris, M. M., Dornmair, K., Gardinier, M. V., Matthieu, J. M., & Baker, D. (1994) Identification of epitopes of myelin oligodendrocyte glycoprotein for the induction of experimental allergic encephalomyelitis in SJL and Biozzi AB/H mice. *J. Immunol.*, 153,4349-4356.

Amor, S., O'Neill, J. K., Morris, M. M., Smith, R. M., Wraith, D. C., Groome, N., Travers, P. J., & Baker, D. (1996) Encephalitogenic epitopes of myelin basic protein, proteolipid protein, myelin oligodendrocyte glycoprotein for experimental allergic encephalomyelitis induction in Biozzi ABH (H-2Ag7) mice share an amino acid motif. *J. Immunol.*, 156,3000-3008.

Angevine, J. B., Jr. (1970) Time of neuron origin in the diencephalon of the mouse. An autoradiographic study. *J. Comp Neurol.*, 139,129-187.

Archer, D. R., Watson, D. F., & Griffin, J. W. (1994) Phosphorylation-dependent immunoreactivity of neurofilaments and the rate of slow axonal transport in the central and peripheral axons of the rat dorsal root ganglion. *J. Neurochem.*, 62,1119-1125.

Arenella, L. S. & Herndon, R. M. (1984) Mature oligodendrocytes. Division following experimental demyelination in adult animals. *Arch. Neurol.*, 41,1162-1165.

Arnett, H. A., Mason, J., Marino, M., Suzuki, K., Matsushima, G. K., & Ting, J. P. (2001) TNF alpha promotes proliferation of oligodendrocyte progenitors and remyelination. *Nat. Neurosci.*, 4,1116-1122.

Artavanistsakonas, S., Matsuno, K., & Fortini, M. E. (1995) Notch Signalling. *Science*, 268,225-232.

Arundine, M. & Tymianski, M. (2003) Molecular mechanisms of calcium-dependent neurodegeneration in excitotoxicity. *Cell Calcium*, 34,325-337.

Asakura, K. & Rodriguez, M. (1998) A unique population of circulating autoantibodies promotes central nervous system remyelination. *Mult. Scler.*, 4,217-221.

Azad, S. C., Marsicano, G., Eberlein, I., Putzke, J., Zieglgansberger, W., Spanagel, R., & Lutz, B. (2001) Differential role of the nitric oxide pathway on delta(9)-THC-induced central nervous system effects in the mouse. *Eur. J. Neurosci.*, 13,561-568.

Baerwald, K. D., Corbin, J. G., & Popko, B. (2000) Major histocompatibility complex heavy chain accumulation in the endoplasmic reticulum of oligodendrocytes results in myelin abnormalities. *J. Neurosci. Res.*, 59,160-169.

Baker, D., O'Neill, J. K., Gschmeissner, S. E., Wilcox, C. E., Butter, C., & Turk, J. L. (1990) Induction of chronic relapsing experimental allergic encephalomyelitis in Biozzi mice. *J. Neuroimmunol.*, 28,261-270.

Baker, D., Pryce, G., Croxford, J. L., Brown, P., Pertwee, R. G., Huffman, J. W., & Layward, L. (2000) Cannabinoids control spasticity and tremor in a multiple sclerosis model.Nature, 404, 84-87.

Baker, D., Pryce, G., Croxford, J. L., Brown, P., Pertwee, R. G., Makriyannis, A., Khanolkar, A., Layward, L., Fezza, F., Bisogno, T., & Di, M., V (2001) Endocannabinoids control spasticity in a multiple sclerosis model. *FASEB J.*, 15,300-302.

Bambakidis, N. C., Wang, R. Z., Franic, L., & Miller, R. H. (2003) Sonic hedgehog-induced neural precursor proliferation after adult rodent spinal cord injury. *J. Neurosurg.*, 99,70-75.

Baranzini, S. E., Elfstrom, C., Chang, S. Y., Butunoi, C., Murray, R., Higuchi, R., & Oksenberg, J. R. (2000) Transcriptional analysis of multiple sclerosis brain lesions reveals a complex pattern of cytokine expression. *Journal Of Immunology*, 165,6576-6582.

Barone, F. C., Irving, E. A., Ray, A. M., Lee, J. C., Kassis, S., Kumar, S., Badger, A. M., Legos, J. J., Erhardt, J. A., Ohlstein, E. H., Hunter, A. J., Harrison, D. C., Philpott, K., Smith, B. R., Adams, J. L., & Parsons, A. A. (2001) Inhibition of p38 mitogen-activated protein kinase provides neuroprotection in cerebral focal ischemia. *Med. Res. Rev.*, 21,129-145.

Barres, B. A., Hart, I. K., Coles, H. S., Burne, J. F., Voyvodic, J. T., Richardson, W. D., & Raff, M. C. (1992) Cell death and control of cell survival in the oligodendrocyte lineage. *Cell*, 70,31-46.

Barres, B. A. & Raff, M. C. (1993) Proliferation of oligodendrocyte precursor cells depends on electrical activity in axons. *Nature*, 361,258-260.

Bartnik, B. L., Juurlink, B. H., & Devon, R. M. (2000) Macrophages: their myelinotrophic or neurotoxic actions depend upon tissue oxidative stress. *Mult. Scler.*, 6,37-42.

Bashir, K. & Whitaker, J. N. (1999) Clinical and laboratory features of primary progressive and secondary progressive MS. *Neurology*, 53,765-771.

Begolka, W. S., Vanderlugt, C. L., Rahbe, S. M., & Miller, S. D. (1998) Differential expression of inflammatory cytokines parallels progression of central nervous system pathology in two clinically distinct models of multiple sclerosis. *J. Immunol.*, 161,4437-4446.

Ben Hur, T., Rogister, B., Murray, K., Rougon, G., & Dubois-Dalcq, M. (1998) Growth and fate of PSA-NCAM+ precursors of the postnatal brain. *J Neurosci.*, 18,5777-5788.

Berrendero, F., Sanchez, A., Cabranes, A., Puerta, C., Ramos, J. A., Garcia-Merino, A., & Fernandez-Ruiz, J. (2001) Changes in cannabinoid CB(1) receptors in striatal and cortical regions of rats with experimental allergic encephalomyelitis, an animal model of multiple sclerosis. *Synapse*, 41,195-202.

Bilsland, J. & Harper, S. (2002) Caspases and neuroprotection. *Curr. Opin. Investig. Drugs*, 3,1745-1752.

Bird, T. D., Farrell, D. F., Stranahan, S., & Austin, E. (1980) Developmental dissociation of myelin synthesis and "myelin-associated" enzyme activities in the shiverer mouse. *Neurochem. Res.*, 5,885-895.

Bjartmar, C., Kidd, G., Mork, S., Rudick, R., & Trapp, B. D. (2000) Neurological disability correlates with spinal cord axonal loss and reduced N-acetyl aspartate in chronic multiple sclerosis patients. *Ann. Neurol.*, 48,893-901.

Bjartmar, C. & Trapp, B. D. (2003) Axonal degeneration and progressive neurologic disability in multiple sclerosis. *Neurotox. Res.*, 5,157-164.

Black, J. A., Kocsis, J. D., & Waxman, S. G. (1990) Ion channel organization of the myelinated fiber. *Trends Neurosci.*, 13,48-54.

Black, M. M. & Baas, P. W. (1989) The basis of polarity in neurons. *Trends Neurosci.*, 12,211-214.

Blakemore, W. F. (1974) Pattern of remyelination in the CNS. *Nature*, 249,577-578.

Blakemore, W. F. (1977) Remyelination of CNS axons by Schwann cells transplanted from the sciatic nerve. *Nature*, 266,68-69.

Blakemore, W. F. & Patterson, R. C. (1978) Suppression of remyelination in the CNS by X-irradiation. *Acta Neuropathol. (Berl)*, 42,105-113.

Blakemore, W. F., Smith, P. M., & Franklin, R. J. (2000) Remyelinating the demyelinated CNS. *Novartis. Found. Symp.*, 231,289-298.

Boatright, K. M. & Salvesen, G. S. (2003) Caspase activation. *Biochem. Soc. Symp.*, 233-242.

Bongarzone, E. R., Pasquini, J. M., & Soto, E. F. (1995) Oxidative damage to proteins and lipids of CNS myelin produced by in vitro generated reactive oxygen species. *J. Neurosci. Res.*, 41,213-221.

Bozyczko-Coyne, D., Saporito, M. S., & Hudkins, R. L. (2002) Targeting the JNK pathway for therapeutic benefit in CNS disease. *Curr. Drug Target CNS. Neurol. Disord.*, 1,31-49.

Bray, D. (1979) Mechanical tension produced by nerve cells in tissue culture. *J. Cell Sci.*, 37,391-410.

Breivogel, C. S., Griffin, G., Di, M., V, & Martin, B. R. (2001) Evidence for a new G protein-coupled cannabinoid receptor in mouse brain. *Mol. Pharmacol.*, 60,155-163.

Brooks, J. W., Pryce, G., Bisogno, T., Jaggar, S. I., Hankey, D. J., Brown, P., Bridges, D., Ledent, C., Bifulco, M., Rice, A. S., Di, M., V, & Baker, D. (2002) Arvanil-induced inhibition of spasticity and persistent pain: evidence for therapeutic sites of action different from the vanilloid VR1 receptor and cannabinoid CB(1)/CB(2) receptors. *Eur. J. Pharmacol.*, 439,83-92.

Brown, K. A. (2001) Factors modifying the migration of lymphocytes across the blood-brain barrier. *Int. Immunopharmacol.*, 1,2043-2062.

Budihardjo, I., Oliver, H., Lutter, M., Luo, X., & Wang, X. (1999) Biochemical pathways of caspase activation during apoptosis. *Annu. Rev. Cell Dev. Biol.*, 15,269-290.

Burlacu, A. (2003) Regulation of apoptosis by Bcl-2 family proteins. *J. Cell Mol. Med.*, 7,249-257.

Burne, J. F., Staple, J. K., & Raff, M. C. (1996) Glial cells are increased proportionally in transgenic optic nerves with increased numbers of axons. . *J. Neurosci.*, 16,2064-2073.

Butt, A. M. & Ransom, B. R. (1989) Visualization of oligodendrocytes and astrocytes in the intact rat optic nerve by intracellular injection of lucifer yellow and horseradish peroxidase. *GLIA*, 2,470-475.

Calignano, A., La Rana, G., Giuffrida, A., & Piomelli, D. (1998) Control of pain initiation by endogenous cannabinoids. *Nature*, 394,277-281.

Calignano, A., La Rana, G., & Piomelli, D. (2001) Antinociceptive activity of the endogenous fatty acid amide, palmitylethanolamide. *Eur. J. Pharmacol.*, 419,191-198.

Campagnoni, A. T. (1988) Molecular biology of myelin proteins from the central nervous system. *J Neurochem.*, 51,1-14.

Campbell, V. A. (2001) Tetrahydrocannabinol-induced apoptosis of cultured cortical neurones is associated with cytochrome c release and caspase-3 activation. *Neuropharmacology*, 40,702-709.

Cannella, B., Hoban, C. J., Gao, Y. L., Garcia-Arenas, R., Lawson, D., Marchionni, M., Gwynne, D., & Raine, C. S. (1998) The neuregulin, glial growth factor 2, diminishes autoimmune demyelination and enhances remyelination in a chronic relapsing model for multiple sclerosis. *Proc. Natl. Acad. Sci. U. S. A*, 95,10100-10105.

Cannella, B., Pitt, D., Capello, E., & Raine, C. S. (2000) Insulin-like growth factor-1 fails to enhance central nervous system myelin repair during autoimmune demyelination. *American Journal Of Pathology*, 157,933-943.

Capello, E., Voskuhl, R. R., McFarland, H. F., & Raine, C. S. (1997) Multiple sclerosis: re-expression of a developmental gene in chronic lesions correlates with remyelination. *Ann. Neurol.*, 41,797-805.

Carafoli, E. (1988) The plasma membrane calcium transporting systems in the regulation of cell calcium. *Adv. Second Messenger Phosphoprotein Res.*, 21,147-155.

Caroni, P. & Schwab, M. E. (1988a) Antibody against myelin-associated inhibitor of neurite growth neutralizes nonpermissive substrate properties of CNS white matter. *Neuron*, 1,85-96.

Caroni, P. & Schwab, M. E. (1988b) Two membrane protein fractions from rat central myelin with inhibitory properties for neurite growth and fibroblast spreading. *J Cell Biol.*, 106,1281-1288.

Carroll, W. M. & Jennings, A. R. (1994) Early recruitment of oligodendrocyte precursors in CNS demyelination. *Brain*, 117 (Pt 3),563-578.

Chang, A., Tourtellotte, W. W., Rudick, R., & Trapp, B. D. (2002) Premyelinating oligodendrocytes in chronic lesions of multiple sclerosis. *N. Engl. J. Med.*, 346,165-173.

Chang, D. W., Ditsworth, D., Liu, H., Srinivasula, S. M., Alnemri, E. S., & Yang, X. (2003a) Oligomerization is a general mechanism for the activation of apoptosis initiator and inflammatory procaspases. *J. Biol. Chem.*, 278,16466-16469.

Chang, D. W., Xing, Z., Capacio, V. L., Peter, M. E., & Yang, X. (2003b) Interdimer processing mechanism of procaspase-8 activation. *EMBO J.*, 22,4132-4142.

Chang, H. Y. & Yang, X. (2000) Proteases for cell suicide: functions and regulation of caspases. *Microbiol. Mol. Biol. Rev.*, 64,821-846.

Chao, C. C., Hu, S., Sheng, W. S., Bu, D., Bukrinsky, M. I., & Peterson, P. K. (1996) Cytokine-stimulated astrocytes damage human neurons via a nitric oxide mechanism. *GLIA*, 16,276-284.

Chinnaiyan, A. M., O'Rourke, K., Yu, G. L., Lyons, R. H., Garg, M., Duan, D. R., Xing, L., Gentz, R., Ni, J., & Dixit, V. M. (1996) Signal transduction by DR3, a death domain-containing receptor related to TNFR-1 and CD95. *Science*, 274,990-992.

Chomczynski, P. & Sacchi, N. (1987) Single-step method of RNA isolation by acid guanidinium thiocyanate-phenol-chloroform extraction. . *Anal. Biochem.*, 162,156-159.

Clarke, P. G. (1981) Chance, repetition, and error in the development of normal nervous systems. *Perspect. Biol. Med.*, 25,2-17.

Clifford, D. B. (1983) Tetrahydrocannabinol for tremor in multiple sclerosis. *Ann. Neurol.*, 13,669-671.

Coffey, R. G., Yamamoto, Y., Snella, E., & Pross, S. (1996) Tetrahydrocannabinol inhibition of macrophage nitric oxide production. *Biochem. Pharmacol.*, 52,743-751.

Coleman, M. P. & Perry, V. H. (2002) Axon pathology in neurological disease: a neglected therapeutic target. *Trends Neurosci.*, 25,532-537.

Colman, D. R., Kreibich, G., Frey, A. B., & Sabatini, D. D. (1982) Synthesis and incorporation of myelin polypeptides into CNS myelin. *J. Cell Biol.*, 95,598-608.

Compton, D. R., Gold, L. H., Ward, S. J., Balster, R. L., & Martin, B. R. (1992) Aminoalkylindole analogs: cannabimimetic activity of a class of compounds structurally distinct from delta 9-tetrahydrocannabinol. *J. Pharmacol. Exp. Ther.*, 263,1118-1126.

Copelman, C. A., Cuzner, M. L., Groome, N., & Diemel, L. T. (2000) Temporal analysis of growth factor mRNA expression in myelinating rat brain aggregate cultures: Increments in CNTF, FGF-2, IGF-I, and PDGF-AA mRNA are induced by antibody-mediated demyelination. *GLIA*, 30,342-351.

Copelman, C. A., Diemel, L. T., Gveric, D., Gregson, N. A., & Cuzner, M. L. (2001) Myelin phagocytosis and remyelination of macrophage-enriched central nervous system aggregate cultures. *J. Neurosci. Res.*, 66,1173-1178.

Cowan, W. M.(1973)Neuronal death as a regulative mechanism in the control of cell number in the nervous system.19-41.

Crang, A. J., Gilson, J., & Blakemore, W. F. (1998) The demonstration by transplantation of the very restricted remyelinating potential of post-mitotic oligodendrocytes. *J. Neurocytol.*, 27,541-553.

Cravatt, B. F., Demarest, K., Patricelli, M. P., Bracey, M. H., Giang, D. K., Martin, B. R., & Lichtman, A. H. (2001) Supersensitivity to anandamide and enhanced

endogenous cannabinoid signaling in mice lacking fatty acid amide hydrolase. *Proc. Natl. Acad. Sci. U. S. A*, 98,9371-9376.

Crespo, D., Verduga, R., Villegas, J., & Fernandez-Viadero, C. (1995) Dimorphic myelin in the rat optic nerve as a result of retinal activity blockage by tetrodotoxin during early postnatal period. *Histol. Histopathol.*, 10,289-299.

Croxford, J. L. & Miller, S. D. (2003) Immunoregulation of a viral model of multiple sclerosis using the synthetic cannabinoid R+WIN55,212. *J. Clin. Invest*, 111,1231-1240.

Cuzner, M. L., Loughlin, A. J., Mosley, K., & Woodroofe, M. N. (1994) The role of microglia macrophages in the processes of inflammatory demyelination and remyelination. *Neuropathol. Appl. Neurobiol.*, 20,200-201.

David, S. & Aguayo, A. J. (1981) Axonal elongation into peripheral nervous system "bridges" after central nervous system injury in adult rats. *Science*, 214,931-933.

Davie, C. A., Hawkins, C. P., Barker, G. J., Brennan, A., Tofts, P. S., Miller, D. H., & McDonald, W. I. (1994) Serial proton magnetic resonance spectroscopy in acute multiple sclerosis lesions. *Brain*, 117 (Pt 1),49-58.

Davis, M. I., Ronesi, J., & Lovinger, D. M. (2003) A predominant role for inhibition of the adenylate cyclase/protein kinase A pathway in ERK activation by cannabinoid receptor 1 in N1E-115 neuroblastoma cells. *J. Biol. Chem.*, 278,48973-48980.

de Andres, B., Cardaba, B., del, P., V, Martin-Orozco, E., Gallardo, S., Tramon, P., Palomino, P., & Lahoz, C. (1994) Modulation of the Fc gamma RII and Fc gamma RIII induced by GM-CSF, IFN-gamma and IL-4 on murine eosinophils. *Immunology*, 83,155-160.

Demerens, C., Stankoff, B., Logak, M., Anglade, P., Allinquant, B., Couraud, F., Zalc, B., & Lubetzki, C. (1996) Induction of myelination in the central nervous system by electrical activity. *Proceedings Of The National Academy Of Sciences Of The United States Of America*, 93,9887-9892.

Devane, W. A., Dysarz, F. A., III, Johnson, M. R., Melvin, L. S., & Howlett, A. C. (1988) Determination and characterization of a cannabinoid receptor in rat brain. *Mol. Pharmacol.*, 34,605-613.

Dewey, W. L. (1986) Cannabinoid pharmacology. *Pharmacol. Rev.*, 38,151-178.

Di, M., V, Breivogel, C. S., Tao, Q., Bridgen, D. T., Razdan, R. K., Zimmer, A. M., Zimmer, A., & Martin, B. R. (2000) Levels, metabolism, and pharmacological activity of anandamide in CB(1) cannabinoid receptor knockout mice: evidence for non-CB(1), non-CB(2) receptor-mediated actions of anandamide in mouse brain. *J. Neurochem.*, 75,2434-2444.

Di, M., V, De Petrocellis, L., Bisogno, T., & Melck, D. (1999) Metabolism of anandamide and 2-arachidonoylglycerol: an historical overview and some recent developments. *Lipids*, 34 Suppl,S319-S325.

Diemel, L. T., Copelman, C. A., & Cuzner, M. L. (1998) Macrophages in CNS remyelination: friend or foe? *Neurochem. Res.*, 23,341-347.

Diemel, L. T., Wolswijk, G., Jackson, S. J., & Cuzner, M. L. (2003) Remyelination of cytokine or antibody demyelinated CNS aggregate cultures is inhibited by macrophage supplementation.GLIA, In Press-

Dinh, T. P., Carpenter, D., Leslie, F. M., Freund, T. F., Katona, I., Sensi, S. L., Kathuria, S., & Piomelli, D. (2002) Brain monoglyceride lipase participating in endocannabinoid inactivation. *Proc. Natl. Acad. Sci. U. S. A*, 99,10819-10824.

Doetsch, F., GarciaVerdugo, J. M., & AlvarezBuylla, A. (1997) Cellular composition and three-dimensional organization of the subventricular germinal zone in the adult mammalian brain. *Journal Of Neuroscience*, 17,5046-5061.

Durbec, P. & Cremer, H. (2001) Revisiting the function of PSA-NCAM in the nervous system. *Mol. Neurobiol.*, 24,53-64.

Earnshaw, W. C., Martins, L. M., & Kaufmann, S. H. (1999) Mammalian caspases: structure, activation, substrates, and functions during apoptosis. *Annu. Rev. Biochem.*, 68,383-424.

Eayers, J. T. & Taylor, S. H. (1951) The effect of thyroid hormone deficency induced by methythiouracil on the maturation of the CNS. *J Anat*, 85,350-358.

Einheber, S., Zanazzi, G., Ching, W., Scherer, S., Milner, T. A., Peles, E., & Salzer, J. L. (1997) The axonal membrane protein Caspr, a homologue of neurexin IV, is a component of the septate-like paranodal junctions that assemble during myelination. *J. Cell Biol.*, 139,1495-1506.

Elder, G. A., Friedrich, V. L., Jr., & Lazzarini, R. A. (2001) Schwann cells and oligodendrocytes read distinct signals in establishing myelin sheath thickness. *J. Neurosci. Res.*, 65,493-499.

Espejo, C., Penkowa, M., Saez-Torres, I., Hidalgo, J., Garcia, A., Montalban, X., & Martinez-Caceres, E. M. (2002) Interferon-gamma regulates oxidative stress during experimental autoimmune encephalomyelitis. *Exp. Neurol.*, 177,21-31.

Facchinetti, F., Del Giudice, E., Furegato, S., Passarotto, M., & Leon, A. (2003) Cannabinoids ablate release of TNFalpha in rat microglial cells stimulated with lypopolysaccharide. *GLIA*, 41,161-168.

Facci, L., Dal Toso, R., Romanello, S., Buriani, A., Skaper, S. D., & Leon, A. (1995) Mast cells express a peripheral cannabinoid receptor with differential sensitivity to anandamide and palmitoylethanolamide. *Proc. Natl. Acad. Sci. U. S. A*, 92,3376-3380.

Felder, C. C., Nielsen, A., Briley, E. M., Palkovits, M., Priller, J., Axelrod, J., Nguyen, D. N., Richardson, J. M., Riggin, R. M., Koppel, G. A., Paul, S. M., & Becker, G. W. (1996) Isolation and measurement of the endogenous cannabinoid receptor agonist, anandamide, in brain and peripheral tissues of human and rat. *FEBS Lett.*, 393,231-235.

Fernandez-Ruiz, J. J., Berrendero, F., Hernandez, M. L., Romero, J., & Ramos, J. A. (1999) Role of endocannabinoids in brain development. *Life Sci.*, 65,725-736.

ffrenchConstant, C., Miller, R. H., Burne, J. F., & Raff, M. C. (1988) Evidence that migratory oligodendrocyte-type-2 astrocyte (O-2A) progenitor cells are kept out of the rat retina by a barrier at the eye-end of the optic-nerve. *Journal Of Neurocytology*, 17,13-25.

Franklin, R. J. (2002) Why does remyelination fail in multiple sclerosis? *Nat. Rev. Neurosci.*, 3,705-714.

Franklin, R. J. (2003) Remyelination by transplanted olfactory ensheathing cells. *Anat. Rec.*, 271B,71-76.

Franklin, R. J. & Gilson, J. M. (1996) Remyelination in the CNS of the hypothyroid rat. . *Neuroreport.*, 7,1526-1530.

Franklin, R. J., Gilson, J. M., & Blakemore, W. F. (1997) Local recruitment of remyelinating cells in the repair of demyelination in the central nervous system. . *J. Neurosci. Res.*, 50,337-344.

Fraser, A. & Evan, G. (1996) A license to kill. *Cell*, 85,781-784.

Fride, E., Ginzburg, Y., Breuer, A., Bisogno, T., Di, M., V, & Mechoulam, R. (2001) Critical role of the endogenous cannabinoid system in mouse pup suckling and growth. *Eur. J. Pharmacol.*, 419,207-214.

Gallily, R., Yamin, A., Waksmann, Y., Ovadia, H., Weidenfeld, J., Bar-Joseph, A., Biegon, A., Mechoulam, R., & Shohami, E. (1997) Protection against septic shock and suppression of tumor necrosis factor alpha and nitric oxide production by dexanabinol (HU-211), a nonpsychotropic cannabinoid. *J. Pharmacol. Exp. Ther.*, 283,918-924.

Galve-Roperh, I., Sanchez, C., Cortes, M. L., del Pulgar, T. G., Izquierdo, M., & Guzman, M. (2000) Anti-tumoral action of cannabinoids: involvement of sustained ceramide accumulation and extracellular signal-regulated kinase activation. *Nat. Med.*, 6,313-319.

Gay, D. & Esiri, M. (1991) Blood-brain barrier damage in acute multiple sclerosis plaques. An immunocytological study. *Brain*, 114,557-572.

Germain, N., Boichot, E., Advenier, C., Berdyshev, E. V., & Lagente, V. (2002) Effect of the cannabinoid receptor ligand, WIN 55,212-2, on superoxide anion and

TNF-alpha production by human mononuclear cells. *Int. Immunopharmacol.*, 2,537-543.

Ghandour, M. S., Langley, O. K., Vincendon, G., Gombos, G., Filippi, D., Limozin, N., Dalmasso, D., & Laurent, G. (1980) Immunochemical and immunohistochemical study of carbonic anhydrase II in adult rat cerebellum: a marker for oligodendrocytes. *Neuroscience*, 5,559-571.

Givogri, M. I., Costa, R. M., Schonmann, V., Silva, A. J., Campagnoni, A. T., & Bongarzone, E. R. (2002) Central nervous system myelination in mice with deficient expression of Notch1 receptor. *J. Neurosci. Res.*, 67,309-320.

Glitsch, M., Llano, I., & Marty, A. (1996) Glutamate as a candidate retrograde messenger at interneurone-Purkinje cell synapses of rat cerebellum. *J. Physiol*, 497 (Pt 2),531-537.

Gold, R., Hartung, H. P., & Toyka, K. V. (2000) Animal models for autoimmune demyelinating disorders of the nervous system. *Mol. Med. Today*, 6,88-91.

Gongora, C., Hose, S., O'Brien, T. P., & Sinha, D. (2004) Downregulation of class II transactivator (CIITA) expression by synthetic cannabinoid CP55,940. *Immunol. Lett.*, 91,11-16.

Goslin, K. & Banker, G. (1989) Experimental observations on the development of polarity by hippocampal neurons in culture. *J. Cell Biol.*, 108,1507-1516.

Gottlieb, R. A. (2000) Role of mitochondria in apoptosis. *Crit Rev. Eukaryot. Gene Expr.*, 10,231-239.

Gran, B. & Rostami, A. (2001) T cells, cytokines, and autoantigens in multiple sclerosis. *Curr. Neurol. Neurosci. Rep.*, 1,263-270.

Grant, P. & Pant, H. C. (2000) Neurofilament protein synthesis and phosphorylation. *J. Neurocytol.*, 29,843-872.

Greenwood, J., Walters, C. E., Pryce, G., Kanuga, N., Beraud, E., Baker, D., & Adamson, P. (2003) Lovastatin inhibits brain endothelial cell Rho-mediated lymphocyte migration and attenuates experimental autoimmune encephalomyelitis. *FASEB J.*, 17,905-907.

Griffiths, I., Klugmann, M., Anderson, T., Yool, D., Thomson, C., Schwab, M. H., Schneider, A., Zimmermann, F., McCulloch, M., Nadon, N., & Nave, K. A. (1998) Axonal swellings and degeneration in mice lacking the major proteolipid of myelin. *Science*, 280,1610-1613.

Groth, R. D., Dunbar, R. L., & Mermelstein, P. G. (2003) Calcineurin regulation of neuronal plasticity. *Biochem. Biophys. Res. Commun.*, 311,1159-1171.

Gruol, D. L., Sweeney, D. D., Conroy, S. M., Trotter, C., Netzeband, J. G., & Qiu, Z. (1998) Cannabinoids alter neurotoxicity produced by interleukin-6 in central nervous system neurons. *Adv. Exp. Med. Biol.*, 437,231-240.

Gveric, D., Hanemaaijer, R., Newcombe, J., van Lent, N. A., Sier, C. F., & Cuzner, M. L. (2001) Plasminogen activators in multiple sclerosis lesions: implications for the inflammatory response and axonal damage. *Brain*, 124,1978-1988.

Hall, G. F. & Yao, J. (2000) Neuronal morphology, axonal integrity, and axonal regeneration in situ are regulated by cytoskeletal phosphorylation in identified lamprey central neurons. *Microsc. Res. Tech.*, 48,32-46.

Hamburger, V. & Levi-Montalcini, R. (1949) Proliferation, Differentiation and Degeneration in the Spinal Ganglia of the Chick Embryo under Normal and Experimental Conditions. *Journal of Experimental Zoology*, 111,457-507.

Hamburger, V. & Oppenheim, R. W. (1982) Naturally occurring neuronal death in vertebrates. *Neuroscience Commentries*, 1,39-55.

Hampson, A. J. & Grimaldi, M. (2001) Cannabinoid receptor activation and elevated cyclic AMP reduce glutamate neurotoxicity. *Eur. J. Neurosci.*, 13,1529-1536.

Hampson, A. J., Grimaldi, M., Axelrod, J., & Wink, D. (1998) Cannabidiol and (-)Delta9-tetrahydrocannabinol are neuroprotective antioxidants. *Proc. Natl. Acad. Sci. U. S. A*, 95,8268-8273.

Hannah, M. J., Schmidt, A. A., & Huttner, W. B. (1999) Synaptic vesicle biogenesis. *Annu. Rev. Cell Dev. Biol.*, 15,733-798.

Hansen, H. H., Azcoitia, I., Pons, S., Romero, J., Garcia-Segura, L. M., Ramos, J. A., Hansen, H. S., & Fernandez-Ruiz, J. (2002) Blockade of cannabinoid CB(1) receptor function protects against in vivo disseminating brain damage following NMDA-induced excitotoxicity. *J. Neurochem.*, 82,154-158.

Hansen, H. H., Schmid, P. C., Bittigau, P., Lastres-Becker, I., Berrendero, F., Manzanares, J., Ikonomidou, C., Schmid, H. H., Fernandez-Ruiz, J. J., & Hansen, H. S. (2001) Anandamide, but not 2-arachidonoylglycerol, accumulates during in vivo neurodegeneration. *J. Neurochem.*, 78,1415-1427.

Hansen, H. S., Moesgaard, B., Hansen, H. H., Schousboe, A., & Petersen, G. (1999) Formation of N-acyl-phosphatidylethanolamine and N-acylethanolamine (including anandamide) during glutamate-induced neurotoxicity. *Lipids*, 34 Suppl,S327-S330.

Hashimoto, R., Nakamura, Y., Komai, S., Kashiwagi, Y., Matsumoto, N., Shiosaka, S., & Takeda, M. (2000) Phosphorylation of neurofilament-L during LTD. *Neuroreport*, 11,2739-2742.

Haydon, P. G., McCobb, D. P., & Kater, S. B. (1984) Serotonin selectively inhibits growth cone motility and synaptogenesis of specific identified neurons. *Science*, 226,561-564.

Hengartner, M. O. (2000) The biochemistry of apoptosis. *Nature*, 407,770-776.

Herkenham, M., Lynn, A. B., Little, M. D., Johnson, M. R., Melvin, L. S., de Costa, B. R., & Rice, K. C. (1990) Cannabinoid receptor localization in brain. *Proc. Natl. Acad. Sci. U. S. A*, 87,1932-1936.

Herring, A. C. & Kaminski, N. E. (1999) Cannabinol-mediated inhibition of nuclear factor-kappaB, cAMP response element-binding protein, and interleukin-2 secretion by activated thymocytes. *J. Pharmacol. Exp. Ther.*, 291,1156-1163.

Hildebrand, C., Remahl, S., Persson, H., & Bjartmar, C. (1993) Myelinated nerve fibres in the CNS. *Prog. Neurobiol.*, 40,319-384.

Hillard, C. J., Muthian, S., & Kearn, C. S. (1999) Effects of CB(1) cannabinoid receptor activation on cerebellar granule cell nitric oxide synthase activity. *FEBS Lett.*, 459,277-281.

Hinks, G. L. & Franklin, R. J. (1999) Distinctive patterns of PDGF-A, FGF-2, IGF-I, and TGF-beta1 gene expression during remyelination of experimentally-induced spinal cord demyelination. *Mol. Cell Neurosci.*, 14,153-168.

Hinks, G. L. & Franklin, R. J. (2000) Delayed changes in growth factor gene expression during slow remyelination in the CNS of aged rats. *Mol. Cell Neurosci.*, 16,542-556.

Hoffman, P. N., Cleveland, D. W., Griffin, J. W., Landes, P. W., Cowan, N. J., & Price, D. L. (1987) Neurofilament gene expression: a major determinant of axonal caliber. *Proc. Natl. Acad. Sci. U. S. A*, 84,3472-3476.

Honegger, P.(1985)Biochemical Differentiation in Serum-Free Aggregating Brain Cell Cultures.223-243.

Honegger, P. & Guentert Lauber, B. (1983) Epidermal growth factor (EGF) stimulation of cultured brain cells. I. Enhancement of the developmental increase in glial enzymatic activity. *Brain Res.*, 313,245-251.

Honegger, P. & Lenoir, D. (1980) Triodothyronine enhancement of neuronal differentiation in aggregating fetal rat brain cells cultured in a chemically defined medium. *Brain Res.*, 199,425-434.

Honegger, P. & Lenoir, D. (1982) Nerve growth factor (NGF) stimulation of cholinergic telencephalic neurons in aggregating cell cultures. *Brain Res.*, 255,229-238.

Honegger, P., Lenoir, D., & Favrod, P. (1979) Growth and differentiation of aggregating fetal brain cells in a serum-free defined medium. *Nature*, 282,305-308.

Honegger, P. & Matthieu, J. M.(1990)Aggregating brain cell cultures: a model to study myelination and demyelination.155-170.

Honegger, P., Matthieu, J. M., & Lassmann, H. (1989) Demyelination in brain cell aggregate cultures, induced by a monoclonal antibody against the myelin/oligodendrocyte glycoprotein (MOG). *Schweiz. Arch. Neurol. Psychiatr.*, 140,10-13.

Honegger, P. & Richelson, E. (1976) Biochemical differentiation of mechanically dissociated mammalian brain in aggregating cell culture. *Brain Res.*, 109,335-354.

Honegger, P. & Richelson, E. (1979) Neurotransmitter synthesis, storage and release by aggregating cell cultures of rat brain. *Brain Res.*, 162,89-101.

Honegger, P. & Werffeli, P. (1988) Use of aggregating cell cultures for toxicological studies. *Experientia*, 44,817-823.

Hooper, D. C., Scott, G. S., Zborek, A., Mikheeva, T., Kean, R. B., Koprowski, H., & Spitsin, S. V. (2000) Uric acid, a peroxynitrite scavenger, inhibits CNS inflammation, blood-CNS barrier permeability changes, and tissue damage in a mouse model of multiple sclerosis. *FASEB J.*, 14,691-698.

Howland, R. D. & Alli, P. (1986) Altered phosphorylation of rat neuronal cytoskeletal proteins in acrylamide induced neuropathy. *Brain Res.*, 363,333-339.

Howlett, A. C. (1995) Pharmacology of cannabinoid receptors. *Annu. Rev. Pharmacol. Toxicol.*, 35,607-634.

Howlett, A. C. (2002) The cannabinoid receptors. *Prostaglandins Other Lipid Mediat.*, 68-69,619-631.

Hu, S., Peterson, P. K., & Chao, C. C. (1997) Cytokine-mediated neuronal apoptosis. *Neurochem. Int.*, 30,427-431.

Huitinga, I., Schmidt, E. D., van der Cammen, M. J., Binnekade, R., & Tilders, F. J. (2000) Priming with interleukin-1beta suppresses experimental allergic encephalomyelitis in the Lewis rat. *J. Neuroendocrinol.*, 12,1186-1193.

Iglesias, A., Bauer, J., Litzenburger, T., Schubart, A., & Linington, C. (2001) T- and B-cell responses to myelin oligodendrocyte glycoprotein in experimental autoimmune encephalomyelitis and multiple sclerosis. *GLIA*, 36,220-234.

Jackowski, A. (1995) Neural injury repair: hope for the future as barriers to effective CNS regeneration become clearer. *Br. J Neurosurg.*, 9,303-317.

Jensen, A. M. & Raff, M. C. (1997) Continuous observation of multipotential retinal progenitor cells in clonal density culture. *Developmental Biology*, 188,267-279.

Johe, K. K., Hazel, T. G., Muller, T., DugichDjordjevic, M. M., & McKay, R. D. G. (1996) Single factors direct the differentiation of stem cells from the fetal and adult central nervous system. *Genes & Development*, 10,3129-3140.

John, G. R., Shankar, S. L., Shafit-Zagardo, B., Massimi, A., Lee, S. C., Raine, C. S., & Brosnan, C. F. (2002) Multiple sclerosis: re-expression of a developmental pathway that restricts oligodendrocyte maturation. *Nat. Med.*, 8,1115-1121.

Jorgensen, O. S., Honegger, P., & Matthieu, J. M. (1984) The neuronal adhesion protein D2 in differentiating aggregates of brain cells. *Brain Res.*, 316,41-49.

Kahl, K. G., Zielasek, J., Uttenthal, L. O., Rodrigo, J., Toyka, K. V., & Schmidt, H. H. (2003) Protective role of the cytokine-inducible isoform of nitric oxide synthase induction and nitrosative stress in experimental autoimmune encephalomyelitis of the DA rat. *J. Neurosci. Res.*, 73,198-205.

Kalman, B., Alder, H., & Lublin, F. D. (1995) Characteristics of the T lymphocytes involved in experimental allergic encephalomyelitis. *J. Neuroimmunol.*, 61,107-116.

Kapoor, R., Davies, M., Blaker, P. A., Hall, S. M., & Smith, K. J. (2003) Blockers of sodium and calcium entry protect axons from nitric oxide-mediated degeneration. *Ann. Neurol.*, 53,174-180.

Keirstead, H. S., BenHur, T., Rogister, B., Oleary, M. T., DuboisDalcq, M., & Blakemore, W. F. (1999) Polysialylated neural cell adhesion molecule-positive CNS precursors generate both oligodendrocytes and schwann cells to remyelinate the CNS after transplantation. *Journal Of Neuroscience*, 19,7529-7536.

Keirstead, H. S. & Blakemore, W. F. (1997) Identification of post-mitotic oligodendrocytes incapable of remyelination within the demyelinated adult spinal cord. *J. Neuropathol. Exp. Neurol.*, 56,1191-1201.

Keirstead, H. S., Levine, J. M., & Blakemore, W. F. (1998) Response of the oligodendrocyte progenitor cell population (defined by NG2 labelling) to demyelination of the adult spinal cord. *GLIA*, 22,161-170.

Kerschensteiner, M., Gallmeier, E., Behrens, L., Leal, V. V., Misgeld, T., Klinkert, W. E., Kolbeck, R., Hoppe, E., Oropeza-Wekerle, R. L., Bartke, I., Stadelmann, C., Lassmann, H., Wekerle, H., & Hohlfeld, R. (1999) Activated human T cells, B cells, and monocytes produce brain-derived neurotrophic factor in vitro and in inflammatory brain lesions: a neuroprotective role of inflammation? *J. Exp. Med.*, 189,865-870.

Killestein, J., Hoogervorst, E. L., Reif, M., Kalkers, N. F., Van Loenen, A. C., Staats, P. G., Gorter, R. W., Uitdehaag, B. M., & Polman, C. H. (2002) Safety,

tolerability, and efficacy of orally administered cannabinoids in MS. *Neurology*, 58,1404-1407.

Kim, D. & Thayer, S. A. (2001) Cannabinoids inhibit the formation of new synapses between hippocampal neurons in culture. *J. Neurosci.*, 21,RC146-

Kollias, G. & Kontoyiannis, D. (2002) Role of TNF/TNFR in autoimmunity: specific TNF receptor blockade may be advantageous to anti-TNF treatments. *Cytokine Growth Factor Rev.*, 13,315-321.

Kotter, M. R., Setzu, A., Sim, F. J., Van Rooijen, N., & Franklin, R. J. (2001) Macrophage depletion impairs oligodendrocyte remyelination following lysolecithin-induced demyelination. *GLIA*, 35,204-212.

Kreitzer, A. C. & Regehr, W. G. (2002) Retrograde signaling by endocannabinoids. *Curr. Opin. Neurobiol.*, 12,324-330.

Kruger, G. M., Diemel, L. T., Copelman, C. A., & Cuzner, M. L. (1999) Myelin basic protein isoforms in myelinating and remyelinating rat brain aggregate cultures. *J. Neurosci. Res.*, 56,241-247.

Lachepelle, F., Duhamel-Clerin, E., Gansmuller, A., Baron-Van Evercooren, A., Villarroya, H., & Gumpel, M. (1994) Transplanted transgenically marked oligodendrocytes survive, migrate and myelinate in the normal mouse brain as they do in the shiverer mouse brain. *Eur. J. Neurosci.*, 6,814-824.

Lachepelle, F., Gumpel, M., Baulac, m., Jacque, C., DUC, P., & Baumann, N. (1984) Transplantation of CNS fragments into the brain of shiverer mutant mice - extensive myelination by implanted oligodendrocytes. 1. Immunohistochemical studies. *Developmental Neuroscience*, 6,325-334.

Lakatos, A., Barnett, S. C., & Franklin, R. J. (2003) Olfactory ensheathing cells induce less host astrocyte response and chondroitin sulphate proteoglycan expression than schwann cells following transplantation into adult cns white matter. *Exp. Neurol.*, 184,237-246.

Lambert, D. M., DiPaolo, F. G., Sonveaux, P., Kanyonyo, M., Govaerts, S. J., Hermans, E., Bueb, J., Delzenne, N. M., & Tschirhart, E. J. (1999) Analogues and homologues of N-palmitoylethanolamide, a putative endogenous CB(2) cannabinoid, as potential ligands for the cannabinoid receptors. *Biochim. Biophys. Acta*, 1440,266-274.

Lambert, S., Davis, J. Q., & Bennett, V. (1997) Morphogenesis of the node of Ranvier: co-clusters of ankyrin and ankyrin-binding integral proteins define early developmental intermediates. *J. Neurosci.*, 17,7025-7036.

Ledent, C., Valverde, O., Cossu, G., Petitet, F., Aubert, J. F., Beslot, F., Bohme, G. A., Imperato, A., Pedrazzini, T., Roques, B. P., Vassart, G., Fratta, W., & Parmentier, M. (1999) Unresponsiveness to cannabinoids and reduced addictive effects of opiates in CB1 receptor knockout mice. *Science*, 283,401-404.

Lee, S. J. & Benveniste, E. N. (1999) Adhesion molecule expression and regulation on cells of the central nervous system. *J. Neuroimmunol.*, 98,77-88.

Leist, M., Volbracht, C., Kuhnle, S., Fava, E., Ferrando-May, E., & Nicotera, P. (1997) Caspase-mediated apoptosis in neuronal excitotoxicity triggered by nitric oxide. *Mol. Med.*, 3,750-764.

Lenoir, D., Barg, J., & Simantov, R. (1983) Down-regulation of opiate receptors in serum-free cultures of aggregating fetal brain cells. *Life Sci.*, 33 Suppl 1,337-340.

Lenoir, D., Barg, J., & Simantov, R. (1984) Characterization and down-regulation of opiate receptors in aggregating fetal rat brain cells. *Brain Res.*, 304,285-290.

Leonard, J. P., Waldburger, K. E., & Goldman, S. J. (1995) Prevention of experimental autoimmune encephalomyelitis by antibodies against interleukin 12. *J. Exp. Med.*, 181,381-386.

Leterrier, J. F., Kas, J., Hartwig, J., Vegners, R., & Janmey, P. A. (1996) Mechanical effects of neurofilament cross-bridges. Modulation by phosphorylation, lipids, and interactions with F-actin. *J. Biol. Chem.*, 271,15687-15694.

Letourneau, P. C. (1981) Immunocytochemical evidence for colocalization in neurite growth cones of actin and myosin and their relationship to cell--substratum adhesions. *Dev. Biol.*, 85,113-122.

Levine, S. & Sowinski, R. (1973) Experimental allergic encephalomyelitis in inbred and outbred mice. *J. Immunol.*, 110,139-143.

Levison, S. W. & Goldman, J. E. (1993) Both oligodendrocytes and astrocytes develop from progenitors in the subventricular zone of postnatal rat forebrain. *Neuron*, 10,201-212.

Li, M., Shibata, A., Li, C., Braun, P. E., McKerracher, L., Roder, J., Kater, S. B., & David, S. (1996) Myelin-associated glycoprotein inhibits neurite/axon growth and causes growth cone collapse. *J Neurosci. Res.*, 46,404-414.

Li, P., Nijhawan, D., Budihardjo, I., Srinivasula, S. M., Ahmad, M., Alnemri, E. S., & Wang, X. (1997) Cytochrome c and dATP-dependent formation of Apaf-1/caspase-9 complex initiates an apoptotic protease cascade. *Cell*, 91,479-489.

Li, X., Kaminski, N. E., & Fischer, L. J. (2001) Examination of the immunosuppressive effect of delta9-tetrahydrocannabinol in streptozotocin-induced autoimmune diabetes. *Int. Immunopharmacol.*, 1,699-712.

Linington, C., Bradl, M., Lassmann, H., Brunner, C., & Vass, K. (1988) Augmentation of demyelination in rat acute allergic encephalomyelitis by circulating mouse monoclonal antibodies directed against a myelin/oligodendrocyte glycoprotein. *Am. J. Pathol.*, 130,443-454.

Linington, C., Webb, M., & Woodhams, P. L. (1984) A novel myelin-associated glycoprotein defined by a mouse monoclonal antibody. *J. Neuroimmunol.*, 6,387-396.

Linker, R. A., Maurer, M., Gaupp, S., Martini, R., Holtmann, B., Giess, R., Rieckmann, P., Lassmann, H., Toyka, K. V., Sendtner, M., & Gold, R. (2002) CNTF is a major protective factor in demyelinating CNS disease: a neurotrophic cytokine as modulator in neuroinflammation. *Nat. Med.*, 8,620-624.

Lipton, S. A., Choi, Y. B., Pan, Z. H., Lei, S. Z., Chen, H. S., Sucher, N. J., Loscalzo, J., Singel, D. J., & Stamler, J. S. (1993) A redox-based mechanism for the neuroprotective and neurodestructive effects of nitric oxide and related nitroso-compounds. *Nature*, 364,626-632.

Liu, Y., Zhu, B., Wang, X., Luo, L., Li, P., Paty, D. W., & Cynader, M. S. (2003) Bilirubin as a potent antioxidant suppresses experimental autoimmune encephalomyelitis: implications for the role of oxidative stress in the development of multiple sclerosis. *J. Neuroimmunol.*, 139,27-35.

Lo, A. C., Black, J. A., & Waxman, S. G. (2002) Neuroprotection of axons with phenytoin in experimental allergic encephalomyelitis. *Neuroreport*, 13,1909-1912.

Lois, C. & Alvarez-Buylla, A. (1993) Proliferating subventricular zone cells in the adult mammalian forebrain can differentiate into neurons and glia. *Proc. Natl. Acad. Sci. U. S. A*, 90,2074-2077.

Lossi, L. & Merighi, A. (2003) In vivo cellular and molecular mechanisms of neuronal apoptosis in the mammalian CNS. *Prog. Neurobiol.*, 69,287-312.

Loughlin, A. J., Copelman, C. A., Hall, A., Armer, T., Young, B. C., Landon, D. N., & Cuzner, M. L. (1997) Myelination and remyelination of aggregate rat brain cell cultures enriched with macrophages. *J. Neurosci. Res.*, 47,384-392.

Lowry, O. H., Rosebrough, L. W., Farr, L. W., & Randall, R. J. (1951) Protein measurement with Folin phenol reagent. *J Biol Chem*, 193,265-275.

Lucchinetti, C., Bruck, W., & Noseworthy, J. (2001) Multiple sclerosis: recent developments in neuropathology, pathogenesis, magnetic resonance imaging studies and treatment. *Curr. Opin. Neurol.*, 14,259-269.

Lucchinetti, C., Bruck, W., Parisi, J., Scheithauer, B., Rodriguez, M., & Lassmann, H. (2000) Heterogeneity of multiple sclerosis lesions: implications for the pathogenesis of demyelination. *Ann. Neurol.*, 47,707-717.

Lucchinetti, C. F., Bruck, W., Rodriguez, M., & Lassmann, H. (1996) Distinct patterns of multiple sclerosis pathology indicates heterogeneity on pathogenesis. *Brain Pathol.*, 6,259-274.

Ludwin, S. K. (1984) Proliferation of mature oligodendrocytes after trauma to the central nervous system. *Nature*, 308,274-275.

Lyman, W. D., Sonett, J. R., Brosnan, C. F., Elkin, R., & Bornstein, M. B. (1989) Delta 9-tetrahydrocannabinol: a novel treatment for experimental autoimmune encephalomyelitis. *J. Neuroimmunol.*, 23,73-81.

Maccarrone, M., Lorenzon, T., Bari, M., Melino, G., & Finazzi-Agro, A. (2000) Anandamide induces apoptosis in human cells via vanilloid receptors. Evidence for a protective role of cannabinoid receptors. *J. Biol. Chem.*, 275,31938-31945.

Madison, D. L., Krueger, W. H., Cheng, D., Trapp, B. D., & Pfeiffer, S. E. (1999) SNARE complex proteins, including the cognate pair VAMP-2 and syntaxin- 4, are expressed in cultured oligodendrocytes. *J. Neurochem.*, 72,988-998.

Madison, D. L., Kruger, W. H., Kim, T., & Pfeiffer, S. E. (1996) Differential expression of rab3 isoforms in oligodendrocytes and astrocytes. *J. Neurosci. Res.*, 45,258-268.

Maejima, T., Ohno-Shosaku, T., & Kano, M. (2001) Endogenous cannabinoid as a retrograde messenger from depolarized postsynaptic neurons to presynaptic terminals. *Neurosci. Res.*, 40,205-210.

Magyar, J. P., Ebensperger, C., Schaeren-Wiemers, N., & Suter, U. (1997) Myelin and lymphocyte protein (MAL/MVP17/VIP17) and plasmolipin are members of an extended gene family. *Gene*, 189,269-275.

Markovic-Plese, S. & McFarland, H. F. (2001) Immunopathogenesis of the multiple sclerosis lesion. *Curr. Neurol. Neurosci. Rep.*, 1,257-262.

Marsicano, G., Moosmann, B., Hermann, H., Lutz, B., & Behl, C. (2002) Neuroprotective properties of cannabinoids against oxidative stress: role of the cannabinoid receptor CB1. *J. Neurochem.*, 80,448-456.

Martin, R. & McFarland, H. F.(1997)Immunology of multiple sclerosis and experimental allergic encephalomyelitis.221-242.

Martyn, C. N., Illis, L. S., & Thom, J. (1995) Nabilone in the treatment of multiple sclerosis. *Lancet*, 345,579-

Mason, J. L., Suzuki, K., Chaplin, D. D., & Matsushima, G. K. (2001) Interleukin-1beta promotes repair of the CNS. *J. Neurosci.*, 21,7046-7052.

Matsuda, L. A. (1997) Molecular aspects of cannabinoid receptors. *Crit Rev. Neurobiol.*, 11,143-166.

Matsuda, L. A., Lolait, S. J., Brownstein, M. J., Young, A. C., & Bonner, T. I. (1990) Structure of a cannabinoid receptor and functional expression of the cloned cDNA. *Nature*, 346,561-564.

Matsushima, G. K. & Morell, P. (2001) The neurotoxicant, cuprizone, as a model to study demyelination and remyelination in the central nervous system. *Brain Pathol.*, 11,107-116.

Matthieu, J. M., Honegger, P., Trapp, B. D., Cohen, S. R., & Webster, H. F. (1978) Myelination in rat brain aggregating cell cultures. *Neuroscience*, 3,565-572.

Mattson, M. P. (2003) Excitotoxic and excitoprotective mechanisms: abundant targets for the prevention and treatment of neurodegenerative disorders. *Neuromolecular. Med.*, 3,65-94.

McCobb, D. P., Haydon, P. G., & Kater, S. B. (1988) Dopamine and serotonin inhibition of neurite elongation of different identified neurons. *J. Neurosci. Res.*, 19,19-26.

McFarlane, S., McNeill, L., & Holt, C. E. (1995) FGF signaling and target recognition in the developing Xenopus visual system. *Neuron*, 15,1017-1028.

McGee, A. W., Topinka, J. R., Hashimoto, K., Petralia, R. S., Kakizawa, S., Kauer, F., Aguilera-Moreno, A., Wenthold, R. J., Kano, M., & Bredt, D. S. (2001) PSD-93 knock-out mice reveal that neuronal MAGUKs are not required for development or function of parallel fiber synapses in cerebellum. *J. Neurosci.*, 21,3085-3091.

McMorris, F. A. & McKinnon, R. D. (1996) Regulation of oligodendrocyte development and CNS myelination by growth factors: prospects for therapy of demyelinating disease. *Brain Pathol.*, 6,313-329.

McQuarrie, I. G., Brady, S. T., & Lasek, R. J. (1986) Diversity in the axonal transport of structural proteins: major differences between optic and spinal axons in the rat. *J. Neurosci.*, 6,1593-1605.

Mechoulam, R., Ben Shabat, S., Hanus, L., Ligumsky, M., Kaminski, N. E., Schatz, A. R., Gopher, A., Almog, S., Martin, B. R., Compton, D. R., & . (1995) Identification of an endogenous 2-monoglyceride, present in canine gut, that binds to cannabinoid receptors. *Biochem. Pharmacol.*, 50,83-90.

Mechoulam, R. & Gaoni, Y. (1965) A total synthesis of dl-delta-1-tetrahydrocannabinol, the active constituent of hashish. *J. Am. Chem. Soc.*, 87,3273-3275.

Mechoulam, R., Lander, N., Varkony, T. H., Kimmel, I., Becker, O., Ben Zvi, Z., Edery, H., & Porath, G. (1980) Stereochemical requirements for cannabinoid activity. *J. Med. Chem.*, 23,1068-1072.

Meinck, H. M., Schonle, P. W., & Conrad, B. (1989) Effect of cannabinoids on spasticity and ataxia in multiple sclerosis. *J. Neurol.*, 236,120-122.

Meller, D., Bellander, B. M., Schmidt-Kastner, R., & Ingvar, M. (1993) Immunohistochemical studies with antibodies to neurofilament proteins on axonal damage in experimental focal lesions in rat. *J. Neurol. Sci.*, 117,164-174.

Merrill, J. E., Ignarro, L. J., Sherman, M. P., Melinek, J., & Lane, T. E. (1993) Microglial cell cytotoxicity of oligodendrocytes is mediated through nitric oxide. . *J. Immunol.*, 151,2132-2141.

Meyer-Franke, A., Shen, S. L., & Barres, B. A. (1999) Astrocytes induce oligodendrocyte processes to align with and adhere to axons. *Molecular And Cellular Neuroscience*, 14,385-397.

Miller, D. J., Bright, J. J., Sriram, S., & Rodriguez, M. (1997) Successful treatment of established relapsing experimental autoimmune encephalomyelitis in mice with a monoclonal natural autoantibody. *J. Neuroimmunol.*, 75,204-209.

Misko, T. P., Trotter, J. L., & Cross, A. H. (1995) Mediation of inflammation by encephalitogenic cells: interferon gamma induction of nitric oxide synthase and cyclooxygenase 2. *J. Neuroimmunol.*, 61,195-204.

Mokhtarian, F., Zhang, Z., Shi, Y., Gonzales, E., & Sobel, R. A. (1999) Molecular mimicry between a viral peptide and a myelin oligodendrocyte glycoprotein peptide induces autoimmune demyelinating disease in mice. *J. Neuroimmunol.*, 95,43-54.

Molina-Holgado, F., Lledo, A., & Guaza, C. (1997) Anandamide suppresses nitric oxide and TNF-alpha responses to Theiler's virus or endotoxin in astrocytes. *Neuroreport*, 8,1929-1933.

Molina-Holgado, F., Pinteaux, E., Moore, J. D., Molina-Holgado, E., Guaza, C., Gibson, R. M., & Rothwell, N. J. (2003) Endogenous interleukin-1 receptor antagonist mediates anti-inflammatory and neuroprotective actions of cannabinoids in neurons and glia. *J. Neurosci.*, 23,6470-6474.

Moller, J. R. (1996) Rapid conversion of myelin-associated glycoprotein to a soluble derivative in primates. *Brain Res.*, 741,27-31.

Monge, M., Kadiiski, D., Jacque, C. M., & Zalc, B. (1986) Oligodendroglial expression and deposition of four major myelin constituents in the myelin sheath during development. An in vivo study. *Dev. Neurosci.*, 8,222-235.

Monory, K., Tzavara, E. T., Leximе, J., Ledent, C., Parmentier, M., Borsodi, A., & Hanoune, J. (2002) Novel, not adenylyl cyclase-coupled cannabinoid binding site in cerebellum of mice. *Biochem. Biophys. Res. Commun.*, 292,231-235.

Morell, P., Quarles, R. H., & Norton, W. T.(1994)Myelin formation, structure and biochemistry.117-141.

Morris-Downes, M. M., McCormack, K., Baker, D., Sivaprasad, D., Natkunarajah, J., & Amor, S. (2002) Encephalitogenic and immunogenic potential of myelin-associated glycoprotein (MAG), oligodendrocyte-specific glycoprotein (OSP) and 2',3'-cyclic nucleotide 3'-phosphodiesterase (CNPase) in ABH and SJL mice. *J. Neuroimmunol.*, 122,20-33.

Moscona, A. A.(1965)Recombination of dissociated cells and the development of cell aggregates.489-529.

Moss, D. W. & Bates, T. E. (2001) Activation of murine microglial cell lines by lipopolysaccharide and interferon-gamma causes NO-mediated decreases in mitochondrial and cellular function. *Eur. J. Neurosci.*, 13,529-538.

Muchmore, S. W., Sattler, M., Liang, H., Meadows, R. P., Harlan, J. E., Yoon, H. S., Nettesheim, D., Chang, B. S., Thompson, C. B., Wong, S. L., Ng, S. L., & Fesik, S. W. (1996) X-ray and NMR structure of human Bcl-xL, an inhibitor of programmed cell death. *Nature*, 381,335-341.

Munro, S., Thomas, K. L., & Abu-Shaar, M. (1993) Molecular characterization of a peripheral receptor for cannabinoids. *Nature*, 365,61-65.

Murphy, L. L., Munoz, R. M., Adrian, B. A., & Villanua, M. A. (1998) Function of cannabinoid receptors in the neuroendocrine regulation of hormone secretion. *Neurobiol. Dis.*, 5,432-446.

Muzio, M., Stockwell, B. R., Stennicke, H. R., Salvesen, G. S., & Dixit, V. M. (1998) An induced proximity model for caspase-8 activation. *J. Biol. Chem.*, 273,2926-2930.

Nadon, N. L., Arnheiter, H., & Hudson, L. D. (1994) A combination of PLP and DM20 transgenes promotes partial myelination in the jimpy mouse. *J Neurochem.*, 63,822-833.

Nagayama, T., Sinor, A. D., Simon, R. P., Chen, J., Graham, S. H., Jin, K., & Greenberg, D. A. (1999) Cannabinoids and neuroprotection in global and focal cerebral ischemia and in neuronal cultures. *J Neurosci.*, 19,2987-2995.

Nait-Oumesmar, B., Decker, L., Lachepelle, F., Avellana-Adalid, V., Bachelin, C., & Van Evercooren, A. B. (1999) Progenitor cells of the adult mouse subventricular zone proliferate, migrate and differentiate into oligodendrocytes after demyelination. *Eur. J. Neurosci.*, 11,4357-4366.

Nakamura, Y., Hashimoto, R., Kashiwagi, Y., Aimoto, S., Fukusho, E., Matsumoto, N., Kudo, T., & Takeda, M. (2000) Major phosphorylation site (Ser55) of neurofilament L by cyclic AMP-dependent protein kinase in rat primary neuronal culture. *J. Neurochem.*, 74,949-959.

Nelson, E. J., Connolly, J., & McArthur, P. (2003) Nitric oxide and S-nitrosylation: excitotoxic and cell signaling mechanism. *Biol. Cell*, 95,3-8.

Neumann, H., Schmidt, H., Cavalie, A., Jenne, D., & Wekerle, H. (1997) Major histocompatibility complex (MHC) class I gene expression in single neurons of the central nervous system: differential regulation by interferon (IFN)-gamma and tumor necrosis factor (TNF)-alpha. *J. Exp. Med.*, 185,305-316.

O'Leary, M. T., Hinks, G. L., Charlton, H. M., & Franklin, R. J. (2002) Increasing local levels of IGF-I mRNA expression using adenoviral vectors does not alter oligodendrocyte remyelination in the CNS of aged rats. *Mol. Cell Neurosci.*, 19,32-42.

Ohno-Shosaku, T., Tsubokawa, H., Mizushima, I., Yoneda, N., Zimmer, A., & Kano, M. (2002) Presynaptic cannabinoid sensitivity is a major determinant of depolarization-induced retrograde suppression at hippocampal synapses. *J. Neurosci.*, 22,3864-3872.

Oldstone, M. B. (1987) Molecular mimicry and autoimmune disease. *Cell*, 50,819-820.

Ossina, N. K., Cannas, A., Powers, V. C., Fitzpatrick, P. A., Knight, J. D., Gilbert, J. R., Shekhtman, E. M., Tomei, L. D., Umansky, S. R., & Kiefer, M. C. (1997) Interferon-gamma modulates a p53-independent apoptotic pathway and apoptosis-related gene expression. *J. Biol. Chem.*, 272,16351-16357.

Ouyang, Y., Hwang, S. G., Han, S. H., & Kaminski, N. E. (1998) Suppression of interleukin-2 by the putative endogenous cannabinoid 2-arachidonyl-glycerol is mediated through down-regulation of the nuclear factor of activated T cells. *Mol. Pharmacol.*, 53,676-683.

Pacheco, M., Childers, S. R., Arnold, R., Casiano, F., & Ward, S. J. (1991) Aminoalkylindoles: actions on specific G-protein-linked receptors. *J. Pharmacol. Exp. Ther.*, 257,170-183.

Pahl, H. L. & Baeuerle, P. A. (1996) Activation of NF-kappa B by ER stress requires both Ca2+ and reactive oxygen intermediates as messengers. *FEBS Lett.*, 392,129-136.

Pahl, H. L. & Baeuerle, P. A. (1997) The ER-overload response: activation of NF-kappa B. *Trends Biochem. Sci.*, 22,63-67.

Panikashvili, D., Simeonidou, C., Ben Shabat, S., Hanus, L., Breuer, A., Mechoulam, R., & Shohami, E. (2001) An endogenous cannabinoid (2-AG) is neuroprotective after brain injury. *Nature*, 413,527-531.

Paria, B. C., Song, H., Wang, X., Schmid, P. C., Krebsbach, R. J., Schmid, H. H., Bonner, T. I., Zimmer, A., & Dey, S. K. (2001) Dysregulated cannabinoid signaling disrupts uterine receptivity for embryo implantation. *J. Biol. Chem.*, 276,20523-20528.

Pavelko, K. D., van Engelen, B. G., & Rodriguez, M. (1998) Acceleration in the rate of CNS remyelination in lysolecithin-induced demyelination. *J. Neurosci.*, 18,2498-2505.

Pescovitz, M. D., Paterson, P. Y., Kelly, J., & Lorand, L. (1978) Serum degradation of myelin basic protein with loss of encephalitogenic activity: evidence for an enzymatic process. *Cell Immunol.*, 39,355-365.

Peterson, J. W., Bo, L., Mork, S., Chang, A., & Trapp, B. D. (2001) Transected neurites, apoptotic neurons, and reduced inflammation in cortical multiple sclerosis lesions. *Ann. Neurol.*, 50,389-400.

Petro, D. J. & Ellenberger, C., Jr. (1981) Treatment of human spasticity with delta 9-tetrahydrocannabinol. *J. Clin. Pharmacol.*, 21,413S-416S.

Petzold, A., Baker, D., Pryce, G., Keir, G., Thompson, E. J., & Giovannoni, G. (2003) Quantification of neurodegeneration by measurement of brain-specific proteins. *J. Neuroimmunol.*, 138,45-48.

Philchenkov, A. A. (2003) Caspases as regulators of apoptosis and other cell functions. *Biochemistry (Mosc.)*, 68,365-376.

Philips, R. J. (1954) Jimpy, a new totally sex-linked gene in house mouse. *Z. Verberbungsl.*, 986,322-322.

Picard-Riera, N., Decker, L., Delarasse, C., Goude, K., Nait-Oumesmar, B., Liblau, R., Pham-Dinh, D., & Evercooren, A. B. (2002) Experimental autoimmune encephalomyelitis mobilizes neural progenitors from the subventricular zone to undergo oligodendrogenesis in adult mice. *Proc. Natl. Acad. Sci. U. S. A*, 99,13211-13216.

Piddlesden, S. J., Lassmann, H., Zimprich, F., Morgan, B. P., & Linington, C. (1993) The demyelinating potential of antibodies to myelin oligodendrocyte glycoprotein is related to their ability to fix complement. *Am. J. Pathol.*, 143,555-564.

Pitt, D., Werner, P., & Raine, C. S. (2000) Glutamate excitotoxicity in a model of multiple sclerosis. *Nat. Med.*, 6,67-70.

Porcella, A., Marchese, G., Casu, M. A., Rocchitta, A., Lai, M. L., Gessa, G. L., & Pani, L. (2002) Evidence for functional CB1 cannabinoid receptor expressed in the rat thyroid. *Eur. J. Endocrinol.*, 147,255-261.

Prineas, J. W.(1985)The neuropathology of multiple sclerosis.213-257.

Puffenbarger, R. A., Boothe, A. C., & Cabral, G. A. (2000) Cannabinoids inhibit LPS-inducible cytokine mRNA expression in rat microglial cells. *GLIA*, 29,58-69.

Pulliam, L., Dix, R. D., Panitch, H. S., & Baringer, J. R. (1984) Use of aggregating brain cultures to study the replication of herpes simplex virus types 1 and 2 in central nervous system tissue. *J. Virol. Methods*, 9,301-316.

Purves, D. & Lichtman, J. W. (1985) Geometrical differences among homologous neurons in mammals. *Science*, 228,298-302.

Raff, M. C., Fields, K. L., Hakomori, S. I., Mirsky, R., Pruss, R. M., & Winter, J. (1979) Cell-type-specific markers for distinguishing and studying neurons and the major classes of glial cells in culture. *Brain Res.*, 174,283-308.

Raine, C. S.(1984)Morphology of myelin and myelination.2,1-50.

Rakic, P. (1972) Mode of cell migration to the superficial layers of fetal monkey neocortex. *J. Comp Neurol.*, 145,61-83.

Rakic, P. (1977) Genesis of the dorsal lateral geniculate nucleus in the rhesus monkey: site and time of origin, kinetics of proliferation, routes of migration and pattern of distribution of neurons. *J. Comp Neurol.*, 176,23-52.

Rakic, P. (1988) Specification of cerebral cortical areas. *Science*, 241,170-176.

Rakic, P., Bourgeois, J. P., Eckenhoff, M. F., Zecevic, N., & Goldman-Rakic, P. S. (1986) Concurrent overproduction of synapses in diverse regions of the primate cerebral cortex. *Science*, 232,232-235.

Readhead, C., Schneider, A., Griffiths, I., & Nave, K. A. (1994) Premature arrest of myelin formation in transgenic mice with increased proteolipid protein gene dosage. *Neuron*, 12,583-595.

Reed, J. C. (1997) Double identity for proteins of the Bcl-2 family. *Nature*, 387,773-776.

Reynolds, R., Dawson, M., Papadopoulos, D., Polito, A., Di Bello, I. C., Pham-Dinh, D., & Levine, J. (2002) The response of NG2-expressing oligodendrocyte progenitors to demyelination in MOG-EAE and MS. *J. Neurocytol.*, 31,523-536.

Reynolds, R. & Wilkin, G. P. (1991) Oligodendroglial progenitor cells but not oligodendroglia divide during normal development of the rat cerebellum. *J Neurocytol.*, 20,216-224.

Richardson, P. M., McGuinness, U. M., & Aguayo, A. J. (1980) Axons from CNS neurons regenerate into PNS grafts. *Nature*, 284,264-265.

Ridet, J. L., Malhotra, S. K., Privat, A., & Gage, F. H. (1997) Reactive astrocytes: cellular and molecular cues to biological function. *Trends Neurosci.*, 20,570-577.

Rivett, A. J., Bose, S., Brooks, P., & Broadfoot, K. I. (2001) Regulation of proteasome complexes by gamma-interferon and phosphorylation. *Biochimie*, 83,363-366.

Roach, A., Boylan, K., Horvath, S., Prusiner, S. B., & Hood, L. E. (1983) Characterization of cloned cDNA representing rat myelin basic protein: absence of expression in brain of shiverer mutant mice. . *Cell*, 34,799-806.

Roberts, P. J., Devereux, S., Pilkington, G. R., & Linch, D. C. (1990) Fc gamma RII-mediated superoxide production by phagocytes is augmented by GM-CSF without a change in Fc gamma RII expression. *J. Leukoc. Biol.*, 48,247-257.

Rodriguez, M., Leibowitz, J. L., & Lampert, P. W. (1983) Persistent infection of oligodendrocytes in Theiler's virus-induced encephalomyelitis. *Ann. Neurol.*, 13,426-433.

Romero, E. M., Fernandez, B., Sagredo, O., Gomez, N., Uriguen, L., Guaza, C., De Miguel, R., Ramos, J. A., & Viveros, M. P. (2002) Antinociceptive, behavioural and neuroendocrine effects of CP 55,940 in young rats. *Brain Res. Dev. Brain Res.*, 136,85-92.

Roos, J. & Kelly, R. B. (2000) Preassembly and transport of nerve terminals: a new concept of axonal transport. *Nat. Neurosci.*, 3,415-417.

Rosenbluth, J., Schiff, R., Liang, W. L., Dou, W. K., & Moon, D. (1999) Antibody-mediated CNS demyelination: focal spinal cord lesions induced by implantation of an IgM anti-galactocerebroside-secreting hybridoma. *J. Neurocytol.*, 28,397-416.

Roth, M. D., Marques-Magallanes, J. A., Yuan, M., Sun, W., Tashkin, D. P., & Hankinson, O. (2001) Induction and regulation of the carcinogen-metabolizing enzyme CYP1A1 by marijuana smoke and delta (9)-tetrahydrocannabinol. *Am. J. Respir. Cell Mol. Biol.*, 24,339-344.

Roy, S., Coffee, P., Smith, G., Liem, R. K., Brady, S. T., & Black, M. M. (2000) Neurofilaments are transported rapidly but intermittently in axons: implications for slow axonal transport. *J. Neurosci.*, 20,6849-6861.

Ruddle, N. H., Bergman, C. M., McGrath, K. M., Lingenheld, E. G., Grunnet, M. L., Padula, S. J., & Clark, R. B. (1990) An antibody to lymphotoxin and tumor necrosis factor prevents transfer of experimental allergic encephalomyelitis. *J. Exp. Med.*, 172,1193-1200.

Ruffini, F., Furlan, R., Poliani, P. L., Brambilla, E., Marconi, P. C., Bergami, A., Desina, G., Glorioso, J. C., Comi, G., & Martino, G. (2001) Fibroblast growth factor-II gene therapy reverts the clinical course and the pathological signs of chronic experimental autoimmune encephalomyelitis in C57BL/6 mice. *Gene Ther.*, 8,1207-1213.

Rushton, W. A. H. (1951) A theory of the effects of fibre size in the medullated nerve. *J. Phisiol. Lond.*, 115,112-122.

Sakaguchi, T., Okada, M., Kitamura, T., & Kawasaki, K. (1993) Reduced diameter and conduction velocity of myelinated fibers in the sciatic nerve of a neurofilament-deficient mutant quail. *Neurosci. Lett.*, 153,65-68.

Salthouse, T. N. (1964) Luxol fast blue G as a myelin stain. *Stain Technol.*, 39,123-

Sanchez, I., Hassinger, L., Paskevich, P. A., Shine, H. D., & Nixon, R. A. (1996) Oligodendroglia regulate the regional expansion of axon caliber and local accumulation of neurofilaments during development independently of myelin formation. *J Neurosci.*, 16,5095-5105.

Sancho, R., Calzado, M. A., Di, M., V, Appendino, G., & Munoz, E. (2003) Anandamide inhibits nuclear factor-kappaB activation through a cannabinoid receptor-independent pathway. *Mol. Pharmacol.*, 63,429-438.

Sandyk, R. (1999) Serotonergic neuronal sprouting as a potential mechanism of recovery in multiple sclerosis. *Int. J. Neurosci.*, 97,131-138.

Sarker, K. P., Obara, S., Nakata, M., Kitajima, I., & Maruyama, I. (2000) Anandamide induces apoptosis of PC-12 cells: involvement of superoxide and caspase-3. *FEBS Lett.*, 472,39-44.

Sarlieve, L. L., Fabre, M., Susz, J., & Matthieu, J. M. (1983) Investigations on myelination in vitro. 4. Myelin-like or premyelin structures in cultures of dissociated brain cells from 14-15 day old embryonic mice. *Journal of Neuroscience Research*, 10,191-210.

Sarlieve, L. L., Neskovic, N. M., Rebel, G., & Mandel, P. (1974) PAPS-cerebroside sulphotransferase activity in developing brain of a neurological mutant of mouse (MSD). *Exp. Brain Res.*, 19,185-65.

Sathornsumetee, S., McGavern, D. B., Ure, D. R., & Rodriguez, M. (2000) Quantitative ultrastructural analysis of a single spinal cord demyelinated lesion predicts total lesion load, axonal loss, and neurological dysfunction in a murine model of multiple sclerosis. *Am. J. Pathol.*, 157,1365-1376.

Sato, K., Ohmae, E., Senoo, E., Mase, T., Tohyama, K., Fujimoto, E., Mizoguchi, A., & Ide, C. (1997) Remyelination in the rat dorsal funiculus following demyelination by laser irradiation. *Neurosci. Res.*, 28,325-335.

Schild, L., Keilhoff, G., Augustin, W., Reiser, G., & Striggow, F. (2001) Distinct Ca2+ thresholds determine cytochrome c release or permeability transition pore opening in brain mitochondria. *FASEB J.*, 15,565-567.

Schulte, S. & Stoffel, W. (1993) Ceramide UDPgalactosyltransferase from myelinating rat brain: purification, cloning, and expression. *Proc. Natl. Acad. Sci. U. S. A*, 90,10265-10269.

Schutgens, R. B., Schrakamp, G., Wanders, R. J., Heymans, H. S., Moser, H. W., Moser, A. E., Tager, J. M., Bosch, H. V., & Aubourg, P. (1985) The cerebro-hepato-renal (Zellweger) syndrome: prenatal detection based on impaired biosynthesis of plasmalogens. *Prenat. Diagn.*, 5,337-344.

Schuurmans, C. & Guillemot, F. (2002) Molecular mechanisms underlying cell fate specification in the developing telencephalon. *Curr. Opin. Neurobiol.*, 12,26-34.

Schwab, M. E. & Schnell, L. (1991) Channeling of developing rat corticospinal tract axons by myelin- associated neurite growth inhibitors. *J Neurosci.*, 11,709-721.

Schwartz, L. M. & Osborne, B. A. (1994) Ced-3/ICE: evolutionarily conserved regulation of cell death. *Bioessays*, 16,387-389.

Scolding, N. J., Rayner, P. J., Sussman, J., Shaw, C., & Compston, D. A. (1995) A proliferative adult human oligodendrocyte progenitor. *Neuroreport*, 6,441-445.

Selmaj, K., Raine, C. S., Farooq, M., Norton, W. T., & Brosnan, C. F. (1991) Cytokine cytotoxicity against oligodendrocytes. Apoptosis induced by lymphotoxin. *J Immunol.*, 147,1522-1529.

Shah, J. V., Flanagan, L. A., Janmey, P. A., & Leterrier, J. F. (2000) Bidirectional translocation of neurofilaments along microtubules mediated in part by dynein/dynactin. *Mol. Biol. Cell*, 11,3495-3508.

Shen, M. & Thayer, S. A. (1998) Cannabinoid receptor agonists protect cultured rat hippocampal neurons from excitotoxicity. *Mol. Pharmacol.*, 54,459-462.

Sheng, M. (2001) Molecular organization of the postsynaptic specialization. *Proc. Natl. Acad. Sci. U. S. A*, 98,7058-7061.

Sheppard, J. R., Brus, D., & Wehner, J. M. (1978) Brain reaggregate cultures: biochemical evidence for myelin membrane synthesis. *J. Neurobiol.*, 9,309-315.

Sherman, M. P., Griscavage, J. M., & Ignarro, L. J. (1992) Nitric oxide-mediated neuronal injury in multiple sclerosis. *Med. Hypotheses.*, 39,143-146.

Sheskin, T., Hanus, L., Slager, J., Vogel, Z., & Mechoulam, R. (1997) Structural requirements for binding of anandamide-type compounds to the brain cannabinoid receptor. *J. Med. Chem.*, 40,659-667.

Shetty, K. T., Link, W. T., & Pant, H. C. (1993) cdc2-like kinase from rat spinal cord specifically phosphorylates KSPXK motifs in neurofilament proteins: isolation and characterization. *Proc. Natl. Acad. Sci. U. S. A*, 90,6844-6848.

Shimizu, S., Narita, M., & Tsujimoto, Y. (1999) Bcl-2 family proteins regulate the release of apoptogenic cytochrome c by the mitochondrial channel VDAC. *Nature*, 399,483-487.

Shine, H. D., Readhead, C., Popko, B., Hood, L., & Sidman, R. L. (1992) Morphometric analysis of normal, mutant, and transgenic CNS: correlation of myelin basic protein expression to myelinogenesis. *J. Neurochem.*, 58,342-349.

Siegrist, H. P., Bologa-Sandru, L., Burkart, T., Wiesmann, U., Hofmann, K., & Herschkowitz, N. (1981) Synthesis of lipids in mouse brain cell cultures during development. *J. Neurosci. Res.*, 6,293-301.

Silverman, B. A., Carney, D. F., Johnston, C. A., Vanguri, P., & Shin, M. L. (1984) Isolation of membrane attack complex of complement from myelin membranes treated with serum complement. *J. Neurochem.*, 42,1024-1029.

Sim, F. J., Zhao, C., Penderis, J., & Franklin, R. J. (2002) The age-related decrease in CNS remyelination efficiency is attributable to an impairment of both

oligodendrocyte progenitor recruitment and differentiation. *J. Neurosci.*, 22,2451-2459.

Singh, V. K., Mehrotra, S., Narayan, P., Pandey, C. M., & Agarwal, S. S. (2000) Modulation of autoimmune diseases by nitric oxide. *Immunol. Res.*, 22,1-19.

Sinor, A. D., Irvin, S. M., & Greenberg, D. A. (2000) Endocannabinoids protect cerebral cortical neurons from in vitro ischemia in rats. *Neurosci. Lett.*, 278,157-160.

Sjostrand, F. (1949) SEM study of the retinal rods in the guinea pig eye. *J. Cell. Comp. Physiol.*, 33,383-398.

Skaper, S. D., Buriani, A., Dal Toso, R., Petrelli, L., Romanello, S., Facci, L., & Leon, A. (1996) The ALIAmide palmitoylethanolamide and cannabinoids, but not anandamide, are protective in a delayed postglutamate paradigm of excitotoxic death in cerebellar granule neurons. *Proc. Natl. Acad. Sci. U. S. A*, 93,3984-3989.

Slavin, A., Ewing, C., Liu, J., Ichikawa, M., Slavin, J., & Bernard, C. C. (1998) Induction of a multiple sclerosis-like disease in mice with an immunodominant epitope of myelin oligodendrocyte glycoprotein. *Autoimmunity*, 28,109-120.

Smith, K. J., Kapoor, R., & Felts, P. A. (1999) Demyelination: the role of reactive oxygen and nitrogen species. *Brain Pathol.*, 9,69-92.

Smith, K. J., Kapoor, R., Hall, S. M., & Davies, M. (2001) Electrically active axons degenerate when exposed to nitric oxide. *Ann. Neurol.*, 49,470-476.

Smith, M. E. (1968) The turnover of myelin in the adult rat. *Biochim. Biophys. Acta*, 164,285-293.

Smith, S. R., Terminelli, C., & Denhardt, G. (2000a) Effects of cannabinoid receptor agonist and antagonist ligands on production of inflammatory cytokines and anti-inflammatory interleukin-10 in endotoxemic mice. *J. Pharmacol. Exp. Ther.*, 293,136-150.

Smith, T., Groom, A., Zhu, B., & Turski, L. (2000b) Autoimmune encephalomyelitis ameliorated by AMPA antagonists. *Nat. Med.*, 6,62-66.

Soilu-Hanninen, M., Eralinna, J. P., Hukkanen, V., Roytta, M., Salmi, A. A., & Salonen, R. (1994) Semliki Forest virus infects mouse brain endothelial cells and causes blood-brain barrier damage. *J. Virol.*, 68,6291-6298.

Sontheimer, H., Trotter, J., Schachner, M., & Kettenmann, H. (1989) Channel expression correlates with differentiation stage during the development of oligodendrocytes from their precursor cells in culture. *Neuron*, 2,1135-1145.

Stangel, M. & Hartung, H. P. (2002a) Despair of repair. *J. Neurol. Neurosurg. Psychiatry*, 72,1-4.

Stangel, M. & Hartung, H. P. (2002b) Remyelinating strategies for the treatment of multiple sclerosis. *Prog. Neurobiol.*, 68,361-376.

Stefferl, A., Brehm, U., & Linington, C. (2000) The myelin oligodendrocyte glycoprotein (MOG): a model for antibody-mediated demyelination in experimental autoimmune encephalomyelitis and multiple sclerosis. *J. Neural Transm. Suppl*, 123-133.

Stein, S. A., Kirkpatrick, L. L., Shanklin, D. R., Adams, P. M., & Brady, S. T. (1991) Hypothyroidism reduces the rate of slow component A (SCa) axonal transport and the amount of transported tubulin in the hyt/hyt mouse optic nerve. *J. Neurosci. Res.*, 28,121-133.

Sternberger, L. A. & Sternberger, N. H. (1983) Monoclonal antibodies distinguish phosphorylated and nonphosphorylated forms of neurofilaments in situ. *Proc. Natl. Acad. Sci. U. S. A*, 80,6126-6130.

Stoffel, W., Boison, D., & Bussow, H. (1997) Functional analysis in vivo of the double mutant mouse deficient in both proteolipid protein (PLP) and myelin basic protein (MBP) in the central nervous system. *Cell Tissue Res.*, 289,195-206.

Sugiura, T., Kobayashi, Y., Oka, S., & Waku, K. (2002) Biosynthesis and degradation of anandamide and 2-arachidonoylglycerol and their possible physiological significance. *Prostaglandins Leukot. Essent. Fatty Acids*, 66,173-192.

Sulston, J. E. & Horvitz, H. R. (1977) Post-embryonic cell lineages of the nematode, Caenorhabditis elegans. *Dev. Biol.*, 56,110-156.

Suzumura, A., Silberberg, D. H., & Lisak, R. P. (1986) The expression of MHC antigens on oligodendrocytes: induction of polymorphic H-2 expression by lymphokines. *J. Neuroimmunol.*, 11,179-190.

Szaro, B. G., Lee, V. M., & Gainer, H. (1989) Spatial and temporal expression of phosphorylated and non-phosphorylated forms of neurofilament proteins in the developing nervous system of Xenopus laevis. *Brain Res. Dev. Brain Res.*, 48,87-103.

Takahashi, H., Nakamura, S., Asano, K., Kinouchi, M., Ishida-Yamamoto, A., & Iizuka, H. (1999) Fas antigen modulates ultraviolet B-induced apoptosis of SVHK cells: sequential activation of caspases 8, 3, and 1 in the apoptotic process. *Exp. Cell Res.*, 249,291-298.

Takahashi, K. A. & Linden, D. J. (2000) Cannabinoid receptor modulation of synapses received by cerebellar Purkinje cells. *J. Neurophysiol.*, 83,1167-1180.

Tang, S., Woodhall, R. W., Shen, Y. J., deBellard, M. E., Saffell, J. L., Doherty, P., Walsh, F. S., & Filbin, M. T. (1997) Soluble Myelin-Associated Glycoprotein (MAG) Found in Vivo Inhibits Axonal Regeneration. *Mol. Cell Neurosci.*, 9,333-346.

Targett, M. P., Sussman, J., Scolding, N., O'Leary, M. T., Compston, D. A., & Blakemore, W. F. (1996) Failure to achieve remyelination of demyelinated rat axons following transplantation of glial cells obtained from the adult human brain. *Neuropathol. Appl. Neurobiol.*, 22,199-206.

Thallmair, M., Metz, G. A., Z'Graggen, W. J., Raineteau, O., Kartje, G. L., & Schwab, M. E. (1998) Neurite growth inhibitors restrict plasticity and functional recovery following corticospinal tract lesions. *Nat. Neurosci.*, 1,124-131.

Tosic, M., Torch, S., Comte, V., Dolivo, M., Honegger, P., & Matthieu, J. M. (1992) Triiodothyronine has diverse and multiple stimulating effects on expression of the major myelin protein genes. . *J. Neurochem.*, 59,1770-1777.

Tourbah, A., Linnington, C., Bachelin, C., Avellana-Adalid, V., Wekerle, H., & Baron-Van Evercooren, A. (1997) Inflammation promotes survival and migration of the CG4 oligodendrocyte progenitors transplanted in the spinal cord of both inflammatory and demyelinated EAE rats. *J. Neurosci. Res.*, 50,853-861.

Trapp, B. D., Honegger, P., Richelson, E., & Webster, H. D. (1979) Morphological differentiation of mechanically dissociated fetal rat brain in aggregating cell cultures. *Brain Res.*, 160,117-130.

Trapp, B. D., Peterson, J., Ransohoff, R. M., Rudick, R., Mork, S., & Bo, L. (1998) Axonal transection in the lesions of multiple sclerosis [see comments]. *N. Engl. J. Med.*, 338,278-285.

Turnley, A. M., Morahan, G., Okano, H., Bernard, O., Mikoshiba, K., Allison, J., Bartlett, P. F., & Miller, J. F. (1991) Dysmyelination in transgenic mice resulting from expression of class I histocompatibility molecules in oligodendrocytes. *Nature*, 353,566-569.

Tzeng, S. F. (2003) Inhibitors of DNA binding in neural cell proliferation and differentiation. *Neurochem. Res.*, 28,45-52.

Ungerleider, J. T., Andyrsiak, T., Fairbanks, L., Ellison, G. W., & Myers, L. W. (1987) Delta-9-THC in the treatment of spasticity associated with multiple sclerosis. *Adv. Alcohol Subst. Abuse*, 7,39-50.

van der Laan, L. J., Ruuls, S. R., Weber, K. S., Lodder, I. J., Dopp, E. A., & Dijkstra, C. D. (1996) Macrophage phagocytosis of myelin in vitro determined by flow cytometry: phagocytosis is mediated by CR3 and induces production of tumor necrosis factor-alpha and nitric oxide. *J. Neuroimmunol.*, 70,145-152.

van der Stelt, M., Veldhuis, W. B., Bar, P. R., Veldink, G. A., Vliegenthart, J. F., & Nicolay, K. (2001a) Neuroprotection by Delta9-tetrahydrocannabinol, the main active compound in marijuana, against ouabain-induced in vivo excitotoxicity. *J. Neurosci.*, 21,6475-6479.

van der Stelt, M., Veldhuis, W. B., van Haaften, G. W., Fezza, F., Bisogno, T., Bar, P. R., Veldink, G. A., Vliegenthart, J. F., Di, M., V, & Nicolay, K. (2001b)

Exogenous anandamide protects rat brain against acute neuronal injury in vivo. *J. Neurosci.*, 21,8765-8771.

Van Noort, J. M. & Amor, S. (1998) Cell biology of autoimmune diseases. *Int. Rev. Cytol.*, 178,127-206.

Van Obberghen, E., Baron, V., Delahaye, L., Emanuelli, B., Filippa, N., Giorgetti-Peraldi, S., Lebrun, P., Mothe-Satney, I., Peraldi, P., Rocchi, S., Sawka-Verhelle, D., Tartare-Deckert, S., & Giudicelli, J. (2001) Surfing the insulin signaling web. *Eur. J. Clin. Invest*, 31,966-977.

Vaney, C., Jobin, P., Tscopp, F., Heinzel, M., & Schnelle, M. (2004) Efficacy, Safety and Tolerability of an orally administered cannabis extract in the treatment of spasticity in patients with multiple sclerosis. *Symposium on thecannabinoids*,

Veeranna, Amin, N. D., Ahn, N. G., Jaffe, H., Winters, C. A., Grant, P., & Pant, H. C. (1998) Mitogen-activated protein kinases (Erk1,2) phosphorylate Lys-Ser-Pro (KSP) repeats in neurofilament proteins NF-H and NF-M. *J. Neurosci.*, 18,4008-4021.

Verstraeten, S. V., Golub, M. S., Keen, C. L., & Oteiza, P. I. (1997) Myelin is a preferential target of aluminum-mediated oxidative damage. *Arch. Biochem. Biophys.*, 344,289-294.

Viehover, A., Miller, R. H., Park, S. K., Fischbach, G., & Vartanian, T. (2001) Neuregulin: an oligodendrocyte growth factor absent in active multiple sclerosis lesions. *Dev. Neurosci.*, 23,377-386.

Villoslada, P., Hauser, S. L., Bartke, I., Unger, J., Heald, N., Rosenberg, D., Cheung, S. W., Mobley, W. C., Fisher, S., & Genain, C. P. (2000) Human nerve growth factor protects common marmosets against autoimmune encephalomyelitis by switching the balance of T helper cell type 1 and 2 cytokines within the central nervous system. *J. Exp. Med.*, 191,1799-1806.

Wade, D. T., Robson, P., House, H., Makela, P., & Aram, J. (2003) A preliminary controlled study to determine whether whole-plant cannabis extracts can improve intractable neurogenic symptoms. *Clin. Rehabil.*, 17,21-29.

Waksman, Y., Olson, J. M., Carlisle, S. J., & Cabral, G. A. (1999) The central cannabinoid receptor (CB1) mediates inhibition of nitric oxide production by rat microglial cells. *J Pharmacol. Exp Ther.*, 288,1357-1366.

Walter, L., Franklin, A., Witting, A., Wade, C., Xie, Y., Kunos, G., Mackie, K., & Stella, N. (2003) Nonpsychotropic cannabinoid receptors regulate microglial cell migration. *J. Neurosci.*, 23,1398-1405.

Waltereit, R. & Weller, M. (2003) Signaling from cAMP/PKA to MAPK and synaptic plasticity. *Mol. Neurobiol.*, 27,99-106.

Wang, L., Ho, C. L., Sun, D., Liem, R. K., & Brown, A. (2000) Rapid movement of axonal neurofilaments interrupted by prolonged pauses. *Nat. Cell Biol.*, 2,137-141.

Wang, S., Sdrulla, A. D., diSibio, G., Bush, G., Nofziger, D., Hicks, C., Weinmaster, G., & Barres, B. A. (1998) Notch receptor activation inhibits oligodendrocyte differentiation. . *Neuron*, 21,63-75.

Waxman, S. G. & Black, J. A.(1995)Axoglial interactions at the cellular and molecular level in CNS myelinated fibres.587-610.

Waxman, S. G. & Sims, T. J. (1984) Specificity in Central Myelination - Evidence for Local Regulation of Myelin Thickness. *Brain Research*, 292,179-185.

Weber, W. E. J.(1988)Cellular auto-immunty in central nervous system disease.

Wekerle, H.(1997)CD4 effector cells in autoimmune diseases of the CNS.460-492.

Werner, P., Pitt, D., & Raine, C. S. (2001) Multiple sclerosis: altered glutamate homeostasis in lesions correlates with oligodendrocyte and axonal damage. *Ann. Neurol.*, 50,169-180.

Whitford, K. L., Dijkhuizen, P., Polleux, F., & Ghosh, A. (2002) Molecular control of cortical dendrite development. *Annu. Rev. Neurosci.*, 25,127-149.

Willard, M. & Simon, C. (1983) Modulations of neurofilament axonal transport during the development of rabbit retinal ganglion cells. *Cell*, 35,551-559.

Willenborg, D. O. & Staykova, M. A. (2003) Cytokines in the pathogenesis and therapy of autoimmune encephalomyelitis and multiple sclerosis. *Adv. Exp. Med. Biol.*, 520,96-119.

Willenborg, D. O., Staykova, M. A., & Cowden, W. B. (1999) Our shifting understanding of the role of nitric oxide in autoimmune encephalomyelitis: a review. *J. Neuroimmunol.*, 100,21-35.

Williams, E. J., Walsh, F. S., & Doherty, P. (2003) The FGF receptor uses the endocannabinoid signaling system to couple to an axonal growth response. *J. Cell Biol.*, 160,481-486.

Wilson, R. I. & Nicoll, R. A. (2001) Endogenous cannabinoids mediate retrograde signalling at hippocampal synapses. *Nature*, 410,588-592.

Wirguin, I., Mechoulam, R., Breuer, A., Schezen, E., Weidenfeld, J., & Brenner, T. (1994) Suppression of experimental autoimmune encephalomyelitis by cannabinoids. *Immunopharmacology*, 28,209-214.

Wolswijk, G. (2000) Oligodendrocyte survival, loss and birth in lesions of chronic-stage multiple sclerosis. *Brain*, 123 (Pt 1),105-115.

Woodruff, R. H. & Franklin, R. J. (1999a) Demyelination and remyelination of the caudal cerebellar peduncle of adult rats following stereotaxic injections of lysolecithin, ethidium bromide, and complement/anti-galactocerebroside: a comparative study. *GLIA*, 25,216-228.

Woodruff, R. H. & Franklin, R. M. (1999b) The expression of myelin protein mRNAs during remyelination of lysolecithin-induced demyelination [Full text delivery]. *Neuropathology And Applied Neurobiology*, 25,226-235.

Wujek, J. R., Bjartmar, C., Richer, E., Ransohoff, R. M., Yu, M., Tuohy, V. K., & Trapp, B. D. (2002) Axon loss in the spinal cord determines permanent neurological disability in an animal model of multiple sclerosis. *J. Neuropathol. Exp. Neurol.*, 61,23-32.

Yabe, J. T., Pimenta, A., & Shea, T. B. (1999) Kinesin-mediated transport of neurofilament protein oligomers in growing axons. *J. Cell Sci.*, 112 (Pt 21),3799-3814.

Yamada, K. M. & Miyamoto, S. (1995) Integrin transmembrane signaling and cytoskeletal control. *Curr. Opin. Cell Biol.*, 7,681-689.

Yamamoto, T. & Hirano, A. (1986) A comparative study of modified Bielschowsky, Bodian and thioflavin S stains on Alzheimer's neurofibrillary tangles. *Neuropathol. Appl. Neurobiol.*, 12,3-9.

Yin, X., Crawford, T. O., Griffin, J. W., Tu Ph, Lee, V. M., Li, C., Roder, J., & Trapp, B. D. (1998) Myelin-associated glycoprotein is a myelin signal that modulates the caliber of myelinated axons. *J. Neurosci.*, 18,1953-1962.

Yoshida, T., Hashimoto, K., Zimmer, A., Maejima, T., Araishi, K., & Kano, M. (2002) The cannabinoid CB1 receptor mediates retrograde signals for depolarization-induced suppression of inhibition in cerebellar Purkinje cells. *J. Neurosci.*, 22,1690-1697.

Young, P. R. & Zygas, A. P. (1987) Secretion of lactic acid by peritoneal macrophages during extracellular phagocytosis. The possible role of local hyperacidity in inflammatory demyelination. . *J. Neuroimmunol.*, 15,295-308.

Zajicek, J., Fox, P., Sanders, H., Wright, D., Vickery, J., Nunn, A., & Thompson, A. (2003) Cannabinoids for treatment of spasticity and other symptoms related to multiple sclerosis (CAMS study): multicentre randomised placebo-controlled trial. *Lancet*, 362,1517-1526.

Zhou, D. & Song, Z. H. (2001) CB1 cannabinoid receptor-mediated neurite remodeling in mouse neuroblastoma N1E-115 cells. *J. Neurosci. Res.*, 65,346-353.

Zhu, Y., Culmsee, C., Klumpp, S., & Krieglstein, J. (2004) Neuroprotection by transforming growth factor-beta1 involves activation of nuclear factor-kappaB through phosphatidylinositol-3-OH kinase/Akt and mitogen-activated protein

kinase-extracellular-signal regulated kinase1,2 signaling pathways. *Neuroscience*, 123,897-906.

Zimmer, A., Zimmer, A. M., Hohmann, A. G., Herkenham, M., & Bonner, T. I. (1999) Increased mortality, hypoactivity, and hypoalgesia in cannabinoid CB1 receptor knockout mice [see comments]. *Proc. Natl. Acad. Sci. U. S. A*, 96,5780-5785.